UNIVERSITÀ DEGLI STUDI DI TRIESTE

UNIVERSITÀ DEGLI STUDI DI UDINE

UNIVERSITÀ DEGLI STUDI DI TRIESTE

XXXV CICLO DEL DOTTORATO DI RICERCA IN

AMBIENTE E VITA

STEM PHOTOSYNTHESIS: AN ALLY FOR TREES FACING DROUGHT?

Settore scientifico-disciplinare: **BIO/04**

DOTTORANDA
SARA NATALE

COORDINATORE
PROF. GIORGIO ALBERTI

SUPERVISORE DI TESI
PROF. ANDREA NARDINI

CO-SUPERVISORE DI TESI
PROF. VALENTINO CASOLO

CO-SUPERVISORE DI TESI
PROF. TOMAS MOROSINOTTO

ANNO ACCADEMICO 2021/2022

TABLE OF CONTENTS

Abstract

Leaves are generally the most important photosynthetic organs in woody plants, but chloroplasts can also be found in organs optimized for other functions. So far, little attention has been paid to the photosynthetic contribution of stem chloroplasts. Specifically, stem photosynthesis is thought to significantly contribute to the tree carbon budget, and this extra carbon source in the form of non-structural carbohydrates (NSCs) has been suggested to be crucial for trees. In particular, this extra carbon gain might be fundamental during a drought stress, under which leaf photosynthesis impairment and/or a reduced phloem transport can occur. Despite some authors have hypothesized that the inhibition of stem photosynthesis might induce a depletion of carbohydrate reserves with consequent failure of embolism repair processes, effective evidence is still lacking.

Considering the current climate change scenarios, an in-depth investigation of both structural and functional characteristics of stem chloroplasts (both at the bark and wood level) and their possible relation on tree drought resistance/resilience was conducted. The knowledge on the features of stem chloroplasts is still highly fragmented since they are species-specific and dependent on stem characteristics (e.g. bark thickness) and age.

In this light, in the first part of this Thesis (Chapter I), I focused my research activities on a model species: *Fraxinus ornus*, a drought-tolerant woody species widespread in the Karst area nearby Trieste (North-east of Italy), characterized by visually green bark and wood. I provided a thoroughly analysis of structural and functional characteristics of bark and wood chloroplasts of *F. ornus* in comparison with the characteristics of leaf chloroplasts (Study 1). I then proposed a new method for the measurement of radial oxygen profile in woody stems, and I provided an analysis of oxygen rates produced by bark and wood chloroplasts in response to light (Study 2). In this section, I proved that the stem photosynthetic apparatus showed features typical of acclimation to low-light environment, with chloroplasts photosynthetically active and fully capable of generating a light-dependent electron transport. In this light, in the second part of this Thesis (Chapter II), I provided an investigation on how much stem photosynthesis is widespread across woody species (both Angiosperms and Gymnosperms) and an analysis of maximum quantum yield of PSII (Fv/Fm) of bark and wood samples in different stem age. In Study 3, I ranked the species in terms of their relative drought tolerance on the basis of their vulnerability to xylem embolism (P_{50}), and I compared stem photosynthetic efficiency of drought tolerant vs drought sensitive species. I observed that Fv/Fm values decreased with increasing stem age and were generally higher for Angiosperms than Gymnosperms. The comparison between drought-tolerant and drought-sensitive species showed a

clear trend of increasing stem photosynthetic activity in species thriving in more arid habitats and biomes. In particular, this study highlighted the potential adaptive role of stem photosynthesis in drought tolerant species.

The third part of the Thesis (Chapter III) aimed at clarifying the role of stem photosynthesis in tree resistance/resilience to drought stress. Specifically, in Study 4 I aimed to investigate how stem photosynthesis was affecting xylem embolism and NSC in relation to dehydration-rehydration experiment in *F. ornus*. Similarly, the corollary Study 5 verified if stem photosynthesis was involved in hydraulic recovery and drought stress relief in *Laurus nobilis* and *Populus alba* exposed to a drought-recovery cycle. Although the inhibition of stem photosynthesis had different outcomes on the three species investigated during the drought-recovery cycle, compared to control-light plants, results showed that inhibition of stem photosynthesis increased the plant hydraulic vulnerability under drought and stem shading affected the saplings capacity to mobilize NSCs during drought. Therefore, these results suggested that stem photosynthesis is involved in local NSC supply and has a key role in the maintenance of hydraulic functioning during drought.

Finally, the corollary Study 6 aimed at verifying if stem photosynthesis could favor bark water uptake and embolism recovery in stem segments soaked in water under illumination. Results denied this hypothesis since, neither in *Olea europaea* stems nor in *F. ornus* stems, refill of embolized conduits was detected, suggesting that this process might be highly species-specific.

In conclusion stem photosynthesis is coherently optimized to the prevailing micro-environmental conditions at bark and wood level. Stem photosynthesis resulted to potentially have an adaptive role in drought tolerant species, thriving under arid conditions. Indeed, stem photosynthesis could be an important source of local NSC. This may be fundamental to enhance the hydraulic resistance to embolism formation and to endure drought when prolonged stomatal closure and halt of leaf-level carbon gain happen.

Finally, this might imply woody trees dependency on stem photosynthesis for survival, especially if frequent drought spells occur.

Riassunto

Le foglie sono generalmente considerate gli organi fotosintetici più importanti nelle piante legnose, ma i cloroplasti si possono trovare anche in organi ottimizzati per altre funzioni. Un esempio sono i cloroplasti del fusto, il cui contributo fotosintetico è stato finora poco studiato. Si ritiene che la fotosintesi del fusto contribuisca in modo significativo al bilancio del carbonio in una pianta, fornendo una cruciale fonte extra di carbonio sotto forma di carboidrati non strutturali (NSC). In particolare, questo carbonio potrebbe essere fondamentale durante uno stress da siccità, in cui può verificarsi una compromissione della fotosintesi fogliare e/o una ridotta capacità di trasporto nel floema. Alcuni autori hanno ipotizzato che l'inibizione della fotosintesi del fusto possa indurre un esaurimento delle riserve di carboidrati con conseguente fallimento dei processi di riparazione dell'embolia. Mancano ancora tuttavia evidenze risolutive.

Considerando gli attuali scenari di cambiamento climatico, è stata condotta un'indagine approfondita sulle caratteristiche strutturali e funzionali dei cloroplasti nel fusto (sia a livello di corteccia che di legno) e sulla loro possibile relazione con la resistenza/resilienza degli alberi alla siccità. La conoscenza delle caratteristiche dei cloroplasti del fusto è ancora molto frammentata poiché sono specie-specifiche e dipendono sia dall'età che dalle caratteristiche del fusto, come lo spessore della corteccia.

In questa prospettiva, nella prima parte di questa Tesi (Capitolo I), ho focalizzato le mie attività di ricerca sulla specie scelta come modello: *Fraxinus ornus*, una pianta legnosa resistente alla siccità diffusa nell'area del Carso vicino a Trieste (Nord-est Italia), caratterizzata da corteccia e legno visivamente verdi. Ho compiuto un'analisi approfondita delle caratteristiche strutturali e funzionali dei cloroplasti di corteccia e legno di *F. ornus* rispetto alle caratteristiche dei cloroplasti fogliari (Studio 1). Ho quindi proposto un nuovo metodo per la misurazione del profilo radiale dell'ossigeno nei fusti legnosi, con cui ho fornito un'analisi dei tassi di ossigeno prodotti dai cloroplasti della corteccia e del legno in risposta alla presenza di luce (Studio 2). In questa sezione ho dimostrato che l'apparato fotosintetico dei cloroplasti del fusto presenta caratteristiche tipiche dell'acclimatazione ad ambienti scarsamente illuminati, con cloroplasti fotosinteticamente attivi e pienamente in grado di generare un trasporto di elettroni dipendente dalla luce. In quest'ottica, nella seconda parte di questa Tesi (Capitolo II), ho verificato un'indagine su quanto la fotosintesi del fusto è diffusa tra le specie legnose (sia Angiosperme che Gimnosperme) e ho analizzato la resa quantica massima del PSII (Fv/Fm) in diverse età del fusto (sia a livello della corteccia, che del legno). Nello Studio 3, ho classificato le specie in termini di relativa tolleranza alla siccità sulla base della loro vulnerabilità

all'embolia xilematica (P_{50}) e ho confrontato l'efficienza fotosintetica delle specie resistenti alla siccità con quelle sensibili alla siccità. Ho osservato che i valori di Fv/Fm diminuivano con l'aumentare dell'età del fusto ed erano generalmente più alti per le Angiosperme rispetto alle Gimnosperme. Il confronto tra specie resistenti alla siccità e sensibili alla siccità ha mostrato una chiara tendenza all'aumento dell'attività fotosintetica del fusto nelle specie che prosperano in habitat e biomi più aridi. In particolare, questo studio ha evidenziato il potenziale ruolo adattativo della fotosintesi del fusto nelle specie resistenti alla siccità.

L'obiettivo della terza parte della Tesi (Capitolo III) è stato quello di chiarire il ruolo della fotosintesi del fusto nella resistenza/resilienza degli alberi sottoposti a stress da siccità. In particolare, nello Studio 4 ho verificato come la fotosintesi del fusto potesse influenzare la resistenza all'embolia xilematica e la concentrazione degli NSC in relazione ad un esperimento di disidratazione-reidratazione in *F. ornus*. Allo stesso modo, lo scopo dello Studio corollario 5 è stato quello di verificare se la fotosintesi del fusto fosse coinvolta nel recupero idraulico e nella riduzione dello stress da siccità in *Laurus nobilis* e *Populus alba*, esposti a un ciclo di stress idrico e successivo recupero (reidratazione). Rispetto alle piante controllo con fusto esposto alla luce, l'inibizione della fotosintesi del fusto ha avuto esiti diversi durante la fase di reidratazione nelle tre specie studiate. Tuttavia, i risultati hanno mostrato che l'inibizione della fotosintesi del fusto ha aumentato la vulnerabilità idraulica delle piante durate lo stress idrico, limitando la capacità delle piante di mobilitare le riserve di NSC. Pertanto, questi risultati hanno suggerito che la fotosintesi del fusto è coinvolta nella produzione locale di NSC e ha un ruolo chiave nel mantenimento del funzionamento idraulico durante lo stress idrico.

Infine, con lo Studio corollario 6, si è voluto verificare se la fotosintesi del fusto potesse favorire l'assorbimento dell'acqua da parte della corteccia e il conseguente recupero dall'embolia nei segmenti di fusto immersi in acqua e illuminati. I risultati hanno smentito questa ipotesi poiché non è stato rilevato refilling di condotti embolizzati né negli steli di *Olea europaea* né in quelli di *F. ornus*, suggerendo che questo processo potrebbe essere altamente specie-specifico.

In conclusione, la fotosintesi del fusto è coerentemente ottimizzata alle condizioni micro-ambientali presenti a livello di corteccia e legno. Inoltre, potrebbe aver avuto un ruolo adattativo nelle specie resistenti alla siccità, che prosperano in condizioni di aridità. Infatti, la fotosintesi del fusto potrebbe essere un'importante fonte locale di NSC, fondamentale per migliorare la resistenza idraulica alla formazione di embolia e per sopportare la siccità quando si verificano una chiusura stomatica prolungata e la conseguente diminuzione della produzione di carbonio a livello fogliare.

Infine, ciò potrebbe implicare la dipendenza degli alberi legnosi dalla fotosintesi del fusto per la sopravvivenza, specialmente se si verificano frequenti periodi di siccità.

General introduction

Climate change and tree mortality

Ongoing climate change is predicted to increase the frequency and severity of drought (IPCC 2022). Indeed, one of the most alarming consequence of climate change is the increasing scarcity of water. Plant life, and as a consequence animal and human life, is critically threatened by water limitation. The increase in temperature co-occurring with increased duration/intensity/frequency of dry periods lead to higher vapor pressure deficit (VPD) and evaporation demand to the atmosphere, exacerbating drought-related damages to plants (e.g. see Williams et al. 2013). As a consequence, also plant mortality rates are predicted to rise (Allen et al. 2010; Nardini et al. 2013; Hember et al. 2017; Neumann et al. 2017).

Trees response to drought

Under drought stress, plants close stomata as a first response to limit water loss and prevent excessive tissue dehydration, embolism formation, and loss of hydraulic conductivity (Brodribb and Holbrook 2003; Bartlett et al. 2016; Choat et al. 2018). Under these environmental and physiological constraints, plants face a reduction of leaf-level photosynthetic carbon gain (Meinzer et al. 2009; Choat et al. 2012; Manzoni et al. 2013; Nardini et al. 2017), potentially leading to depletion of stored non-structural carbohydrates (NSC) to maintain primary and secondary metabolism (McDowell et al. 2022). Therefore, prolonged drought stress might lead to the exhaustion of NSC pools (McDowell et al. 2008; Adams et al. 2009). Most researchers agree that the decline of tree health due to drought is mainly linked to hydraulic failure and/or carbon starvation (McDowell et al. 2022), and commonly these two phenomena can co-occur together (Lloret et al. 2018; McDowell et al. 2011; McDowell et al. 2015). This happens because plant hydraulic and carbon dynamics are strictly related (Adams et al. 2009; McDowell 2011; Tomasella et al. 2020).

Tree resistance/resilience to drought stress

In order to predict how climate change, and in particular drought stress, will affect trees' life, it is crucial to identify and understand the physiological drivers inducing tree mortality and those that allow/help plants to withstand/cope with the detrimental effects of drought.

Drought can induce tree mortality mainly through three mechanisms: hydraulic failure, phloem transport failure, and carbon starvation.

- *Xylem embolism and hydraulic failure*: in a situation of water limitation, xylem tension can shift to a critical threshold, interrupting long-distance water transport. In this situation, gaseous bubbles might enter into the conduits ("air-seeding" hypothesis, Tyree and Zimmermann 2002) inducing embolism formation, thus reducing tree water transport efficiency. Under such a situation, xylem integrity might be compromised and hydraulic failure might occur (McDowell et al. 2008). Xylem vulnerability varies across species and biomes (Maherali et al. 2004; Choat et al. 2012), and to overcome the threat of drought, some woody species adjust their hydraulic characteristics to become more resistant to embolism or to recover the lost xylem functionality through embolism repair mechanisms after drought relief (Zwieniecki and Secchi 2015).
- *Phloem transport failure*: during drought stress, the lack of water might also induce a reduction in phloem turgor and/or an increase in phloem sap viscosity, ending in a phloem transport failure (Sevanto et al. 2014; Nardini et al. 2011). When phloem transport is impaired, carbohydrates are barely transported from source to sink and since during drought stress plants may need to mobilize reserves, this situation might promote carbon starvation and reduce overall plant metabolism. Furthermore, the transport of carbohydrates and/or their reallocation is fundamental to sustain the refilling of embolized xylem conduits, so that phloem failure can contribute to hydraulic failure (Sevanto et al. 2014; Nardini et al. 2018).
- *Carbon starvation*: as mentioned above, stomatal closure is an early response to drought stress, to control water loss and prevent excessive drop of water potential. In this way though, CO_2 uptake is limited and carbohydrate production is reduced. Hence, plants must account on their reserves, but when stored carbon is not sufficient to sustain cell turgor and metabolism, "carbon starvation" might occur (McDowell et al. 2008, 2011). Drought-tolerant species can maintain their stomata open for a longer time during drought and sustain a relatively higher transpiration rate, reducing the possibility to fall into carbon starvation (McDowell et al. 2011). Nevertheless, independently on plant water use strategy, since transpiration is intimately connected to air temperature and temperatures are predicted to rise, also drought-tolerant species will be forced to close stomata, especially during prolonged drought periods. In the initial period of drought, growth rates decline stronger than photosynthesis, inducing little increase or no changes in NSC content. On the contrary, during a prolonged period of drought, also photosynthesis rates decline with a consequent low carbon assimilation and thus, a theoretical decline in the NSC reserves (McDowell et al. 2011).

Stem photosynthesis

Leaves are the primary photosynthetic organs for most woody species and are generally assumed to be the major source of carbon assimilation. Nonetheless, a wide range of woody plants can carry out

photosynthesis even at the stem level (Pfanz and Aschan 2001), with a net photosynthetic rate of stems that can be up to 60% of those recorded for leaves (Ávila et al. 2014). Since these rates are also maintained during the dry season, when leaves close their stomata, reducing the leaf-level net carbon uptake, (Ávila-Lovera et al. 2017), stem photosynthesis appears as an extra source of carbon assimilation helping plants to face drought events. Indeed, since prolonged drought stress might provoke exhaustion of the carbohydrate pools (McDowell et al. 2008; Adams et al. 2009), an additional carbon gain at the stem level might represent a significant adaptive advantage for such species under drought.

It is now well known that stem photosynthesis comprises both net photosynthesis supplied by atmospheric CO_2 and recycling photosynthesis, which is associated with the re-fixation of internal CO_2 released by local cell respiration from the stem tissues (Teskey et al. 2008; Ávila et al. 2014), leading to some carbon recovery with minimal associated water losses. Indeed, some woody species possess functional stomata on the stem surface, that facilitate the carbon uptake from the atmosphere, thus allowing stem photosynthesis (Comstock and Ehleringer 1990; Nilsen 1995; Aschan and Pfanz 2003; Ávila et al. 2014). Furthermore, since respiratory CO_2 inside the stem reaches concentrations up to 1-26%, this can favor photosynthesis while minimizing photorespiration (e.g. Cernusak and Marshall 2000; Cernusak et al. 2001; Teskey et al. 2008). Stem photosynthesis can further prevent the risk of hypoxia due to local oxygen production (Pfanz et al. 2002; Wittmann and Pfanz 2014), and is involved in several processes, as bud development, stem growth and re-sprouting after biotic attack (Saveyn et al. 2010; Cernusak and Hutley 2011; Bloemen et al. 2013a,b; Steppe et al. 2015). Moreover, although it is not clear how the regulation of stem photosynthesis is achieved, it has been hypothesized its participation in the local supply of carbohydrates (Schmitz et al. 2012; Bloemen et al. 2016; De Baerdemaeker et al. 2017; Trifilò et al. 2021), facilitating the generation of osmotic gradients necessary for post-drought refilling of embolized vessels (Zwieniecki and Holbrook 2009; Nardini et al. 2011; Secchi and Zwieniecki 2011; Liu et al. 2019; Secchi et al. 2021).

The species-specific chloroplasts' distribution in the different stem compartments is related to several traits, e.g. chlorophyll/nitrogen content, the amount of light that penetrates through the stems (c. 20% in one-year-old stems, Damesin 2003; Pfanz and Aschan 2001) and to the bark structural features (e.g. colour/thickness) (Schmitz et al. 2012). Anyway, irradiance is considered one of the most important factors that can limit chloroplasts activity, since photosynthetically active radiation is necessary for the differentiation of active chloroplasts (van Cleve et al. 1993). Few studies have reported that usually the outer bark mainly absorbs blue-light (short wavelengths) whereas the wood and the pith are reached by the red- and far-red light (long wavelengths) (Kharouk et al. 1995; Solhaug et al. 1995; Pfanz and Aschan 2001; Sun et al. 2003; Wittmann and Pfanz 2016). Generally, the

amount of light transmitted through stems decreases as stems age increases and the bark grows thicker (Wiebe 1975; Aschan and Pfanz 2003; Saveyn et al. 2010). These differences in light quantity and quality, might induce modification on the structural and functional characteristics of stem chloroplasts. Therefore, the distribution of chloroplasts in the stems is highly species-specific and generally chloroplasts have been observed at bark, wood and pith level (e.g. see Pfanz and Aschan 2001; Dima et al. 2006; Berveiller et al. 2007; Burrows and Connor 2020). For these reasons, to date the knowledge of stem chloroplasts features is still largely fragmented. Recently, some studies have highlighted that the maximum quantum yield of PSII (Fv/Fm) of stem tissues, especially of bark chlorenchyma, might have values from 0.71 to 0.81, close to the maximum values measured for healthy leaves (Damesin 2003; Manetas 2004; Alessio et al. 2005; Manetas and Pfanz 2005; Tausz et al. 2005; Filippou et al. 2007).

Despite this knowledge, the interest of the scientific community on this topic is still relatively limited and this, coupled with a huge species-specific heterogeneity of stem photosynthesis, leads to largely fragmented and incomplete information on functional and structural features of stem chloroplasts.

For instance, one issue still unresolved regards the coordination between stem photosynthesis and hydraulics, since the actual relationship of stem photosynthetic efficiency with adaptation to drought has been only proposed. Indeed, only a few studies have highlighted that photosynthetic stems could have evolved more than once as an adaptation to life in tropical-dry and Mediterranean-like ecosystems (Ávila-Lovera and Garcillán 2020; Ávila-Lovera et al. 2020), and have suggested that stem photosynthesis contributes to the maintenance of hydraulic functioning [e.g. in mangroves (Schmitz et al. 2012), *Populus nigra* (De Baerdemaeker et al. 2017), *Salix matsudana* (Liu et al. 2019), *Populus deltoides* (Bloemen et al. 2016) and *Populus alba* (Trifilò et al. 2021)].

In particular, inhibition of stem photosynthesis can induce stems to shrink more drastically in response to severe drought stress, suggesting that sugars locally produced at stem level could potentially be involved in maintaining the turgor of wood parenchyma cells, which are supposed to assist xylem hydraulic functioning (Secchi et al. 2021; Tomasella et al. 2021; Kawai et al. 2022). Therefore, based on the above, stem photosynthesis might have an impact on hydraulic functioning under drought, or on recovery capacity after drought release. Nonetheless, the actual contribution of stem photosynthesis to the non-structural carbohydrates pool in the wood, and how this interacts with hydraulic responses during and after drought, are still under-investigated topics.

Eventually, understanding the functional role of bark and especially wood chloroplasts in embolism repair might help us to better understand these mechanisms and elucidate why chloroplasts are present also in deep tissues, such as pith, so far from incident light.

Aims

Due to the increase in the frequency and intensity of drought events, understanding the structural and functional characteristics of stem chloroplasts in comparison to those of the leaves is fundamental to understand if stem photosynthesis will provide an additional advantage to trees in terms of drought tolerance. As a final aim, deepening the knowledge on stem photosynthesis will allow to plan adequate management actions in several different sectors, e.g. utilization of species and selection of varieties more tolerant to drought in agro-forestry systems.

To this end, I have conducted a series of experimental studies on different tree species under controlled or field conditions, that are presented in this thesis.

In the first part (Chapter 1), I aimed at:

a) investigating the light spectra that can reach both bark and wood chloroplasts. Studying the distribution and the ultrastructure of stem chloroplasts. Assessing their functionality by applying spectroscopy techniques that until now have been applied only to leaf samples (Study 1);
b) quantifying the light-induced oxygen production at stem level and identifying the contribution of specific compartments (bark and wood). Testing and validating a new method to measure oxygen production *in vivo* through the stem radial profile (Study 2).

The second aim of this Thesis (Chapter 2) was to investigate how much stem photosynthesis is widespread across woody species (both Angiosperms and Gymnosperms) and to propose a new approach in exploring the possible association of stem photosynthetic efficiency with species-specific adaptation to drought. Specifically, I aimed at:

a) testing eventual differences in Fv/Fm between Angiosperms and Gymnosperms in both bark and wood, from stems of different age (Study 3);
b) ranking species in terms of relative drought tolerance on the basis of their vulnerability to xylem embolism (P_{50}), and comparing stem photosynthetic efficiency of drought tolerant vs drought sensitive species.

In the last chapter (Chapter 3), I finally tested the possible role of stem photosynthesis in drought stress responses. Specifically, I tested whether:

a) xylem vulnerability to drought stress was higher in plants with stem photosynthesis inhibited, and any potential consequence in carbohydrates production/dynamics (Study 4);
b) there was a different significance of stem photosynthesis between an evergreen vs deciduous species (corollary study – Study 5);
c) bark water uptake could help stems to recover from embolism (corollary study – Study 6).

References

IPCC. 2022. Climate Change 2022: Impacts, Adaptation, and Vulnerability. Contribution of Working Group II to the Sixth Assessment Report of the Intergovernmental Panel on Climate Change [H.-O. Pörtner, D.C. Roberts, M. Tignor, E.S. Poloczanska, K. Mintenbeck, A. Alegría, M. Craig, S. Langsdorf, S. Löschke, V. Möller, A. Okem, B. Rama (eds.)]. Cambridge University Press. Cambridge University Press, Cambridge, UK and New York, NY, USA, 3056 pp.

Adams HD, Guardiola–Claramonte M, Barron–Gafford GA, Villegas JC, Breshears DD, Zou CB, Troch PA, Huxman TE. 2009. Reply to Leuzinger et al.: drought-induced tree mortality temperature sensitivity requires pressing forward with best available science. *Proceedings of the National Academy of Sciences* **106:** E107.

Alessio GA, Pietrini F, Brilli F, Loreto F. 2005. Characteristics of CO_2 exchange between peach stems and the atmosphere. *Functional Plant Biology* **32:** 787-795.

Allen CD, Macalady AK., Chenchouni H, Bachelet D, McDowell N, Vennetier M, et al. 2010. A global overview of drought and heat-induced tree mortality reveals emerging climate change risks for forests. *Forest ecology and management* **259:** 660–684.

Aschan G, Pfanz H. 2003. Non-foliar photosynthesis–a strategy of additional carbon acquisition. *Flora-Morphology, Distribution, Functional Ecology of Plants* **198:** 81–97.

Ávila E, Herrera A, Tezara W. 2014. Contribution of stem CO_2 fixation to whole–plant carbon balance in nonsucculent species. *Photosynthetica* **52:** 3–15.

Ávila-Lovera E, Garcillán PP. 2020. Phylogenetic signal and climatic niche of stem photosynthesis in the mediterranean and desert regions of California and Baja California Peninsula. *American Journal of Botany* **108:** 334–345.

Ávila-Lovera E, Zerpa AJ, Santiago LS. 2017. Stem photosynthesis and hydraulics are coordinated in desert plant species. *New Phytologist* **216:** 1119–1129.

Ávila-Lovera E, Garcillán PP, Silva-Bejarano C, Santiago LS. 2020. Functional traits of leaves and photosynthetic stems of species from a sarcocaulescent scrub in the southern Baja California Peninsula. *American Journal of Botany* **107:** 1410–1422.

Bartlett MK, Klein T, Jansen S, Choat B, Sack L. 2016. The correlations and sequence of plant stomatal, hydraulic, and wilting responses to drought. *Proceedings of the National Academy of Sciences* **113:** 13098–13103.

Berveiller D, Kierzkowski D, Damesin C. 2007. Interspecific variability of stem photosynthesis among tree species. *Tree Physiology* **27:** 53–61.

Bloemen J, Overlaet-Michiels L, Steppe K. 2013. Understanding plant responses to drought: how important is woody tissue photosynthesis? *Acta Horticulturae* **991:** 149–157.

Bloemen J, McGuire MA, Aubrey DP, Teskey RO, Steppe K. 2013a. Internal recycling of respired CO_2 maybe important for plant functioning under changing climate regimes. *Plant Signaling & Behavior* **8:** e27530.

Bloemen J, Overlaet-Michiels L, Steppe K. 2013b. Understanding plant responses to drought: how important is woody tissue photosynthesis? *Acta Horticulturae* **991:** 149–157.

Bloemen J, Vergeynst LL, Overlaet-Michiels L, Steppe K. 2016. How important is woody tissue photosynthesis in poplar during drought stress?. *Trees* **30:** 63–72.

Brodribb TJ, Holbrook NM. 2003. Stomatal closure during leaf dehydration, correlation with other leaf physiological traits. *Plant Physiology* **132:** 2166–2173.

Burrows GE, Connor C. 2020. Chloroplast Distribution in the Stems of 23 Eucalypt Species. *Plants* **9:** 1814.

Cernusak LA, Marshall JD. 2000. Photosynthetic refixation in branches of western white pine. *Functional Ecology* **14:** 300–311.

Cernusak LA, Marshall JD, Comstock JP, Balster NJ. 2001. Carbon isotope discrimination in photosynthetic bark. *Oecologia* **128:** 24–35.

Cernusak LA, Hutley LB. 2011. Stable isotopes reveal the contribution of corticular photosynthesis to growth in branches of *Eucalyptus miniata*. *Plant physiology* **155:** 515–523.

Choat B, Jansen S, Brodribb TJ, Cochard H, Delzon S, Bhaskar R, et al. 2012. Global convergence in the vulnerability of forests to drought. *Nature* **491:** 752–755.

Choat B, Brodribb TJ, Brodersen CR, Duursma RA, López R, Medlyn BE. 2018. Triggers of tree mortality under drought. *Nature* **558:** 531–539.

Comstock J, Ehleringer J. 1990. Effect of variations in leaf size on morphology and photosynthetic rate of twigs. *Functional Ecology* **4:** 209–221.

Damesin C. 2003. Respiration and photosynthesis characteristics of current-year stems of *Fagus sylvatica*: from the seasonal pattern to an annual balance. *New Phytologist* **158:** 465–475.

De Baerdemaeker NJ, Salomón RL, De Roo L, Steppe K. 2017. Sugars from woody tissue photosynthesis reduce xylem vulnerability to cavitation. *New Phytologist* **216:** 720–727.

Filippou M, Fasseas C, Karabourniotis G. 2007. Photosynthetic characteristics of olive tree (*Olea europaea*) bark. *Tree physiology* **27:** 977–984.

Hember RA, Kurz WA, Coops NC. 2017. Relationships between individual-tree mortality and water-balance variables indicate positive trends in water stress-induced tree mortality across North America. *Global Change Biology* **23:** 1691–1710.

Kawai K, Minagi K, Nakamura T, Saiki ST, Yazaki K, Ishida A. 2022. Parenchyma underlies the interspecific variation of xylem hydraulics and carbon storage across 15 woody species on a subtropical island in Japan. *Tree Physiology* **42:** 337–350.

Kharouk VI, Middleton EM, Spencer SL, Rock BN, Williams DL. 1995. Aspen bark photosynthesis and its significance to remote sensing and carbon budget estimates in the boreal ecosystem. *Water, Air and Soil Pollution* **82:** 483–497.

Liu J, Gu L, Yu Y, Huang P, Wu Z, Zhang Q, Qian Y, Sun Z. 2019. Corticular photosynthesis drives bark water uptake to refill embolized vessels in dehydrated branches of *Salix matsudana*. *Plant, Cell & Environment* **42:** 2584–2596.

Lloret F, Sapes G, Rosas T, Galiano L, Saura-Mas S, Sala A, Martínez-Vilalta J. 2018. Non-structural carbohydrate dynamics associated with drought-induced die-off in woody species of a shrubland community. *Annals of botany* **121:** 1383–1396.

Maherali H, Pockman WT, Jackson RB. 2004. Adaptive variation in the vulnerability of woody plants to xylem cavitation. *Ecology* **85:** 2184–2199.

Manetas Y. 2004. Probing corticular photosynthesis through in vivo chlorophyll fluorescence measurements: evidence that high internal CO_2 levels suppress electron flow and increase the risk of photoinhibition. *Physiologia Plantarum* **120:** 509–517.

Manetas Y, Pfanz H. 2005. Spatial heterogeneity of light penetration through periderm and lenticels and concomitant patchy acclimation of corticular photosynthesis. *Trees* **19:** 409–414.

Manzoni S, Vico G, Katul G, Porporato A. 2013. Biological constraints on water transport in the soil-plant-atmosphere system. *Advances in Water Resources* **51:** 292–304.

McDowell N, Pockman WT, Allen CD. 2008. Mechanisms of plant survival and mortality during drought: why do some plants survive while others succumb to drought? *New Phytologist* **178:** 719–739.

McDowell NG. 2011. Mechanisms linking drought, hydraulics, carbon metabolism, and vegetation mortality. *Plant Physiology* **155:** 1051–1059.

McDowell NG, Beerling DJ, Breshears DD, Fisher RA, Raffa KF, Stitt M. 2011. The interdependence of mechanisms underlying climate-driven vegetation mortality. *Trends in Ecology & Evolution* **26:** 523–532.

McDowell NG, Coops NC, Beck PS, Chambers JQ, Gangodagamage C, Hicke JA, et al. 2015. Global satellite monitoring of climate-induced vegetation disturbances. *Trends in plant science* **20:** 114–123.

McDowell NG, Sapes G, Pivovaroff A, Adams HD, Allen CD, Anderegg WR, et al. 2022. Mechanisms of woody-plant mortality under rising drought, CO_2 and vapour pressure deficit. *Nature Reviews Earth & Environment* **3:** 294–308.

Meinzer FC, Johnson DM, Lachenbruch B, McCulloh KA, Woodruff DR. 2009. Xylem hydraulic safety margins in woody plants: coordination of stomatal control of xylem tension with hydraulic capacitance. *Functional Ecology* **23:** 922–930.

Nardini A, Lo Gullo MA, Salleo S. 2011. Refilling of embolized conduits: is it a matter of phloem unloading? *Plant Science* **180**: 604–611.

Nardini A, Battistuzzo M, Savi T. 2013. Shoot desiccation and hydraulic failure in temperate woody angiosperms during an extreme summer drought. *New Phytologist* **200:** 322–329.

Nardini A, Savi T, Trifilò P, Lo Gullo MA. 2018. Drought stress and the recovery from xylem embolism in woody plants. In Cánovas FM, Luettge U, Matyssek R, eds. *Progress in Botany*. Berlin, DE, Springer, 197–231.

Neumann M, Mues V, Moreno A, Hasenauer H, Seidl R. 2017. Climate variability drives recent tree mortality in Europe. *Global Change Biology* **23:** 4788–4797.

Nilsen ET. 1995. Stem photosynthesis: extent, patterns and role in plant carbon economy. In: Gartner B, eds. *Plant stems: physiology and functional morphology*. San Diego, CA, USA: Academic Press, 223–240.

Park Williams A, Allen CD, Macalady AK, Griffin D, Woodhouse CA, Meko DM, et al. 2013. Temperature as a potent driver of regional forest drought stress and tree mortality. *Nature climate change* **3:** 292–297.

Pfanz H, Aschan G. 2001. The existence of bark and stem photosynthesis in woody plants and its significance for the overall carbon gain. An eco-physiological and ecological approach. In: Essr K, Luttge U, Kadereit JW, Beyshlag W, eds. *Progress in Botany*, Berlin, DE: Springer-Verlag, 477–510.

Pfanz H, Aschan G, Langenfeld-Heyser R, Wittmann C, Loose M. 2002. Ecology and ecophysiology of tree stems: corticular and wood photosynthesis. *Naturwissenschaften* **89:** 147–162.

Saveyn A, Steppe K, Ubierna N, Dawson TE. 2010. Woody tissue photosynthesis and its contribution to trunk growth and bud development in young plants. *Plant, Cell & Environment* **33**: 1949–1958.

Schmitz N, Egerton JJG, Lovelock CE, Ball MC. 2012. Light-dependent maintenance of hydraulic function in mangrove branches: do xylary chloroplasts play a role in embolism repair? *New Phytologist* **195:** 40–46

Secchi F, Zwieniecki MA. 2011. Sensing embolism in xylem vessels: the role of sucrose as a trigger for refilling. *Plant, cell & environment* **34:** 514–524.

Secchi F, Pagliarani C, Cavalletto S, Petruzzellis F, Tonel G, Savi T, et al. 2021. Chemical inhibition of xylem cellular activity impedes the removal of drought-induced embolisms in poplar stems-new insights from micro-CT analysis. *New Phytologist* **229:** 820–830.

Sevanto S, Mcdowell NG, Dickman LT, Pangle R, Pockman WT. 2014. How do trees die? A test of the hydraulic failure and carbon starvation hypotheses. *Plant, cell & environment* **37:** 153–161.

Solhaug KA, Gauslaa Y, Haugen J. 1995. Adverse effects of epiphytic crustose lichens upon stem photosynthesis and chlorophyll of *Populus tremula* L. *Botanica Acta* **108:** 233–239.

Steppe K, Sterck F, Deslauriers A. 2015. Diel growth dynamics in tree stems: linking anatomy and ecophysiology. *Trends in Plant Science* **20:** 335–343.

Sun Q, Kiyotsugu Y, Mitsuo S, Hitoshi S. 2003. Vascular tissue in the stem and roots of woody plants can conduct light. *Journal of Experimental Botany* **54:** 1627–1635.

Tausz M, Warren CR, Adams MA. 2005. Is the bark of shining gum (*Eucalyptus nitens*) a sun or a shade leaf? *Trees* **19:** 415–421.

Teskey RO, Saveyn A, Steppe K, McGuire MA. 2008. Origin, fate and significance of CO_2 in tree stems. *New Phytologist* **177:** 17–32.

Tyree MT, Zimmermann MH. 2002. *Xylem structure and the ascent of sap*. 2nd Edn. Berlin, DE: Spriger Verlag.

Tomasella M, Petrussa E, Petruzzellis F, Nardini A, Casolo V. 2019. The possible role of non-structural carbohydrates in the regulation of tree hydraulics. *International journal of molecular sciences* **21:** 144.

Tomasella M, Casolo V, Natale S, Petruzzellis F, Kofler W, Beikircher B, Stefan Mayr, Nardini A. 2021. Shade-induced reduction of stem nonstructural carbohydrates increases xylem vulnerability to embolism and impedes hydraulic recovery in *Populus nigra*. *New Phytologist* **231:** 108–121.

Trifilò P, Natale S, Gargiulo S, Abate E, Casolo V, Nardini A. 2021. Stem photosynthesis affects hydraulic resilience in the deciduous *Populus alba* but not in the evergreen *Laurus nobilis*. *Water* **13:** 2911.

van Cleve B, Forreiter C, Sauter JJ, Apel K. 1993. Pith cells of poplar contain photosynthetically active chloroplasts. Planta **189:** 70–73.

Wiebe HH. 1975. Photosynthesis in wood. *Physiologia Plantarum* **33:** 245–246.

Wittmann C, Pfanz H. 2014. Bark and woody tissue photosynthesis: a means to avoid hypoxia or anoxia in developing stem tissues. *Functional Plant Biology* **41:** 940–953.

Wittmann C, Pfanz H. 2016. The optical, absorptive and chlorophyll fluorescence properties of young stems of five woody species. *Environmental and Experimental Botany* **121:** 83–93.

Zwieniecki MA, Holbrook NM. 2009. Confronting Maxwell's demon: biophysics of xylem embolism repair. *Trends in Plant Science* **14:** 530–534.

ZwienieckiMA, Secchi F. 2015. Threats to xylem hydraulic function of trees under 'new climate normal' conditions. *Plant, Cell & Environment* **38:** 1713–1724.

Chapter I

Study 1

Structure and function of bark and wood chloroplasts in a drought tolerant tree (*Fraxinus ornus* L.)

Sara Natale[1], Nicoletta La Rocca[2], Mariano Battistuzzi[2], Tomas Morosinotto[2], Andrea Nardini[1], Alessandro Alboresi[2]

[1] Department of Life Sciences, University of Trieste, Trieste, Italy

[2] Department of Biology, University of Padova, Padova, Italy

Manuscript resubmitted after a minor revision to Tree Physiology

Abstract

Leaves are the most important photosynthetic organs in most woody plants, but chloroplasts are found also in organs optimized for other functions. However, the actual photosynthetic efficiency of these chloroplasts is still unclear. We analysed bark and wood chloroplasts of *Fraxinus ornus* L. saplings. Optical and spectroscopic methods were applied to stem samples and compared to leaves. A sharp light gradient was detected along the stem radial direction, with blue light mainly absorbed by the outer bark, and far-red enriched light reaching the underlying xylem and pith. Chlorophylls were evident in the xylem rays and the pith and showed an increasing concentration gradient toward the bark. The stem photosynthetic apparatus showed features typical of acclimation to a low-light environment, like larger grana stacks, lower chlorophyll *a/b* and photosystem I/II ratios compared to leaves. Despite likely receiving very few photons, wood chloroplasts were photosynthetically active and fully capable of generating a light-dependent electron transport. Our data provide a comprehensive scenario of the functional features of bark and wood chloroplasts in a woody species and suggest that stem photosynthesis is coherently optimized to the prevailing micro-environmental conditions at the bark and wood level.

Keywords: bark, chlorophyll fluorescence, chloroplast ultrastructure, electron transport, stem photosynthesis, wood

Introduction

Leaves are the most important photosynthetic organs in most extant vascular plants, but early-diverging tracheophytes also relied on stems to assure a positive carbon gain (Nilsen 1995). Plants void of leaves and with photosynthetically active stems are widely spread in a diversity of ecosystems and families and comprise both herbaceous and woody species (Gibson 1983; Nilsen 1995; Teskey et al. 2008). These specialized plants are generally found in hot, dry, and high-irradiance environments, whereby the more favourable surface-to-volume ratio of stems allows sufficient CO_2 fixation while minimizing water loss to the atmosphere, compared to leaf-level photosynthesis (Gibson 1983; Nilsen 1995). The presence of photosynthetic stems has been documented also in several leaf-bearing species of tropical and temperate habitats, but their possible functional role and contribution to plant metabolism have never been fully elucidated (Nilsen and Sharifi 1997; Pfanz et al. 2002; Ávila et al. 2014).

Functional stomata are frequently observed on the stem surface of herbaceous species, and even of woody plants. These stomatal apertures apparently facilitate carbon uptake from the atmosphere, thus leading to stem-level net photosynthesis, generally indicated as "stem photosynthesis" (Comstock and Ehleringer 1990; Nilsen 1995; Aschan and Pfanz 2003; Ávila et al. 2014).

Stem photosynthesis comprises both net photosynthesis supplied by atmospheric CO_2 and recycling photosynthesis, which is involved in the re-fixation of internal CO_2 released by respiration from the surrounding heterotrophic stem tissues (Ávila et al. 2014), leading to some carbon recovery with minimal associated water losses. Because the bark limits gas exchange between wood and atmosphere, respiratory CO_2 accumulates inside the stem reaching concentrations up to 1-26%, thus providing sufficient substrate for photosynthetic activity while also limiting photorespiration (Cernusak and Marshall 2000; Cernusak et al. 2001; Teskey et al. 2008). Stem photosynthesis may have the additional advantage of maintaining sufficiently high O_2 concentration within the stems, thus preventing the risk of hypoxia (Pfanz et al. 2002; Wittmann and Pfanz 2014). Stem photosynthesis is known to be involved in several processes such as bud development, stem growth, re-sprouting after biotic attack, and local exudate synthesis (Saveyn et al. 2010; Cernusak and Hutley 2011; Bloemen et al. 2013 a,c; Steppe et al. 2015). Stem photosynthesis could be also involved in the local supply of energy and photosynthates for embolism repair (Schmitz et al. 2012; Bloemen et al. 2016; De Baerdemaeker et al. 2017; Trifilò et al. 2021). Hence, stem photosynthesis can be a source of sugars that facilitate the generation of osmotic gradients necessary for post-drought refilling of embolized vessels (Zwieniecki and Holbrook 2009; Nardini et al. 2011; Secchi and Zwieniecki 2011; Liu et al. 2019; Secchi et al. 2021).

Stem photosynthetic efficiency depends on chlorophyll content, nitrogen content, structural bark composition, and spatial distribution of chloroplasts (e.g. Wittmann et al. 2005; Wittmann and Pfanz 2007; Ávila et al. 2014). Environmental conditions such as light availability and temperature also play important roles. Light is necessary for the differentiation of active chloroplasts (van Cleve et al. 1993) so that species-specific differences in axial and radial light transmission through stems might drive the spatial distribution of chloroplasts in different tissues (Schmitz et al. 2012). Depending on bark structural features (e.g. colour or thickness), the light reaching the inner portions of stems varies also in quantity and quality. In general, shorter wavelengths are mainly absorbed in the outer bark whereas longer wavelengths penetrate better through the stem (Kharouk et al. 1995; Solhaug et al. 1995; Pfanz and Aschan 2001; Sun et al. 2003).

The amount of light transmitted through stems depends on species and stem age (Wiebe 1975; Aschan and Pfanz 2003; Wittmann and Pfanz 2016). Light transmission and CO_2 fixation usually decrease as stems age and the bark grows thicker (Saveyn et al. 2010). Gradients of light quantity and quality across stems may lead to modifications in relative chlorophyll concentration, chloroplast ultrastructure and photosynthetic efficiency. To date, due to the huge species-specific heterogeneity and the relatively low research efforts on this topic, the information the on functional features of stem chloroplasts is still largely fragmented. Recent studies have shown that in some species, the maximum quantum yield of PSII (Fv/Fm) of stem tissues, especially of bark chlorenchyma, has values from 0.71 to 0.81, close to the maximum values recorded for healthy leaves (Damesin 2003; Manetas 2004; Alessio et al. 2005; Manetas and Pfanz 2005; Tausz et al. 2005; Filippou et al. 2007).

Despite this knowledge, it is not clear how the regulation of stem photosynthesis is achieved, and if the photosynthetic efficiency of stem chloroplasts is comparable to that of leaf ones.

Based on the above, refixation of CO_2 by wood photosynthesis might have an important metabolic role (e.g. crucial role in the local production of carbohydrates), while corticular photosynthesis may also fix CO_2 directly transported from the atmosphere through stomata and/or lenticels (Wittmann et al. 2001; Pfanz et al. 2002; Damesin 2003; Alessio et al. 2005; Berveiller et al. 2007; Teskey et al. 2008; Ávila et al. 2014; Vandegehuchte et al. 2015). Thus, according to present knowledge, both bark and wood photosynthesis can contribute to the overall plant carbon economy, but their physiological relevance and the quantitative contribution of stem photosynthesis to the carbon balance of a tree are still unclear (Pfanz 2008; Teskey et al. 2008; Saveyn et al. 2010; Bloemen et al. 2013b; Bloemen et al. 2016).

To gain advanced knowledge on the structure and function of stem chloroplasts, we investigated the ultrastructural, biophysical, biochemical and physiological features of bark and wood chloroplasts in current-year and one-year-old stems of *Fraxinus ornus* L., a thermophilous, sun-adapted and drought-

tolerant deciduous tree (Nardini et al. 2003; Gortan et al. 2009; Nardini et al. 2021). We specifically aimed at (1) characterizing light transmission through stems, (2) identifying radial gradients of chloroplasts distribution, (3) describing in detail the ultrastructure, functionality, and efficiency of stem chloroplasts, compared to chloroplasts found in leaves. We hypothesized that chloroplasts display different characteristics and functionality, depending on the stem region where they are located.

Material and Methods

Plant material

In this study, we have applied to stems several methodologies so far applied only on leaf samples. Therefore, before starting our experiments measures, we conducted a preliminary analysis to test for the reliability of such methods when used on bark and wood samples. To avoid differences in terms of acclimation to specific growing conditions, all data presented were collected in July 2021 on three-year-old saplings of *Fraxinus ornus* L. (*F. ornus*). In March 2021, 15 saplings provided by a public nursery (Vivai Pascul, Regional Forestry Service FVG, Tarcento, Italy) were transplanted in 3.5 L pots in a greenhouse at the University of Trieste, Italy. Plants were regularly irrigated at field capacity and their position in the greenhouse was randomly shifted weekly, to assure exposure to uniform light conditions. A slow-release fertilizer (Flortis, universal fertilizer, Orvital, Milano, Italy) was added to each pot in April (4 g) and May (3 g) to prevent nutritional deficiency. Before each measurement (see below) the plants were collected from the greenhouse and moved to the laboratory, and when necessary acclimatized to dark conditions. Analyses were performed on fresh samples of leaves, as well as on stem samples. Specifically, 1-2 cm long stem segments were cut, and bark and wood were carefully separated both for the current year (B_{cy} and W_{cy} respectively), and for one-year-old stems (B_{1y} and W_{1y} respectively).

For each measure described below, we sampled the stem segments always from the same plant region (i.e. in the apical end of each growth year investigated, about 1 cm below the corresponding apex/node).

Radial light transmission in stems

To characterize light conditions experienced by stem chloroplasts as compared to leaf ones, we initially measured the light transmission spectra through leaves as well as through bark and wood. Measurements were performed when stem cambial cells were active, favouring stem girdling.

Accordingly, we separated the bark and wood from a 2 cm long stem segment to measure the light transmitted from these two stem regions.

The custom-made apparatus used for detecting light transmission in plant samples is illustrated in Fig. S1. A light source (KL 2500, Schott, Wolverhampton, UK) providing a photosynthetic photon flux density (PPFD) of 495 μmol m^{-2} s^{-1} was used to illuminate perpendicularly a sample held in place on a wooden stand, at a distance of 20 cm. The stand was covered on the front with a sheet of black plastic to reduce light scattering. A central hole was drilled in the stand and the sample was placed on it to completely cover the hole. A high-resolution fibre-optic connected to a spectrometer (Flame, Ocean Optics) was then placed behind the stand and carefully inserted in the hole of the stand, to measure only the light emitted from the light source and then transmitted through the sample to the fibre. The entire system was placed in a dark room for measurements. Before sample measurements, blank and dark readings were recorded at an integration time (i.t) of 110 ms. Blank corresponds to the lamp light spectrum measured by spectrometer without any sample, while dark corresponds to the "dark spectrum", i.e. the spectrum measured with the lamp switched off and with no sample. Measurements were performed on samples obtained from three different saplings, from 400 to 800 nm, at an integration time of 110 ms. All measurements (blank, dark, and samples) were repeated 10 times, and the final light transmission spectra were obtained by averaging results. Data were smoothed to eliminate the background instrument error through Origin 9.0 software (Northampton, MA, USA).

Pigment analysis

Since both bark and wood were apparently green (Fig. S2), we quantified the pigment contents of these tissues and of leaves upon extraction of fresh material in *N,N'*-dimethylformamide (DMF). Leaves were cut into small pieces to facilitate the extraction, and 50 mg of sample were placed in a 2 mL Eppendorf filled up with 0,5 mL of DMF. The same procedure was applied to bark and wood. For the extraction, 50 mg of bark in 0,5 mL of DMF and 200 mg of wood in 0,75 mL of DMF were used. From each sample, the same amount of fresh material (i.e. 50 mg for leaves and bark, 200 mg for wood) was dried in an oven at 60 °C for 48 h to determine the corresponding dry weight (DW). Samples were kept in the dark at 4°C for at least 48 h to ensure complete extraction of the pigments and then centrifuged for 3 min at 10000 rpm. Absorption spectra were recorded (Cary 300 UV-Vis, Agilent) between 350 and 750 nm. Pure DMF was used as blank. The final pigment concentration was assessed using Wellburn equations (Wellburn 1994). The pigment analysis was performed on samples obtained from four different saplings.

Epifluorescence and transmission electron microscopy

To investigate chlorophyll distribution along the stem transverse section and to define the chloroplasts structure, fluorescence and electron microscopy analyses were carried out. Light and fluorescent light microscopy analyses were made using a 5000 Leica (Leica, Wetzlar, Germany) microscope, equipped with a digital image acquisition system. A light microscope was used to visualize and describe the various tissues of the stem. Chlorophyll localization was obtained by excitation with UV light. Leaf and stem 40 µm thick transverse sections were obtained from fresh material with a sliding microtome. Three to five sections per sample were made and analysed, and observations were repeated for two different saplings, as well as for the following analyses.

For transmission electron microscopy (TEM), fresh samples of leaf, bark and wood were rapidly cut into 2 mm^3 blocks and fixed overnight at 4°C in 6% glutaraldehyde in 0.1 M sodium cacodylate buffer, with a pH 6.9, and then fixed for 2 h in 1 % osmium tetroxide in the same buffer. The samples were dehydrated in a graded series of ethanol and propylene oxide and finally embedded in Araldite. Ultrathin sections (80-100 nm) were prepared with an ultramicrotome (Ultracut; Reichert-Jung, Vienna, Austria) and treated with lead citrate and uranyl acetate. Samples were analysed with a transmission electron microscope (Tecnai G2; FEI, Hillsboro, Oregon) operating at 100 kV. We analysed images (n=8-15 images per each tissue) with ImageJ to obtain data on grana number, starch number and stromal area, following Mazur et al. (2021).

Fluorescence spectroscopy

To quantify the relative fluorescence intensities emitted from PSI (F735 nm) and PSII (F685 and F695 nm), we characterized the low-temperature (77K) chlorophyll fluorescence emission spectra of leaves, bark and wood. The 685 nm and 695 nm fluorescence emission components originate from the antenna complex and reaction center of PSII subunits CP43 and CP47, respectively (Krause and Weis 1991; Govindjee 1995; Andrizhiyevskaya et al. 2005; Lamb et al. 2015). The fluorescence emission band at 735 nm is instead due to PSI and its associated light-harvesting complex I (LHCI) (Breton 1982; Govindjee 1995; Krause and Weis 1991; Morosinotto et al. 2003; Dobrev et al. 2016; Lamb et al. 2018; Dymova et al. 2018). Therefore, these LT fluorescence spectra give information on the relative composition of photosynthetic apparatus. Specifically, the F735/695 ratio provides a reliable estimate of the distribution of excitation energy to each of the photosystems and/or their relative abundance within the thylakoid membranes (Krause and Weis 1984).

Fresh material (i.e. 50 mg for leaves and bark, 200 mg for wood) was rapidly cut into small pieces and finely ground with liquid nitrogen in a mortar. The material was then quickly transferred in a 2 mL Eppendorf with 0.5 mL of 60% w/v glycerol, 10 mM Hepes, pH 7.5. Each sample was set up for

the measurements in a glass Pasteur pipette and put in a Dewar vessel filled with liquid nitrogen. Low-temperature (77 K) emission spectra measurements were performed through a fluorimeter (Varian Cary Eclipse, Agilent, USA), exciting samples at 440 nm (excitation and emission slits were set to 2.5 nm) and recording the emission spectra from 600 to 800 nm. Data for W_{1y} were smoothed to eliminate the background instrument error through Origin 9.0 software (Northampton, MA, USA).

SDS-PAGE electrophoresis and Western blot analysis

Western blot analyses were performed to evaluate the composition of the photosynthetic apparatus of bark and wood compared to the leaves. Total protein extracts were obtained from fresh material *(*i.e. 50 mg for leaves, 110-130 mg for bark, 200-300 mg for wood) finely ground with liquid nitrogen in a mortar. The material was then quickly put in a 2 mL Eppendorf with 0,5 mL of sample buffer (SB) 3× (125 mM TRIS pH 6.8, 100 mM DTT, 9% (w/v) SDS, and 30% (w/v) glycerol) for leaves and bark and 700 µL SB3× for wood. The protein concentration of extracts was quantified using the BCA protein assay, and samples were loaded accordingly to the quantification (1× samples corresponding to 10 mg/µL) in an acrylamide gel at a final concentration of 12%. Western blot analysis was performed by transferring the protein to nitrocellulose (Bio Trace, Pall Corporation, Auckland, New Zealand). The membranes were hybridized with specific primary antibodies: anti-PsaA (Agrisera, catalogue number AS06172), custom-made anti-D2, anti-PsbS (Storti et al. 2019); custom-made anti-Rubisco, anti-LHCII, anti-CP47 were also used. After hybridization, signals were detected with an alkaline phosphatase-conjugated antibody (Sigma Aldrich). Measurements were repeated for three different saplings.

In vivo imaging fluorescence measurements

Photosynthetic efficiency of leaves, bark and wood was estimated by *in vivo* chlorophyll fluorescence measurements, using a closed-imaging PAM chlorophyll fluorometer (Photon Systems Instruments, Brno, Czech Republic).

Saplings were dark-acclimated for at least 1 hour before measurements. Leaf and stem segments approximately 1 cm long were sampled from 4 different saplings. Bark and wood were separated, and wood segments were sectioned both longitudinally and radially. Samples were placed in a petri dish resting on damp paper and were maintained hydrated by covering them with a thin layer of distilled water. The petri dish was then placed in the closed-imaging PAM chlorophyll FluorCam to obtain chlorophyll fluorescence images.

The optimal quantum yield of PSII (Fv/Fm) was measured for the different areas of internal stem tissues (Maxwell and Johnson 2000).

Spectroscopy measurements

In vivo spectroscopic analysis was performed to gain insights into the regulation of electron flow via absorbance changes. The measurements were performed at room temperature with a JTS-10 spectrophotometer (Bio-Logic, France) on fresh samples of leaf, bark and wood collected from the same sapling, and repeated for five different saplings. The plants were dark-acclimated for 1 hour before measurements. We separated bark and wood from a 1 cm long stem segment. For the wood, we prepared longitudinal thin sections to place on the sample holder. The samples were kept hydrated by wrapping them in a transparent cellulose filter.

We assessed the photosynthetic activity by monitoring the electrochemical gradient across thylakoid membranes as generated during photosynthesis, using the electrochromic shift (ECS) (Witt 1979; Bailleul et al. 2010; Allorent et al. 2015; Allorent et al. 2018). Such a signal is in fact modified when light drives an electron transport and thus the generation of an electrochemical gradient. An evaluation of functional photosynthetic complexes and electron transport rates (ETR) was done by measuring the electrochromic shift (ECS), according to the protocol described by Bailleul et al. (2010) and Mellon et al. (2021). The ECS signal provides accurate data on the function of the photosynthetic complexes (Bailleul et al. 2010), and photosystem charge separation can be evaluated by DIRK (dark-induced relaxation kinetic (Sacksteder and Kramer 2000)). ETR was obtained by subtracting the slope of ECS during the dark (SD) from the slope in the light (SL) and normalized to the total PSs content (PSI + PSII). To remove the contribution of scattering and cytochromes, the background signal at 546 nm was subtracted from the 520 nm signal. Functional total photosystems (PSs) were quantified using a single flash turnover emitted by a xenon lamp (Gerotto et al. 2016).

P700 concentration was measured at 705 nm using an extinction calculated from Ke (1972). Samples were illuminated with continuous red (630 nm) light, which was transiently switched off to measure P700 absorption changes at 705 nm. Each measurement was repeated on 3-8 different saplings.

Statistics

All statistical analyses were performed with R software (R Core Team 2021). The normality of residuals and homogeneity of variances were tested, and when these assumptions were not violated one-way ANOVA analysis through “aov” function in “stats” R package was used. For significance tests, *Post-hoc* Tukey's Honestly Significant Difference test (Tukey HSD) was performed through “Tukey HSD” function in “stats” R package.

When the homogeneity of variances assumption was violated, generalized least square (GLS) models were performed, using “gls” function including the ‘varPower’ variance structure. Pigments data were log-transformed to respect the assumption of normality, before performing GLS model. Differences

between groups were tested post hoc with “Holm” contrasts using the *emmeans* function (*emmeans* package).

Results

Light transmission in stems

Measurements of light transmission through the bark (B_{cy} and B_{1y}) and wood (W_{cy} and W_{1y}) of different ages and through leaves revealed a progressive modification of light quantity and quality (Fig. 1; S3). The transmission spectra of B_{cy} and B_{1y} were very similar to that of the leaf. All these spectra showed a peak at 550 nm and suggested a maximum light absorption between 400-500 and 600-700 nm, as expected from chlorophyll-containing samples. W_{cy} and W_{1y} also showed decreases in transmission at 400-500 and 600-700 nm associated with chlorophyll absorption. They also showed a significant contribution at all wavelengths associated with scattering. The analysis of non-normalized spectra (Fig. S3) clearly shows that while light can penetrate both bark and wood, its transmission is attenuated going from leaves to bark to wood. Photons were better transmitted through the xylem to the pith in the younger stem, compared to the one-year-old one. Moreover, blue and red light was highly absorbed in the bark, while green- and far-red light penetrated much better toward the xylem parenchyma. The observed transmission spectra suggested a change in light quantity and quality from the outermost towards the innermost portions of the stem. This indicated that the inner stem compartments are reached by limited light intensity, also with an altered spectrum.

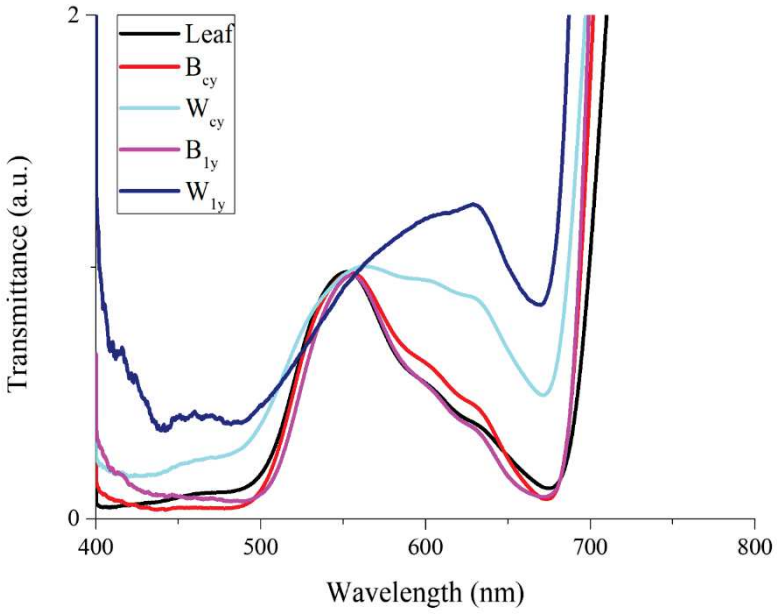

Fig. 1 Light transmission spectra of leaf, bark and wood of current (B_{cy} and W_{cy}) and one-year-old stems (B_{1y} and W_{1y}) of *Fraxinus ornus* L. Data normalized at 550 nm (arbitrary units). Each measurement was replicated 10 times and the average value was calculated. Spectra were corrected for dark pixels.

Bark and wood chloroplasts of Fraxinus ornus saplings acclimate to light conditions

Chlorophylls and carotenoids were detected throughout the stem, both in the bark and in the wood. In both compartments, chlorophyll (Chl) content was lower compared to leaves. However, the Chl content of bark was higher than that of wood (Tab. 1). The pigment concentration in the bark decreased with increasing stem age. This was also coupled to a qualitative change, with a relatively larger decrease of chlorophyll *a* (Chl*a*) as compared to chlorophyll *b* (Chl*b*) (Tab. 1).

Sample	**Chl*a*** (mg g^{-1} FW)	**Chl*b*** (mg g^{-1} FW)	**Total Chl** (mg g^{-1} FW)	**Car** (mg g^{-1} FW)
Leaf	2.589±0.801 a	0.949±0.336 a	3.538±1.136 a	0.514±0.139 a
B_{cy}	0.409±0.136 b	0.165±0.061 b	0.574±0.196 b	0.076±0.024 b
B_{1y}	0.293±0.076 b	0.126±0.040 b	0.419±0.117 b	0.060±0.015 b
W_{cy}	0.018±0.009 c	0.008±0.004 c	0.026±0.012 c	0.004±0.001 c
W_{1y}	0.018±0.005 c	0.009±0.002 c	0.027±0.007 c	0.005±0.001 c

Tab. 1 Chlorophyll *a* (Chl*a*), chlorophyll *b* (Chl*b*), total Chl (Chl*a*+Chl*b*) and carotenoid (Car) concentration for leaf, bark and wood of current (B_{cy} and W_{cy}) and one-year-old stems (B_{1y} and W_{1y}) of *Fraxinus ornus* L. Mean values are reported ± S.D. (n = 4). Different letters indicate significant differences between samples ($P < 0.05$).

Therefore, the Chl*a*/*b* ratio of the leaf was similar to that of B_{cy}, while it decreased progressively in B_{1y}, W_{cy} and W_{1y} (Fig. 2A). Chl*a*/*b* of W_{cy} and W_{1y} was significantly lower compared to leaf and B_{cy} ($P < 0.0005$ and $P < 0.05$ respectively, Fig. 2A). Carotenoid (Car) / Chl ratios were similar in leaves, B_{cy} and B_{1y}, with a slight relative increase in W_{1y} and W_{cy} (Fig. 2B).

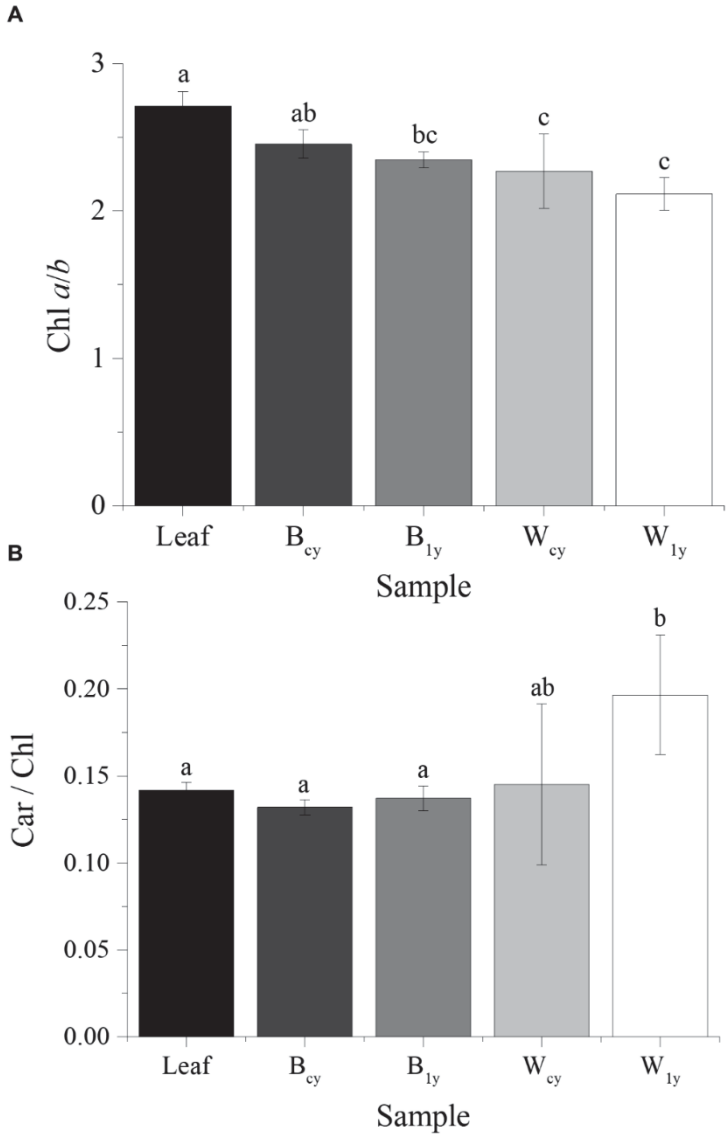

Fig. 2 Mean chlorophyll *a*/*b* (Chl*a*/*b*) (A), carotenoids/total chlorophyll (Car/Chl) (B) comparison between leaf, bark and wood of current (B_{cy} and W_{cy}) and one-year-old stems (B_{1y} and W_{1y}) of *Fraxinus ornus* L. Standard deviation bars are included on each of the bar graphs (n = 4). Different letters indicate significant differences between samples ($P < 0.05$).

The Chl distribution and ultrastructural features of chloroplasts were further investigated for leaves, B_{cy}, W_{cy}, B_{1y} and W_{1y}, by epifluorescence and transmission electron microscopy (EM). A detailed anatomical transverse section is presented in Fig. S4, showing the different tissues composing the bark, i.e. phelloderm, cortex and phloem (Angyalossy et al. 2016).

Analyses showed that the majority of stem Chl was present in the bark mainly in the parenchyma cells of phelloderm, cortex and phloem, but chlorophyllous cells were detected also along xylem rays and around the pith (Fig. 3). At higher magnification, plastids are visible as chlorophyll autofluorescence in red whereas the green colour is given by lignified or suberified components. EM analysis defined the ultrastructure of stem chloroplasts that showed intact and well-defined organization (Fig. 4 and Fig. S5). Fig. S5 reports images acquired at lower magnification, useful to visualize the general features of the different tissues. Fig. 4 shows images at higher magnification to better appreciate the different characteristics of the chloroplast ultrastructure and thylakoid distribution.

The phelloderm cells contained well-developed chloroplasts, with both stroma lamellae and grana stacks resembling those of leaves (Fig. 4B, D, Tab. S1). Chloroplasts found towards the cortex and the phloem presented a significantly lower number of grana, with a higher number of stacks (Tab. S1). A significant reduction of the stromal area was observed from bark to wood, specifically between chloroplasts found in the phelloderm/cortex and those in the wood of both growth years (Tab. S1). A similar starch amount was found in the chloroplasts of different samples.

Due to the hardness of the material, the image quality did not allow us to make accurate measurements of the number of stromal thylakoids, and we can only draw some conclusions from a visual/descriptive analysis of the images. In particular, chloroplasts found in the wood of each growth year apparently, have very few stromal thylakoids (Fig. 4S; S5E, F).

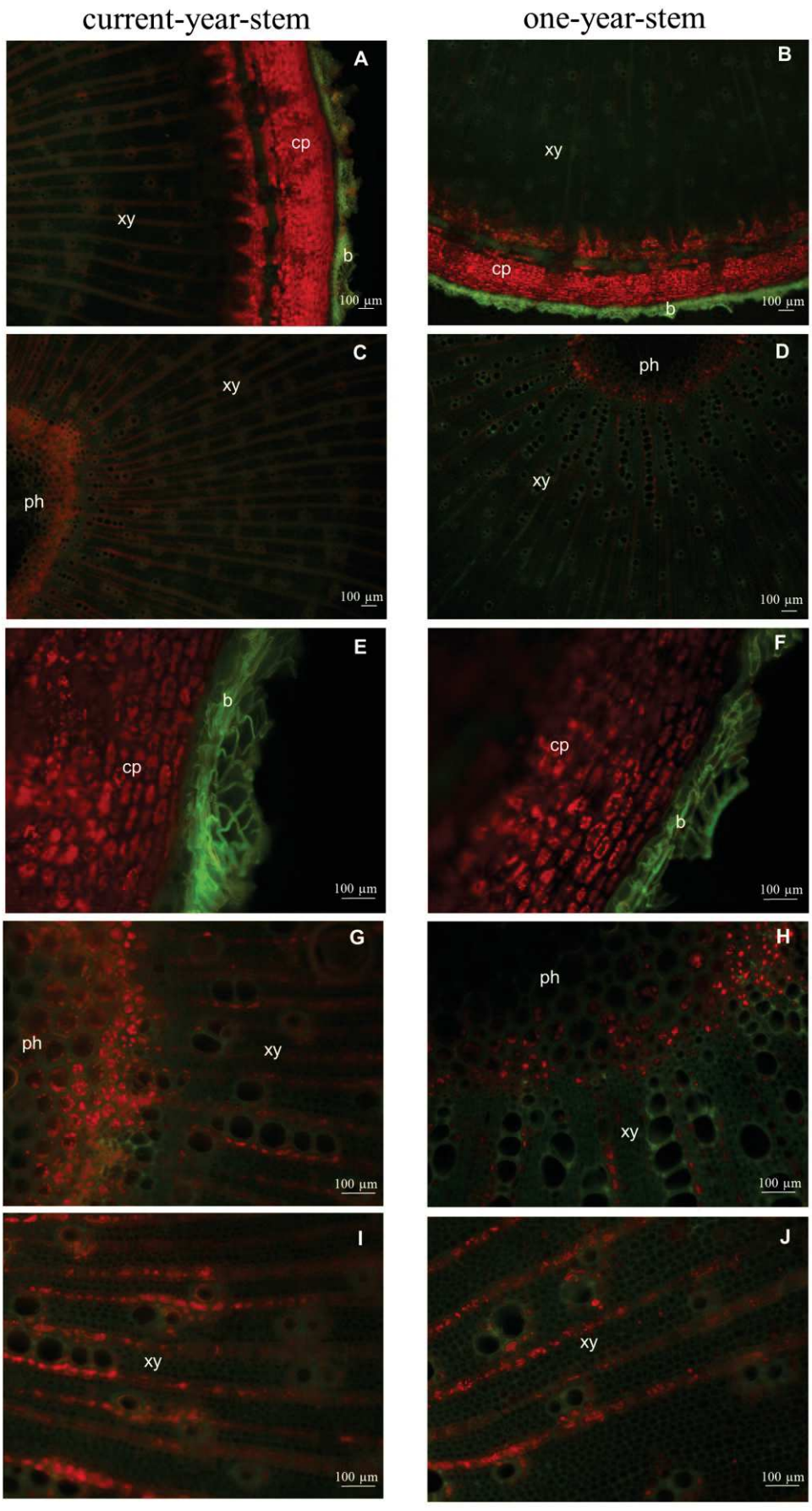
current-year-stem
one-year-stem
A
cp
xy
b
100 µm
B
xy
cp
b
100 µm
C
xy
ph
100 µm
D
ph
xy
100 µm
E
b
cp
100 µm
F
cp
b
100 µm
G
ph
xy
100 µm
H
ph
xy
100 µm
I
xy
100 µm
J
xy
100 µm

Fig. 3 Representative transverse-section images of current year and one-year-old stems of *Fraxinus ornus* L. observed by epifluorescence microscopy. The red color is given by chlorophyll fluorescence when excited by UV light; the green colour is given by lignified or suberified components. Periderm of current (A, E) and one-year-old stems (B, F). Xylem rays and pith of current (C, G, I) and one-year-old stems (D, H, J). Abbreviations: b, phellem; cp, cortical parenchyma; xy, xylem and ph, pith.

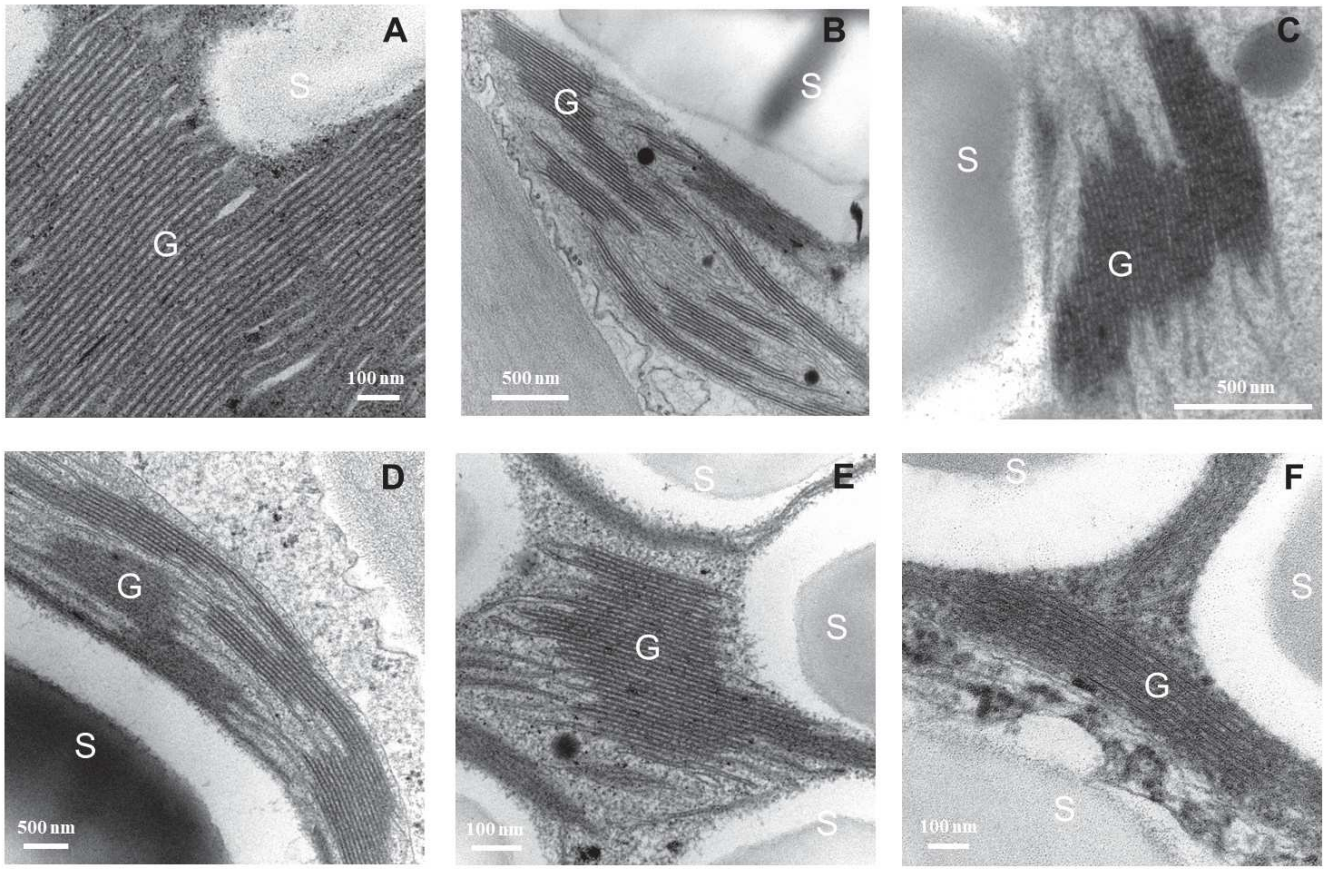

Fig. 4 Representative electron micrographs of chloroplast thylakoids of different stem samples of *Fraxinus ornus* L. (A) Leaf; (B) Periderm of current year stems; (C) Xylem rays of wood of current year stems; (D) Cortical parenchyma of one-year-old stems; (E) Phloem of one-year-old stems; (F) Xylem rays of one-year-old stems. Abbreviations: G, grana thylakoids; S, starch.

Changes of composition of photosynthetic apparatus in different tissues

Upon excitation at 440 nm, the low-temperature (LT, 77K) fluorescence emission spectra of leaves, bark and wood of current and one-year-old stems showed three major emission bands (685 nm, 695 nm, 735 nm) (Fig. 5A).

As shown in Fig. 5A, there is a significant decrease in the relative intensity of fluorescence from the PSI and LHCI complexes (at 735 nm) in B_{cy} and B_{1y}. This trend is further amplified in W_{cy} and W_{1y}. In accordance, the F735/F685 ratio (Fig. 5B) gradually decreased from bark to wood. Such a lower value of the ratio for bark and wood compared to leaf suggests a reduced content of PSI complexes relative to PSII.

The F685/F695 ratio (Fig. 5C) of B_{cy} and B_{1y} was similar to that of both leaf and wood. Compared to the leaves, the values were significantly higher for both W_{cy} and W_{1y}. The alteration in the F685/F695 ratio might be attributed to a relative increase in the fluorescence emitted by the antenna system of PSII with respect to the reaction center.

Photosynthetic apparatus composition was also investigated using specific antibodies. An equal protein amount was loaded for each sample (Fig. 6). As expected, samples that accumulated less Chl, also showed a lower abundance of photosynthetic proteins. Nevertheless, western blot analysis allowed the detection of LHCII protein in all samples investigated, confirming their presence even in wood.

RuBisCO was also detected in all samples i.e. leaf, bark and wood, with a signal progressively lower and particularly weak in the latter. PSAD was detected in leaf and B_{cy}, whereas only a faint band was detected in B_{1y}. No PSAD signal was detected for the wood. The band of D2 proteins was detected only in the leaf and weakly in B_{cy}.

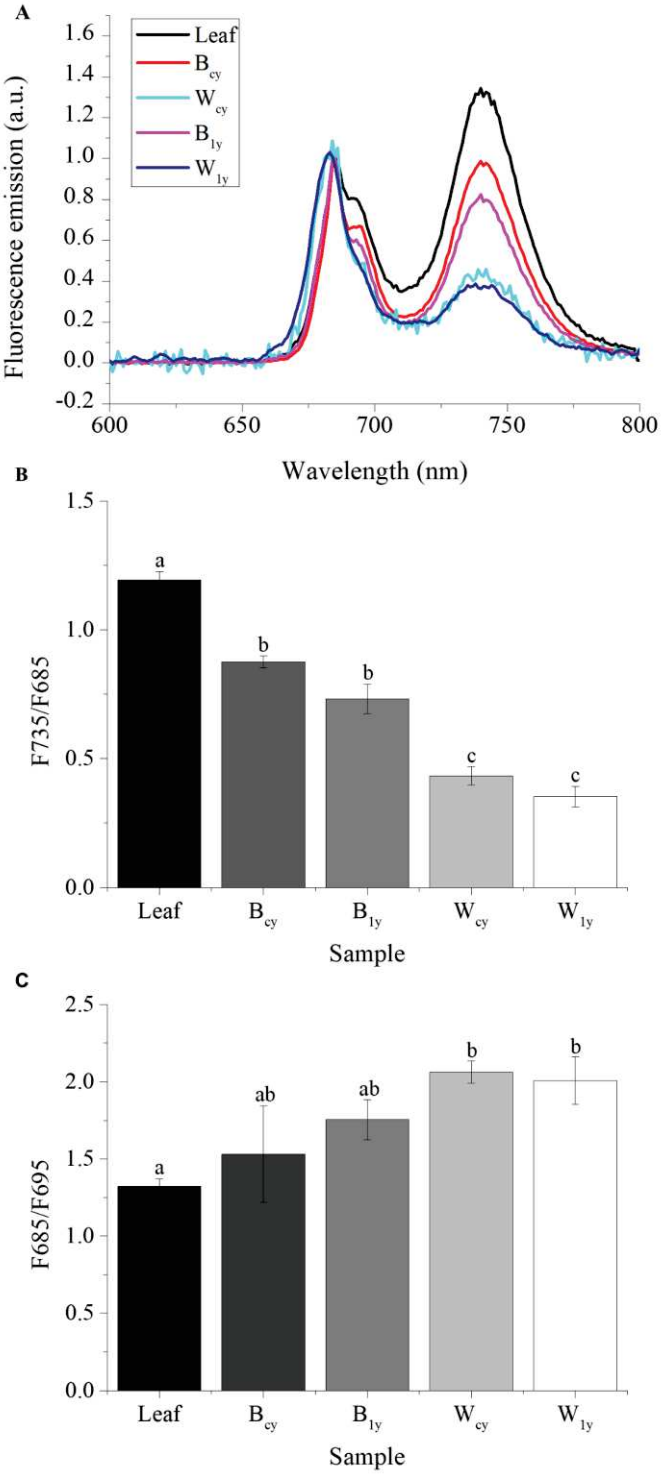

Fig. 5 (A) 77K fluorescence emission spectra of leaf, bark and wood of current (B_{cy} and W_{cy}) and one-year-old stems (B_{1y} and W_{1y}) stems of *Fraxinus ornus* L. Spectra are normalized on PSII emission (685 nm). Excitation wavelength was 440 nm. (B) Fluorescence ratio F735/F685 and (C) F685/F695 for leaf, bark and wood of current (B_{cy} and W_{cy}) and one-year-old stems (B_{1y} and W_{1y}). Mean values are reported ± S.D. (n = 2). Different letters indicate significant differences between samples ($P < 0.05$).

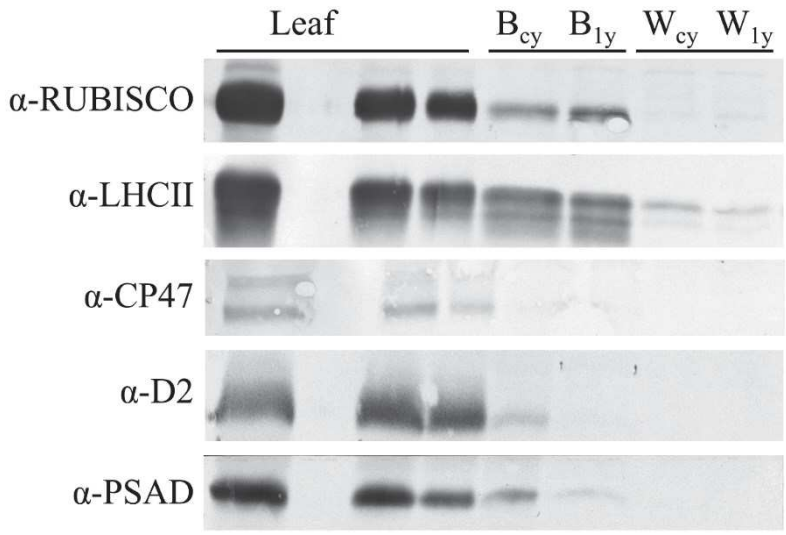

Fig. 6 Immunoblot analysis of leaf, bark and wood of current year (B_{cy} and W_{cy}) and one-year-old stems (B_{1y} and W_{1y}) of *Fraxinus ornus* L., using antibodies against different components of the photosynthetic apparatus from Rubisco, antenna complexes (LHCII, CP47), PSII (D2) and PSI (PSAD). Different dilutions of total protein extracts were loaded. The first column of Leaf, B_{cy}, B_{1y}, W_{cy} and W_{1y} were loaded with 1×, which corresponds to 10 mg/μL of total proteins. The second and third columns of leaf have 0.2× and 0.5× (Rubisco, LHCII), 0.25× and 0.13× (CP47), 0.33× and 0.16× (D2, PSAD) respectively.

The stem contains photosynthetically active cells

Chlorophyll fluorescence imaging (Fig. 7A) across longitudinal sections of current- and one-year-old stems detected significant signals, consistent with all the above results. Analysis of maximal PSII photochemical efficiency (Fv/Fm) showed that leaf, B_{cy}, W_{cy}, B_{1y} and W_{1y} have no statistically significant different activities (Fig. 7B). This means that even in wood PSII displays a maximum potential quantum efficiency resembling the one of leaves.

Despite the non-ideal optical features of the samples and the presence of a strong scattering, we were able to detect for the first time an ECS signal also in bark and wood samples (Fig. S6). These results demonstrate the presence of an active photosynthetic electron transport in illuminated tissues mediated by PSI and PSII charge separation activity capable of generating and sustaining a membrane potential, clearly confirming that the photosynthetic apparatus of both bark and wood is fully functional.

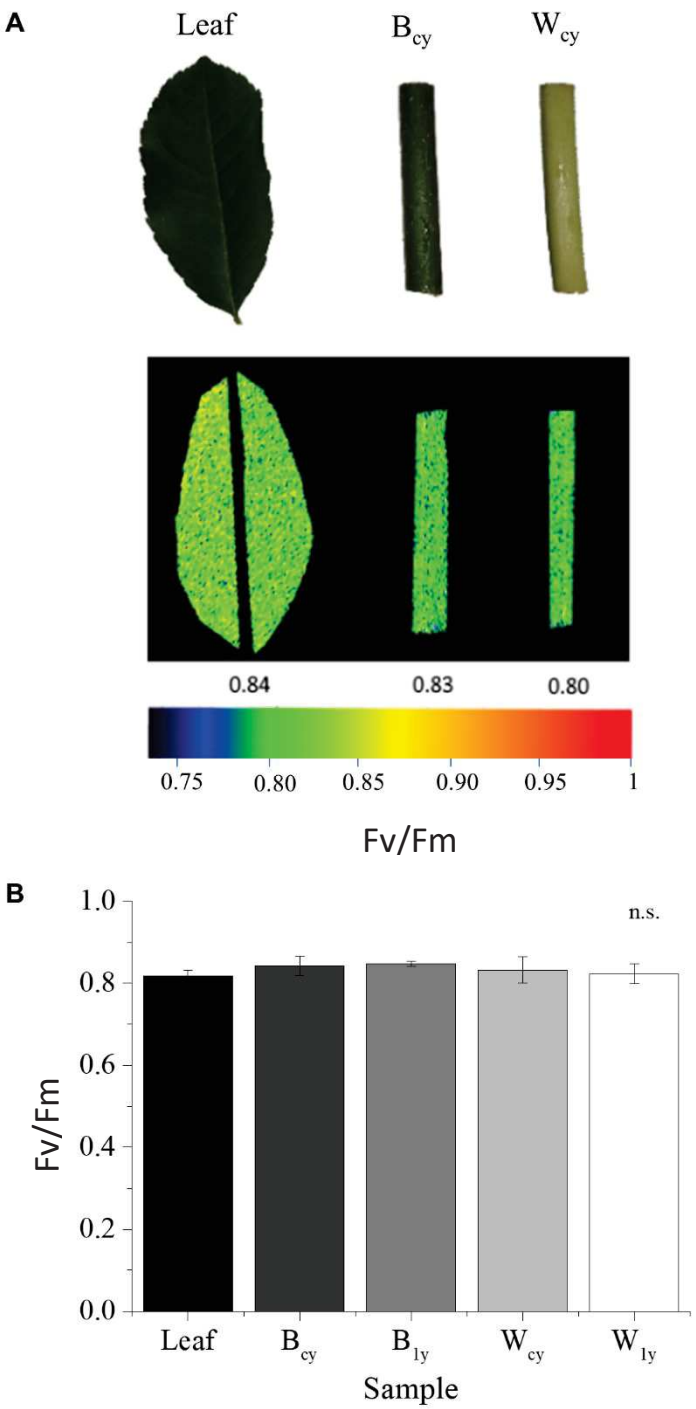

Fig. 7 (A) Example of optical analysis of leaf, bark and wood of current year stem (B_{cy} and W_{cy}) of *Fraxinus ornus* L. to analyse the different photosynthetic efficiency, shown in terms of maximum quantum efficiency (Fv/Fm) of PSII. (B) Maximum quantum efficiency (Fv/Fm) of PSII of leaf, bark and wood of current year (B_{cy} and W_{cy}) and one-year-old stems (B_{1y} and W_{1y}) of *Fraxinus ornus* L. Mean values are reported ± S.D. (n = 4); n.s.: not statistically significant.

The ETR was quantified by comparing the ECS when the light was switched off (S_D) and when the light was on (S_L) (Fig. 8A), an approach that enables to distinguish the light-dependent signal from other contributions. Even if the ETR values should be considered semi-quantitative because of the inability to use inhibitors in these samples for internal standardization (see Methods for details), data indicate that B_{cy} ETR was comparable to that of the leaf, while a lower electron transport capacity was observed with increasing stem age in B_{1y} (Fig. 8B). ETR in the wood (both W_{cy} and W_{1y}) was even lower compared to leaf and B_{cy}.

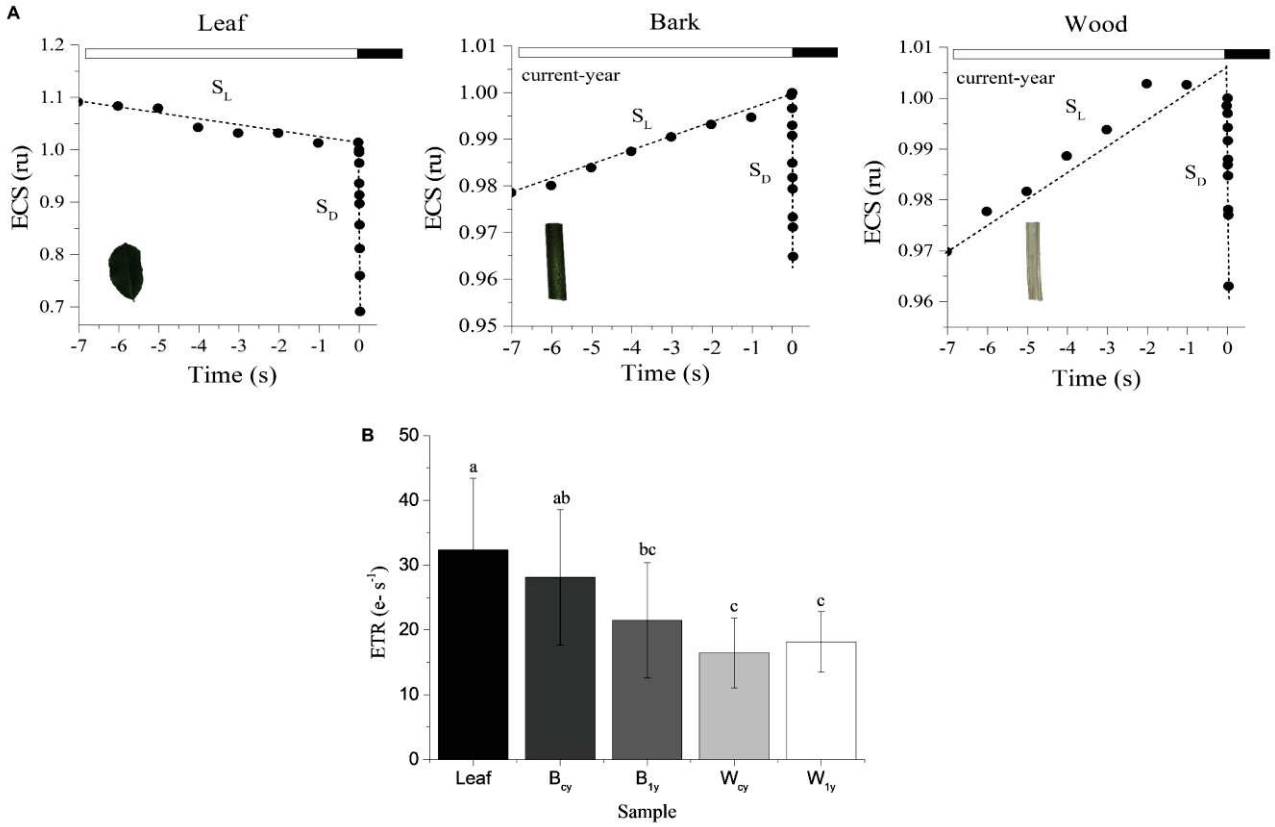

Fig. 8 (A) Examples of changes in the electrochromic shift (ECS) signal measured at 520-546 nm upon normalization on the first data point in the dark to one, to allow for a better comparison. A slope of the ECS changing during a transition from light (S_L) to dark (S_D) is reported for leaf, bark and wood of current year (B_{cy} and W_{cy}) of *Fraxinus ornus* L. White box: the actinic light was on; black box: the actinic light was switched off. (B) Electron transport rate (ETR) of leaf, bark and wood of current year (B_{cy} and W_{cy}) and one-year-old stems (B_{1y} and W_{1y}) of *Fraxinus ornus* L. Data are normalized on functional total photosystems (PSs). The error bars represent mean values ± S.D. ($n \geq 5$). Different letters indicate significant differences between samples ($P < 0.05$).

A further confirmation that photosynthesis is fully functional in these tissues can be obtained by looking at the oxidized P700 ($P700^+$) signal (Fig. 9A). When P700 is oxidized during photosynthesis, it generates a difference in absorption at 705 nm that can be detected. Since this signal only detects a difference in absorption generated by light, it demonstrates the presence of a photo-oxidizable PSI, enabling to distinguish it from other optical signals. As shown in Fig. 9a, all samples show the ability to generate a $P700^+$ signal dependent on illumination. The signal is high in samples such as leaves and bark, where Chl (and PSI) content is higher.

Fig. 9B shows in more detail the reduction kinetics of P700 when the light is switched off after illumination with actinic light. When the light is switched off, the $P700^+$ is reduced back to P700 restoring the initial level of light absorption. Since samples are pre-illuminated for several minutes and have fully activated steady photosynthetic activity, the kinetics of P700 reduction is indicative of their electron transport capacity. These measurements show a much faster re-oxidation in leaf samples, indicative of a higher electron transport capacity. On the other hand, the kinetic is much slower for B_{cy} (τ: 66.45±1.06 ms), W_{cy} (τ: 57.15±18.19 ms), B_{1y} (τ: 50.18±22.37 ms) and W_{1y} (τ: 37.13±22.92 ms) compared to leaves (τ: 17.69±9.87 ms), indicating a lower electron transport activity in these samples.

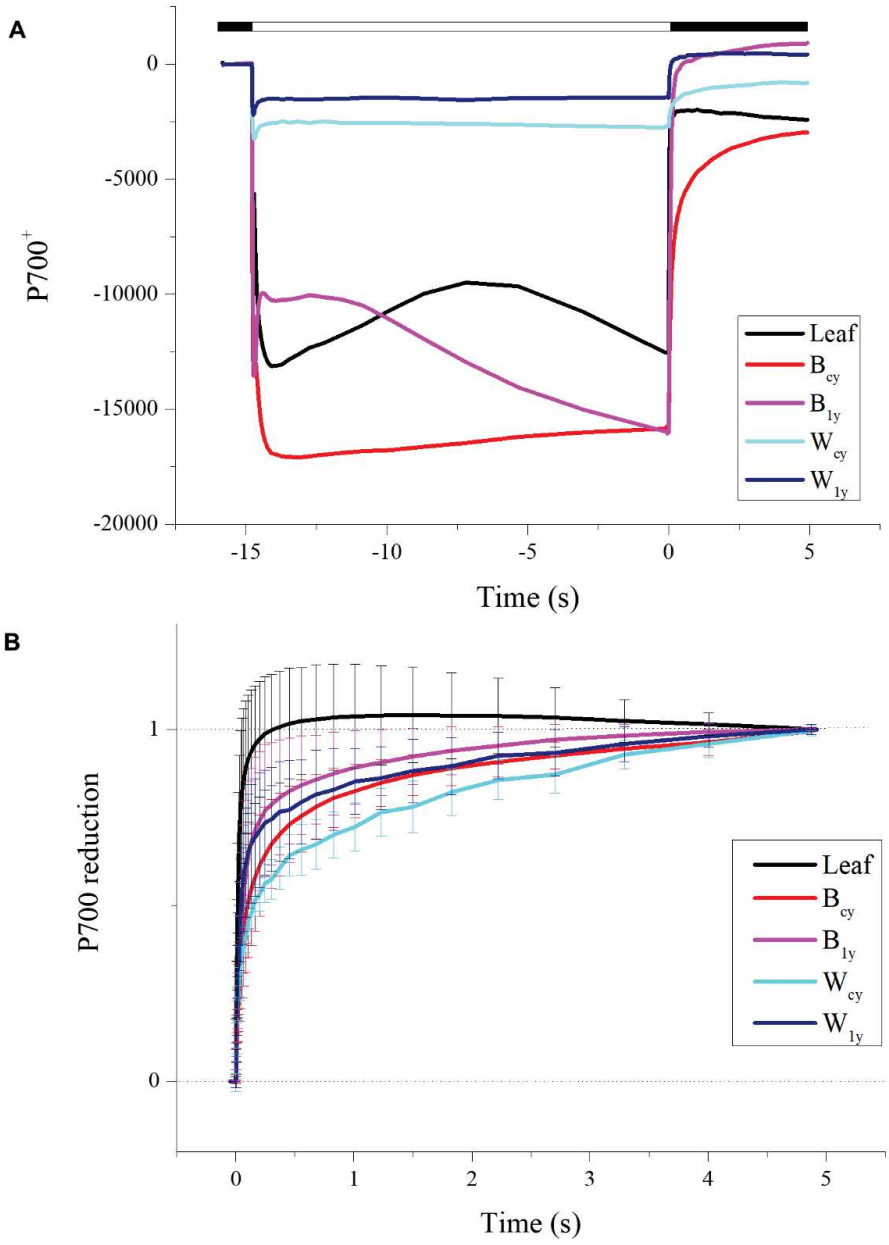

Fig. 9 (A) Examples of oxidation of P700 ($P700^+$) kinetics of leaf, bark and wood of current year (B_{cy} and W_{cy}) and one-year-old stems (B_{1y} and W_{1y}) of *Fraxinus ornus* L. White box: the actinic light was on; black box: the actinic light was switched off. (B) $P700^+$ reduction kinetics of leaf, bark and wood of current year (B_{cy} and W_{cy}) and one-year-old stems (B_{1y} and W_{1y}) of *Fraxinus ornus* L. Curves shown are average of 3-8 independent measurements.

Discussion

Our study represents one of the first examples of an in-depth analysis of ultrastructural and functional features of bark and wood chloroplasts and stem photosynthetic activity. Our data offer new insights into the functional traits of the photosynthetic apparatus in the different stem regions.

Light environment across the stem section

Transmission of light through isolated portions of bark and wood of *F. ornus* changed with stem age, decreasing from current-year to one-year-old stems. This can be explained by the gradual increment of the protective cork tissues (Pilarski 1989; Pfanz and Aschan 2001; Aschan et al. 2001; Filippou et al. 2007). The optical properties of stems resulted in a different light environment between bark and wood compartments in terms of both intensity and spectral composition. The blue band of the spectrum is mainly absorbed by the bark, and consequently, the wood is reached by green- and far-red enriched light. Our findings strongly suggest that light is attenuated when travelling through the wood layer and are in accordance with previous studies (e.g. Pfanz and Aschan 2001; Pfanz et al. 2002; Manetas and Pfanz 2005; Wittmann and Pfanz 2016), which also showed that stems absorb most of the visible spectrum, except for far-red light that might be conducted also in the axial direction of stems and roots (Sun et al. 2003, 2005).

Pigment composition and chloroplasts' structure

Despite the low light transmittance in the radial stem direction, we could confirm the presence of Chl and Car in both bark and wood of *F. ornus* stems. This was evident in fluorescence microscopy images, showing Chl accumulated in the bark (in the parenchyma cells of phelloderm, cortex and phloem) but also present along the xylem rays and around the pith. The detailed analysis, however, revealed a gradual decrease in the concentration of both pigments going from leaves to bark and wood, and also with the tissue age (Tab. 1). For this reason, we deemed it important to compare the chloroplast ultrastructure and photosynthetic apparatus organization and function of stems and leaves. In accordance with previous observations (Larcher et al. 1988; Ivanov et al. 1990; Pfanz et al. 2002; Liu et al. 2021), leaf and stem chloroplasts had different ultrastructural organization, showing clear patterns along the stem radial profile with progressively larger grana, smaller stroma lamellae and lower stromal area (mostly occupied by accumulated starch). These modifications in the chloroplasts' ultrastructure along the stem profile are likely induced by the gradient in light quantity/quality. As previously suggested by other researchers (e.g. Larcher et al. 1988; Ivanov et al. 1990; Pfanz et al. 2002; Hu et al. 2020; Liu et al. 2021), broader grana stacks are fundamental to harvest the limited

light energy penetrating through the stem, and highly stacked thylakoid membranes are a typical acclimation response to low light environments.

Light is an important requisite for the differentiation of active chloroplasts, but Chl can be synthesized at light intensities below those necessary to fuel the photosynthetic process, suggesting that the mere presence of pigments does not necessarily indicate active photosynthesis in stem chloroplasts (Schaedle 1975). Consistently with the observed light gradient (e.g. Larcher et al. 1988; van Cleve et al. 1993; Pilarski 1999; Pfanz et al. 2002; Filippou et al. 2007; Wittmann and Pfanz 2016), a progressive decrease of Chl*a/b* ratio was also observed in *F. ornus* when moving into innermost stem regions (Fig. 2), suggesting that chloroplasts are acclimated to lower light availability. The analysis of wood samples is particularly interesting since they show other typical features of acclimation to a low light environment, such as a lower Chl*a/b* ratio, larger number of grana stacks, and higher PSII/PSI ratios (Anderson et al. 1973; Lee and Whitmarsh 1989; Brugnoli et al. 1994; Murchie and Horton 1997). All these findings suggest efficient optimization of the stem photosynthetic apparatus to low and red-enhanced irradiation, especially in the wood parenchyma.

Any change in light quantity/quality can induce modifications in the structure and organization of the main pigment-protein complexes of chloroplasts (Anderson et al. 1995; Eberhard et al. 2008; Anderson et al. 2012; La Rocca et al. 2015; Albanese et al. 2016; Storti et al. 2020). Indeed, PSI is preferably excited by far-red light ($\lambda > 700$ nm) whereas PSII absorbs better at wavelengths shorter than 680 nm (Chow et al. 1990). An increase in red and far-red light is expected to induce an increase of the PSII abundance and a decrease in that of PSI, and hence a decrease in PSI/PSII ratio in order to maintain an equal electron transport capacity of the two photosystems despite the different excitation levels (Ruban and Johnson 2009; Lemeille and Rochaix 2010; Minagawa 2011; Mukherjee 2020; Hu et al. 2020). In line with this, the low temperature (77K) peak of the PSI-related complex was much lower in bark and wood than in leaves of *F. ornus*, indicating lower relative accumulation of PSI proteins, consistent with previous studies (Ivanov et al. 1990; Ivanov et al. 2006). This also supports the hypothesis that wood chloroplasts are acclimated not only to low light but also to a different light spectrum, enriched in far-red wavelengths. Overall, data suggest the ability of stem chloroplast to modify the stoichiometry of the two photosystems to retain a high quantum efficiency of photosynthesis as observed in plants exposed to different light regimes (Chow et al. 1990) and thus an acclimation response, dynamically modifying the composition and function of thylakoids membranes in response to different light conditions is activated here (Melis and Harvey 1981; Anderson 1986).

Chloroplasts activity/efficiency

In addition to their capability of activating an acclimation response, bark and wood chloroplasts had PSII with good photochemical activity, as shown by Fv/Fm values similar to those measured for leaves (Björkman and Demmig 1987). Our results are in line with other studies focused on current-year stems of several deciduous species (Damesin 2003; Manetas and Pfanz 2005; Berveiller et al. 2007; Wittmann and Pfanz 2007, 2008). The novel data that we present in this paper, have been acquired using ECS spectroscopy applied to the analysis of bark and wood chloroplasts. With this methodology, we were able to quantify the number of active PSs for each sample type, thus determining the effective ETR for leaves, bark and wood. Using ECS spectroscopy it was also possible to demonstrate that bark and wood chloroplasts are capable of light-dependent electron transport. Moreover, the bark of current-year stems had similar photosynthetic capacity, measured by ETR, as leaves. In older stems, the bark ETR decreased whereas the photosynthetic capacity of wood was lower compared to both bark and leaves. Interestingly, all these results suggest that current-year bark has photosynthetic characteristics comparable to those of the leaves, as already noted by Berveiller et al. (2007). Data on the photochemical activities of PSII and PSI show that the few chlorophyllous cells buried deep in the wood are still able to perform photosynthesis. Indeed, as expected, the size of $P700^+$ re-reduction was lower in bark and wood than in leaves, suggesting a lower potential electron transport activity, which is also in agreement with the lower abundance of PSI found with immunoblot analysis (Fig. 6). Moreover, the P700 re-reduction kinetics depend on both linear and cyclic electron transport, and a slower kinetic might depend on a unbalance contribution by one of these two, therefore future studies might focus on it. Finally, this hypothesis is supported also by the presence of LHCII proteins in the bark as well as in wood, that suggested efficient light-harvesting for the photosystems in stems even in the low light environment. Indeed, LHCII is an antenna that can connect energetically the entire photosynthetic apparatus, both PSI and PSII, and according to different light intensities can associate preferentially to one PS rather than the other (Wientjes et al. 2013; Grieco et al. 2015).

To summarize, stem chloroplasts accumulate relatively more LHCII and PSII, by increasing the amount of thylakoid membrane stacking. On the other hand, they show less PSI and fewer stroma lamellae than leaves. Once again, these characteristics are a typical acclimation response to a red-enhanced and low-light environment, to increase light use efficiency. Many of these characteristics have been observed also in shade leaves. Compared to sun leaves, shade leaves show more grana stacks, lower Chl*a/b* ratio and higher numbers of light-harvesting complexes per reaction centres (e.g. Lichtenthaler et al. 1981; Anderson 1986; Ballottari et al. 2007; Lichtenthaler et al. 2013; Flannery et al. 2021).

Our data thus provide support for the hypothesis that chlorophyll-containing cells near the vascular system, in a region receiving mostly green or far-red light, are indeed photosynthetically active. On the other hand, the precise physiological role of this photosynthetic activity still needs to be explored and proven (Pfanz and Aschan 2001; Hibberd and Quick 2002; Berveiller and Damesin 2008).

Available data on the enzymatic features of bark and wood photosynthesis are particularly scarce in the literature. The presence of Rubisco was detected in leaves and bark and weakly in the wood, indicating a capacity to fix CO_2 also in the stem compartments. The lower signal of the protein present in the wood might be explained by the lower sensitivity of the antibodies that indeed showed weaker signals also in leaf samples.

Both the ETR values and presence of Rubisco in the wood corroborate the hypothesis that wood photosynthesis can recycle the CO_2 dissolved in the xylem sap (Alessio et al. 2005; Berveiller and Damesin 2008; Wittmann et al. 2006; Bloemen et al. 2013a,c; Vandegehuchte et al. 2015).

Recent research has suggested that local production of carbohydrates by bark photosynthesis may facilitate osmotic adjustment to support turgor maintenance and xylem functioning under drought stress (Zwieniecki and Holbrook 2009; Nardini et al. 2011; Secchi and Zwieniecki 2012; Cernusak and Cheesman 2015; Nardini et al. 2018; Ávila-Lovera et al. 2017; De Roo et al. 2020; Tomasella et al. 2020). Our data let us speculate that even wood chloroplasts might play a very local role in these processes, especially in post-drought hydraulic recovery, paving the way for future studies on this topic.

Conclusions

In conclusion, our experimental setup enabled us to define in detail the functional features of stem chloroplasts of *F. ornus*, and their potential photosynthetic efficiency. The comparison of the P700 kinetics in different compartments raises interesting questions on the relative amount of linear and cyclic electron flow in the wood. From the current literature, it is known that the presence of chloroplasts and the related photosynthetic activity decrease with increasing stem age. In accordance, we found that the bark of current year stems has a conformation of the photosynthetic apparatus almost comparable to that of the adjacent leaves. Moreover, already in the one-year-old stem, there is a decrease in electron transport rates, compatible with decreased light transmittance. In accordance with our expectations, chloroplasts in the wood of different ages showed good photosynthetic efficiency, supporting the idea that stem photosynthesis participates in the production of photosynthates that might support plant carbon balance. This functional feature invites to speculate that stem photosynthesis might play an adaptive advantage, especially for woody plant species

occurring in habitats where seasonal drought can strongly limit leaf photosynthesis, which is, in fact, the case of *F. ornus*.

Author contributions

AN, TM, AA, NLR and SN designed the experiment; NLR, AA, MB and SN performed pigments analysis and fluorescence spectroscopy measurements; SN and MB performed light-transmission measurements and analysis; NLR and SN performed epifluorescence microscopy and TEM observations; AA and SN performed SDS-PAGE electrophoresis and western blot analysis; TM, AA and SN contributed to imaging and spectroscopy data acquisition and analyses. SN and AN wrote the manuscript, with contributions and revisions from all authors.

Acknowledgements

We are very grateful to the 'Direzione centrale risorse agroalimentari, forestali e ittiche – area foreste e territorio' of the 'Regione Autonoma Friuli Venezia Giulia', and to the public nursery Vivai Pascul (Tarcento, Italy) for providing the plant material for the glasshouse experiment. We thank the Electron Microscopy Facility of the Department of Biology at the University of Padova.

References

Albanese P, Manfredi M, Meneghesso A, Marengo E, Saracco G, Barber J, Morosinotto T, Pagliano C. 2016. Dynamic reorganization of photosystem II supercomplexes in response to variations in light intensities. *Biochimica et Biophysica Acta (BBA)-Bioenergetics* **1857:** 1651–1660.

Alessio GA, Pietrini F, Brilli F, Loreto F. 2005. Characteristics of CO_2 exchange between peach stems and the atmosphere. *Functional Plant Biology* **32:** 787–795.

Allorent G, Osorio S, Ly Vu J, et al. 2015. Adjustments of embryonic photosynthetic activity modulate seed fitness in *Arabidopsis thaliana*. *New Phytologist* **205:** 707–719.

Allorent G, Byrdin M, Carraretto L, Morosinotto T, Szabo I, Finazzi G. 2018. Global spectroscopic analysis to study the regulation of the photosynthetic proton motive force: A critical reappraisal. *Biochimica et Biophysica Acta (BBA)-Bioenergetics* **1859:** 676–683.

Anderson JM, Goodchild DJ, Boardman NK. 1973. Composition of the photosystems and chloroplast structure in extreme shade plants. *Biochimica et Biophysica Acta (BBA)-Bioenergetics* **325:** 573–585.

Anderson JM. 1986. Photoregulation of the composition, function, and structure of thylakoid membranes. *Annual review of plant physiology* **37:** 93–136.

Anderson JM, Chow WS, Park YI. 1995. The grand design of photosynthesis: acclimation of the photosynthetic apparatus to environmental cues. *Photosynthesis Research* **46:** 129–139.

Anderson JM, Horton P, Kim EH, Chow WS. 2012. Towards elucidation of dynamic structural changes of plant thylakoid architecture. *Philosophical Transactions of the Royal Society B: Biological Sciences* **367:** 3515–3524.

Andrizhiyevskaya EG, Chojnicka A, Bautista JA, Diner BA, van Grondelle R, Dekker JP. 2005. Origin of the F685 and F695 fluorescence in photosystem II. *Photosynthesis Research* **84:** 173–180.

Angyalossy V, Pace MR, Evert RF, Marcati CR, Oskolski AA, Terrazas T, et al. 2016. IAWA list of microscopic bark features. *Iawa Journal* **37:** 517–615.

Aschan G, Wittmann C, Pfanz H. 2001. Age-dependent bark photosynthesis of aspen twigs. *Trees* **15:** 431–437.

Aschan G, Pfanz H. 2003. Non-foliar photosynthesis–a strategy of additional carbon acquisition. *Flora-Morphology, Distribution, Functional Ecology of Plants* **198:** 81–97.

Ávila E, Herrera A, Tezara W. 2014. Contribution of stem CO_2 fixation to whole-plant carbon balance in nonsucculent species. *Photosynthetica* **52:** 3–15.

Ávila-Lovera E, Zerpa AJ, Santiago LS. 2017. Stem photosynthesis and hydraulics are coordinated in desert plant species. *New Phytologist* **216:** 1119–1129.

Bailleul B, Cardol P, Breyton C, Finazzi G. 2010. Electrochromism: a useful probe to study algal photosynthesis. *Photosynthesis Research* **106:** 179–189.

Ballottari M, Dall'Osto L, Morosinotto T, Bassi R. 2007. Contrasting behavior of higher plant photosystem I and II antenna systems during acclimation. *Journal of Biological Chemistry* **282:** 8947–8958.

Berveiller D, Damesin C. 2008. Carbon assimilation by tree stems: potential involvement of phosphoenolpyruvate carboxylase. *Trees* **22:** 149–157.

Berveiller D, Kierzkowski D, Damesin C. 2007. Interspecific variability of stem photosynthesis among tree species. *Tree Physiology* **27:** 53–61.

Björkman O, Demmig B. 1987. Photon yield of O_2 evolution and chlorophyll fluorescence characteristics at 77 K among vascular plants of diverse origins. *Planta* **170:** 489–504.

Bloemen J, McGuire MA, Aubrey DP, Teskey RO, Steppe K. 2013a. Internal recycling of respired CO_2 may be important for plant functioning under changing climate regimes. *Plant Signaling and Behavior* **8:** e27530.

Bloemen J, McGuire MA, Aubrey DP, Teskey RO, Steppe K. 2013b. Transport of root-respired CO_2 via the transpiration stream affects aboveground carbon assimilation and CO_2 efflux in trees. *New Phytologist* **197:** 555–565.

Bloemen J, Overlaet-Michiels L, Steppe K. 2013c. Understanding plant responses to drought: how important is woody tissue photosynthesis? *Acta Horticulturae* **991:** 149–157.

Bloemen J, Vergeynst L, Overlaet-Michiels L, Steppe K. 2016. How important is woody tissue photosynthesis in poplar during drought stress? *Trees* **30:** 63–72.

Breton J. 1982. The 695 nm fluorescence (F 695) of chloroplasts at low temperature is emitted from the primary acceptor of photosystem II. *FEBS Letters* **147:** 16–20.

Brugnoli E, Cona A, Lauteri M. 1994. Xanthophyll cycle components and capacity for non-radiative energy dissipation in sun and shade leaves of *Ligustrum ovalifolium* exposed to conditions limiting photosynthesis. *Photosynthesis Research* **41:** 451–463.

Buns R, Acker G, Beck E. 1993. The plastids of the yew tree (*Taxus baccata* L.): ultrastructure and immunocytochemical examination of chloroplastic enzymes. *Botanica Acta* **106:** 32–41.

Cernusak LA, Marshall JD. 2000. Photosynthetic refixation in branches of western white pine. *Functional Ecology* **14:** 300–311.

Cernusak LA, Marshall JD, Comstock JP, Balster NJ. 2001. Carbon isotope discrimination in photosynthetic bark. *Oecologia* **128:** 24–35.

Cernusak LA, Hutley LB. 2011. Stab. Isotopes reveal the contribution of corticular photosynthesis to growth in branches of *Eucalyptus 46iniate*. *Plant Physiology* **155:** 515–523.

Cernusak LA, Cheesman AW. 2015. The benefits of recycling: how photosynthetic bark can increase drought tolerance. *New Phytologist* **208:** 995–997.

Chow WS, Melis A, Anderson J. 1990. Adjustments of photosystem stoichiometry in chloroplasts improve the quantum efficiency of photosynthesis. *Proceedings of the National Academy of Sciences* **87:** 7502–7506.

Comstock J, Ehleringer J. 1990. Effect of variations in leaf size on morphology and photosynthetic rate of twigs. *Functional Ecology* **4:** 209–221.

Damesin C. 2003. Respiration and photosynthesis characteristics of current-year stems of *Fagus sylvatica*: from the seasonal pattern to an annual balance. *New Phytologist* **158:** 465–475.

De Baerdemaeker NJ, Salomón RL, De Roo L, Steppe K. 2017. Sugars from woody tissue photosynthesis reduce xylem vulnerability to cavitation. *New Phytologist* **216:** 720–727.

De Roo L, Salomón RL, Steppe K. 2020. Woody tissue photosynthesis reduces stem CO_2 efflux by half and remains unaffected by drought stress in young *Populus tremula* trees. *Plant, Cell & Environment* **43:** 981–991.

Dobrev K, Stanoeva D, Velitchkova M, Popova AV. 2016. The lack of lutein accelerates the extent of light-induced bleaching of photosynthetic pigments in thylakoid membranes of *Arabidopsis thaliana*. *Photochemistry and Photobiology* **92:** 436–445.

Dymova O, Khristin M, Miszalski Z, Kornas A, Strzalka K, Golovko T. 2018. Seasonal variations of leaf chlorophyll-protein complexes in the wintergreen herbaceous plant *Ajuga reptans* L. *Functional Plant Biology* **45:** 519–527.

Eberhard S, Finazzi G, Wollman FA. 2008. The dynamics of photosynthesis. *Annual Review of Genetics* **42:** 463–515.

Flannery SE, Hepworth C, Wood WH, Pastorelli F, Hunter CN, Dickman MJ, Jackson PJ, Johnson MP. 2021. Developmental acclimation of the thylakoid proteome to light intensity in *Arabidopsis*. *The Plant Journal* **105:** 223–244.

Filippou M, Fasseas C, Karabourniotis G. 2007. Photosynthetic characteristics of olive tree (*Olea europaea*) bark. *Tree physiology* **27:** 977–984.

Gerotto C, Alboresi A, Meneghesso A, Jokel M, Suorsa M, Aro EM, Morosinotto T. 2016. Flavodiiron proteins act as safety valve for electrons in *Physcomitrella patens*. *Proceedings of the National Academy of Sciences* **113:** 12322–12327.

Gibson A. 1983. Anatomy of photosynthetic old stems of nonsucculent dicotyledons from North American deserts. *Botanical Gazette* **144:** 347–362.

Gortan E, Nardini A, Gascó A, Salleo S. 2009. The hydraulic conductance of *Fraxinus ornus* leaves is constrained by soil water availability and coordinated with gas exchange rates. *Tree Physiology* **29:** 529–539.

Govindjee. 1995. Sixty-three years since Kautsky: chlorophyll a fluorescence. *Australian Journal of Plant Physiology* **22:** 131–160.

Grieco M, Suorsa M, Jajoo A, Tikkanen M, Aro EM. 2015. Light-harvesting II antenna trimers connect energetically the entire photosynthetic machinery—including both photosystems II and I. *Biochimica et Biophysica Acta (BBA)-Bioenergetics* **1847:** 607–619.

Hibberd JM, Quick WP. 2002. Characteristics of C4 photosynthesis in stems and petioles of C3 flowering plants. *Nature* **415:** 451–454.

Hu C, Nawrocki WJ, Croce R. 2021. Long-term adaptation of *Arabidopsis thaliana* to far-red light. *Plant, Cell & Environment* **44:** 3002–3014.

Ivanov AG, Ignatova NS, Christov AM. 1990. Comparative ultrastructural and fluorescence studies of grapevine (*Vitis vinifera* L.) chloroplasts isolated from stem and leaf tissues. *Plant Science* **67:** 253–257.

Ivanov AG, Krol M, Sveshnikov D, Malmberg G, Gardeström P, Hurry V, Öquist G, Huner NPA. 2006. Characterization of the photosynthetic apparatus in cortical bark chlorenchyma *of Scots pine*. *Planta* **223:** 1165–1177.

Jensen KF. 1969. Oxygen and carbon dioxide concentrations in sound and decaying red oak trees. *Forest Science* **15:** 246–251.

Ke B. 1972. The rise time of photoreduction, difference spectrum, and oxidation-reduction potential of P430. *Archives of Biochemistry and Biophysics* **152:** 70–77.

Kharouk VI, Middleton EM, Spencer SL, Rock BN, Williams DL. 1995. Aspen bark photosynthesis and its significance to remote sensing and carbon budget estimates in the boreal ecosystem. *Water, Air and Soil Pollution* **82:** 483–497.

Krause GH, Weis E. 1984. Chlorophyll fluorescence as a tool in plant physiology II. Interpretation of fluorescence signals. *Photosynthesis research* **5:** 139–157.

Krause GH, Weis E. 1991. Chlorophyll fluorescence and photosynthesis—the basics. *Annual Review of Plant Physiology and Plant Molecular Biology* **42:** 313–349.

La Rocca N, Sciuto K, Meneghesso A, Moro I, Rascio N, Morosinotto T. 2015. Photosynthesis in extreme environments: responses to different light regimes in the Antarctic alga *Koliella antarctica*. *Physiologia Plantarum* **153:** 654–667.

Lamb J, Forfang K, Hohmann-Marriott M. 2015. A practical solution for 77 K fluorescence measurements based on LED excitation and CCD array detector. *PloS One* **10:** e0132258.

Lamb JJ, Røkke G, Hohmann-Marriott MF. 2018. Chlorophyll fluorescence emission spectroscopy of oxygenic organisms at 77 K. *Photosynthetica* **56:** 105–124.

Lemeille S, Rochaix JD. 2010. State transitions at the crossroad of thylakoid signaling pathways. *Photosynthesis Research* **106:** 33–46.

Larcher W, Lütz C, Nagele M, Bodner M. 1988. Photosynthetic functioning and ultrastructure of chloroplasts in stem tissues of *Fagus sylvatica*. *Journal of Plant Physiology* **132:** 731–737.

Lee WJ, Whitmarsh J. 1989. Photosynthetic apparatus of pea thylakoid membranes: Response to growth light intensity. *Plant Physiology* **89:** 932–940.

Levizou E, Petropoulou Y, Manetas Y. 2004. Carotenoid composition of peridermal twigs does not fully conform to a shade acclimation hypothesis. *Photosynthetica* **42:** 591–596.

Lichtenthaler HK, Buschman C, Pahmsdorf U. 1980. The importance of blue light for the development of sun-type chloroplasts. In: Senger H, eds. *The Blue Light Syndrome*. Berlin, DE: Springer-Verlag, 485–494.

Lichtenthaler HK, Buschmann C, Döll M, Fietz HJ, Bach T, Kozel U, Meier D, Rahmsdorf U. 1981. Photosynthetic activity, chloroplast ultrastructure, and leaf characteristics of high-light and low-light plants and of sun and shade leaves. *Photosynthesis Research* **2:** 115–141.

Lichtenthaler HK, Babani F, Navrátil M, Buschmann C. 2013. Chlorophyll fluorescence kinetics, photosynthetic activity, and pigment composition of blue-shade and half-shade leaves as compared to sun and shade leaves of different trees. *Photosynthesis Research* **117:** 355–366.

Liu J, Gu L, Yu Y, Huang P, Wu Z, Zhang Q, Qian Y, Wan X, Sun Z. 2019. Corticular photosynthesis drives bark water uptake to refill embolized vessels in dehydrated branches of *Salix matsudana*. *Plant, Cell & Environment* **42:** 2584–2596.

Liu J, Sun C, Zhai FF, Li Z, Qian Y, Gu L, Sun Z. 2021. Proteomic insights into the photosynthetic divergence between bark and leaf chloroplasts in *Salix matsudana*. *Tree Physiology* **41:** 2142–2152.

Manetas Y. 2004. Probing corticular photosynthesis through in vivo chlorophyll fluorescence measurements: evidence that high internal CO_2 levels suppress electron flow and increase the risk of photoinhibition. *Physiologia Plantarum* **120:** 509–517.

Manetas Y, Pfanz H. 2005. Spatial heterogeneity of light penetration through periderm and lenticels and concomitant patchy acclimation of corticular photosynthesis. *Trees* **19:** 409–414.

Maxwell K, Johnson GN. 2000. Chlorophyll fluorescence-a practical guide. *Journal of Experimental Botany* **51:** 659–668.

Melis A, Harvey GW. 1981. Regulation of photosystem stoichiometry, chlorophyll-A and chlorophyll-B content and relation to chloroplast ultrastructure. *Biochimica et Biophysica Acta (BBA)-Bioenergetics* **637:** 138–145.

Mellon M, Storti M, Vera-Vives AM, Kramer DM, Alboresi A, Morosinotto T. 2021. Inactivation of mitochondrial complex I stimulates chloroplast ATPase in *Physcomitrium patens*. *Plant Physiology* **187:** 931–946.

Mazur R, Mostowska A, Kowalewska Ł. 2021. How to measure grana-ultrastructural features of thylakoid membranes of plant chloroplasts. *Frontiers in Plant Science* **12:** 756009.

Minagawa J. 2011. State transitions—the molecular remodeling of photosynthetic supercomplexes that controls energy flow in the chloroplast. *Biochimica et Biophysica Acta (BBA)-Bioenergetics* **1807:** 897–905.

Morosinotto T, Breton J, Bassi R, Croce R. 2003. The nature of a chlorophyll ligand in Lhca proteins determines the far red fluorescence emission typical of photosystem I. *Journal of Biological Chemistry* **278:** 49223–49229.

Mukherjee A. 2020. State transition regulation in *Chlamydomonas reinhardtii*. *Plant Physiology* **183:** 1418–1419.

Murchie EH, Horton P. 1997. Acclimation of photosynthesis to irradiance and spectral quality in British plant species: chlorophyll content, photosynthetic capacity and habitat preference. *Plant, Cell & Environment* **20:** 438–448.

Nardini A, Salleo S, Trifilò P, Lo Gullo MA. 2003. Water relations and hydraulic characteristics of three woody species co-occurring in the same habitat. *Annals of Forest Science* **60:** 297–305.

Nardini A, L Gullo MA, Salleo S. 2011. Refilling embolized xylem conduits. Is it a matter of xylem unloading? *Plant Science* **180:** 604–611.

Nardini A, Savi T, Trifilò P, Lo Gullo MA. 2018. Drought stress and the recovery from xylem embolism in woody plants. In Cánovas FM, Luettge U, Matyssek R, eds. *Progress in Botany*. Berlin, DE, Springer, 197–231.

Nardini A, Petruzzellis F, Marusig D, *et al.* 2021. Water 'on the rocks': a summer drink for thirsty trees? *New Phytologist* **229:** 199–212.

Nilsen ET, Sharifi MR. 1994. Seasonal acclimation of stem photosynthesis in woody legume species from the Mojave and Sonoran Deserts of California. *Plant Physiology* **105:** 1385–391.

Nilsen ET. 1995. Stem photosynthesis: extent, patterns and role in plant carbon economy. In: Gartner B, eds. *Plant stems: physiology and functional morphology*. San Diego, CA, USA: Academic Press, 223–240.

Pfanz H, Aschan G. 2001. The existence of bark and stem photosynthesis in woody plants and its significance for the overall carbon gain. An eco-physiological and ecological approach. In: Essr K, Luttge U, Kadereit JW, Beyshlag W, eds. *Progress in Botany*, Berlin, DE: Springer-Verlag, 477–510.

Pfanz H, Aschan G, Langenfeld-Heyser R, Wittmann C, Loose M. 2002. Ecology and ecophysiology of tree stems: corticular and wood photosynthesis. *Naturwissenschaften* **89:** 147–162.

Pfanz H. 2008. Bark photosynthesis. *Trees* **22:** 137–138.

Pilarski J. 1989. Optical properties of bark and leaves of *Syringa vulgaris* L. *Bulletin of the Polish Academy of Sciences. Biological Sciences* **37:** 253–260.

Pilarski J. 1999. Gradient of photosynthetic pigments in the bark and leaves of lilac (*Syringa vulgaris* L.). *Acta Physiologiae Plantarum* **21:** 365–373.

R Core Team. 2021. R: A language and environment for statistical computing. R Foundation for Statistical Computing, Vienna, Austria. https://www.R-project.org/.

Ruban AV, Johnson MP. 2009. Dynamics of higher plant photosystem cross-section associated with state transitions. *Photosynthesis Research* **99:** 173–183.

Sacksteder CA, Kramer DM. 2000. Dark-interval relaxation kinetics (DIRK) of absorbance changes as a quantitative probe of steady-state electron transfer. *Photosynthesis Research* **66:** 145–158.

Saveyn A, Steppe K, Ubierna N, Dawson TE. 2010. Woody tissue photosynthesis and its contribution to trunk growth and bud development in young plants. *Plant, Cell & Environment* **33:** 1949–1958.

Schaedle M. 1975. Tree photosynthesis. *Annual Review of Plant Physiology* **26:** 101–115.

Schmitz N, Egerton JJG, Lovelock CE, Ball MC. 2012. Light-dependent maintenance of hydraulic function in mangrove branches: do xylary chloroplasts play a role in embolism repair? *New Phytologist* **195:** 40–46.

Secchi F, Zwieniecki MA. 2011. Sensing embolism in xylem vessels: the role of sucrose as a trigger for refilling. *Plant, Cell & Environment* **34:** 514–524.

Secchi F, Zwieniecki MA. 2012. Analysis of xylem sap from functional (Nonembolized) and nonfunctional (Embolized) vessels of *Populus nigra*: chemistry of refilling. *Plant Physiology* **160:** 955–964.

Secchi F, Pagliarani C, Cavalletto S, *et al.* 2021. Chemical inhibition of xylem cellular activity impedes the removal of drought- induced embolisms in poplar stems – new insights from micro-CT analysis. *New Phytologist* **229:** 820–830.

Solhaug KA, Gauslaa Y, Haugen J. 1995. Adverse effects of epiphytic crustose lichens upon stem photosynthesis and chlorophyll of *Populus tremula* L. *Botanica Acta* **108:** 233–239.

Steppe K, Sterck F, Deslauriers A. 2015. Diel growth dynamics in tree stems: linking anatomy and ecophysiology. *Trends in Plant Science* **20:** 335–343.

Storti M, Segalla A, Mellon M, Alboresi A, Morosinotto T. 2020. Regulation of electron transport is essential for photosystem I stability and plant growth. *New Phytologist* **228:** 1316–1326.

Sun Q, Kiyotsugu Y, Mitsuo S, Hitoshi S. 2003. Vascular tissue in the stem and roots of woody plants can conduct light. *Journal of Experimental Botany* **54:** 1627–1635.

Sun Q, Yoda K, Suzuki H. 2005. Internal axial light conduction in the stems and roots of herbaceous plants. *Journal of Experimental Botany* **56:** 191–203.

Tausz M, Warren CR, Adams MA. 2005. Is the bark of shining gum (*Eucalyptus nitens*) a sun or a shade leaf? *Trees* **19:** 415–421.

Teskey RO, Saveyn A, Steppe K, McGuire MA. 2008. Origin, fate and significance of CO_2 in tree stems. *New Phytologist* **177:** 17–32.

Tomasella M, Petrussa E, Petruzzellis F, Nardini A, Casolo V. 2020. The possible role of non-structural carbohydrates in the regulation of tree hydraulics. *International Journal of Molecular Sciences* **21:** 144.

Trifilò P, Natale S, Gargiulo S, Abate E, Casolo V, Nardini A. 2021. Stem photosynthesis affects hydraulic resilience in the deciduous *Populus alba* but not in the evergreen *Laurus nobilis*. *Water* **13:** 2911.

Van Cleve B, Forreiter C, Sauter JJ, Apel K. 1993. Pith cells of poplar contain photosynthetically active chloroplasts. *Planta* **189:** 70–73.

Vandegehuchte MW, Bloemen J, Vergeynst LL, Steppe K. 2015. Woody tissue photosynthesis in trees: salve on the wounds of drought? *New Phytologist* **208:** 998–1002.

Wellburn AR. 1994. The spectral determination of chlorophylls a and b, as well as total carotenoids, using various solvents with spectrophotometers of different resolution. *Journal of Plant Physiology* **144:** 307–313.

Wiebe HH. 1975. Photosynthesis in wood. *Physiologia Plantarum* **33:** 245–246.

Witt HT. 1979. Energy conversion in the functional membrane of photosynthesis. Analysis by light pulse and electric pulse methods. The central role of the electric field. *Biochimica et Biophysica Acta (BBA)-Reviews on Bioenergetics* **505:** 355–427.

Wittmann C, Aschan G, Pfanz H. 2001. Leaf and twig photosynthesis of young beech *(Fagus sylvatica*) and aspen (*Populus tremula*) trees grown under different light intensity regimes. *Basic and Applied Ecology* **2:** 145–154.

Wittmann C, Pfanz H, Pietrini F. 2005. Light-modulation of corticular CO_2-refixation in young birch stems (*Betula pendula* Roth.). *Phyton-Annales Rei Botanicae* **45:** 195–212.

Wittmann C, Pfanz H, Loreto F, Centritto M, Pietrini F, Alessio G. 2006. Stem CO_2 release under illumination: corticular photosynthesis, photorespiration or inhibition of mitochondrial respiration? *Plant, Cell & Environment* **29:** 1149–1158.

Wittmann C, Pfanz H. 2007. Temperature dependency of bark photosynthesis in beech (*Fagus sylvatica* L.) and birch (*Betula pendula* Roth.) trees. *Journal of Experimental Botany* **58:** 4293–4306.

Wittmann C, Pfanz H. 2008. General trait relationships in stems: a study on the performance and interrelationships of several functional and structural parameters involved in corticular photosynthesis. *Physiologia Plantarum* **134:** 636–648.

Wittmann C, Pfanz H. 2014. Bark and woody tissue photosynthesis: a means to avoid hypoxia or anoxia in developing stem tissues. *Functional Plant Biology* **41:** 940–953.

Wittmann C, Pfanz H. 2016. The optical, absorptive and chlorophyll fluorescence properties of young stems of five woody species. *Environmental and Experimental Botany* **121:** 83–93.

Wientjes E, van Amerongen H, Croce R. 2013. LHCII is an antenna of both photosystems after long-term acclimation. *Biochimica et Biophysica Acta (BBA)-Bioenergetics* **1827:** 420–426.

Zwieniecki MA, Holbrook NM. 2009. Confronting Maxwell's demon: biophysics of xylem embolism repair. *Trends in Plant Sciences* **14:** 1360–1385.

Supplementary material

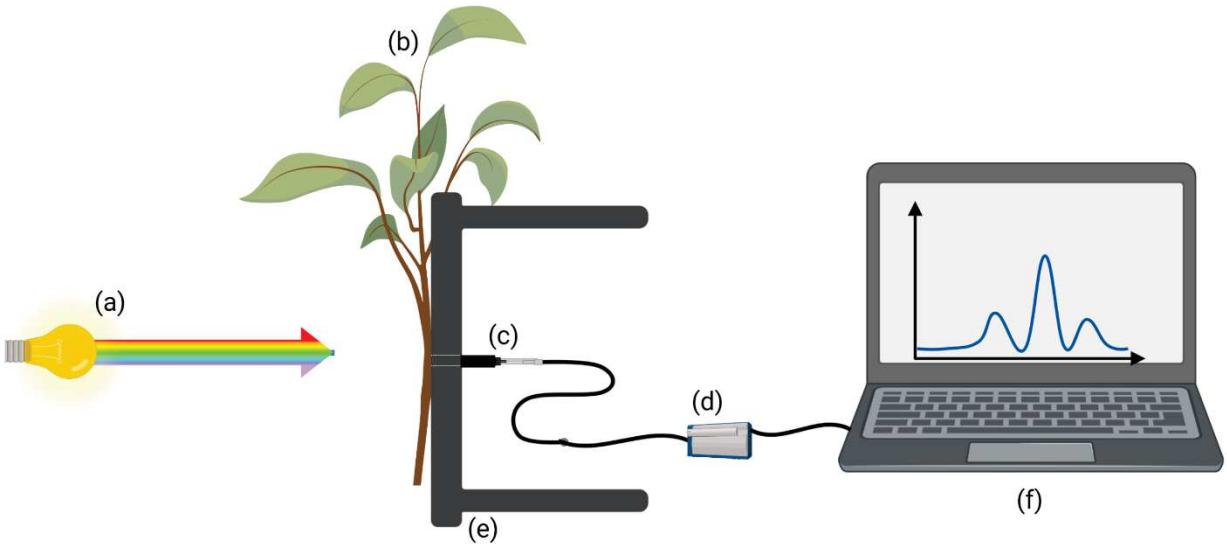

Fig. S1 Schematic representation of the radial light transmittance experimental setup. A wooden stand (e) covered on the front with a sheet of black Plexiglas was used to reduce light scattering. A small circular hole was drilled in the center. The light source (a) illuminated perpendicularly a leaf, bark or wood sample (b). Photons of light transmitted through the samples were collected by a high-resolution optical fiber (c), inserted in the hole of the wooden stand, and conveyed to a spectrometer (d). The acquired photon counts were analyzed and converted to transmission spectra with the aid of dedicated software (f). Created with Biorender.

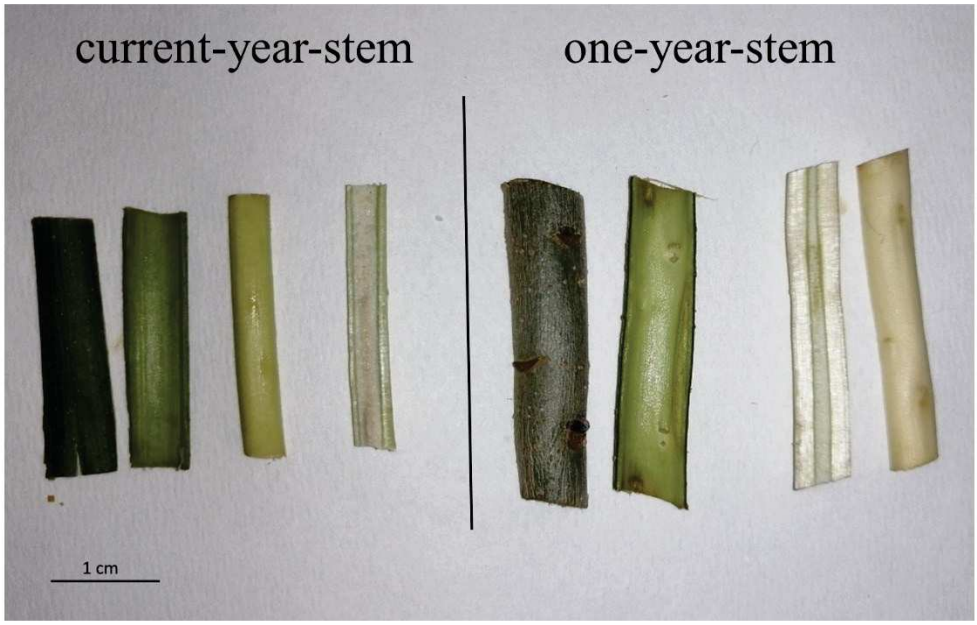

Fig. S2 Examples of samples of *Fraxinus ornus* L. used for measurements and experiments: bark and wood of current-year are shown on the left, while bark and wood of one-year-old stems are shown on the right.

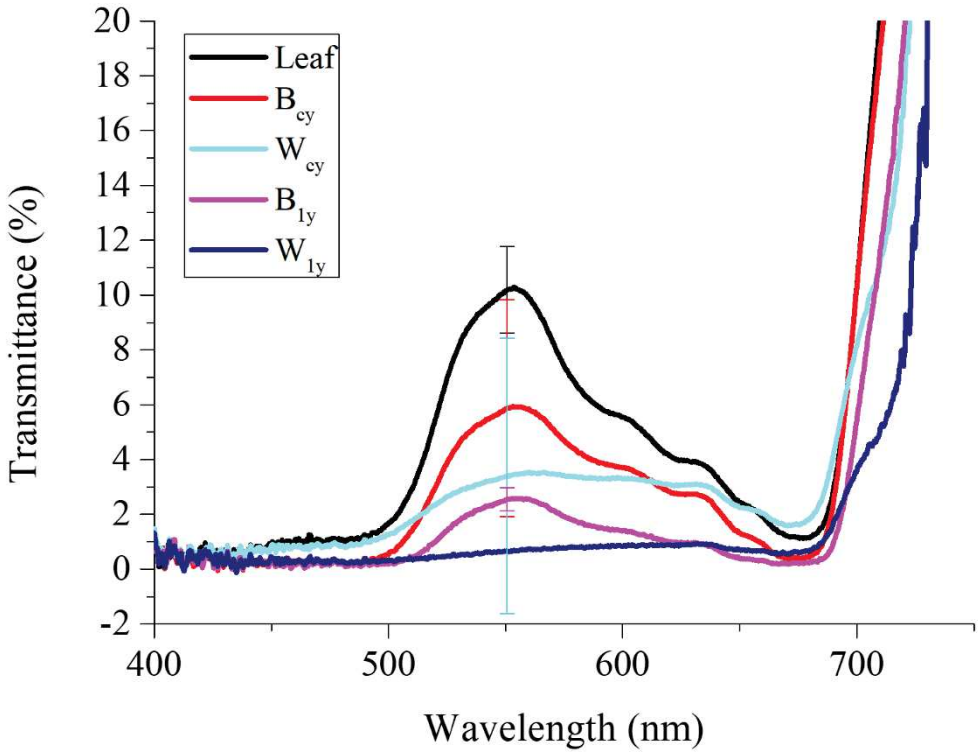

Fig. S3 Light transmission spectra of leaf, bark and wood of current (B_{cy} and W_{cy}) and one-year-old stems (B_{1y} and W_{1y}). Each measurement was averaged 10 times. Spectra were corrected for dark pixels. 100% transmittance is white light.

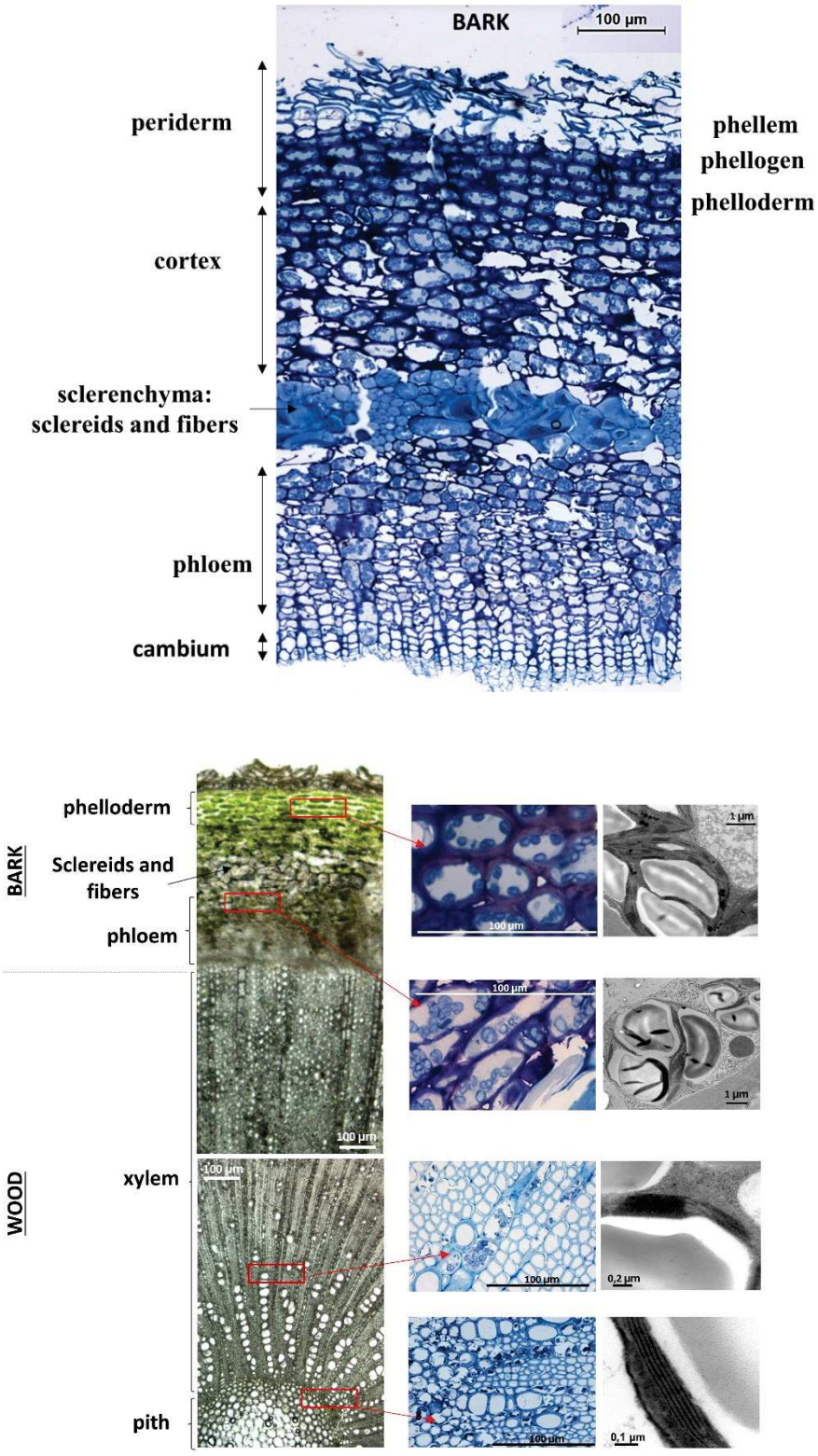

Fig. S4 Representative anatomical transverse-section images of current year stem of *Fraxinus ornus* L.

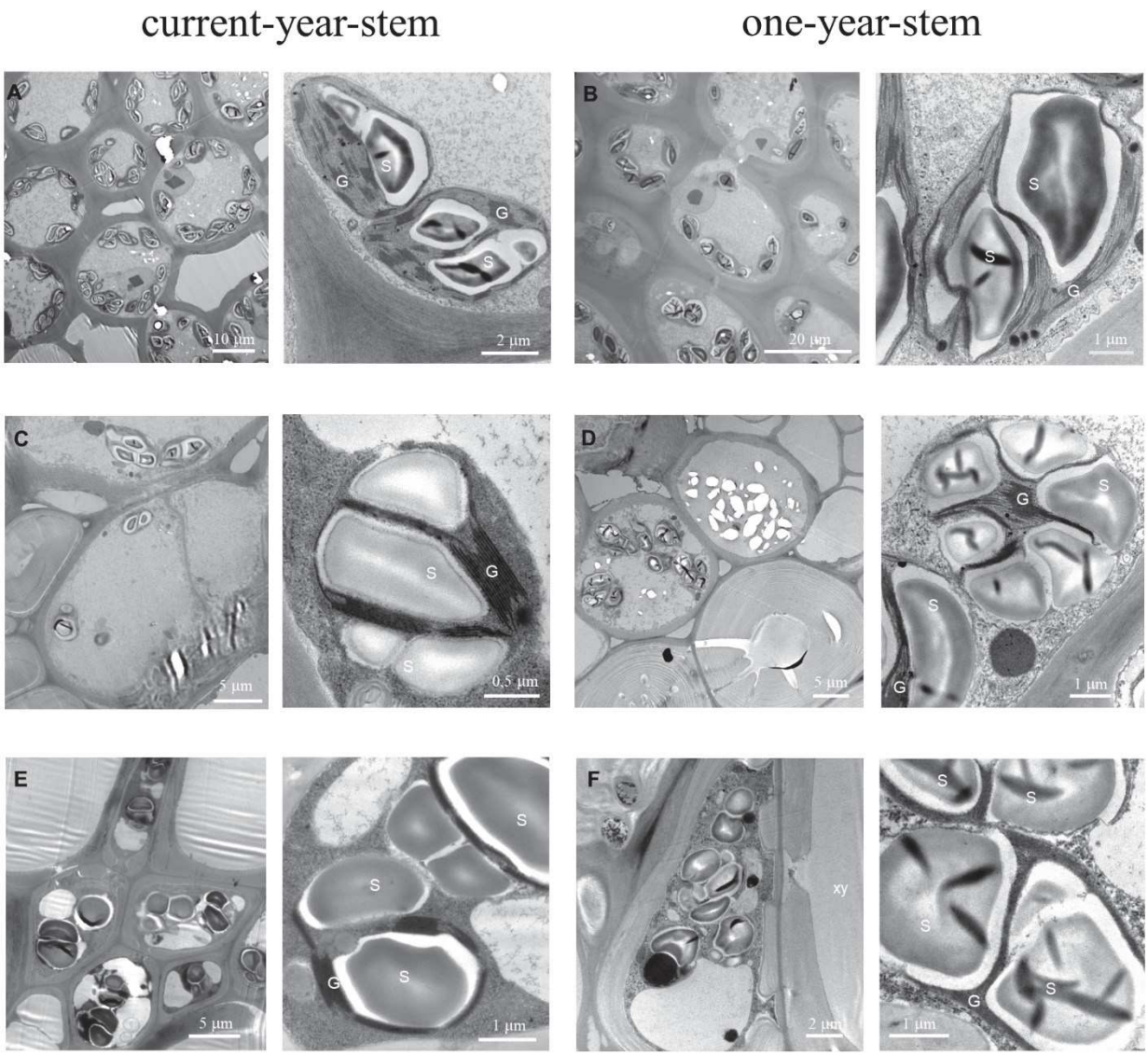

Fig. S5 Electron micrographs of chloroplasts of different stem samples of *Fraxinus ornus* L. For each pair of images, a lower magnification image is shown on the left and a higher magnification focused on chloroplasts is shown on the right. (A, B) Cortical parenchyma of current and one-year-stems. (C, D) Phloem of current and one-year stems. (E, F) Xylem rays of current and one-year-old stems. Abbreviations: G, grana thylakoids; S, starch; xy, xylem rays.

Tissue	Grana n°	Starch n°	Stromal area, µm
Bark – current-year stem (total)	(18±7.89)	(2.81±0.98)	(0.014±0.006)
phelloderm/cortex	24±4.72 a	2.55±1.01	0.015±0.006 a
phloem	11±3.92 b	3.14±0.90	0.011±0.005 ab
Bark – one-year-old stem (total)	(18±8.69)	(2.69±1.14)	(0.018±0.007)
phelloderm/cortex	23±6.23 a	2.3±0.67	0.020±0.008 a
phloem	9±2.04 bc	3.33±1.5	0.014±0.005 ab
Wood – current-year stem	4±2.3 c	2±0.5	0.009±0.004 b
Wood – one-year-old stem	5±1.5 c	3±1.8	0.010±0.004 b

Tab. S1. Mean and the respective standard deviation of grana number (n°), starch n° and stromal area of bark and wood of both current and one-year-old stems of *Fraxinus ornus* L. Different letters indicate significant differences between samples ($P < 0.05$).

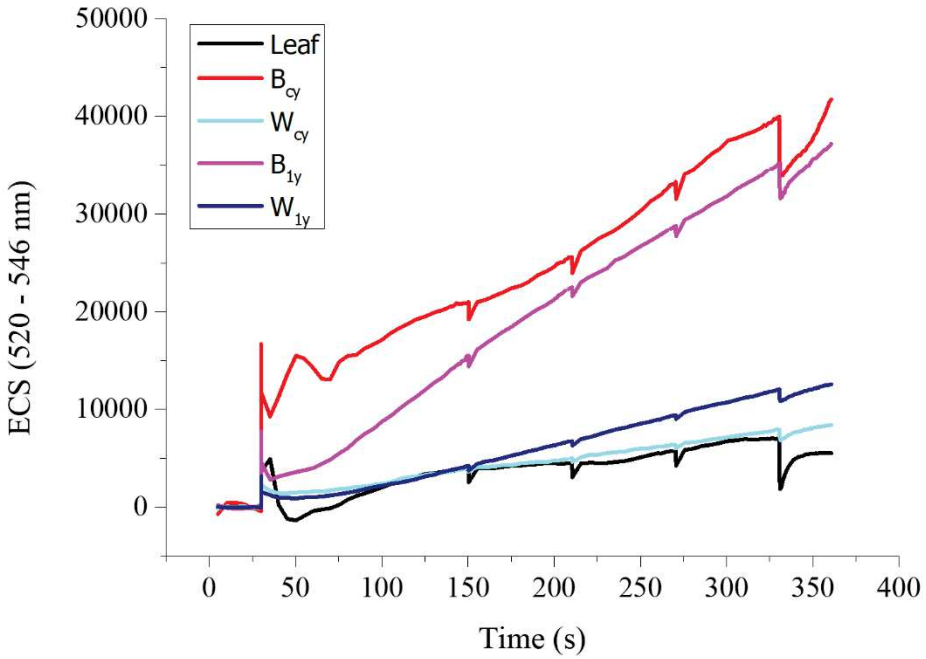

Fig. S6 Kinetics of the ECS (ElectroChromic Shift) of leaf, bark and wood of current year (B_{cy} and W_{cy}) and one-year-old stems (B_{1y} and W_{1y}) of *Fraxinus ornus* L.

Study 2

Light-induced oxygen evolution along the radial profile of *Fraxinus ornus* stems

Sara Natale[1], Lucas Léon Peralta Ogorek[2], Valentino Casolo[3], Ole Pedersen[2], Andrea Nardini[1]

[1] Dipartimento di Scienze della Vita - University of Trieste, Trieste, Italy

[2] The Freshwater Biological Laboratory, Department of Biology, University of Copenhagen, Universitetsparken 4, Copenhagen 2100, Denmark

[3] Dipartimento di Scienze Agroalimentari, ambientali e animali – University of Udine, Udine, Italy

Manuscript under preparation for submission to New Phytologist

Abstract

Most of the woody species possess green stems able to photosynthesize. Photosynthetic stems depend on both on atmospheric CO_2 and internal CO_2, but the actual photosynthetic rate in response to light is still poorly understood.

Here, we decided to apply microsensor technology to stem samples of different ages of *Fraxinus ornus*, to assess the oxygen production in leaves, intact stems, as well as in bark and wood separately. We show that the implementation of these microsensors might significantly increase the understanding of the adaptive responses of stem chloroplasts under different and adverse ambient conditions.

Our study showed a light-induced changes in O_2 production, both of intact stems, and also of isolated bark and wood. Our results confirmed the hypothesis that the younger stems are able to have both a higher light-induced O_2 production and respiration rates compared to older ones. Bark was identified as the most significant contributor to oxygen production.

Furthermore, we report the first radial profile of O_2 production in current-year stems of F. ornus under dark and light conditions. In this way, we were able to finally prove a photosynthetic response of both bark and wood chloroplasts and corroborate the hypothesis that stem chloroplasts are perfectly able to have a light-dependent electron transport.

In conclusion, the radial oxygen profile represents an accurate measurement of stem photosynthesis and can be used in future studies with a focus on the role of stem photosynthesis in drought tolerance.

Keywords: oxygen, stem photosynthesis, microsensor, radial O_2 profile, oxygen evolution rate

Introduction

The occurrence of stem photosynthesis in leaf-bearing woody plants is relatively common (Pfanz and Aschan 2001), recent years have seen a renewed interest in this physiological phenomenon and its possible role in tree resistance/resilience to drought stress (Cernusak and Cheesman 2015; Vandegehuchte et al. 2015). However, while leaf-level photosynthesis has been investigated in detail, the actual functioning and efficiency of stem-level carbon gain, and in particular the relative contributions of bark and wood, are still poorly understood.

Stem photosynthesis can rely on the uptake of atmospheric CO_2 (stem net photosynthesis) and/or re-fixation of CO_2 respired by living stem cells or transported by the transpiration stream (stem recycling photosynthesis) (Ávila et al. 2014; Wittmann et al. 2006; Berveiller et al. 2007; Pfanz et al. 2002; Teskey et al. 2008; Cernusak and Cheesman 2015). Indeed, some studies (e.g. Powers and Marshall 2011; Bloemen et al. 2013) based on isotopic labelling have shown that CO_2 added to the xylem sap was partly transported upward and released to the atmosphere, and partly refixed by photosynthetic stems and petioles.

Due to the very high [CO_2] in the inner portions of stems (ranging from 1 to 26%), and because of the significantly lower surface-to-volume ratio, stem photosynthesis has some advantages compared to leaf photosynthesis, like high water use efficiency and low photorespiration rates (Cernusak and Marshall 2000; Pfanz et al. 2002; Pfanz et al. 2008; Teskey et al. 2008). Hence, stem photosynthesis has been suggested to be an important contributor to the carbon balance of woody plants (Saveyn et al. 2010), especially under stressful conditions imposing stomatal closure and impeding leaf-level carbon gain.

Because stem photosynthesis depends on species-specific traits (e.g. chlorophyll content, bark features) and environmental conditions (e.g. light availability), its efficiency largely differs between/within species, stem age and habitat. In general, young stems appear greenish and are covered by epidermis or a thin bark, allowing efficient transmission of incident light inside the stem, up to 20% for 1-year-old stems compared to about 8% in older ones covered by thicker bark (Damesin, 2003; Pfanz and Aschan 2001; Sun et al. 2003; Wittmann and Pfanz 2016). In fact, young stems might compensate for 60-90% of the potential respiratory carbon loss, with supposedly decreasing contribution to carbon uptake as stems grows older and or in inner stem regions reached by limited amounts of light (Berveiller et al. 2007; Wittmann et al. 2006; Wittmann and Pfanz 2008; Rosell et al. 2015; Tarvainen et al. 2018). However, stem photosynthesis might also be important to raise internal O_2 concentration, avoiding hypoxia in the inner stem portions (Wittmann et al. 2006; Wittmann and Pfanz 2014,2018). Some studies have reported that [O_2] in the sapwood varied between

c. 14-24% and 72-95% values with respect to the atmospheric concentration (e.g. Spicer and Holbrook 2005; Wittmann and Pfanz 2015), with large changes related to species and stem age.

Yet, our knowledge of [O_2] profiles inside the stem, and its changes under variable light conditions, is still poor and generally limited to bark-level corticular photosynthesis (e.g. Wittmann and Pfanz 2014,2018). This is largely due to methodological limitations, which have been overcome by the development of oxygen-sensitive micro-sensors, offering the capability to accurately measure changes in [O_2] concentration at very small spatial scales inside different plant samples (Rolletschek et al. 2009; Pedersen et al. 2020). Indeed, micro-sensors have enabled some detailed studies of O_2 status at bark and sapwood level (e.g. Wittmann and Pfanz 2014, 2018). To date, we still lack accurate data of [O_2] gradients across/within woody stems in response to light presence/absence, and only a static picture of radial [O_2] profile has been described in the stem of a 4-week-old *Ricinus communis* plants (van Dongen et al. 2003).

In this study, we present the first example of high-resolution measurements of light-induced O_2 evolution in the stems of a drought tolerant tree (*Fraxinus ornus* L.). We specifically aimed at: 1) characterizing the photosynthetic activity of bark and wood parenchyma, and their relative contribution to total photosynthesis in stems with increasing age; 2) characterizing the light-response curve of O_2 evolution of current-year stems; 3) measuring radial profile of O_2 evolution from different compartments in a current-year stem. To this aim, we implemented an experimental system based on micro-sensor-based detection of O_2.

Material and methods

Plant material

On June 2022, 25 three-year-olds saplings of *Fraxinus ornus* L. were purchased by a nursery (Planteskoler.dk, Holstebro, Denmark) and grown in 3 L pots in the greenhouse at the University of Copenhagen (DK). Two Tab.ts of OsmocotePlus fertilizer were added to each pot. Plants were regularly irrigated at field capacity and their position in the greenhouse was randomly shifted every week to assure exposure of different plants to uniform light conditions. Analyses were performed on fresh samples of leaves, as well as on bark and wood of current-year (B_{cy} and W_{cy} respectively) and one-year-old (B_{1y} and W_{1y} respectively), and two-year-old stems (B_{2y} and W_{2y} respectively).

Pigment analyses

Pigment analysis was performed on the same samples used for the oxygen evolution measurements (see below). We measured the pigments content of leaves, whole stems (bark+wood), bark and wood

upon extraction of frozen material in 99% ethanol. Samples were cut into small pieces to facilitate the extraction and placed in 2 mL Eppendorf filled up with 1.9mL of ethanol. Samples were stored at 4 °C in the dark for at least 48 h to ensure complete extraction. Then, samples were centrifuged for 3 min (MiniStar silverline, VWR). Absorption spectra were recorded (UV-1800 spectrophotometer, Shimadzu) at 750, 665, 649, and 470 nm, and the final pigment concentration was calculated according to Lichtenthaler et al. (1983). The pigment analysis was performed on samples obtained from four different saplings. Pure 99% ethanol was used as blank.

Measurements of oxygen concentration and evolution

This experiment was aimed at estimating the photosynthetic activity of leaves and stem samples by measuring O_2 production/consumption. Measurements of [O_2] and its changes were made at 26°C using an O_2 optode (Opto-430) connected to an optode-meter (Opto-F4, UniAmp, MicroOptode Meter, Unisense) and inserted into glass vials containing a leaf/stem sample. Vials were kept in a bath at constant temperature. A temperature sensor was connected to the optode meter and placed inside the tank to correct [O_2] for temperature. Time-dependent changes in [O_2] were used to calculate O_2 evolution rate, and normalized by sample fresh weight.

Leaf samples (n=5 x each measurement) were obtained by cutting a piece of 2cmx4cm at the base of each leaf. Outer edges were removed about 1 cm of petiole was maintained for immersion in water, thus allowing to maintain adequate hydration of the sample throughout the measurement. Stem samples were prepared by cutting two pieces of c. 1 cm each of current-year, one-year- and two-year-old stems. One sample was left intact, whereas bark was carefully separated from the wood (cambium was active) in the second sample (n=5 x each measurement).

Each sample was promptly insert in a 10 mL glass-vial containing 0.3 mL of distilled water to maintain hydrated the sample. The vial was sealed with crimp butyl caps of 20 mm (10 mm central hole) and 1.2 mL of air were removed with a syringe, while and 1.2 mL of CO_2 were injected to increase [CO_2] by 10% compared to atmospheric concentration and thus saturate the photosynthetic process. Samples were fixed on a transparent block with Pattafix and submerged in a tank full of distilled water kept at 26 °C (Fig. S1). The water level was set just below the surface of the cap, so that the tip of the sensor did not get wet during the measurement. After 20 min of both dark and temperature adaptation, the first measurement (starting point) was taken, thereafter samples were dark adapted overnight and a second reading was taken in the following morning (dark respiration). Then, light was switched on (PPFD = 1000 μmol m^{-2} s^{-1} for 4 h, and a third measurement was performed (light-response). After this last measurement, samples were immediately weighted to obtain their fresh weight, using an analytical balance (Mettler Toledo Analytical Balance ME54), and stored at -

20°C until pigment extraction (see above). For each measurement, the sensor was inserted in the vial, waiting about 1 minute to balance the sensor and then reading [O_2] value.

Another set of leaf and current-year stem samples, prepared as described above, was used to measure the light-response curve of oxygen evolution. The lamp was moved backward in order to obtain different light intensities with PPFD of 50, 100, 300 and 1000 μmol m^{-2} s^{-1} (n=3 x each measurement). In this case, stem samples were initially dark adapted for 4 h and then light adapted overnight before taking measurements. Leaves were dark adapted for 2 h and light adapted for 1 h. PPFD was measured with quantum meter (LI-250A, LI-COR).

Radial stem profile of O_2 evolution

Radial profiles of [O_2] were measured to confirm light-mediated oxygen release by stem parenchyma cells, as a proxy of net photosynthetic rates at bark, wood and pith level. Measurements were based on the approach described in Colmer et al. (2020) and Peralta Ogorek et al. (2021), with some modifications. Clark-type micro-sensors measuring oxygen partial pressure (OX-50, Unisense A/S) were connected to a meter (*fx*-6, UniAmp, Unisense A/S) and a motor controller. Micro-sensors were calibrated before each set of measurements. Calibration was made under [O_2] = 0 (2 g ascorbate in 100 mL deionized water in 0.1 N NaOH) and deionized water at air equilibrium ([O_2] = 257.9 μmol l^{-1} at 25°C, pO_2 = 20.6 kPa).

A current-year stem segment (n=5) was cut underwater and the cut ends were sealed with parafilm. A hole (c. 1 mm) was made with a drill in the center of the stem and the sample was fixed on a metal mesh placed in a plastic tank (Fig. S2). The hole was filled with de-oxygenized agar 0.1%, using a syringe. By using a micro-manipulator, the micro-sensor was positioned in the middle of the hole, and the exact starting position (at the level of the cortex) was set. Sample was then submerged in agar 0.1%, and flushed with N_2 nitrogen to lower [O_2]. The bulk agar was monitored using an O_2 optode (OP-MR and MicroOptode Meter; Unisense A/S). Temperature was also monitored to adjust [O_2] to the temperature.

[O_2] profiles were taken with a spatial resolution of 25 μm starting at the stem surface (0 point) and then moving to bark, wood, and down to the pith. The O_2 microsensor was left in each position for 5 s to allow for a full response. [O_2] measurements were taken also 1000, 500, 400, 300, 200 and 100 μm away from the 0 point to monitor oxygen concentration in the bulk medium close to the sample. Each sample was adapted in the medium for 15 minutes before taking the first measurement (not shown) to overcome the temporary increase in the stem respiration due to the drilling's wound (Levy et al. 1999). Light with a PPFD of 700 (μmol m^{-2} s^{-1}) was provided by a fiber-optic illuminator (Schott KL1500). After the measurement period, the stem was dissected along the insertion point of the

microsensor with a Leica VT1200 S vibrating blade microtome, and visualized using an Olympus BX60 light microscope, to obtain the exact measurement positions along the stem radial profile.

Statistics

Statistical analyses were performed with R software (R Core Team 2022). The normality of residuals and homogeneity of variances were tested. When homogeneity of variances assumption was violated, generalized least square (GLS) models were performed, using "gls" function including the 'varPower' variance structure. Three-way Anova analysis through "aov" function in "stats" R package was used. For significance tests, differences between groups were tested post hoc with "Holm" contrasts using the emmeans function (emmeans package). Boxplot panels were made using "ggplot2" package in R. Light-response curves and radial oxygen profile graph were prepared with Origin 9.0 software (Northampton, MA, USA).

Results

Pigment content

Chlorophylls (Chl) and carotenoids (Car) were detected throughout the stems, both in the bark and in the wood. In wood of one- and two-year-old stems pigment content was too low to be detected . However, total Chl content (Chl*a*+*b*) was higher in current-year stems and decreased with increasing stem age (Tab. 1). The same trend was observed also when considering isolated bark samples. Therefore, the Chl*a*/*b* ratios were similar intact stems and bark samples, with a decrease in current-year wood. On the contrary, Car/Chl ratios were similar intact stems and bark samples, with a slight relative increase in current-year wood.

Sample	Chl*a*+*b*, mg/g	Chl *a*/*b*	Car/Chl
Leaf	4.17±0.80a	3.11±0.33a	0.14±0.02a
Scy	0.27±0.05b	2.63±0.15b	0.20±0.01bcd
S1y	0.15±0.03c	2.44±0.25b	0.22±0.01d
S2y	0.13±0.01c	2.68±0.36b	0.22±0.02cd
Bcy	0.76±0.17d	2.58±0.12b	0.18±0.01bc
B1y	0.47±0.14ed	2.50±0.14b	0.18±0.01bcd
B2y	0.39±0.11e	2.47±0.22b	0.18±0.02b
Wcy	0.03±0.01f	1.61±0.08c	0.30±0.03e

Tab. 1 Total chlorophyll (Chl*a*+*b*) concentration, chlorophyll *a*/*b* (Chl *a*/*b*) ratio and carotenoid (Car) / Total chlorophyll (Car/Chl) ratio measured in leaves, in intact stems and isolated bark and wood samples of current-year, one-year and two-year stem segments of *Fraxinus ornus* L. saplings. S: stem; B: bark; W: wood; cy:

current-year; 1y: one-year-stem; 2y: two-year-stem. Mean values ± S.D are reported. (n = 5). Different letters indicate significant difference between samples ($P < 0.05$).

Net oxygen exchange under dark and light conditions

As expected, leaves had the highest O_2 release rate under light conditions (111.74±11.38, nmol O_2 g^{-1} FM sec^{-1}), compared to stems samples (Fig. 1). Light-induced O_2 production was tendentially higher in current-year stems (2.03±1.22, nmol O_2 g^{-1} FM sec^{-1}) compared to one- and two-year-old ones, independently if we were considering intact stems or bark and wood separately (Fig. 1). Under dark conditions, net O_2 exchange became negative for all samples investigated (Fig. 1), indicating oxygen consumption via respiration. Measurement in dark-adapted samples revealed higher respiration rates for leaves and bark (especially of current-year stem) compared to wood. Once corrected by subtracting the oxygen evolution rate obtained in the dark and normalized on the mean value of total chlorophyll (Chl*a*+*b*) concentration for each tissue, the photosynthetic oxygen evolution rate was positive for samples of stem current year and bark of current and one-year old stems (Tab. S1).

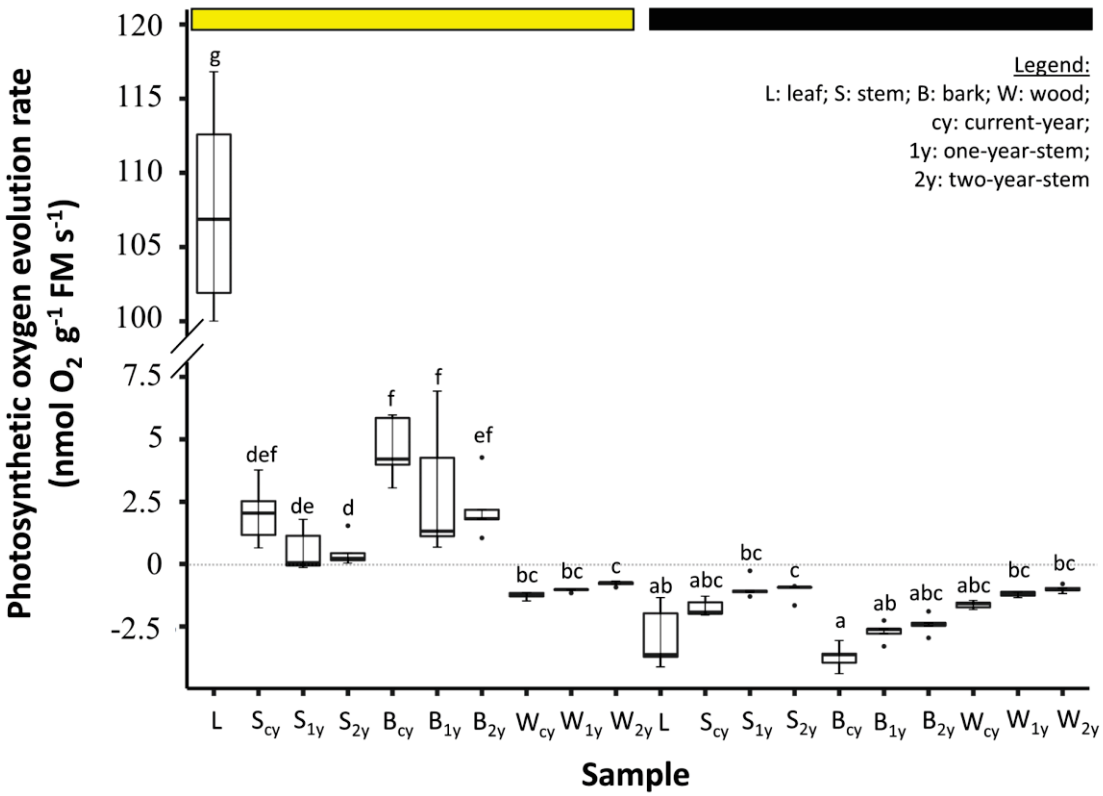

Fig. 1 Median values, 25th and 75th percentiles of mass-based photosynthetic O_2 evolution rate measured in leaves as well in intact stems and isolated bark and wood samples of current-year, one-year and two-year stem segments of *Fraxinus ornus* L. saplings (n=5 x each sample). Yellow box: the light was on (1000 µmol m^{-2} s^{-}

[1]); black box: the light was switched off. Different letters indicate significant differences between samples ($P < 0.05$).

The same trend was observed in the light-response curves, both in intact stems and isolated bark and wood compartments (Fig. 2). Bark showed a larger increase in light-induced O_2 release compared both to intact stem and isolated wood. Besides the lower photosynthetic response of wood, all the samples showed a light-induced photosynthetic response. Specifically, net oxygen production was reached at 100 PPFD (µmol/m^2/s) for intact stems and isolated bar.

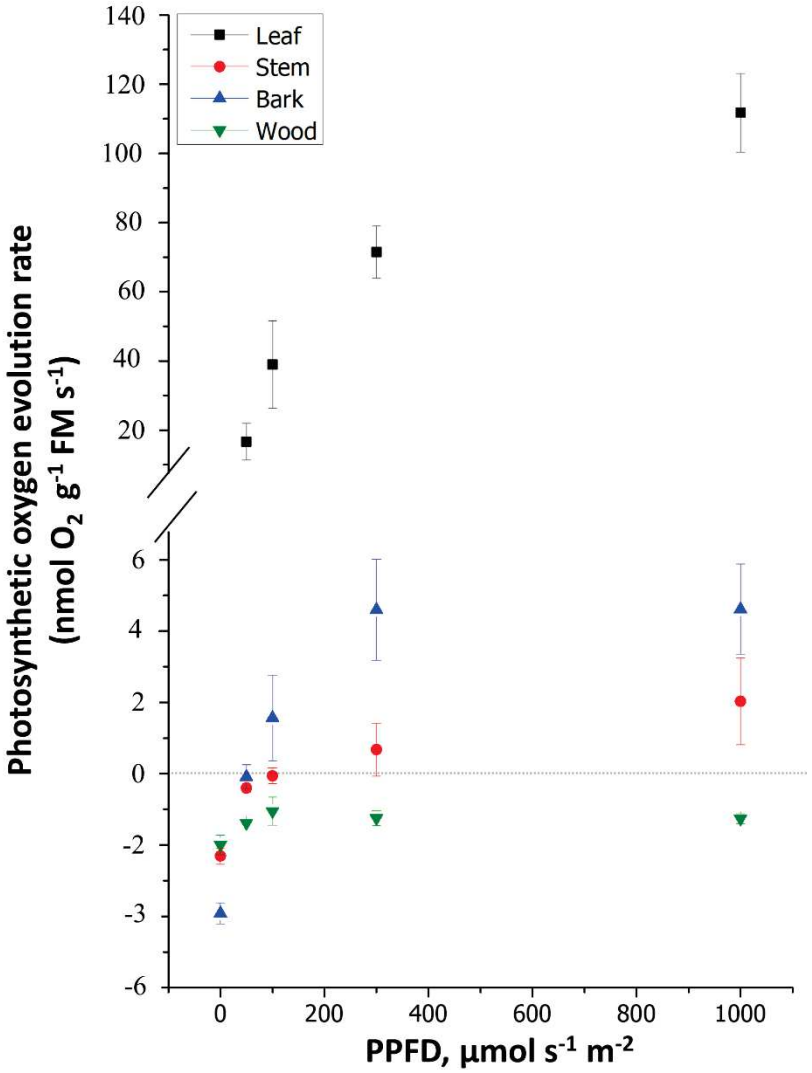

Fig. 2 Light-response curves of photosynthetic O_2 evolution rate, normalized on sample fresh mass (nmol O_2 g^{-1} FM s^{-1}), measured in leaves as well as in intact stems and isolated bark and wood samples of current-year stem segments of *Fraxinus ornus* L. saplings. Curves shown are average of 3-5 independent measurements. Positive rate indicates positive net photosynthesis; respiration is always negative.

Radial stem profile of light-induced O_2 evolution

The novel O_2 microsensor approach enabled us to accurately measure of small-scale changes of [O_2] in illuminated stems (Fig. 3). After dark adaptation, measurements showed a complete equilibration of [O_2] across all the stem tissues. On the contrary, after 1h of light exposure we detected revealed higher [O_2] with a peak at bark level and declining values toward the wood, approaching zero at pith level. The bulk medium showed significantly lower [O_2] throughout measurements.

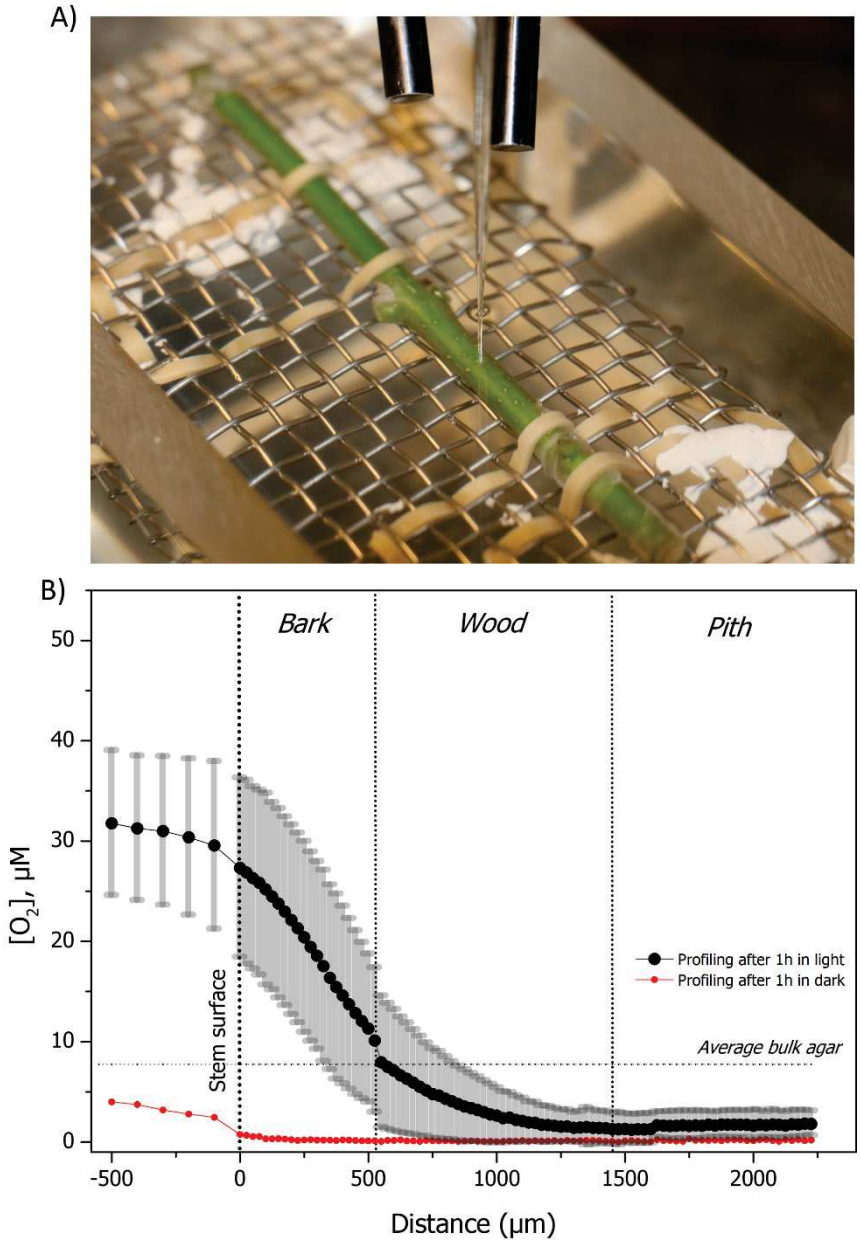

Fig. 3 A) Photograph of the experimental setup with a zoom on the microsensor insertion point. B) Oxygen profile across the current-year stems (n=5) of *Fraxinus ornus* L. saplings, grown under normal light conditions in a greenhouse at the University of Copenhagen (Denmark).

Discussion

Our study represents one of the first examples of light-induced changes in O_2 production of whole stems and, most importantly, of isolated compartments (bark and wood) from stems with different age. Our data offer new insights into patterns of O_2 release, and hence photosynthetic activity in different stem regions. Furthermore, we report a highly detailed radial profile of O_2 exchange along current-year stems, providing strong evidence for the photosynthetic competence of living cells at bark and wood level.

Current-year stems showed both higher light-induced O_2 production and dark respiration rates, compared to one-year and two-year-old stem segments, implying higher photosynthetic rates and a potentially important contribution to net carbon gain and/or in preventing the risk of hypoxia in internal stem tissues. In any case, regardless of the stem age, intact stem segments always showed the ability to perform positive net photosynthesis, with rate of oxygen evolution up to 2.03 nmol O_2 g^{-1} FM s^{-1} (Fig. 1).

Experiments performed on isolated bark and wood samples led to contrasting results. Bark emerged as the compartment contributing most to the production of oxygen, especially in current-year samples. Even for isolated bark, O_2 evolution rates progressively decreased for older stems. On the contrary, wood was never capable to display a net oxygen release, regardless of the age considered. Different results were obtained by Wittmann et al. (2006), who observed no net O_2 production when considering intact branches of *Betula pendula*, but a positive net photosynthetic rate after bark removal. It is possible that this discrepancy marks species-specific characteristics of stem photosynthetic apparatus in terms of size and/or specific features, maybe dependent on the optical properties of the bark, which influence both the light penetration capacity and gas permeability. The bark represents a barrier to radial CO_2 diffusion, and its removal from the wood allowed a better gas diffusion as well as light penetration trough wood compartment. Here, we cannot quantify stem photosynthesis based on net atmospheric CO_2 uptake or internal CO_2 recycling, but we can safely conclude that stem photosynthesis of *F. ornus* saplings is mainly sustained by bark photosynthesis, whereas wood photosynthesis hardly counterbalanced O_2 depletion related to the respiratory activity of the living cells of stem tissues. These results are in accordance with observations showing that the proportion of living cells generally decreases from the outer bark towards the pith (Stockfors and Linder 1998). In accordance, bark of current-year stem showed higher respiration rates then wood of one- and two-year-old stems. In line with our results, Pruyn et al. (2002) found 2-3 fold higher respiration rates for inner bark than sapwood in Douglas-fir. Furthermore, [O_2] measured in the bark was always higher than values measured in sapwood in different species from different authors (e.g.

Gansert 2001; Sorz and Hietz 2008; Wittmann et al. 2018), corroborating the hypothesis that stem photosynthesis is mainly driven by bark chloroplasts.

The progressive decrease in pigment concentration and chloroplast density from the bark to the pith observed in *F. ornus* (Tab. 1; Natale et al. submitted, study#1), might be responsible for the lower photosynthetic activity of the wood compared to bark. As stated in the introduction, an important limiting factor for corticular and wood photosynthesis is available light. It is important here to remind that only a minor fraction of the photosynthetically active radiation (mainly red- far-red light) can reach the inner woody tissues (e.g. Pfanz et al. 2002), possibly further restricting the photosynthetic activation of wood chloroplasts. In this light, to determine the potential photosynthetic capacity and oxygen release rate of each stem compartment (bark and wood), light-response curves of $[O_2]$ release were performed on isolated stem tissues were conducted.

Our data showed that peeled bark had higher maximum net photosynthetic rates than both intact stem and wood. Indeed, net photosynthetic oxygen release could be measured already at 100 PPFD for bark and intact stem. Interestingly, although wood photosynthesis never produced a positive net O_2 release upon illumination, a light-induced increased of oxygen production could be indeed detected. These results induce us speculate that stem chloroplasts at wood level might still be involved into partial re-fixation of respiratory CO_2 and might help plants to buffer NSC depletion under prolonged drought conditions.

We present here the first radial profile of O_2 production within current-year stems in response to light (Fig. 3). These data show an increase in O_2 production in stems exposed to light for 1 h, with different rates in the different stem compartments. O_2 production sharply decreased when moving from the bark to the pith. Specifically, c. 10-30 µM O_2 were measured at the bark level, 0-8 µM O_2 at the wood level and c. 0-2 µM O_2 at pith level. Considering that dark adaptation $[O_2]$ was c. 0 µM throughout the stem profile, while the bulk medium had $[O_2]$ = 8 µM O_2, we are confident that the oxygen released after 1 h of light exposure was produced by the photosynthetic activity of chloroplasts, and was not a result of oxygen diffusion from the medium to the sample.

Precise measurements of net O_2 exchange within stems are crucial for understating bark and wood photosynthesis, and their actual contribution to the plant carbon metabolism or to the regulation of oxygen levels inside thick organs like stems. In this view oxygen micro-sensors offer the possibility to investigate radial oxygen profiled in stems of different species and under different environmental conditions, opening new doors to our understanding of stem photosynthesis and its role in both wild and cultivated plants facing a warmer and drier future, that might impose more frequent and longer period of stomatal closure.

Author contributions

SN, AN, VC, OP, LLPO designed the experiment; SN performed pigments analysis; SN and LLPO performed microsensor measurements and analysis; SN and AN wrote the manuscript, with contributions and revisions from all authors.

References

Ávila E, Herrera A, Tezara W. 2014. Contribution of stem CO_2 fixation to whole-plant carbon balance in nonsucculent species. *Photosynthetica* **52:** 3–15.

Berveiller D, Kierzkowski D, Damesin C. 2007. Interspecific variability of stem photosynthesis among tree species. *Tree Physiology* **27:** 53–61.

Bloemen J, Overlaet–Michiels L, Steppe K. 2013. Understanding plant responses to drought: how important is woody tissue photosynthesis? *Acta Horticulturae* **991:** 149–157.

Cernusak LA, Cheesman AW. 2015. The benefits of recycling: how photosynthetic bark can increase drought tolerance. *New Phytologist* **208:** 995–997.

Colmer TD, Winkel A, Kotula L, Armstrong W, Revsbech NP, Pedersen O. 2020. Root O_2 consumption, CO_2 production and tissue concentration profiles in chickpea, as influenced by environmental hypoxia. *New Phytologist* **226:** 373–384.

Damesin C. 2003. Respiration and photosynthesis characteristics of current-year stems of *Fagus sylvatica*: from the seasonal pattern to an annual balance. *New Phytologist* **158:** 465–475.

Gansert D, Burgdorf M, Lösch R. 2001. A novel approach to the in situ measurement of oxygen concentrations in the sapwood of woody plants. *Plant, Cell & Environment* **24:** 1055–1064.

Levy PE, Meir P, Allen SJ, Jarvis PG. 1999. The effect of aqueous transport of CO_2 in xylem sap on gas exchange in woody plants. *Tree Physiology* **19:** 53–58.

Lichtenthaler HK, Wellburn AR. 1983. Determinations of total carotenoids and chlorophylls *a* and *b* of leaf extracts in different solvents. *Biochemical Society Transactions* **11:** 591–592.

Peralta Ogorek LL, Pellegrini E, Pedersen O. 2021. Novel functions of the root barrier to radial oxygen loss–radial diffusion resistance to H_2 and water vapour. *New Phytologist* **231:** 1365–1376.

Pedersen O, Revsbech NP, Shabala S. 2020. Microsensors in plant biology: in vivo visualization of inorganic analytes with high spatial and/or temporal resolution. *Journal of Experimental Botany* **71:** 3941–3954.

Pfanz H, Aschan G. 2001. The existence of bark and stem photosynthesis in woody plants and its significance for the overall carbon gain. An eco-physiological and ecological approach. In: Essr K, Luttge U, Kadereit JW, Beyshlag W, eds. *Progress in Botany*, Berlin, DE: Springer-Verlag, 477–510.

Pfanz H, Aschan G, Langenfeld-Heyser R, Wittmann C, Loose M. 2002. Ecology and ecophysiology of tree stems: corticular and wood photosynthesis. *Naturwissenschaften* **89:** 147–162.

Powers EM, Marshall JD. 2011. Pulse labeling of dissolved ^{13}C-carbonate into tree xylem: developing a new method to determine the fate of recently fixed photosynthate. *Rapid Communications in Mass Spectrometry* **25:** 33–40.

Pruyn ML, Gartner BL, Harmon ME. 2002. Within-stem variation of respiration in *Pseudotsuga menziesii* (Douglas-fir) trees. *New Phytologist* **154:** 359–372.

R Core Team. 2022. R: A language and environment for statistical computing. R Foundation for Statistical Computing, Vienna, Austria. URL https://www.R-project.org/.

Rolletschek H, Stangelmayer A, Borisjuk L. 2009. Methodology and significance of microsensor-based oxygen mapping in plant seeds–an overview. *Sensors* **9:** 3218–3227.

Rosell, JA, Castorena M, Laws CA, Westoby M. 2015. Bark ecology of twigs vs. main stems: functional traits across eighty-five species of angiosperms. *Oecologia* **178:** 1033–1043.

Saveyn A, Steppe K, Ubierna N, Dawson TE. 2010. Woody tissue photosynthesis and its contribution to trunk growth and bud development in young plants. *Plant, Cell & Environment* **33:** 1949–1958.

Sorz J, Hietz P. 2008. Is oxygen involved in beech (*Fagus sylvatica*) red heartwood formation? *Trees* **22:** 175–185.

Spicer R, Holbrook NM. 2005. Within-stem oxygen concentration and sap flow in four temperate tree species: does long-lived xylem parenchyma experience hypoxia? *Plant, Cell & Environment* **28:** 192–201.

Stockfors J, Linder S. 1998. Effect of nitrogen on the seasonal course of growth and maintenance respiration in stems of Norway spruce trees. *Tree Physiology* **18:** 155–166.

Sun Q, Yoda K, Suzuki M, Suzuki H. 2003. Vascular tissue in the stem and roots of woody plants can conduct light. *Journal of Experimental Botany* **54:** 1627–1635.

Tarvainen L, Wallin G, Lim H, Linder S, Oren R, Löfvenius MO, Räntfors M, Tor-Ngern P, Marshall J. 2018. Photosynthetic refixation varies along the stem and reduces CO_2 efflux in mature boreal *Pinus sylvestris* trees. Tree Physiology **38:** 558–569.

Teskey RO, Saveyn A, Steppe K, McGuire MA. 2008. Origin, fate and significance of CO_2 in tree stems. *New Phytologist* **177:** 17–32.

Vandegehuchte MW, Bloemen J, Vergeynst LL, Steppe K. 2015. Woody tissue photosynthesis in trees: salve on the wounds of drought? *New Phytologist* **208:** 998–1002.

van Dongen JT, Schurr U, Pfister M, Geigenberger P. 2003. Phloem metabolism and function have to cope with low internal oxygen. *Plant Physiology* **131:** 1529–1543.

Wittmann C, Pfanz H, Loreto F, Centritto M, Pietrini F, Alessio G. 2006. Stem CO_2 release under illumination: corticular photosynthesis, photorespiration or inhibition of mitochondrial respiration? *Plant, Cell & Environment* **29:** 1149–1158.

Wittmann C, Pfanz H. 2008. General trait relationships in stems: a study on the performance and interrelationships of several functional and structural parameters involved in corticular photosynthesis. *Physiologia Plantarum* **134:** 636–648.

Wittmann C, Pfanz H. 2014. Bark and woody tissue photosynthesis: a means to avoid hypoxia or anoxia in developing stem tissues. *Functional Plant Biology* **41:** 940–953.

Wittmann C, Pfanz H. 2016. The optical, absorptive and chlorophyll fluorescence properties of young stems of five woody species. *Environmental and Experimental Botany* **121:** 83–93.

Wittmann C, Pfanz H. 2018. More than just CO_2-recycling: corticular photosynthesis as a mechanism to reduce the risk of an energy crisis induced by low oxygen. *New Phytologist* **219:** 551–564.

Supplementary material

Fig. S1 Photograph of the experimental MicroRespiration setup.

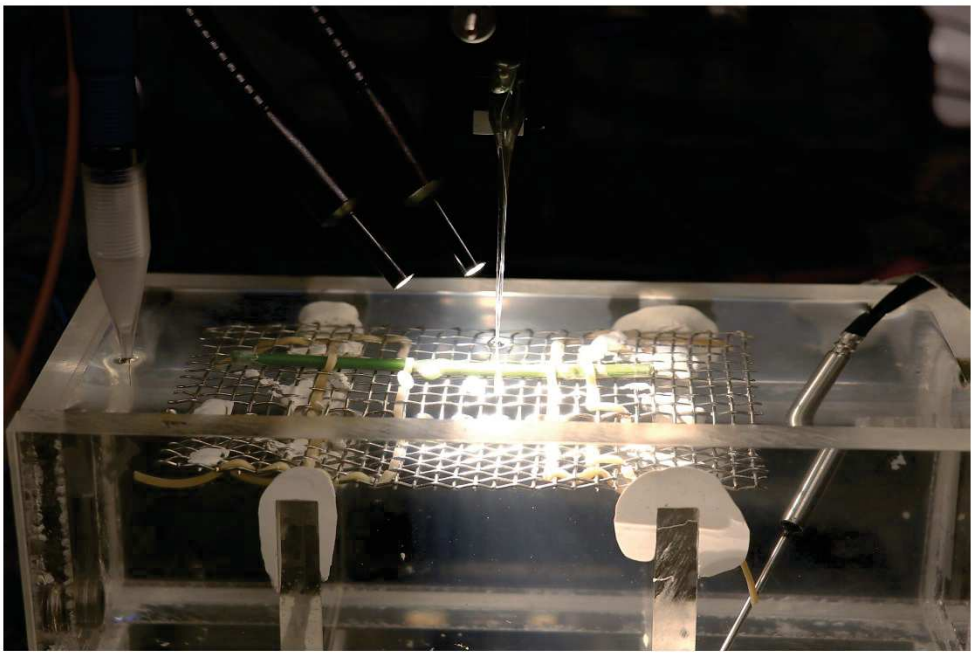

Fig. S2 Photograph of the experimental setup of microsensor system.

Sample	Photosynthetic O_2 evolution rate ($nmol\ O_2\ mg^{-1}\ Chl\ sec^{-1}$)
Leaf	3.20 ± 0.5
S_{cy}	0.11 ± 2.4
S_{1y}	-2.75 ± 4.0
S_{2y}	-2.26 ± 5.1
B_{cy}	0.33 ± 0.6
B_{1y}	0.09 ± 2.1
B_{2y}	-0.13 ± 1.2
W_{cy}	-4.77 ± 0.8

Tab. S1 Photosynthetic oxygen evolution rate corrected by subtracting the oxygen evolution rate obtained in the dark and normalized on the mean value of total chlorophyll (Chl*a*+*b*) concentration for each tissue, measured in leaves, in intact stems and isolated bark and wood samples of current-year, one-year and two-year stem segments of *Fraxinus ornus* saplings. S: stem; B: bark; W: wood; cy: current-year; 1y: one-year-stem; 2y: two-year-stem. Mean values ± S.D. are reported (n = 5).

Chapter II

Study 3

Stem photosynthetic efficiency across woody Angiosperms and Gymnosperms with contrasting drought tolerance

Sara Natale[1], Francesco Petruzzellis[1], Alessandro Alboresi[2], Nicoletta La Rocca[2], Tomas Morosinotto[2], Andrea Nardini[1]

[1]Department of Life Sciences, University of Trieste, Trieste, Italy

[2]Department of Biology, University of Padova, Padova, Italy

Manuscript submitted to Trees - Structure and Function

Abstract

Stem photosynthesis is thought to be involved in tree resistance/resilience to water shortage. Recent studies have focused on the coordination between stem photosynthesis and hydraulics, but the generality of association of stem photosynthetic efficiency with species-specific adaptation to drought is still unclear. We quantified bark and wood chlorophyll *a* fluorescence (in terms of Fv/Fm) in current-year, one-year and two-year-old stems of several woody species harvested in diverse habitats. We ranked species in terms of relative drought tolerance on the basis of their vulnerability to xylem embolism (P_{50}), and compared stem photosynthetic efficiency of drought tolerant vs drought sensitive species. Fv/Fm values decreased with increasing stem age, and were generally higher for Angiosperms than Gymnosperms. Fv/Fm both at the bark and wood level was higher for drought tolerant Angiosperms compared to drought sensitive ones. Our results highlight the potential adaptive role of stem photosynthesis in drought tolerant species, thriving under arid conditions likely leading to prolonged stomatal closure and halt of leaf-level carbon gain.

Keywords: bark, P_{50}, stem photosynthesis, drought, wood, Fv/Fm

Introduction

Leaves are the most important photosynthetic organs in most woody plants, but nearly all of them can also perform this fundamental physiological process at stem level. Early observations of 'green stems' date back to the early 20th century (e.g. Cannon 1908). Since then, photosynthetically competent stems have been detected in a wide range of woody plants typical of Mediterranean ecosystems, subtropical warm deserts, and tropical arid lands worldwide (e.g. Dima et al. 2006; Ávila et al. 2014). Indeed, photosynthetic stems are widely spread throughout different species and biomes (Teskey et al. 2008; Ávila et al. 2014). Stem photosynthesis is obviously common in succulent stems of CAM plants, but it occurs also in bark, wood and pith of woody plants (Pfanz et al. 2002; Wittmann et al. 2016). Stem photosynthetic efficiency is apparently species-specific and varies on a seasonal scale, thus suggesting that it might be very important from a functional and ecological point of view (Rentzou and Psaras 2008).

Although stems are not specialized for photosynthesis, due to their unfavorable surface-to-volume ratio and low light transmittance, it is known that chlorophyll is synthetized in functional chloroplasts even in deep wood layers of aged stems (Pfanz et al. 2002). Most woody species show a greenish inner bark and cortical parenchyma (e.g. Pfanz et al. 2002; Wittmann and Pfanz 2008, 2014), but chloroplasts can also be found along the xylem rays and in the pith, suggesting that they are not restricted to the relatively more illuminated outer cell layers of the stem (Dima et al. 2006; Berveiller et al. 2007; Yiotis et al. 2009). Among these, bark exhibits higher chlorophyll concentration and photochemical efficiency than other stem compartments (e.g. Yiotis et al. 2009; Wittmann and Pfanz 2016; Liu et al. 2018).

The amount and quality of light transmitted through the stem might be a key factor governing stem photosynthetic capacity (Manetas et al. 2005; Cernusak and Cheesman 2015; Wittmann and Pfanz 2016). Typically, about 15% of incident PAR can penetrate the periderm, (Cernusak and Marshall 2000), but light transmittance changes according to stem anatomy (bark thickness, cell-wall lignification), age and environment (Cernusak and Marshall 2000; Pfanz et al. 2002; Wittmann and Pfanz 2008). Blue light photons are largely absorbed by the outer bark, while red and far-red light penetrate more in depth, reaching the underlying xylem and pith. In addition, it is also possible that the optical properties of vascular tissue allow some axial light conduction to the pith cells (Sun et al. 2003).

Stems covered by an outer epidermis with stomata and/or periderm with lenticels, can rely on net uptake of atmospheric CO_2 (Ávila et al. 2014). Otherwise, internal re-assimilation of CO_2 released by respiration of underlying heterotrophic tissues is also possible (e.g. Cernusak and Marshall 2000;

Pfanz et al. 2002; Wittmann and Pfanz 2008; Berveiller et al. 2007). Internal CO_2 might be available at much higher concentrations within the stem (Teskey et al. 2008) compared to leaves, up to levels inhibiting photorespiration thus increasing quantum yield of photosynthesis (Berveiller et al. 2007). Previous studies have shown that net photosynthetic rates of stems can be up to 60% of those recorded for leaves (Ávila et al. 2014), and these rates are maintained even throughout the dry season when stomatal closure reduces leaf-level net carbon uptake (Ávila-Lovera et al. 2017). Hence, stem photosynthesis might provide an extra carbon gain under conditions imposing stomatal closure and limiting leaf photosynthesis. The carbon gain assured by stem photosynthesis might also contribute to bud development, flowering, and recovery after herbivores attack (Saveyn et al. 2010). More recently, stem photosynthesis has been suggested to contribute to the maintenance and recovery of xylem hydraulic function (Saveyn et al. 2010; Schmitz et al. 2012; Bloemen et al. 2016; De Baerdemaeker et al. 2017; Trifilò et al. 2017; Tomasella et al. 2021).

Based on the above, stem photosynthesis might be particularly useful to maintain carbon uptake and physiological activities of plants during leafless periods, or under environmental conditions limiting leaf gas exchange (Ávila et al. 2014), with specific reference to drought. In particular, locally produced photosynthates might be used to sustain stem non-structural carbohydrates (NSC) pools to buffer carbon starvation under drought stress (De Roo and Salomón 2020), and refill embolized xylem upon drought relief (Schmitz et al. 2012; Liu et al. 2019).

In this study, we investigated possible differences in terms of stem photosynthetic efficiency across a set of woody plants from different habitats. Our analysis was based on 39 woody species (both Angiosperms and Gymnosperms) from a broad phylogenetic range that were categorized in terms of relative drought tolerance in terms of species-specific vulnerability to xylem embolism. We specifically addressed the following questions: i) are there differences in maximum quantum yield of photosystem II (Fv/Fm) of bark and wood in stems of different ages, and between various Angiosperm and Gymnosperm species? ii) Are there any significant differences in terms of stem Fv/Fm in drought tolerant vs drought sensitive species?

Material and methods

Plant material and experimental design

All experiments and measurements were carried out at the University of Trieste. Sampling of plant material was done in three different geographical areas to obtain stems from species with contrasting phylogenies and/or adapted to different environmental conditions: i) the botanical garden at the University of Trieste; ii) the Classical Karst, a limestone plateau extending by ~500 km^2, nearby

Trieste; iii) montane forests nearby the village of Forni di Sopra, located in the Friulian Dolomites. Sampling was done between 6-8 a.m. in June 2021 for sites i) and ii), and in mid-July for site iii). Three individuals per species were randomly selected, and two sun-exposed branches (about 3-4 years old) were sampled from each tree, for a total of 6 branches per species. Branches were immediately re-cut for 2-5 cm underwater and stored in a bucket with the cut section immersed in water to avoid dehydration until processing in the laboratory. Three branches (one per individual) were used for chlorophyll fluorescence measurements, while the other three branches were used to measure wood density, as described below. The complete list of species is reported in Tab. S1. Analyses of photosynthetic efficiency were made on current-year, one-year and two-year-old stem segments, both at bark and wood level (Fig. 1).

Fig. 1 Example of a stem sample selected for the measurements.

Chlorophyll fluorescence

Measurement of chlorophyll *a* fluorescence is a powerful technique for *in vivo* analysis of different photosynthetic parameters (Maxwell and Johnson 2000). One of the most relevant parameters to estimate the effective yield (or maximal photochemical efficiency) of PSII is the Fv/Fm ratio (Maxwell and Johnson 2000; Schreiber 2004), which indicates the intrinsic efficiency of PSII photochemistry of dark-adapted samples (Aschan et al. 2005). Chlorophyll fluorescence was measured in the laboratory using an imaging PAM chlorophyll fluorometer equipped with a high-resolution camera (6.45 µm x 6.45 µm, resolution 1360 x 1024 px) (Open FluorCam SN-FC800-398, Photon Systems Instruments, Brno, Czech Republic) to quantify Fv/Fm for both bark, wood (Fig. S1) and leaves. Branches, still maintained with their cut end in water, were dark adapted for 2 h before measurements to ensure relaxation of photosystems. 3 to 5 mature leaves were detached from each branches and carefully placed on a petri dish, as explained below for stem samples. Stem segments

of different age were sampled from branches. Stem segments were sectioned both longitudinally and radially, and bark and wood were manually and carefully separated. Samples were placed on a petri dish with a bottom layer of moisten paper towels, and kept hydrated via partial immersion in a water film during the analysis with the PAM fluorometer.

Vulnerability to xylem embolism and wood density

Data of xylem pressure values inducing 50% loss of xylem hydraulic conductivity (P_{50}) for the study species were derived from the Xylem Functional Traits (XFT) database (Choat et al. 2012), and integrated with more recent studies not included in the XFT. In accordance with previous studies (e.g Petruzzellis et al. 2021), we considered only P_{50} data obtained for stems and we discarded values based on r-shaped vulnerability curves (Cochard et al. 2013). When more than one value was available for a given species, we considered the average value from different studies for subsequent analysis. Mean values of traits for each species included in the study, along with the relative references, are reported in Tab. S1 and S2.

Based on global relationships between P_{50} and environmental water availability (Maherali et al. 2004; Choat et al. 2012), we set a threshold of P_{50} = -3.0 MPa to separate relatively drought tolerant (P_{50} < -3.0 MPa) from relatively drought sensitive (P_{50} > -3.0 MPa) species. We were thus able to separate two groups of Angiosperms based on their P_{50} values. The same approach was not possible for Gymnosperms, due to the relatively low number of species included in the study.

Wood density (WD) is a key functional trait indicating variation in wood structure/carbon investment, and often used as a proxy for vulnerability to embolism due to its general correlation with P_{50} (Hacke and Sperry 2001; Kiorapostolou et al. 2019). WD was measured on 3 cm long segments from two-year-old stems (one stem per individual), as:

WD = Wood dry weight / Wood fresh volume (g cm^{-3})

Bark was removed and samples were rehydrated overnight by immersion in vials filled with tap water. The following morning, samples were weighed, and their fresh volume was measured using a water displacement method (Hughes 2005; Petruzzellis et al. 2019). Samples were then oven-dried at 70 °C for 24 h and weighed again to obtain their dry weight.

Statistical and phylogenetic analysis

Statistical analyses were performed with R (version 3.4.4) software (R Core Team 2022).

Boxplot panels were made using “ggplot2” package in R. Bar charts were prepared with Origin 9.0 software (Northampton, MA, USA). To test possible significant differences in Fv/Fm, three way Anova tests were performed setting Fv/Fm as the response variable and the drought sensitiveness

(drought-tolerant or sensitive species) and each sample (e.g. bark of current-year stem) as the first and second explanatory variables, respectively. Since homogeneity of variance assumption was violated, generalized least square (GLS) models were run, using the 'nlme' R package (Pinheiro et al. 2019), specifying a 'varPower' variance structure. Differences between groups were tested post hoc with Holm contrasts using the emmeans function ("emmeans" package). For GLS models, the pseudo R^2 was calculated using the Nagelkerke method ("rcompanion" R package; Nagelkerke 1991). To disentangle eventual phylogenetic signals from general trends of variation in stem photosynthesis and drought-tolerance traits, we constructed a phylogenetic tree according to Fletcher et al. (2018) and used *"pgls"* function in the "caper" R package to analyze data using a phylogenetic generalized least-squares (PGLS) approach. The PGLS approach enabled calculations of relationships between variables controlling for phylogeny (OU, Garland et al. 2005). Specifically, the analysis takes into account for phylogenetic autocorrelation when testing the relationship between the considered traits. Covariance analysis is based on the Brownian evolution model. To estimate the phylogenetic distance/length of branches, we included the Lambda factor in the model. Lambda was calculated using the «maximum likelihood» method (Lambda = 1: phylogenetic covariation is equal to that estimated by the model, Lambda = 0: traits' relationship is independent of the phylogenetic relationship).

We also used the "phylobase" R package to combine the phylogenetic data with the dataset containing the P_{50} values. Then, we used "ggtree" R package to create a phylogenetic tree in which each species is color-coded according the corresponding P_{50} value, to highlight the evolutionary differences between species in terms of resistance to drought stress (Maherali et al. 2004).

Results

We were able to retrieve data of P_{50} for all the species under study (Tab. S1, references in Tab. S2). We mapped a phylogenetic tree according to P_{50} values, and high resistance to embolism (more negative P_{50}) appeared in several species, both Angiosperms and Gymnosperms (Fig. 2). The highest value was found in *Sambucus nigra* (-1.2 MPa), while *Juniperus communis* had the lowest value (-5.7 MPa).

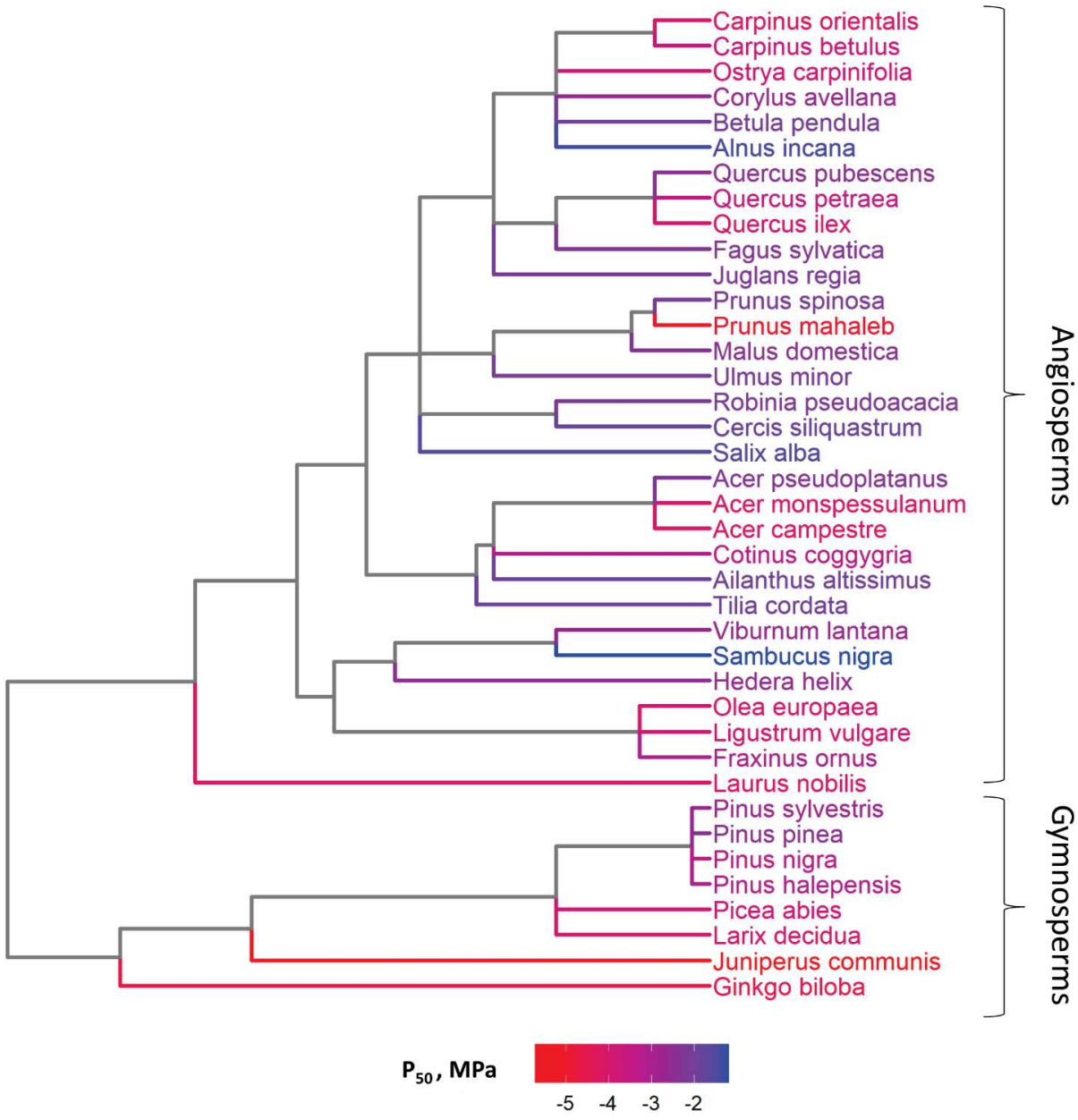

Fig. 2 Phylogenetic tree showing species selected for this study, color-coded according to their values of xylem water potential inducing 50% loss of hydraulic conductivity (P_{50}). Note that more negative values characterize more resistant species. Data are retrieved from literature.

Mean values of WD for each species are reported in Tab. S1. The lowest WD was measured in *Tilia cordata* (0.30±0.01 g cm^{-3}) while *Quercus ilex* had the highest value (0.68±0.07 g cm^{-3}). A significant negative relationship was found between P_{50} and WD (Fig. 3).

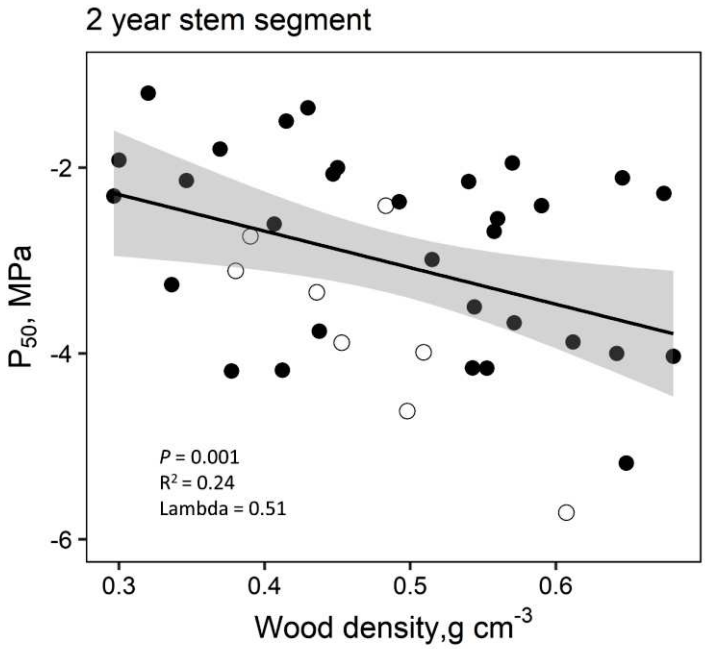

Fig. 3 Relationship between xylem water potential inducing 50% loss of hydraulic conductivity (P_{50}) and wood density (WD). P_{50} data are retrieved from literature; WD was measured in the species selected for this study. Solid and open circles represent angiosperm and gymnosperm species, respectively. Solid line represents the overall regression, while shaded area represents 95% confidence intervals.

Fv/Fm of leaves, bark and wood for each species and each growth year are also reported in Tab. S3. Values of Fv/Fm for leaves were above 0.80 for all the study species. The lowest Fv/Fm value for wood was recorded in *Pinus halepensis* (0.42±0.5), with *Cercis siliquastrum* scoring the highest one (0.81±0.02). Instead, the lowest Fv/Fm value at bark level was measured in *Prunus spinosa* (0.62±0.08), while *Laurus nobilis* had the highest value (0.83±0.004). In both Angiosperms and Gymnosperms, average Fv/Fm values for leaves were similar and higher than those measured at bark and wood level. When considering the wood, Angiosperms showed higher values of Fv/Fm than Gymnosperms, especially when considering the wood (Fig. 4). We found a decreasing trend of photosynthetic efficiency with increasing stem age. This trend was more evident for Gymnosperms than for Angiosperms, and more marked when considering the wood, compared to the bark (Fig. 4).

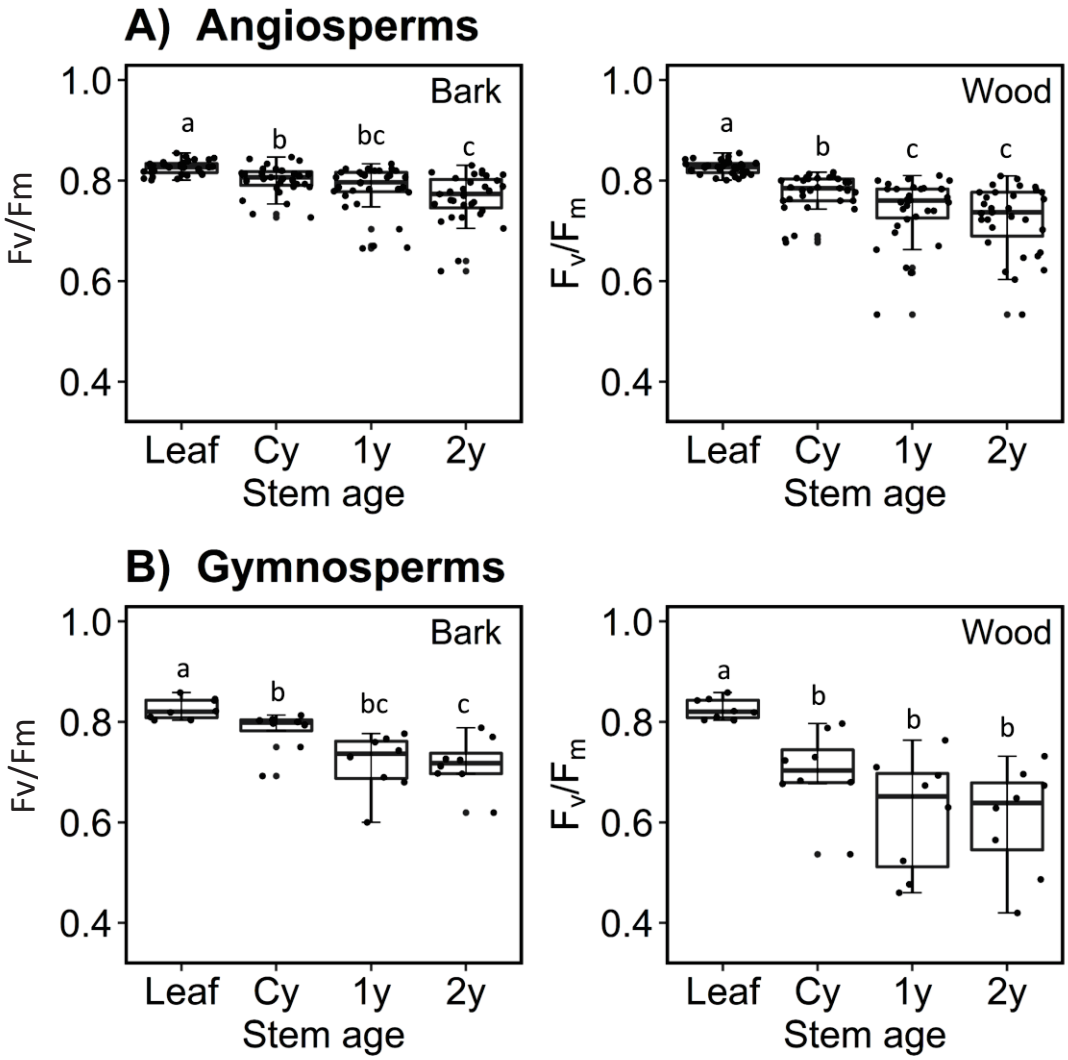

Cy: current-year stem; 1y: 1-year stem; 2y: 2-year stem.

Fig. 4 Median values, 25th and 75th percentiles of Fv/Fm values measured in A) Angiosperms and B) Gymnosperms in leaf as well as bark and wood of current-year, 1-year and 2-year stem segments. Different letters indicate significant differences between samples ($P < 0.05$).

When exploring possible differences in terms of Fv/Fm according to the relative drought tolerance of different species based on the P_{50} threshold, we found that Fv/Fm values for the leaves were similar for drought-tolerant and drought-sensitive species. However, significant differences emerged between the two groups when considering bark of 1-year-old (p = 0.02) and 2-year-old (p = 0.02) (Fig. 5A, Tab. S4A). When considering wood, we found significant differences between the two groups in the current-year (p = 0.007) and 1-year-old stems (p = 0.023) (Fig. 5B, Tab. S4B). The trend toward lower Fv/Fm values in drought-sensitive compared to drought-tolerant species was maintained also in the 2-year-old wood, although no significant differences were found in this case due to high variability of data.

Values of Fv/Fm in the bark did not change over different stem ages for drought-tolerant species. On the contrary, in the drought-sensitive species bark Fv/Fm showed a decreasing trend with age (Tab. S4A). Fv/Fm values in the wood tended to decrease with age in both groups (Tab. S4B).

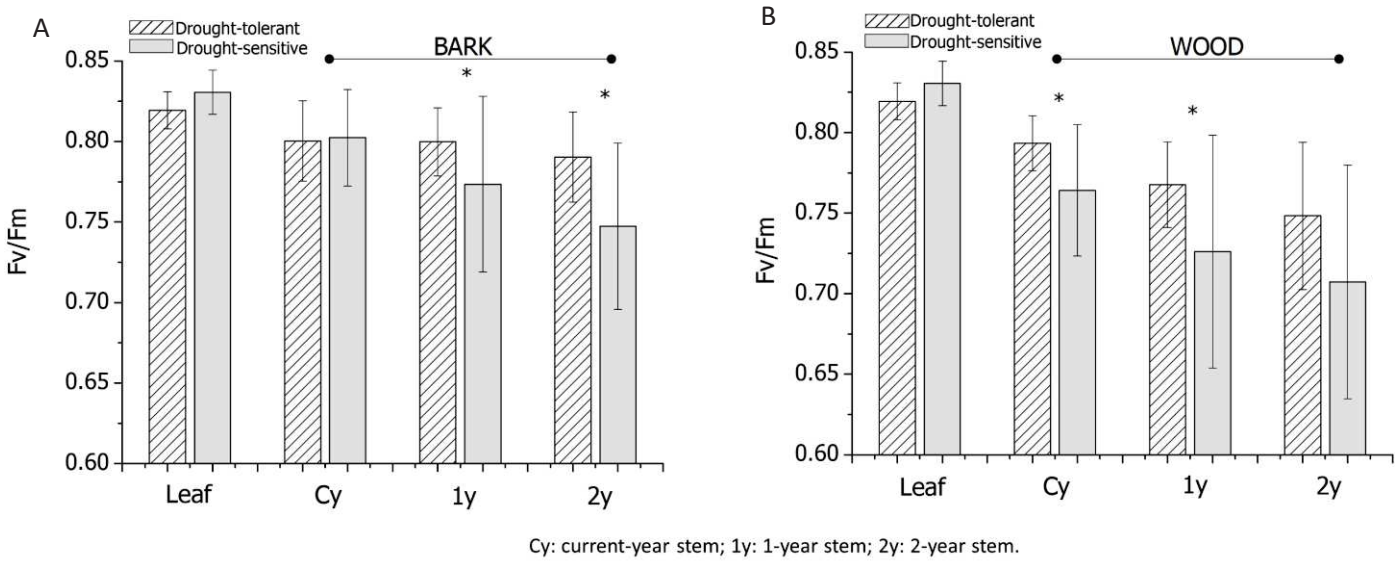

Fig. 5 Mean maximum quantum yield of PSII (Fv/Fm) in drought-tolerant and drought-sensitive Angiosperm species, according to values of xylem water potential inducing 50% loss of hydraulic conductivity (P_{50}). Values are reported for leaves as well as for A) bark and B) wood samples of different age. Vertical bars indicated standard deviation. Asterisks indicate significant differences between groups ($P < 0.05$).

Discussion

Stem photosynthesis is thought to play different roles in tree resistance/resilience to water shortage, but the actual correlation of stem photosynthetic efficiency with adaptation to drought has never been clearly demonstrated. Our data reveal significant differences in terms of Fv/Fm for both bark and wood of species with contrasting levels of drought tolerance, highlighting possible functional roles of stem photosynthesis for woody plants thriving in water-limited habitats.

Chlorophyll *a* fluorescence is considered an excellent tool to quantify the physiological status of photosynthetic tissues (Govindjee 2004), and Fv/Fm is the parameter most commonly used to this aim. The average Fv/Fm for photosynthetically active and healthy leaves is 0.83 (Harbinson et al. 2018). Lower values indicate reduced maximum quantum efficiency, due to intrinsic features of the photosynthetic apparatus or to damage resulting from environmental stress (Maxwell and Johnson 2000). Hence, Fv/Fm emerges as a convenient parameter to assess stem photosynthetic efficiency.

Fv/Fm for leaves of the study species was above 0.80, and similar among Angiosperms and Gymnosperms. Interestingly, the Fv/Fm of bark for both current-year stems and one-year-old stems was very close to values measured in leaves (although significantly lower based on statistics), suggesting that the bark of young stems can perform photosynthesis with an efficiency very similar to that of leaves. In Angiosperms (but not in Gymnosperms), also current-year wood displayed Fv/Fm comparable to that of leaves, indicating that even this compartment might significantly contribute to carbon uptake in this group of plants.

We found Fv/Fm to be stem-age dependent, with relatively high values in current-year stems, but then decreasing in bark and especially wood of older stems. This finding is consistent with the observation that light transmitted through the stem and CO_2 diffusion from the atmosphere inside the stem generally decrease as stems age and grow thicker (Saveyn et al. 2010). In fact, blue light is mainly absorbed by the bark, while the wood can be reached by far-red enriched light (Wittmann and Pfanz 2016; Natale et al. submitted) that is far from optimal for the photosynthetic process. However, it is interesting to note that even 2-year-old wood displayed appreciable levels of Fv/Fm (especially in Angiosperms), consistent with possible residual CO_2 fixation even in this compartment. This finding would be in agreement with the role proposed for wood chloroplast as 'recyclers' of CO_2 released by respiration of wood parenchyma (Ávila et al. 2014). This process might help plants to buffer NSC depletion during periods of stress leading to stomatal closure (see below).

As expected, statistical analyses revealed that Fv/Fm values of bark and wood differed between Angiosperm and Gymnosperm species. Specifically, Angiosperms had higher Fv/Fm values, especially in the wood, compared to Gymnosperms. These differences are consistent with the xylem

anatomical features in the two groups, with specific reference to the percentage wood volume occupied by parenchymatic cells. In fact, Gymnosperms have typically low amounts of parenchyma in their wood (in the range of 5-10% of the total volume), in sharp contrast with Angiosperms where 25-50% of the wood volume can be occupied by parenchyma (Morris et al. 2016; Kiorapostolou et al. 2019). Hence, Gymnosperm wood can accommodate relatively fewer chloroplasts and is likely less efficient in light transmission below the bark.

The vulnerability to xylem embolism (P_{50}) is considered one of the most reliable proxies to quantify plant tolerance to drought stress (e.g. Choat et al. 2012; Petruzzellis et al. 2021). P_{50} is a measure of the apoplastic vulnerability to dehydration, since drought stress can affect the soil-to-leaf pathway by causing dysfunction of water columns in xylem conduits (e.g. Nardini and Luglio 2014), potentially inducing embolism formation and further desiccation (e.g. Nardini et al. 2017; McDowell et al. 2008; Adams et al. 2009). Indeed, P_{50} values show large inter-specific variation, and are generally coordinated with climatic conditions of the species' natural range with specific reference to precipitation, evapotranspiration and temperature (Maherali et al. 2004; Bartlett et al. 2012). Values of P_{50} in our dataset spanned a twofold range for both Angiosperms and Gymnosperms, and allowed us to separate two groups of relatively drought-tolerant (11 species) and drought-sensitive (20 species) Angiosperms. The same classification was not possible for Gymnosperms, due to the relatively small number of species analyzed. Drought-tolerant and drought-sensitive species were distributed along independent phylogenetic trajectories (Fig. 2). A possible pitfall of our analysis lies in the fact that P_{50} values were retrieved form the literature, and not measured on the same individuals used for Fv/Fm measurements. Although species-specific vulnerability to xylem embolism displays limited genotypic variability (Wortemann et al. 2011; Unterholzner et al. 2020), we decided to measure wood density in the same plants used for analysis of stem photosynthetic efficiency to further test the overall reliability of the P_{50} dataset as based on literature data. WD is recognized as a good proxy for species-specific vulnerability to xylem embolism (Nardini et al. 2013; Kiorapostolou et al. 2019), and in fact this trait was well correlated with P_{50} values across our dataset, confirming the overall validity of our classification of Angiosperms according to their relative drought tolerance.

We found that woody species with more negative P_{50} values were also characterized by higher Fv/Fm values in bark and wood, although not for all age ranges. This finding might suggest that drought-tolerant species have greater stem photosynthetic efficiency, as a possible adaptation to environmental conditions imposing prolonged stomatal closure. This conclusion would be in accordance with previous studies suggesting that photosynthetic stems could have evolved more than once as an adaptation to life in tropical-dry and Mediterranean-like ecosystems (Ávila-Lovera and Ezcurra 2016; Ávila-Lovera and Garcillán 2020). In fact, under prolonged drought stomata close to prevent

excessive tissue dehydration (Brodribb and Holbrook 2003; Bartlett et al. 2016; Choat et al. 2018). Stomatal closure cannot fully prevent residual water loss and progressive drop of xylem pressure, so that these species gain an adaptive advantage from developing xylem conduits highly resistant to xylem embolism that can assure the integrity of the root-to-leaf water pathway. Under such conditions, plants face a reduction of leaf-level photosynthetic carbon gain (Meinzer et al. 2009; Choat et al. 2012; Manzoni et al. 2013; Nardini et al. 2017), potentially leading to depletion of stored non-structural carbohydrates (NSC) to maintain primary and secondary metabolism (McDowell et al. 2022). Prolonged drought stress might provoke exhaustion of NSC pools (McDowell et al. 2008; Adams et al. 2009), so that additional carbon gain at the stem level might represent a significant adaptive advantage for such species.

In this study, we used P_{50} values to disentangle drought-sensitive form drought-tolerant species, and to compare stem photosynthetic efficiency in these two groups. Hence, our data cannot provide any insight into possible mechanistic relationships between vulnerability to xylem embolism and stem photosynthesis. However, some observations lead to interesting speculations. In particular, it is interesting to note that wood photosynthetic efficiency was higher in Angiosperms than in Gymnosperms. Locally produced non-structural carbohydrates have been suggested to be involved in the post-drought recovery of stem hydraulics, pending refilling of embolized conduits (Schmitz et al. 2012; Bloemen et al. 2016; Nardini et al. 2018). In this light, it is worth noting that embolism repair, although debated, has been observed more frequently in Angiosperms compared to Gymnosperms (Johnson et al. 2012; Klein et al. 2018). Thus, it is tempting to speculate that the limited ability of Gymnosperms to recover their hydraulic functions after drought partly depends on the low photosynthetic efficiency at wood level, that would prevent adequate production and of non-structural carbohydrates to be invested in the generation of osmotic forces which are thought to be required for embolism reversal (Nardini et al. 2011; Secchi and Zwieniecki 2016; Secchi et al. 2021).

To conclude, our data suggest an adaptive role for stem photosynthesis for woody plants thriving in hot and dry ecosystems. Considering that this is the first study showing the connection between stem photosynthesis and drought-related functional traits, we call for more studies aimed at verifying these findings at larger geographical, ecological and taxonomic scales, to better understand the ecophysiological importance of photosynthetic stems for plants facing ongoing climate changes.

Author contributions

AN, SN and FP planned and designed the research. SN performed experimental measurements. SN, FP and AN analyzed the data. TM, NLR and AA contributed to the interpretation of the data. SN and AN wrote the manuscript, with contribution by all co-authors.

References

Adams HD, Guardiola-Claramonte M, Barron-Gafford GA, Villegas JC, Breshears DD, Zou CB, Troch PA, Huxman TE. 2009. Reply to Leuzinger et al.: drought-induced tree mortality temperature sensitivity requires pressing forward with best available science. *Proceedings of the National Academy of Sciences* **106:** e107.

Aschan G, Pfanz H, Vodnik D, Batič F. 2005. Photosynthetic performance of vegetative and reproductive structures of green hellebore (*Helleborus viridis* L. agg.). *Photosynthetica* **43:** 55–64.

Ávila E, Herrera A, Tezara W. 2014. Contribution of stem CO_2 fixation to whole-plant carbon balance in nonsucculent species. *Photosynthetica* **52:** 3–15.

Ávila-Lovera E, Ezcurra E. 2016. Stem-succulent trees from the Old and New World tropics. In: G. Goldstein and L. S. Santiago, eds. *Tropical tree physiology*. Cham, CH: Springer International, 45–65.

Ávila-Lovera E, Zerpa AJ, Santiago LS. 2017. Stem photosynthesis and hydraulics are coordinated in desert plant species. *New Phytologist* **216:** 1119–1129.

Ávila-Lovera E, Haro R, Ezcurra E, Santiago LS. 2018. Costs and benefits of photosynthetic stems in desert species from southern California. *Functional Plant Biology* **46:** 175–186.

Ávila-Lovera E, Garcillán PP, Silva-Bejarano C, Santiago LS. 2020. Functional traits of leaves and photosynthetic stems of species from a sarcocaulescent scrub in the southern Baja California Peninsula. *American Journal of Botany* **107:** 1410–1422.

Ávila-Lovera E, Garcillán PP. 2020. Phylogenetic signal and climatic niche of stem photosynthesis in the mediterranean and desert regions of California and Baja California Peninsula. *American Journal of Botany* **108:** 334–345.

Berveiller D, Kierzkowski D, Damesin C. 2007. Interspecific variability of stem photosynthesis among tree species. *Tree Physiology* **27:** 53–61.

Bartlett MK, Scoffoni C, Sack L. 2012. The determinants of leaf turgor loss point and prediction of drought tolerance of species and biomes: a global meta-analysis. *Ecology Letters* **15:** 393–405.

Bartlett MK, Zhang Y, Kreidler N, Sun S, Ardy R, Cao K, Sack L. 2014. Global analysis of plasticity in turgor loss point, a key drought tolerance trait. *Ecology Letters* **17:** 1580–1590.

Bartlett MK, Klein T, Jansen S, Choat B, Sack L. 2016. The correlations and sequence of plant stomatal, hydraulic and wilting responses to drought. *Proceedings of the National Academy of Sciences* **113:** 13098–13103.

Bloemen J, Overlaet-Michiels L, Steppe K. 2013. Understanding plant responses to drought: how important is woody tissue photosynthesis? *Acta Horticulturae* **991:** 149–157.

Bloemen J, Vergeynst L, Overlaet-Michiels L, Steppe K. 2016. How important is woody tissue photosynthesis in poplar during drought stress? *Trees* **30:** 63–72.

Brodersen CR, McElrone AJ. 2013. Maintenance of xylem network transport capacity: a review of embolism repair in vascular plants. *Frontiers in Plant Science* **4:** 108.

Brodribb TJ, Holbrook NM. 2003. Stomatal closure during leaf dehydration, correlation with other leaf physiological traits. *Plant Physiology* **132:** 2166–2173.

Cannon W. 1908. The topography of the chlorophyll apparatus in desert plants. *Carnegie Institution of Washington Publication* **98**.

Cernusak LA, Marshall JD. 2000. Photosynthetic refixation in branches of western white pine. *Functional Ecology* **14:** 300–311.

Cernusak LA, Cheesman AW. 2015. The benefits of recycling: how photosynthetic bark can increase drought tolerance. *New Phytologist* **208:** 995–997.

Choat B, Jansen S, Brodribb TJ, Cochard H, Delzon S, Bhaskar R, et al. 2012. Global convergence in the vulnerability of forests to drought. *Nature* **491:** 752–755.

Choat B, Brodribb TJ, Brodersen CR, Duursma RA, López R, Medlyn BE. 2018. Triggers of tree mortality under drought. *Nature* **558:** 531–539.

Cochard H, Badel E, Herbette S, Delzon S, Choat B, Jansen S. 2013. Methods for measuring plant vulnerability to cavitation: a critical review. *Journal of Experimental Botany* **64:** 4779–4791.

De Baerdemaeker NJ, Salomón RL, De Roo L, Steppe K. 2017. Sugars from woody tissue photosynthesis reduce xylem vulnerability to cavitation. *New Phytologist* **216:** 720–727.

De Roo L, Salomón RL, Steppe K. 2020. Woody tissue photosynthesis reduces stem CO_2 efflux by half and remains unaffected by drought stress in young *Populus tremula* trees. *Plant, Cell & Environment* **43:** 981–991.

Dima E, Manetas Y, Psaras GK. 2006. Chlorophyll distribution pattern in inner stem tissues: evidence from epifluorescence microscopy and reflectance measurements in 20 woody species. *Trees* **20:** 515–521.

Fletcher LR, Cui H, Callahan H, Scoffoni C, John GP, Bartlett MK, Burge DO, Sack L. 2018. Evolution of leaf structure and drought tolerance in species of Californian *Ceanothus*. *American Journal of Botany* **105:** 1672–1687.

Garland JrT, Bennett AF, Rezende EL. 2005. Phylogenetic approaches in comparative physiology. *Journal of Experimental Biology* **208:** 3015–3035.

Govindjee G. 2004. Chlorophyll a fluorescence: a bit of basics and history. In: Papageorgiou GC, Govindjee G, eds. *Chlorophyll a fluorescence a signature of photosynthesis*. Dordrecht, NL: Springer, 1–41.

Hacke UG, Sperry JS. 2001. Functional and ecological xylem anatomy. *Perspective in Plant Ecology, Evolution and Systematics* **4:** 97–115.

Harbinson J. 2018. Chlorophyll fluorescence as a tool for describing the operation and regulation of photosynthesis in vivo. In: Croce R, van Grondelle R, van Amerongen H, van Stokkum I, eds. *Light harvesting in photosynthesis*. Boca Raton, USA: CRC Press, 539–571.

Hughes SW. 2005. Archimedes revisited: a faster, better, cheaper method of accurately measuring the volume of small objects. *Physics Education* **40:** 468–474.

Johnson DM, McCulloh KA, Woodruff DR, Meinzer FC. 2012. Hydraulic safety margins an embolism reversal in stems and leaves: why are conifers and angiosperms so different? *Plant Science* **195:** 48–53.

Kiorapostolou N, Da Sois L, Petruzzellis F, Savi T, Trifilò P, Nardini A, Petit G. 2019. Vulnerability to xylem embolism correlates to wood parenchyma fraction in angiosperms but not in gymnosperms. *Tree Physiology* **39:** 1675–1684.

Klein T, Zeppel MJ, Anderegg WR, Bloemen J, De Kauwe MG, Hudson P, et al. 2018. Xylem embolism refilling and resilience against drought-induced mortality in woody plants: processes and trade-offs. *Ecological Research* **33:** 839–855.

Lamy JB, Delzon S, Bouche PS, Alia R, Vendramin GG, Cochard H, Plomion C. 2014. Limited genetic variability and phenotypic plasticity detected for cavitation resistance in a Mediterranean pine. *New Phytology* **201:** 874–886.

Liu J, Gu L, Yu, Y, Ju G, Sun Z. 2018. Stem Photosynthesis of Twig and Its Contribution to New Organ Development in Cutting Seedlings of *Salix Matsudana* Koidz. *Forests* **9:** 207–219.

Liu J, Gu L, Yu Y, Huang P, Wu Z, Zhang Q, Qian Y, Wan X, Sun Z. 2019. Corticular photosynthesis drives bark water uptake to refill embolized vessels in dehydrated branches of *Salix Matsudana*. *Plant, Cell & Environment* **42:** 2584–2596.

Maherali H, Pockman WT, Jackson RB. 2004. Adaptive variation in the vulnerability of woody plants to xylem cavitation. *Ecology* **85:** 2184–2199.

Manetas Y, Pfanz H. 2005. Spatial heterogeneity of light penetration through periderm and lenticels and concomitant patchy acclimation of corticular photosynthesis. *Trees* **19:** 409–414.

Manzoni S, Vico G, Katul G, Palmroth S, Jackson RB, Porporato A. 2013. Hydraulic limits on maximum plant transpiration and the emergence of the safety-efficiency trade-off. *New Phytologist* **198:** 169–178.

Maxwell K, Johnson GN. 2000. Chlorophyll fluorescence-a practical guide. *Journal of Experimental Botany* **51:** 659–668.

McDowell N, Pockman WT, Allen CD, Breshears DD, Cobb N, Kolb T, Plaut J, Sperry J, West A, Williams DG, et al. 2008. Mechanisms of plant survival and mortality during drought: why do some plants survive while others succumb to drought? *New Phytologist* **178:** 719–739.

McDowell NG. 2011. Mechanisms linking drought, hydraulics, carbon metabolism, and vegetation mortality. *Plant Physiology* **155:** 1051–1059.

McDowell NG, Sapes G, Pivovaroff A, Adams HD, Allen CD, Anderegg WR, et al. 2022. Mechanisms of woody-plant mortality under rising drought, CO_2 and vapour pressure deficit. *Nature Reviews Earth & Environment* **3:** 294–308.

Meinzer FC, Johnson DM, Lachenbruch B, McCulloh KA, Woodruff DR. 2009. Xylem hydraulic safety margins in woody plants: coordination of stomatal control of xylem tension with hydraulic capacitance. *Functional Ecology* **23:** 922–930.

Méndez-Alonzo R, Paz H, Zuluaga RC, Rosell JA, Olson ME. 2012. Coordinated evolution of leaf and stem economics in tropical dry forest trees. *Ecology* **93:** 2397–2406.

Mitchell PJ, O'Grady AP, Tissue DT, White DA, Ottenschlaeger ML, Pinkard EA. 2013. Drought response strategies define the relative contributions of hydraulic dysfunction and carbohydrate depletion during tree mortality. *New Phytologist* **197:** 862–872.

Morris H, Plavcová L, Cvecko P, Fichtler E, Gillingham MAF, Martínez Cabrera HI, McGlinn DJ, Wheeler E, Zheng J, Ziemińska K, Jansen S. 2016. A global analysis of parenchyma tissue fractions in secondary xylem of seed plants. *New Phytologist* **209:** 1553–1565.

Nagelkerke NJD. 1991. A note on a general definition of the coefficient of determination. *Biometrika* **78:** 691–692.

Nardini A, Battistuzzo M, Savi T. 2013. Shoot desiccation and hydraulic failure in temperate woody angiosperms during an extreme summer drought. *New Phytologist* **200:** 322–329.

Nardini A, Luglio J. 2014. Leaf hydraulic capacity and drought vulnerability: possible trade-offs and correlations with climate across three major biomes. *Functional Ecology* **28:** 810–818.

Nardini A, Savi T, Trifilò P, Lo Gullo MA. 2018. Drought stress and the recovery from xylem embolism in woody plants. In Cánovas FM, Luettge U, Matyssek R, eds. *Progress in Botany*. Berlin, DE, Springer, 197–231.

Petruzzellis F, Nardini A, Savi T, Tonet V, Castello M, Bacaro G. 2019. Less safety for more efficiency: water relations and hydraulics of the invasive tree *Ailanthus altissima* (Mill.) Swingle compared with native *Fraxinus ornus* L. *Tree physiology* **39:** 76–87.

Petruzzellis F, Tordoni E, Di Bonaventura A, Tomasella M, Natale S, Panepinto F, Bacaro G, Nardini A. 2021. Turgor loss point and vulnerability to xylem embolism predict species-specific risk of drought-induced decline of urban trees. *Plant Biology*. https://doi.org/10.1111/plb.13355

Pfanz H, Aschan G, Langenfeld-Heyser R, Wittmann C, Loose M. 2002. Ecology and ecophysiology of tree stems: corticular and wood photosynthesis. *Naturwissenschaften* **89:** 147–162.

R Core Team. 2022. R: A language and environment for statistical computing. R Foundation for Statistical Computing, Vienna, Austria. URL https://www.R-project.org/.

Pivovaroff AL, Cook VM, Santiago LS. 2018. Stomatal behavior and stem xylem traits are coordinated for woody plant species under exceptional drought conditions. *Plant, Cell & Environment* **41:** 2617–2626.

Rentzou A, Psaras GK. 2008. Green plastids, maximal PSII photochemical efficiency and starch content of inner stem tissues of three Mediterranean woody species during the year. *Flora: Morphology, Distribution, Functional Ecology of Plants* **203:** 350–357.

Saveyn A, Steppe K, Ubierna N, Dawson TE. 2010. Woody tissue photosynthesis and its contribution to trunk growth and bud development in young plants. *Plant, Cell & Environment* **33:** 1949–1958.

Schmitz N, Egerton JJG, Lovelock CE, Ball MC. 2012. Light-dependent maintenance of hydraulic function in mangrove branches: do xylary chloroplasts play a role in embolism repair? *New Phytologist* **195:** 40–46.

Schreiber U. 2004. Pulse-amplitude-modulation (PAM) fluorometry and saturation pulse method: an overview. In: Papageorgiou, G.C., Govindjee, eds. *Chlorophyll a Fluorescence: A Signature of Photosynthesis. Advances in Photosynthetic Respiration*. Dordrecht, NL: Springer, 279–319.

Secchi F, Zwieniecki MA. 2016. Accumulation of sugars in the xylem apoplast observed under water stress conditions is controlled by xylem pH. *Plant, Cell & Environment* **39:** 2350–2360.

Secchi F, Pagliarani C, Cavalletto S, Petruzzellis F, Tonel G, Savi T, et al. 2021. Chemical inhibition of xylem cellular activity impedes the removal of drought-induced embolisms in poplar stems–new insights from micro-CT analysis. *New Phytologist* **229:** 820–830.

Steppe K, Sterck F, Deslauriers A. 2015. Diel growth dynamics in tree stems: linking anatomy and ecophysiology. *Trends in Plant Science* **20:** 335–343.

Sun Q, Kiyotsugu Y, Mitsuo S, Hitoshi S. 2003. Vascular tissue in the stem and roots of woody plants can conduct light. *Journal of Experimental Botany* **54:** 1627–1635.

Teskey RO, Saveyn A, Steppe K, McGuire MA. 2008. Origin, fate and significance of CO_2 in tree stems. *New Phytologist* **177:** 17–32.

Tomasella M, Petrussa E, Petruzzellis F, Nardini A, Casolo V. 2019. The possible role of non-structural carbohydrates in the regulation of tree hydraulics. *International Journal of Molecular Science* **21:** 144.

Tomasella M, Casolo V, Natale S, Petruzzellis F, Kofler W, Beikircher B, et al. 2021. Shade-induced reduction of stem nonstructural carbohydrates increases xylem vulnerability to embolism and impedes hydraulic recovery in *Populus nigra*. *New Phytologist* **231:** 108–121.

Trifilò P, Casolo V, Raimondo F, Petrussa E, Boscutti F, Lo Gullo MA, Nardini A. 2017. Effects of prolonged drought on stem non- structural carbohydrates content and post-drought hydraulic recovery in *Laurus nobilis* L.: The possible link between carbon starvation and hydraulic failure. *Plant Physiology and Biochemistry* **120:** 232–241.

Trifilò P, Kiorapostolou N, Petruzzellis F, Vitti S, Petit G, Lo Gullo MA, Nardini A, Casolo V. 2019. Hydraulic recovery from xylem embolism in excised branches of twelve woody species: relationships with parenchyma cells and non-structural carbohydrates. *Plant Physiology and Biochemistry* **139:** 513–520.

Trifilò P, Natale S, Gargiulo S, Abate E, Casolo V, Nardini A. 2021. Stem Photosynthesis Affects Hydraulic Resilience in the Deciduous *Populus alba* but Not in the Evergreen *Laurus nobilis*. *Water* **13:** 2911.

Unterholzner L, Carrer M, Bär A, Beikircher B, Dämon B, et al. 2020. *Juniperus communis* populations exhibit low variability in hydraulic safety and efficiency. *Tree Physiology* **40:** 1668–1679.

Vandegehuchte MW, Bloemen J, Vergeynst LL, Steppe K. 2015. Woody tissue photosynthesis in trees: salve on the wounds of drought? *New Phytologist* **208:** 998–1002.

Wittmann C, Pfanz H. 2008. General trait relationships in stems: a study on the performance and interrelationships of several functional and structural parameters involved in corticular photosynthesis. *Physiologia Plantarum* **134:** 636–648.

Wittmann C, Pfanz H. 2014. Bark and woody tissue photosynthesis: a means to avoid hypoxia or anoxia in developing stem tissues. *Functional Plant Biology* **41:** 940–953.

Wittmann C, Pfanz H. 2016. The optical, absorptive and chlorophyll fluorescence properties of young stems of five woody species. *Environmental and Experimental Botany* **121:** 83–93.

Wortemann R, Herbette S, Barigah TS, Fumanal B, Alia R, Ducousso A, Gomory D, Roeckel-Drevet P, Cochard H. 2011. Genotypic variability and phenotypic plasticity of cavitation resistance in Fagus sylvatica L. across Europe. *Tree Physiology* **31:** 1175–1182.

Yiotis C, Petropoulou Y, Manetas Y. 2009. Evidence for light-independent and steeply decreasing PSII efficiency along twig depth in four tree species. *Photosynthetica* **47:** 223–231.

Supplementary material

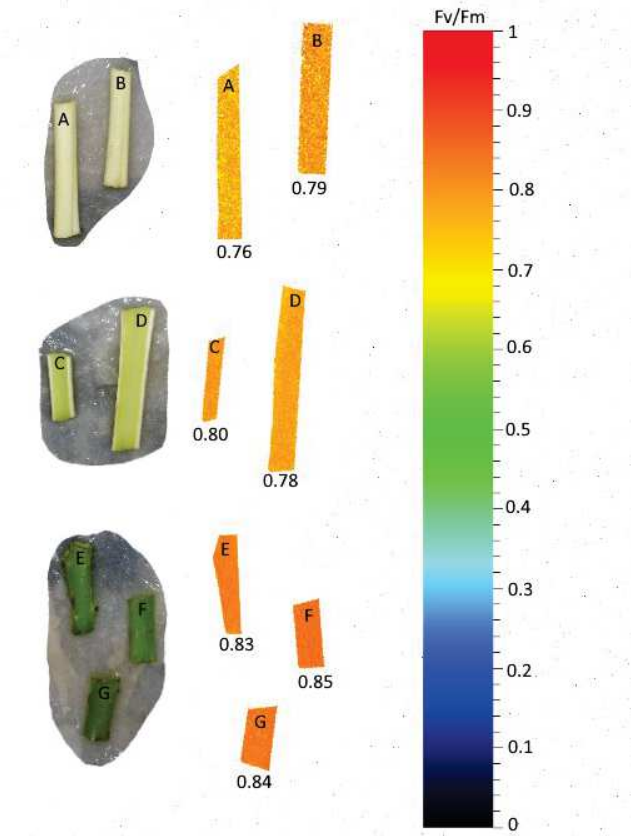

Fig. S1 Example of maximum quantum yield of PSII (Fv/Fm) measured in stem samples used for the experiment. (A-B) Wood, (C-D) wood + pith (exposing the cut side) and (E-G) bark were analyzed separately. The example showed measurements conducted on the current-year stem of *Juglans regia*. Values displayed under each picture are the average Fv/Fm value of the sample.

	Species	P_{50} (MPa)	WD, g cm^{-3}
Angiosperms	*Acer campestre*	–4.18±0.01	0.41±0.04
	Acer monspessulanum	–4.16±0.85	0.55±0.03
	Acer pseudoplatanus	–2.31±0.63	0.30±0.0
	Ailanthus altissima	–1.95±1.43	0.57±0.06
	Alnus incana	–1.36±0.49	0.43±0.02
	Betula pendula	–2.00±0.28	0.45±0.02
	Carpinus betulus	–3.67	0.57±0.03
	Carpinus orientalis	–4.16±0.30	0.54±0.08
	Cercis siliquastrum	–1.80	0.37±0.02
	Corylus avellana	–2.61±0.44	0.41±0.03
	Cotinus coggygria	–3.26±0.88	0.34±0.05
	Fagus sylvatica	–2.28±0.63	0.67±0.01
	Fraxinus ornus	–2.99±0.69	0.52±0.03
	Hedera helix	–2.55±0.41	0.56±0.06
	Juglans regia	–2.14±0.34	0.35±0.02
	Laurus nobilis	–4.19±2.75	0.38±0.02
	Ligustrum vulgare	–3.88±1.07	0.61±0.03
	Malus domestica	–2.37±1.38	0.49±0.02
	Olea europaea	–4.00	0.64±0.09
	Ostrya carpinifolia	–3.76±0.77	0.44±0.04
	Prunus mahaleb	–5.18±0.25	0.65±0.03
	Prunus spinosa	–2.11	0.65±0.03
	Quercus ilex	–4.03±1.37	0.68±0.07
	Quercus petraea	–3.5	0.54±0.02
	Quercus pubescens	–2.41±0.79	0.59±0.07
	Robinia pseudoacacia	–2.15±0.74	0.54±0.04
	Salix alba	–1.50	0.41±0.02
	Sambucus nigra	–1.20	0.32±0.02
	Tilia cordata	–1.92±0.49	0.30±0.01
	Ulmus minor	–2.07±1.47	0.45±0.03
	Viburnum lantana	–2.69±0.94	0.56±0.03
Gymnosperms	*Ginkgo biloba*	–4.62	0.50±0.01
	Juniperus communis	–5.71±0.92	0.61±0.04
	Larix decidua	–3.99±0.55	0.51±0.04
	Picea abies	–3.88	0.45±0.01
	Pinus halepensis	–3.11	0.38±0.01
	Pinus nigra	–3.34±0.21	0.44±0.01
	Pinus pinea	–2.41±0.12	0.48±0.03
	Pinus sylvestris	–2.74±0.71	0.39±0.03

Tab. S1 Mean values and associated standard deviation of water potential inducing 50% loss of hydraulic conductivity (P_{50}) and wood density (WD) of wood of the second-year stem segment, retrieved from literature and measured on the selected species, respectively. Note that for some species it was not possible to calculate the standard deviation because only one value was available.

	Species	References
Angiosperms	*Acer campestre*	Rosner et al. 2019; Savi et al. 2019
	Acer monspessulanum	Tissier et al. 2004 ; Petruzzellis et al. 2021; Kiorapostolou et al. 2019
	Acer pseudoplatanus	Tissier et al. 2004; Losso et al. 2019; Cochard et al unplublished
	Ailanthus altissima	Chen et al. 2019; Kröber et al. 2014; Petruzzellis et al. 2019
	Alnus incana	Sperry et al. 1994
	Betula pendula	Charrier et al 2013; Cochard et al. 2005; Zhang et al. 2018
	Carpinus betulus	Savi et al. 2019
	Carpinus orientalis	Kiorapostolu et al. 2019; Savi et al. 2019; Zhang et al. 2018;Iovi et al. 2009
	Cercis siliquastrum	Nardini et al. 2003
	Corylus avellana	Kiorapostolu et al. 2019; Savi et al. 2019; Zhang et al. 2018
	Cotinus coggygria	Chen et al. 2019; Savi et al. 2017,2019
	Fagus sylvatica	Barigah et al 2013; Charrier et al 2014; Losso et al. 2019; Rosas et al. 2019; Savi et al. 2019; Cochard et al. 1999
	Fraxinus ornus	Tognetti et al. 1999, Petruzzellis et al. 2019; Savi et al. 2019
	Hedera helix	Kiorapostolu et al. 2019; Savi et al. 2019
	Juglans regia	Tyree et al. 1993; Chen et al. 2019
	Laurus nobilis	Salleo et al. 1996; Hacke & Sperry 2003; Klepsch et al. 2016; Nardini et al. 2017; Lamarque et al. 2018
	Ligustrum vulgare	Savi et al. 2017; Beikircher & Mayr 2009
	Malus domestica	Nolf et al. 2015; De Baerdemaeker et al. 2018
	Olea europaea	Trifilò et al. 2015; Zhu et al. 2018; Trifilò et al. 2007; Diaz-Espejo et al. 2012;Torres-Ruiz et al. 2017
	Ostrya carpinifolia	Kiorapostolu et al. 2019; Savi et al. 2019
	Prunus mahaleb	Savi et al. 2017; Savi et al. 2019
	Prunus spinosa	Savi et al. 2017
	Quercus ilex	Lo Gullo & Salleo 1992; Tognetti et al. 1998; Tognetti et al. 1999; Martinez-Vilalta et al. 2002; Pita et al. 2005; Quero et al. 2011; Limousin et al. 2012; Pinto et al. 2012; Peguero-Pina et al. 2014; Trifilò et al. 2015; Rodriguez-Calcerrada et al. 2017; Domec et al. 2017; Peguero-Pina et al. 2018;
	Quercus petraea	Kiorapostolu et al. 2019; Rosas et al. 2019; Savi et al. 2019 Cochard et al. 1992a; Tyree & Cochard 1996
	Quercus pubescens	Cochard et al. 1992; Tognetti et al. 1998; Tognetti et al. 1999; Cochard et al. 1992; Tognetti et al. 1998; Tognetti et al. 1999; Pita et al. 2005; Domec et al. 2017; Kiorapostolu et al. 2019; Savi et al. 2019
	Robinia pseudoacacia	Wang et al. 2014; Chen et al. 2019; Kiorapostolu et al. 2019; Savi et al. 2019; Dai et al. 2020
	Salix alba	Charrier et al 2014; Cochard et al. 1992b
	Sambucus nigra	Vogt 2001
	Tilia cordata	Li et al. 2008; Kiorapostolu et al. 2019; Savi et al. 2019
	Ulmus minor	Venturas et al. 2014
	Viburnum lantana	Beikircher & Mayr 2009

Gymnosperms	*Ginkgo biloba*	Cochard 2006
	Juniperus communis	Bouche et al. 2014; Beikircher & Mayr 2008;Mayr et al. 2006; Tognetti et al. 2001
	Larix decidua	Mayr et al 2006; Rosner et al. 2019a; Cochard 2006; Bouche et al. 2014
	Picea abies	Mayr et al. 2003; Chumura et al. 2016; Luss et al. 2019; Nolf et al. 2015; Rosner et al 2019a; Cochard et al. 1992;
	Pinus halepensis	Oliveras et al. 2003
	Pinus nigra	Martinez-Vilalta & Piñol 2002; Rosas et al. 2019
	Pinus pinea	Oliveras et al. 2003; Johnson et al. 2016
	Pinus sylvestris	Mencuccini et al. 1997; Martinez-Vilalta & Piñol 2002; Poyatos et al. 2007; Aguadé et al. 2015; Torres-Ruiz et al. 2016; Jin et al. 2018

Tab. S2 List of the species selected in this study along with sources of water potential inducing 50% loss of hydraulic conductivity (P_{50}) values.

pseudo R^2 = 0.58

A) YEAR = 1: contrast	estimate	SE	df	t.ratio	p.value
(Drought-sensitive) - (Drought-tolerant)	-0.03	0.01	84.40	-2.44	**0.02**
YEAR = 2: contrast					
(Drought-sensitive) - (Drought-tolerant)	-0.04	0.02	30.30	-2.24	**0.03**
YEAR = c: contrast					
(Drought-sensitive) - (Drought-tolerant)	0.00	0.01	102.60	-0.36	0.72
Leaf contrast					
(Drought-sensitive) - (Drought-tolerant)	0.01	0.01	45.20	1.87	0.07

pseudo R^2 = 0.57

B) YEAR = 1: contrast	estimate	SE	df	t.ratio	p.value
(Drought-sensitive) - (Drought-tolerant)	-0.04	0.02	78.60	-2.32	**0.02**
YEAR = 2: contrast					
(Drought-sensitive) - (Drought-tolerant)	-0.04	0.02	48.30	-1.66	0.10
YEAR = c: contrast					
(Drought-sensitive) - (Drought-tolerant)	-0.03	0.01	109.60	-2.86	**0.01**
Leaf contrast					
(Drought-sensitive) - (Drought-tolerant)	0.01	0.01	40.20	2.21	0.06

Tab. S4:**A)** Results of *emmeans* model. Bark Fv/Fm was the response variable, and year and drought-sensitivity the explanatory variables. *P values* are reported. **B)** Results of *emmeans* model. Wood Fv/Fm was the response variable, and year and drought-sensitivity the explanatory variables. *P values* are reported.

P_{50} references

Aguadé D, Poyatos R, Gòmez M, Oliva J, Martínez–Vilalta J. 2015. The role of defoliation and root rot pathogen infection in driving the mode of drought–related physiological decline in Scots pine (*Pinus sylvestris* L.). *Tree Physiology* **35:** 229–242.

Beikircher B, Mayr S. 2008. The hydraulic architecture of Juniperus communis L. ssp. communis: shrubs and trees compared. *Plant, Cell & Environment* **31:** 1545–1556.

Beikircher B, Mayr S. 2009. Intraspecific differences in drought tolerance and acclimation in hydraulics of *Ligustrum vulgare* and *Viburnum lantana*. *Tree Physiology* **29:** 765–775.

Bouche PS, Larter M, Domec JC, Burlett R, Gasson P, Jansen S, Delzon S. 2014. A broad survey of hydraulic and mechanical safety in the xylem of conifers. *Journal of Experimental Botany* **65:** 4419–4431.

Charrier G, Cochard H, Améglio T. 2013. Evaluation of the impact of frost resistances on potential altitudinal limit of trees. *Tree Physiology* **33:** 891–902.

Charrier G, Charra–Vaskou K, Kasuga J, Cochard H, Mayr S, Améglio T. 2014. Freeze–thaw stress: effects of temperature on hydraulic conductivity and ultrasonic activity in ten woody angiosperms. *Plant Physiology* **164:** 992–998.

Chen Z, Li S, Luan J, Zhang Y, Zhu S, Wan X, Liu S. 2019. Prediction of temperate broadleaf tree species mortality in arid limestone habitats with stomatal safety margins. *Tree Physiology* **39:** 1428–1437.

Chmura DJ, Guzicka M, McCulloh KA, Żytkowiak R. 2016. Limited variation found among Norway spruce half–sib families in physiological response to drought and resistance to embolism. *Tree Physiology* **36:** 252–266.

Cochard H, Bréda N, Granier A, Aussenac G. 1992a. Vulnerability to air embolism of three European oak species (*Quercus petraea* (Matt) Liebl, *Q pubescens* Willd, *Q robur* L). In Annales des Sciences Forestières, Vol. 49, EDP Sciences, 225–233.

Cochard H, Cruiziat P, Tyree MT. 1992b. Use of positive pressures to establish vulnerability curves: further support for the air–seeding hypothesis and implications for pressure–volume analysis. *Plant Physiology* **100:** 205–209.

Cochard H, Lemoine D, Dreyer E. 1999. The effects of acclimation to sunlight on the xylem vulnerability to embolism in *Fagus sylvatica* L. *Plant, Cell & Environment* **22:**101–108.

Cochard H, Damour G, Bodet C, Tharwat I, Poirier M, Améglio T. 2005. Evaluation of a new centrifuge technique for rapid generation of xylem vulnerability curves. *Physiologia Plantarum* **124:** 410–418.

Cochard H. 2006. Cavitation in trees. *Comptes Rendus Physique* **7:** 1018–1026.

Dai Y, Wang L, Wan X. 2020. Frost fatigue and its spring recovery of xylem conduits in ring–porous, diffuse–porous, and coniferous species in situ. *Plant Physiology and Biochemistry* **146:** 177–186.

Díaz–Espejo A, Buckley TN, Sperry JS, Cuevas MV, de Cires A, Elsayed–Farag S, Fernandez JE. 2012. Steps toward an improvement in process–based models of water use by fruit trees: a case study in olive. *Agricultural Water Management* **114:** 37–49.

De Baerdemaeker NJ, Hias N, Van den Bulcke J, Keulemans W, Steppe K. 2018. The effect of polyploidization on tree hydraulic functioning. *American Journal of Botany* **105:** 161–171.

Domec J–C, Smith DD, McCulloh KA. 2017. A synthesis of the effects of atmospheric carbon dioxide enrichment on plant hydraulics: implications for whole-plant water use efficiency and resistance to drought. *Plant, Cell & Environment* **40:** 921–937.

Hacke UG, Sperry JS. 2003. Limits to xylem refilling under negative pressure in *Laurus nobilis* and *Acer negundo*. *Plant, Cell & Environment* **26:** 303–311.

Jin Y, Wang C, Zhou Z. 2018. Conifers but not angiosperms exhibit vulnerability segmentation between leaves and branches in a temperate forest. *Tree Physiology* **39:** 454–462.

Johnson DM, Wortemann R, McCulloh KA, Jordan–Meille L, Ward E, Warren JM, et al. 2016. A test of the hydraulic vulnerability segmentation hypothesis in angiosperm and conifer tree species. *Tree Physiology* **36:** 983–993.

Kiorapostolou N, Da Sois L, Petruzzellis F, Savi T, Trifilò P, Nardini A, Petit G. 2019. Vulnerability to xylem embolism correlates to wood parenchyma fraction in angiosperms but not in gymnosperms. *Tree Physiology* **39:** 1675–1684.

Klepsch M, Zhang Y, Kotowska M, Lamarque LJ, Nolf M, Schuldt B, Torres–Ruiz JM, Qin D–W, Choat B, Delzon S, Scoffoni C, Cao K–F, Jansen S. 2016. Is xylem of angiosperm leaves less resistant to embolism than branches? Insights from microCT, hydraulics, and anatomy. *Journal of Experimental Botany* **22:** 5611–5623.

Kröber W, Zhang S, Ehmig M, Bruelheide H. 2014. Linking xylem hydraulic conductivity and vulnerability to the leaf economics spectrum—a cross–species study of 39 evergreen and deciduous broadleaved subtropical tree species. *Public Library of Science One* **9:** e109211.

Lamarque LJ, Corso D, Torres–Ruiz JM, Badel E, Brodribb TJ, Burlett R, Charrier G, Choat B, Cochard H, Gambetta GA, et al. 2018. An inconvenient truth about xylem resistance to embolism in the model species for refilling *Laurus nobilis* L. *Annals of Forest Science* **75:** 88.

Li Y, Sperry JS, Taneda H, Bush SE, Hacke UG. 2008. Evaluation of centrifugal methods for measuring xylem cavitation in conifers, diffuse– and ring–porous angiosperms. *New Phytologist* **177:** 558–568.

Lo Gullo MA, Salleo S. 1992. Water storage in the wood and xylem cavitation in 1–year–old twigs of *Populus deltoides* Bartr. *Plant, Cell & Environment* **15:** 431–438.

Losso A, Bär A, Dämon B, Dullin C, Ganthaler A, Petruzzellis F, et al. 2019. Insights from in vivo micro-CT analysis: testing the hydraulic vulnerability segmentation in *Acer pseudoplatanus* and *Fagus sylvatica* seedlings. *New Phytologist* **221:** 1831–1842.

Lovi K, Kolovou C, Kyparissis A. 2009. An ecophysiological approach of hydraulic performance for nine Mediterranean species. *Tree Physiology* **29:** 889–900.

Luss S, Lundqvist SO, Evans R, Grahn T, Olsson L, Petit G, Rosner S. 2019. Within–ring variability of wood structure and its relationship to drought sensitivity in Norway spruce trunks. *IAWA Journal* **40:** 288–310.

Martínez–Vilalta J, Piñol J. 2002. Drought–induced mortality and hydraulic architecture in pine populations of the NE Iberian Peninsula. *Forest Ecology and Management* **161:** 247–256.

Martínez–Vilalta J, Prat E, Oliveras I, Piñol J. 2002. Xylem hydraulic properties of roots and stems of nine Mediterranean woody species. *Oecologia* **133:** 19–29.

Mayr S, Gruber A, Bauer H. 2003. Repeated freeze–thaw cycles induce embolism in drought stressed conifers (Norway spruce, stone pine). *Planta* **217:** 436–441.

Mayr S, Hacke U, Schmid P, Schwienbacher F, Gruber A. 2006. Frost drought in conifers at the alpine timberline: xylem dysfunction and adaptations. *Ecology* **87:** 3175–3185.

Mencuccini M, Grace J, Fioravanti M. 1997. Biomechanical and hydraulic determinants of tree structure in Scots pine: anatomical characteristics. *Tree Physiology* **17:** 105–113.

Nardini A, Salleo S, Raimondo F. 2003. Changes in leaf hydraulic conductance correlate with leaf vein embolism in *Cercis siliquastrum* L. *Trees* **17:** 529–534.

Nardini A, Savi T, Losso A, Petit G, Pacilè S, Tromba G, Mayr S, Trifilò P, Lo Gullo MA, Salleo S. 2017. X-ray microtomography observations of xylem embolism in stems of *Laurus nobilis* are consistent with hydraulic measurements of percentage loss of conductance. *New Phytologist* **213:** 1068–1075.

Nolf M, Beikircher B, Rosner S, Nolf A, Mayr S. 2015. Xylem cavitation resistance can be estimated based on time-dependent rate of acoustic emissions. *New Phytologist* **208:** 625–632.

Oliveras I, Martínez–Vilalta J, Jimenez–Ortiz T, José Lledó M, Escarré A, Piñol J. 2003. Hydraulic properties of *Pinus halepensis*, *Pinus pinea* and *Tetraclinis articulata* in a dune ecosystem of Eastern Spain. *Plant Ecology* **169:** 131–141.

Peguero–Pina JJ, Sancho–Knapik D, Barrón E, Camarero JJ, Vilagrosa A, Gil–Pelegrín E. 2014. Morphological and physiological divergences within *Quercus ilex* support the existence of different ecotypes depending on climatic dryness. *Annals of Botany* **114:** 301–313.

Peguero–Pina JJ, Mendoza–Herrer Ó, Gil–Pelegrín E, Sancho–Knapik D. 2018. Cavitation Limits the Recovery of Gas Exchange after Severe Drought Stress in Holm Oak (*Quercus ilex* L.). *Forests* **9:** b443.

Petruzzellis F, Nardini A, Savi T, Tonet V, Castello M, Bacaro G. 2019. Less safety for more efficiency: water relations and hydraulics of the invasive tree *Ailanthus altissima* (Mill.) Swingle compared with native *Fraxinus ornus* L. *Tree Physiology* **39:** 76–87.

Petruzzellis F, Tordoni E, Tomasella M, Savi T, Tonet V, Palandrani C, et al. 2021. Functional differentiation of invasive and native plants along a leaf efficiency/safety trade–off. *Environmental and Experimental Botany* **188:** 104518.

Pinto CA, David JS, Cochard H, Caldeira MC, Henriques MO, Quilhó T, Paço TA, Pereira JS, David TS. 2012. Drought–induced embolism in current–year shoots of two Mediterranean evergreen oaks. *Forest Ecology and Management* **285:** 1–10.

Pita P, Cañas I, Soria F, Ruiz F, Toval G. 2005. Use of physiological traits in tree breeding for improved yield in drought–prone environments. The case of *Eucalyptus globulus*. *Investigación agraria. Sistemas y recursos forestales* **14:** 383–393.

Quero JL, Sterck F, Martinez–Vilalta J, Villar R. 2011. Water–use strategies of six co–existing Mediterranean woody species during a summer drought. *Oecologia* **166:** 45–57.

Rodríguez-Calcerrada J, Li M, López R, Cano FJ, Oleksyn J, Atkin OK, Pita P, Aranda I, Gil L. 2017. Drought-induced shoot dieback starts with massive root xylem embolism and variable depletion of nonstructural carbohydrates in seedlings of two tree species. *New Phytologist* **213:** 597–610.

Rosas T, Mencuccini M, Barba J, Cochard H, Saura-Mas S, Martínez-Vilalta J. 2019. Adjustments and coordination of hydraulic, leaf and stem traits along a water availability gradient. *New Phytologist* **223:** 632–646.

Rosner S, Heinze B, Savi T, Dalla-Salda G. 2019. Prediction of hydraulic conductivity loss from relative water loss: new insights into water storage of tree stems and branches. *Physiologia Plantarum* **165:** 843–854.

Salleo S, Gullo MAL, De Paoli D, Zippo M. 1996. Xylem recovery from cavitation-induced embolism in young plants of *Laurus nobilis*: a possible mechanism. *New Phytologist* **132:** 47–56.

Savi T, Love VL, Dal Borgo A, Martellos S, Nardini A. 2017. Morpho–anatomical and physiological traits in saplings of drought–tolerant Mediterranean woody species. *Trees* **31:** 1137–1148.

Savi T, Tintner J, Da Sois L, Grabner M, Petit G, Rosner S. 2019. The potential of Mid–Infrared spectroscopy for prediction of wood density and vulnerability to embolism in woody angiosperms. *Tree Physiology* **39:** 503–510.

Sperry JS, Nichols KL, Sullivan JE, Eastlack SE. 1994. Xylem embolism in ring-porous, diffuse-porous, and coniferous trees of northern Utah and interior Alaska. *Ecology* **75:** 1736–1752.

Tissier J, Lambs L, Peltier J P, Marigo G. 2004. Relationships between hydraulic traits and habitat preference for six *Acer* species occurring in the French Alps. *Annals of Forest Science* **61:** 81–86.

Tognetti R, Longobucco A, Raschi A. 1998. Vulnerability of xylem to embolism in relation to plant hydraulic resistance in *Quercus pubescens* and *Quercus ilex* co–occurring in a Mediterranean coppice stand in central Italy. *New Phytologist* **139:** 347–448.

Tognetti R, Longobucco A, Raschi A. 1999. Seasonal embolisms and xylem vulnerability in deciduous and evergreen Mediterranean trees influenced by proximity to a carbon dioxide spring. *Tree Physiology* **19:** 271–277.

Tognetti R, Longobucco A, Raschi A, Jones MB. 2001. Stem hydraulic properties and xylem vulnerability to embolism in three co–occurring Mediterranean shrubs at a natural CO_2 spring. *Functional Plant Biology* **28:** 257–268.

Torres-Ruiz JM, Cochard H, Mencuccini M, Delzon S, Badel E. 2016. Direct observation and modelling of embolism spread between xylem conduits: a case study in Scots pine. *Plant, Cell & Environment* **39:** 2774–2785.

Torres-Ruiz JM, Cochard H, Choat B, Jansen S, López R, Tomášková I, et al. 2017. Xylem resistance to embolism: presenting a simple diagnostic test for the open vessel artefact. *New Phytologist* **215:** 489–499.

Trifilò P, Lo Gullo MA, Nardini A, Pernice F, Salleo S. 2007. Rootstock effects on xylem conduit dimensions and vulnerability to cavitation of *Olea europaea* L. *Trees* **21:** 549–556.

Trifilò P, Nardini A, Gullo MAL, Barbera PM, Savi T, Raimondo F. 2015. Diurnal changes in embolism rate in nine dry forest trees: relationships with species–specific xylem vulnerability, hydraulic strategy and wood traits. *Tree Physiology* **35:** 694–705.

Tyree MT, Cochard H, Cruiziat P, Sinclair B, Ameglio T. 1993. Drought–induced leaf shedding in walnut: evidence for vulnerability segmentation. *Plant, Cell & Environment* **16:** 879–882.

Tyree MT, Cochard H. 1996. Summer and winter embolism in oak: impact on water relations. In *Annales des sciences forestières*, Vol. 53, EDP Sciences, 173–180.

Venturas M, López R, Martín JA, Gascó A, Gil L. 2014. Heritability of *Ulmus minor* resistance to Dutch elm disease and its relationship to vessel size, but not to xylem vulnerability to drought. *Plant Pathology* **63:** 500–509.

Vogt UK. 2001. Hydraulic vulnerability, vessel refilling, and seasonal courses of stem water potential of *Sorbus aucuparia* L. and *Sambucus nigra* L. Journal of Experimental Botany **52:** 1527–1536.

Wang R, Zhang L, Zhang S, Cai J, Tyree MT. 2014. Water relations of *Robinia pseudoacacia* L.: do vessels cavitate and refill diurnally or are R-shaped curves invalid in *Robinia*? *Plant, Cell & Environment* **37:** 2667–2678.

Zhang Y, Lamarque LJ, Torres–Ruiz JM, Schuldt B, Karimi Z, Li S, Jansen S. 2018. Testing the plant pneumatic method to estimate xylem embolism resistance in stems of temperate trees. *Tree Physiology* **38:** 1016–1025.

Zhu SD, Chen YJ, Ye Q, He PC, Liu H, Li RH, Cao KF. 2018. Leaf turgor loss point is correlated with drought tolerance and leaf carbon economics traits. *Tree Physiology* **38:** 658–663.

Species	**Fv/Fm Leaf**		**Year**	**Fv/Fm Bark**		**Fv/Fm Wood**	
	Mean	SD		Mean	SD	Mean	SD
Acer campestre	0.81	0.04	current	0.73	0.12	0.76	0.03
			1y	0.81	0.02	0.76	0.02
			2y	0.73	0.03	0.65	0.03
Acer monspessulanum	0.80	0.01	current	0.79	0.02	0.81	0.01
			1y	0.75	0.04	0.71	0.02
			2y	0.76	0.04	0.68	0.02
Acer pseudoplatanus	0.83	0.01	current	0.82	0.01	0.77	0.01
			1y	0.80	0.04	0.73	0.02
			2y	0.79	0.03	0.73	0.02
Ailanthus altissima	0.82	0.01	current	0.79	0.01	0.68	0.02
			1y	0.67	0.02	0.53	0.05
			2y	0.64	0.06	0.60	0.02
Alnus incana	0.82	0.01	current	0.73	0.16	0.69	0.13
			1y	0.67	0.18	0.66	0.16
			2y	0.75	0.03	0.70	0.02
Betula pendula	0.83	0.02	current	0.75	0.02	0.75	0.04
			1y	0.77	0.03	0.78	0.03
			2y	0.75	0.02	0.72	0.07
Carpinus betulus	0.83	0.01	current	0.80	0.00	0.80	0.00
			1y	0.79	0.01	0.78	0.01
			2y	0.78	0.02	0.79	0.01
Carpinus orientalis	0.82	0.01	current	0.81	0.01	0.81	0.02
			1y	0.82	0.01	0.80	0.02
			2y	0.81	0.01	0.80	0.02
Cercis sliquatrum	0.84	0.00	current	0.80	0.02	0.81	0.02
			1y	0.78	0.01	0.81	0.01
			2y	0.73	0.03	0.81	0.01
Corylus avellana	0.84	0.01	current	0.81	0.01	0.78	0.00
			1y	0.78	0.01	0.78	0.01
			2y	0.75	0.05	0.78	0.01
Cotinus coggygria	0.83	0.00	current	0.81	0.01	0.80	0.02
			1y	0.81	0.01	0.79	0.01
			2y	0.79	0.02	0.78	0.03
Fagus sylvatica	0.83	0.01	current	0.78	0.04	0.78	0.04
			1y	0.75	0.02	0.79	0.01
			2y	0.72	0.03	0.79	0.02
Fraxinus ornus	0.83	0.01	current	0.84	0.00	0.74	0.02
			1y	0.82	0.01	0.62	0.08
			2y	0.82	0.02	0.65	0.06
Hedera helix	0.80	0.01	current	0.79	0.01	0.81	0.01

			1y	0.81	0.01	0.78	0.01
			2y	0.77	0.02	0.53	0.08
Juglans regia	0.85	0.01	current	0.84	0.01	0.78	0.01
			1y	0.79	0.05	0.63	0.08
			2y	0.73	0.05	0.62	0.09
Laurus nobilis	0.82	0.01	current	0.82	0.01	0.80	0.02
			1y	0.82	0.01	0.80	0.01
			2y	0.83	0.00	0.78	0.01
Ligustrum vulgare	0.80	0.04	current	0.82	0.01	0.79	0.01
			1y	0.82	0.00	0.79	0.01
			2y	0.81	0.00	0.75	0.02
Malus domestica	0.81	0.01	current	0.85	0.01	0.80	0.04
			1y	0.83	0.02	0.70	0.06
			2y	0.82	0.01	0.77	0.04
Olea europaea	0.83	0.01	current	0.80	0.01	0.80	0.02
			1y	0.81	0.01	0.78	0.02
			2y	0.81	0.01	0.79	0.02
Ostrya carpinifolia	0.81	0.02	current	0.81	0.01	0.79	0.01
			1y	0.80	0.01	0.76	0.01
			2y	0.80	0.01	0.77	0.01
Prunus mahaleb	0.83	0.01	current	0.80	0.02	0.82	0.02
			1y	0.78	0.02	0.74	0.03
			2y	0.77	0.02	0.75	0.01
Prunus spinosa	0.84	0.01	current	0.81	0.02	0.81	0.01
			1y	0.67	0.05	0.80	0.01
			2y	0.62	0.08	0.78	0.01
Quercus ilex	0.81	0.01	current	0.79	0.01	0.76	0.01
			1y	0.78	0.01	0.74	0.01
			2y	0.81	0.01	0.72	0.02
Quercus petraea	0.84	0.01	current	0.82	0.01	0.80	0.02
			1y	0.81	0.01	0.76	0.02
			2y	0.76	0.05	0.74	0.05
Quercus pubescens	0.86	0.01	current	0.83	0.01	0.81	0.02
			1y	0.82	0.01	0.67	0.11
			2y	0.74	0.08	0.62	0.13
Robinia pseudoacacia	0.83	0.01	current	0.80	0.01	0.79	0.01
			1y	0.81	0.02	0.77	0.02
			2y	0.81	0.02	0.75	0.03
Salix alba	0.82	0.01	current	0.76	0.03	0.75	0.01
			1y	0.70	0.01	0.74	0.03
			2y	0.71	0.00	0.72	0.02
Sambucus nigra	0.84	0.01	current	0.82	0.01	0.76	0.03
			1y	0.82	0.01	0.75	0.07
			2y	0.78	0.01	0.71	0.01
Tilia cordata	0.83	0.01	current	0.81	0.01	0.78	0.03
			1y	0.82	0.01	0.76	0.01
			2y	0.80	0.03	0.74	0.02

Ulmus minor	0.83	0.01	current	0.81	0.02	0.76	0.04
			1y	0.82	0.01	0.72	0.03
			2y	0.76	0.07	0.66	0.02
Viburnum lantana	0.85	0.01	current	0.79	0.03	0.68	0.14
			1y	0.78	0.03	0.77	0.02
			2y	0.78	0.04	0.76	0.02
Ginkgo biloba	0.84	0.01	current	0.80	0.03	0.80	0.05
			1y	0.69	0.06	0.63	0.08
			2y	0.62	0.02	0.67	0.09
Juniperus communis	0.80	0.03	current	0.69	0.07	0.68	0.04
			1y	0.77	0.02	0.76	0.02
			2y	0.79	0.01	0.73	0.03
Larix decidua	0.85	0.02	current	0.79	0.01	0.54	0.15
			1y	0.74	0.04	0.67	0.08
			2y	0.71	0.03	0.65	0.06
Picea abies	0.86	0.00	current	0.75	0.00	0.68	0.06
			1y	0.76	0.01	0.69	0.04
			2y	0.73	0.02	0.63	0.07
Pinus halepnsis	0.80	0.01	current	0.80	0.01	0.73	0.01
			1y	0.68	0.06	0.46	0.07
			2y	0.70	0.01	0.42	0.05
Pinus nigra	0.82	0.02	current	0.80	0.03	0.68	0.06
			1y	0.60	0.05	0.48	0.03
			2y	0.72	0.02	0.57	0.01
Pinus pinea	0.81	0.01	current	0.81	0.01	0.72	0.03
			1y	0.78	0.01	0.52	0.11
			2y	0.77	0.00	0.49	0.02
Pinus sylvestris	0.82	0.01	current	0.81	0.01	0.79	0.01
			1y	0.73	0.03	0.71	0.07
			2y	0.70	0.02	0.70	0.02
Abies cephalonica	0.85	0.01	current	0.77	0.02	0.68	0.04
			1y	0.76	0.01	0.56	0.01
			2y	0.76	0.04	0.51	0.11

Tab. S3 Mean values and associated standard deviation (SD) of maximum quantum yield of PSII (Fv/Fm) of leaf and both bark and wood, measured on the selected species in the different stem years. Current: current-year stem; 1y: 1-year stem; 2y: 2-year stem.

Chapter III

Study 4

Stem photosynthesis contributes to non-structural carbohydrates pool and modulates xylem vulnerability to embolism in *Fraxinus ornus* L.

Sara Natale[1], Martina Tomasella[1], Sara Gargiulo[2], Francesco Petruzzellis[1], Giuliana Tromba[3], Enrico Boccato[1], Valentino Casolo[2], Andrea Nardini[1]

[1] Dipartimento di Scienze della Vita - University of Trieste, Trieste, Italy

[2] Dipartimento di Scienze Agroalimentari, ambientali e animali – University of Udine, Udine, Italy

[3] Elettra-Sincrotrone Trieste, Area Science Park, Basovizza, Trieste 34149, Italy

Manuscript submitted to Environmental and Experimental Botany

Abstract

Leaves are the main photosynthetic organs in woody plants, but in some species stem photosynthesis can significantly contribute to the tree carbon budget. This extra carbon gain has been suggested to be crucial, especially when drought stress causes leaf photosynthesis impairment and/or a reduced phloem transport.

Stems of potted *Fraxinus ornus* L. saplings were covered with aluminium foil to verify if inhibition of stem photosynthesis increases plant vulnerability to drought. The plants reached the target xylem water potentials of -3.5 MPa (corresponding to 50% loss of xylem hydraulic conductivity, PLC) in ca. one week and were then re-irrigated to field capacity to quantify their recovery capacity. Vulnerability was assessed in light-exposed and stem-shaded saplings with both the hydraulic method and in vivo with X-ray micro-computed tomography. We also measured non-structural carbohydrate (NSC) concentration and osmotic potentials in bark and wood separately.

Stem shading affected the hydraulic response during a drought event, but did not influence the recovery phase. Both hydraulic and imaging methods revealed higher vulnerability to xylem embolism in stem-shaded saplings. This difference was coupled with modification of the NSC pool and impaired osmoregulation, in particular in the wood of stem-shaded saplings compared to control ones.

Our results indicate stem photosynthesis as an important source of local NSCs, directly or indirectly involved in osmoregulation processes, which could be crucial to enhance the hydraulic resistance to embolism formation and to endure drought.

Keywords: stem photosynthesis; drought; wood parenchyma; X-ray micro-CT; embolism; xylem vulnerability

Introduction

Ongoing climate change is producing an increase in the frequency/severity of anomalous drought events (IPCC 2022), leading to higher rates of tree dieback and mortality (Allen et al. 2010; Hember et al. 2017; Neumann et al. 2017). Drought-induced tree decline is mainly related to hydraulic failure and/or carbon starvation (McDowell et al. 2022). Since xylem and phloem functioning are strongly inter-related (Holtta et al. 2009; Hubeau and Steppe 2015), plant hydraulic and carbon dynamics are intimately linked (Adams et al. 2009; McDowell, 2011; Adams et al. 2017), so that these two events are likely to co-occur to some extent under drought (Lloret et al. 2018; McDowell et al. 2011; McDowell et al. 2015). Hence, when considering the effects of drought stress on plant survival, it is fundamental to consider both processes (Adams et al. 2017; Sevanto et al. 2014; Nardini et al. 2011). A recent review highlighted the relationships between stem xylem embolism and non-structural carbohydrates (NSCs) dynamics (Tomasella et al. 2020), as mediated by water and solutes exchanges between xylem conduits and parenchyma cells where NSCs are stored.

Leaves are the primary photosynthetic organs for most woody species, and are generally assumed to be the major source of carbon assimilation. Nonetheless, a wide range of woody plants can carry out photosynthesis even at stem level (Pfanz and Aschan 2001), which appears as an extra source of carbon assimilation helping plants to face drought events. Generally, the spatial distribution of chloroplasts within stems strongly depends on the interspecific characteristics in axial and radial light transmission through stem tissues (Sun et al. 2003,2005; Schmitz et al. 2012), which generally depends on bark features (Aschan et al. 2001; Cernusak and Cheesman 2015). The functional advantage of stem photosynthesis is that it can be sustained either from the external CO_2 uptake (at bark level) and/or from the re-fixation of internally respired CO_2 (Pfanz et al. 2002; Teskey et al 2008; Ávila et al. 2014). Stem photosynthesis has been reported to substantially contribute to wood production, thus playing a key role in stem growth (Saveyn et al. 2010; Cernusak and Hutley 2011; Bloemen et al. 2013; Steppe et al. 2015), and bud development (Saveyn et al. 2010). As an example, stem photosynthesis was reported to contribute to stem growth by 25-56% in three evergreen woody species (Saveyn et al. 2010), by about 10% in mature *Eucalyptus* species (Cernusak and Hutley 2011), and by 30% in *Populus tremuloides* (Bloemen et al. 2016).

The peculiar capacity of stems to rely on endogenous CO_2 (Pfanz et al. 2002; Aschan and Pfanz 2003; Wittmann and Pfanz 2008), might represent an important advantage when leaf photosynthesis is impaired by stomatal closure and phloem transport is limited (Vandegehuchte et al. 2015). The photosynthetic activity of stems might also minimize the impact of absence of leaves due to seasonality (e.g. deciduous species), and might become particularly important under stress conditions

(e.g. drought stress) (Eyles et al. 2009; Teskey et al. 2008). Indeed, the first observations of photosynthetic stems were referred to desert plants (Gibson 1983; Nilsen 1995), and recent studies have suggested a coordination between stem photosynthesis and hydraulics in these species (Ávila-Lovera et al. 2017).

The first clear evidence of an involvement of stem photosynthesis in hydraulic functioning was provided by Schmitz et al. (2012), who highlighted a reduction in stem hydraulic conductivity in detached branches of different mangrove species after branches were covered to block light penetration. This led to the hypothesis that the inhibition of stem photosynthesis induced a depletion of carbohydrate reserves with consequent failure of embolism repair processes (Nardini et al. 2018). Moreover, inhibition of stem photosynthesis can induce stems to shrink more drastically in response to severe drought stress (Bloemen et al. 2016). Hence, sugars produced at stem level might potentially be involved in maintaining the turgor of wood parenchyma cells, which are supposed to assist xylem hydraulic functioning (Secchi et al. 2021; Tomasella et al. 2021; Kawai et al. 2022). Similarly, light-excluded branches of *Populus nigra* displayed a steeper increase in embolism formation for any given water potential, compared to control stems (De Baerdemaeker et al. 2017). A recent study pointed out that stem shading had a different impact on an evergreen woody species (*Laurus nobilis*) compared to a deciduous one (*Populus alba*) (Trifilò et al. 2021). Specifically, the inhibition of stem photosynthesis affected the growth of *Laurus nobilis* but not of *Populus alba*. Conversely, stem shading affected the ability to recover from xylem embolism in *P. alba*, but not in *L. nobilis*.

All the above studies suggest that stem photosynthesis might have an impact on hydraulic functioning under drought, or on recovery capacity after drought release. An important unresolved issue concerns the contribution of stem photosynthesis to the NSC pool in the wood, and how this interacts with hydraulic responses during and after drought. In this study, we report a set of experiments aiming to test the impact of long- and short-term stem shading on drought response of *Fraxinus ornus*. This species was selected because it is known to have functional chloroplasts at bark and wood level (Natale et al. submitted), and because it is a drought-tolerant tree facing prolonged summer periods with partial or full stomatal closure (Nardini et al. 2003; Tomasella et al. 2019).

Material and Methods

Experimental design and plant material

Three-year-old potted saplings of *Fraxinus ornus* L. (n=83) were provided by a public nursery (Vivai Pascul, Regional Forestry Service, Tarcento, Italy). Plants were transplanted on February 2020 in 3.5 L pots filled with a light mineral substrate designed for green roof installations (Savi et al. 2013), and

randomly allocated in a greenhouse of the botanical garden of the University of Trieste (Italy). The plant's height (h) and the diameter at the stem base (ø) were measured both at the start and end of the experiment.

Plants were regularly irrigated at field capacity until the start of experimental drought treatments, and their position in the greenhouse was randomly shifted weekly, to assure exposure to uniform light conditions. A slow-release fertilizer (Flortis, universal fertilizer, Orvital, Milano, Italy) was added to each pot in April (4 g) and May (3 g) to prevent nutritional deficiency. Saplings were divided in three groups (c. 30 plants each) (Fig. 1): i) plants maintained under greenhouse light conditions for the whole experiment (Li, Light plants); ii) plants with stems covered with aluminum foil for 30 days before starting the drought experiment (LS, Long-shading plants); iii) plants with stems covered with aluminum foil at the starting of the drought experiment (SS, Short-shading plants). By covering the whole stem, we aimed at inhibiting stem photosynthesis and favoring the depletion of local non-structural carbohydrates (NSC) reserves. For each group, plants were further divided in three treatments: i) well-watered (C, control), ii) drought-stress (D), and iii) recovery (R). The drought stress was induced by suspending irrigation for 5-10 days, until the xylem water potential (Ψ_{xyl}) dropped to about -3.5 MPa, i.e. a value known to induce 50% loss of xylem hydraulic conductance due to embolism in this species (Petit et al. 2016). Plants for the recovery experiment were re-irrigated to field capacity and harvested 24 h later to assess possible hydraulic recovery. C plants (Li_C, LS_C, SS_C) were harvested and measured within the same period as D and R plants. For each group, five to ten plants were harvested for pigments quantification as well as hydraulic and NSC measurements between 12:00 and 14:30 h, to avoid diurnal fluctuation effects on carbohydrate content (Tixier et al. 2018).

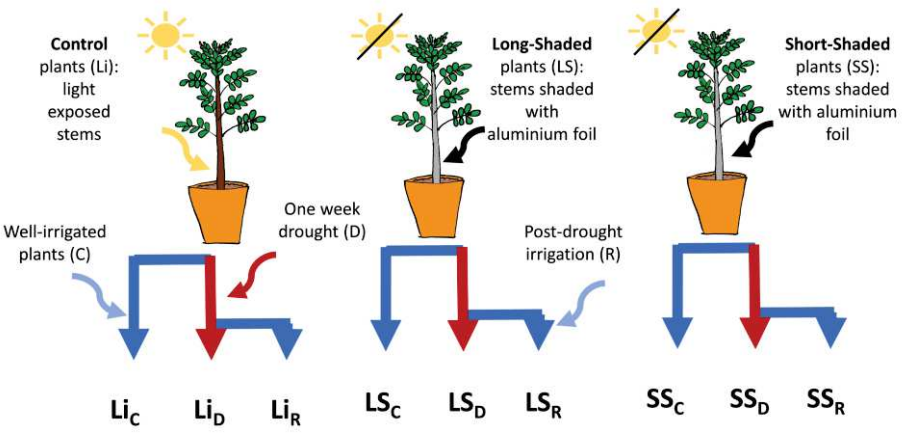

Fig. 1 Schematic representation of the experimental design. *Fraxinus ornus* plants with stems light-exposed (Li) and shaded (LS, SS) are shown with brown and grey stems respectively. Blu and red arrows indicate irrigation and drought treatments. The drought-recovery experiment aimed to compare control (Li_C, LS_C, SS_C), drought (Li_D, LS_D, SS_D), and recovery (Li_R, LS_R, SS_R) plants.

Leaf water relations and stem osmotic potential

To assess eventual effects of water and/or light treatments on plant water status, we measured midday stem xylem water potential (Ψ_{xyl}), leaf conductance to water vapor (g_L), and stem osmotic potential. In particular, g_L (mmol m^{-2} s^{-1}) was measured with a steady-state porometer (SC-1, Decagon Devices Inc., Pullman, USA) between 11.00 h and 14.00 h on 2 mature and healthy leaves per sapling. Measurements were coupled to quantification of photosynthetic photon flux density (PPFD, µmol m^{-2} s^{-1}) with a Quantum photo-radiometer (HD 9021, Delta OHM S.r.l., Padova, Italy) at the selected leaf surface.

To assess Ψ_{xyl}, 1-2 mature leaves per sapling were bagged in cling film and covered with aluminum foil in the early morning. Leaves were then collected between 11:00 and 14:00 h and water potential was measured using a pressure chamber (mod. 1505D, PMS Instrument co., Albany, OR, USA).

Additionally, stem osmotic potential at full turgor was estimated on 5-10 saplings for each group/treatment. Bark and wood were carefully separated, re-hydrated for 20 minutes by immersion in bi-distilled water, wrapped in parafilm and placed at -20°C until measurements. Samples were thawed for c. 10 min, chopped quickly and wrapped in cling film, and placed in liquid nitrogen for 60 seconds. Half of the sample was put immediately in a dewpoint hygrometer to measure the osmotic water potential (WP4, Decagon Devices Inc., Pullman, USA), and the other half was stored in 1 mL Eppendorf filled with bi-distilled water, and shaken for 30 seconds before measuring the electrical conductivity (C, µS cm^{-1}) of the solution with a conductivity meter (LAQUAtwin-EC-11, Horiba Ltd., Kyoto, Japan). Data of osmotic water potential and electrical conductivity collected during the greenhouse experiment were combined with those obtained during the micro-CT experiment (see below).

Pigment analysis

To investigate the possible effects of stem shading and water treatments on pigment concentration, we quantified chlorophyll *a*, chlorophyll *b* and carotenoids content in both bark and wood upon extraction of fresh material in 80% acetone solution. Bark and wood samples (5-10 saplings for each group/treatment) were cut into small pieces to facilitate the extraction. About 50 mg of bark samples were placed in a 2 mL Eppendorf filled up with 1.5 mL of acetone solution. About 300 mg of wood were placed in 1.5 mL of acetone solution. Absorption spectra were recorded using an UV-Vis spectrophotometer (model 7315; Jenway, Worcestershire, UK) between 250 and 750 nm. The final pigment concentration was assessed using Wellburn equations (Wellburn 1994).

Hydraulic Measurements

In order to quantify eventual impacts of stem shading on xylem vulnerability to embolism or on post-drought hydraulic recovery, we measured the percentage loss of hydraulic conductivity (PLC) in one-year-old stem segments in Li, LS, and SS saplings (5-10 saplings per group/treatment). PLC was measured in well-watered saplings, as well as in plants exposed to D and R treatments.

To minimize any possible excision artifact in PLC quantification, we followed the protocol by Torres-Ruiz et al. (2015). We optimized the method by making the first cut underwater. Whole pots wrapped in a plastic bag were immersed in a bucket filled with tap water, and the stem was cut at the base under water. Then, the stem was transferred in clean tap water and a second cut was made at a minimum distance of 0.2 times the maximum vessel length (MVL). The residual xylem tension was released by immersing the cut end in water for 20 min. MVL was estimated with the "air injection method" described by Wang et al. (2014), and averaged 23 ± 9 cm in our saplings. Then, the xylem segment to be used for hydraulic measurements was excised under water at the minimum distance of 1.5 MVL from the initial cut, to remove any artificial embolism generated during previous cuts. Hydraulic conductance was measured with a hydraulic apparatus (Tomasella et al. 2019a), using filtered (0.45 μm) and degassed mineral water added with 10 mM KCl as perfusion solution (Nardini et al. 2007). Stem hydraulic conductance was measured gravimetrically under a water head of 4 kPa before (initial hydraulic conductance, K_i) and after (maximum hydraulic conductance, K_{max}) flushing the sample at high pressure (0.15 MPa) for 3 min to remove embolism. Maximum stem specific hydraulic conductivity (kg m^{-1} s^{-1} MPa^{-1}) was calculated as:

$$K_s = K_{max} \times l/A_x$$

where l is sample length and A_x is the xylem transverse area, as calculated on the basis of the radius of the stem cross section area occupied by xylem, measured using a caliper.

Finally, PLC was calculated as:

$$PLC=100\times[1-(K_i/K_{max})]$$

Micro-CT imaging

In order to validate results obtained with destructive hydraulic techniques, we performed micro-CT scans on intact saplings (n=26) at the SYRMEP beamline of the Elettra Synchrotron light source (Trieste, Italy), on 17-21 July 2020. Since we had a short facility-time access and data obtained with the "classical hydraulic technique" revealed a statistically significant higher PLC only in long-shaded plants (see below), we decided to perform micro-CT scans only on "light" and "long-shaded" plants. Therefore, one month before Synchrotron access, the whole stems of 12 plants were shaded with aluminum foil (LS, long-shaded plants), whereas other 12 plants were kept under ambient light

conditions (Li, light plants). Eight plants per group were subjected to drought stress by withholding irrigation until Ψ_{xyl} reached the critical threshold (see above). Stems were quickly fixed to the sample holder and the plant was wrapped in cling film to avoid water loss. For image acquisition, the average X-ray source energy was 22 keV and pixel size was set at 2 μm to clearly visualize xylem conduits. The exposure time was 200 milliseconds (ms) per image, except for some taller saplings where this value was set at 100 ms to reduce plant movement during rotation. Scan range was 180°, with 1800 projections per sample. The slice reconstructions were performed using SYRMEP Tomo Project (STP) software (Brun et al. 2015). A phase retrieval pre-processing algorithm (Paganin et al. 2002) was applied prior to the conventional filtered back-projection algorithm to increase the image contrast. Reconstructed images were processed using ImageJ. Due to the larger diameter of the stems compared to the field of view (ca. 4 mm × 4 mm), analyses were conducted on about one-quarter of the stem section, excluding the immature xylem next to the vascular cambium. The embolized sapwood area (A_{embol}) was calculated by dividing the total embolized pixel area by the analyzed mature sapwood area, and expressed as percentage (Secchi et al. 2021). Immediately after each scan, a stem segment was collected just below the scan point from each sapling, and used to quantify carbohydrate content and estimate stem osmotic potential at full turgor (see above).

Stem non-structural carbohydrate content

In order to investigate the effects of the experimental treatments on carbohydrate dynamics, non-structural carbohydrate (NSC) analysis was performed on 4 cm long stem segments, sampled next to those used for hydraulic measurements immediately after cutting (5-10 saplings for each treatment). Bark and wood were separated, microwaved for 3 min at 700 W in order to stop enzymatic activity, oven-dried at 70 °C for 24 h, then grinded with a mixer mill (MM400; Retsch GmbH, Haan, Germany), and stored at -20 °C until NSC extraction. Aliquots of 15 ± 2 mg of powder were processed following Tomasella et al. (2019), with the following modifications: after extraction with 80% ethanol, soluble carbohydrates were recovered in the alcoholic supernatant, while the pellet (containing both starch and maltodextrin oligosaccharide fractions) was incubated in 0.5 mL 2 mM HEPES-Tris pH 6.7 at 25 °C overnight. The remaining starch in the pellet was processed according to Landhäusser et al. (2018). Soluble NSC were measured as mg g^{-1} DW of glucose by the Anthrone assay method (Yemm and Willis 1954), comparing sugars content of samples with known amount of glucose.

Starch hydrolysis was performed according to Landhäusser et al. (2018). The glucose resulting from the starch enzymatic digestion was quantified as NADPH using a spectrophotometer (Perkin Elmer, Boston, MA, USA), following Bergmeyer and Bernt (1974). Starch amount was expressed as mg of

glucose equivalent per g of DW, by comparison with standard solutions of amylose.
Mannitol concentration was determined enzymatically, according to the method described by Lunn et al. (1989) slightly modified as follows: a buffer of Tris-HCl pH 7.5 was prepared and NAD^+ was suspended. 1 mg/mL di BAS was added to stabilize ROS formation and the buffer was adjusted to pH 8.6. 5 µL of sample was added to 294 µL of buffer-NAD reagent. After mixing, the absorbance at 340 nm was recorded and 2 µL (0.6U) of mannitol dehydrogenase added per each sample and the absorbance was measured again. The measurements were carried out at 40°C.

Statistical Analysis

Statistical analyses were carried out with R (R Core Team, 2021). Boxplot graph were prepared with the 'ggplot2' package. We used generalized least squares (GLS) analyses ('nmle' R package), setting each parameter measured (e.g. g_L, Ψ_{xyl}, π_0, etc) as the response variable and the light treatment (L) and the water treatment (W) as the first and second explanatory variables, respectively. When homogeneity of variance assumption was violated we used the "varPower()" variance structure (Pinheiro et al. 2016). When the interaction was statistically significant ($p < 0.05$), differences between groups were tested and p-values were adjusted using the Holm correction through the emmeans function in 'emmeans' R package.

Results

The plant's height (h) and the diameter of the stem base (ø) measured both at the start and end of the experiment are reported in Tab. S1. Plant size was similar in all experimental groups, and did not change significantly along the duration of the experiment.

Stem shading's effects on pigments concentration

As reported in Fig. S1, we did not observe any significant effect of the interaction of light and water treatments on chlorophyll and carotenoid concentration. We observed a significant effect of light treatment in Chl*a* and Chl*b* concentration of wood samples. In particular, compared to LS_C plants, SS_C showed a slightly higher amount of total chlorophyll concentration (Chl *a*+*b*) (Fig. S2, Appendix 1). Nonetheless, it is worth noting that Chl*a*, Chl*b* and Car concentration tended to be lower in bark samples of both shaded treatments, with a marked decrease for LS ones.
The investigated interaction (Light × Water, Fig. S2) was significant for Chl *a/b* in wood and Car/Chl tot in bark. LS_D plants had overall highest Chl *a/b* in wood, and SS_C plants had lowest Car/Chl tot.

Plant water relations

Midday values of g_L and Ψ_{xyl} during the experimental period were statistically similar in well irrigated light (Li) and shaded (LS, SS) samples (Fig. 2, 3A respectively). Drought induced a drop of xylem water potential that reached the value of c. -3.5 MPa in all light treatments, leading to marked stomatal closure and reduction of g_L. Upon recovery, plant water status returned to the values detected for controls, but g_L remained well below control values.

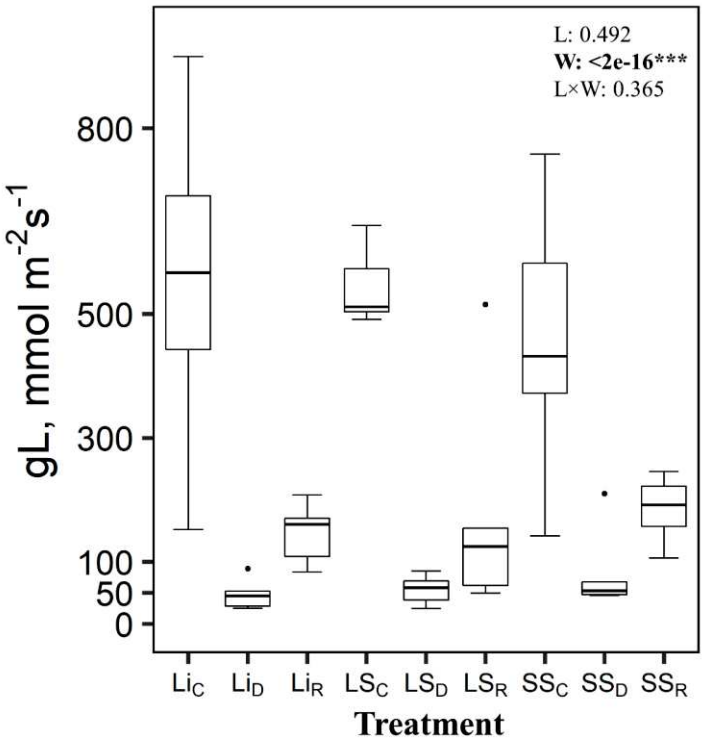

Fig. 2 Median values, 25th and 75th percentiles of leaf conductance to water vapour (g_L) measured in light (Li), long-shaded (LS) and short-shaded (SS) control (Li_C, LS_C, SS_C), drought (Li_D, LS_D, SS_D) and recovery (Li_R, LS_R, SS_R) *Fraxinus ornus* saplings at midday. Explanatory variables (light treatment, L, and water treatment, W) and associated p-values are reported. * = $p < 0.05$; ** = $p < 0.01$; *** = $p < 0.001$.

Values of PLC for well irrigated plants averaged 20-30% in all light treatments. Despite similar drops of Ψ_{xyl} (Fig. 3A) under drought, hydraulic measurements showed that PLC was markedly higher in LS_D plants compared to Li_D ones (50.03±10.13 and 78.57±7.78 respectively). A non-significant tendency toward higher PLC values was detected also in SS_D plants compared to Li_D. Upon re-irrigation, PLC returned to control values within 24 h, and stem shading apparently did not affect the

ability to recover xylem hydraulic function (Fig. 3B, Appendix 1). No differences were detected in terms of maximum stem hydraulic conductivity across different groups/treatments (Fig. 3C).

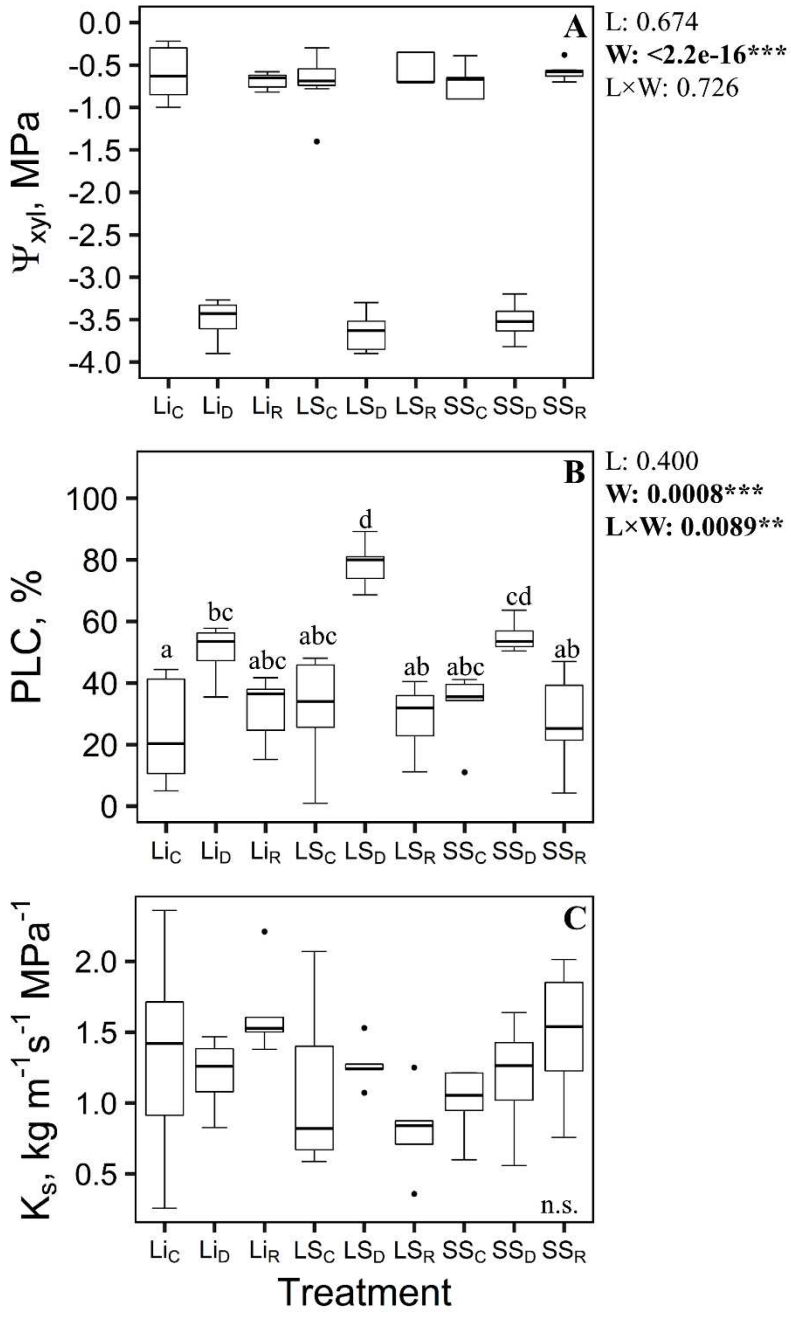

Fig. 3 Median values, 25th and 75th percentiles of A) xylem water potential (Ψ_{xyl}), B) percentage loss of hydraulic conductance (PLC) and C) maximum stem specific hydraulic conductivity (K_s) measured in light (Li), long-shaded (LS) and short-shaded (SS) control (Li_C, LS_C, SS_C), drought (Li_D, LS_D, SS_D) and recovery (Li_R, LS_R, SS_R) *Fraxinus ornus* saplings. Different letters indicate statistically significant differences among

treatments ($p < 0.05$). n.s. = not statistically significant. Explanatory variables (light treatment, L, and water treatment, W) and associated p-values are reported. * = $p < 0.05$; ** = $p < 0.01$; *** = $p < 0.001$.

Micro-CT analysis of xylem in intact plants allowed us to identify water-filled (functional) from gas-filled (non-functional) vessels (Fig. 4C) in saplings exposed to different light and water treatments. Changes in AEV/AMX are shown in Fig. 4B. Changes in plant water status in C, D and R plants were similar to those detected in the main experiment (Fig. 4A). We observed that the number of embolized vessels increased in drought-treated plants compared to controls, but these apparently returned to the functional status upon re-irrigation. Consistent with results obtained in hydraulic measurements, LS_D plants had higher embolism levels compared to Li_D ones, although the low number of samples masked the statistical significance in this set of plants.

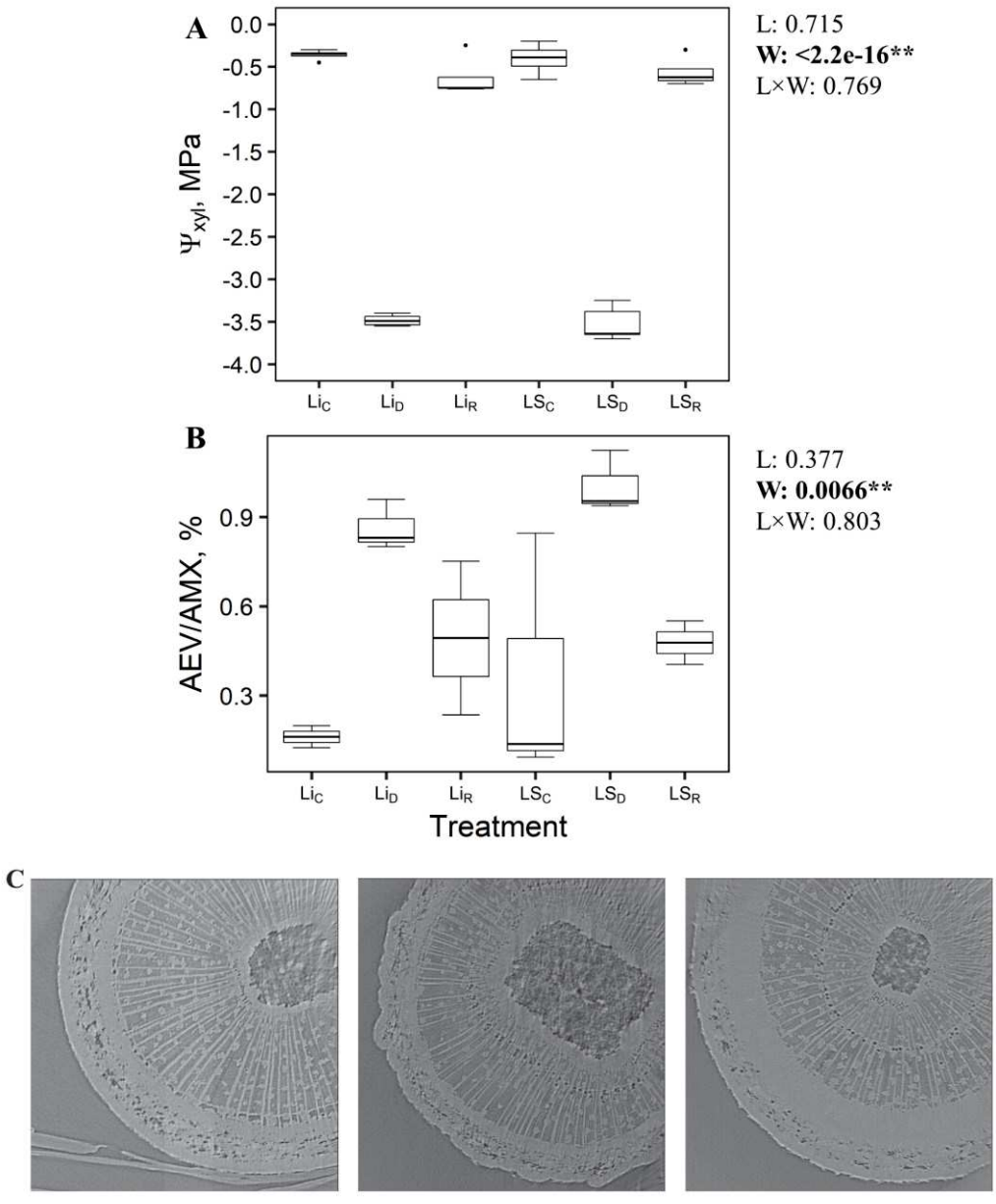

Fig. 4 Median values, 25th and 75th percentiles of A) xylem water potential (Ψ_{xyl}), B) percentage of total area of embolized vessels (AEV) over total area of mature xylem (AMX) in response to changes in xylem pressure during drought and recovery treatments. Data were measured in light (Li) and long-shaded (LS) control (Li_C, LS_C), drought (Li_D, LS_D) and recovery (Li_R, LS_R) *Fraxinus ornus* saplings. Explanatory variables (light treatment, L, and water treatment, W) and associated p-values are reported. * = $p < 0.05$; ** = $p < 0.01$; *** = $p < 0.001$. C) In vivo visualization by X-ray microtomography (micro-CT) in stems of intact *Fraxinus ornus* saplings. Reconstructed cross-sections showing embolized (air-filled vessels, dark circles) and functional conduits (water-filled, light gray circles) in well-watered, stressed and recovered plants, respectively.

Electrical conductivity was similar in all groups/treatments, both in bark and wood (Fig. 5). Osmotic potential (Fig. 6) was also similar across experimental groups at bark level. However, a different pattern of osmoregulation was observed at wood level in light vs shaded plants. In fact, under drought stress only plants with light exposed stems (Li) adjusted the wood osmotic potential at full turgor (π_0) to more negative values than control plants (Fig. 6B). Interestingly, SS plants had the highest (less negative) osmotic potential, although the high variability of data masked any eventual statistical significance.

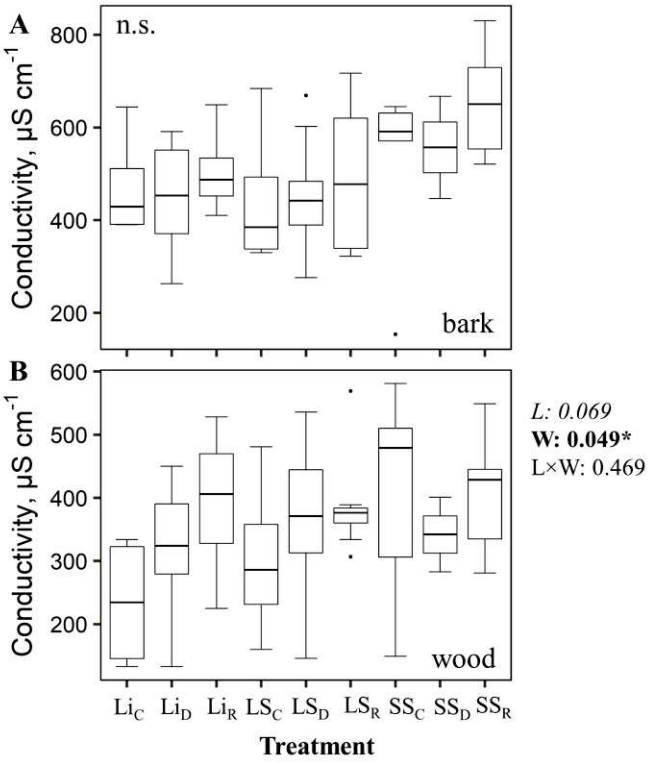

Fig. 5 Median values, 25th and 75th percentiles of A) bark and B) wood conductivity, measured in light (Li), long-shaded (LS) and short-shaded (SS) control (Li_C, LS_C, SS_C), drought (Li_D, LS_D, SS_D) and recovery (Li_R, LS_R, SS_R) *Fraxinus ornus* saplings. N.s. = not statistically significant. Explanatory variables (light treatment, L, and water treatment, W) and associated p-values are reported. * = $p < 0.05$; ** = $p < 0.01$; *** = $p < 0.001$.

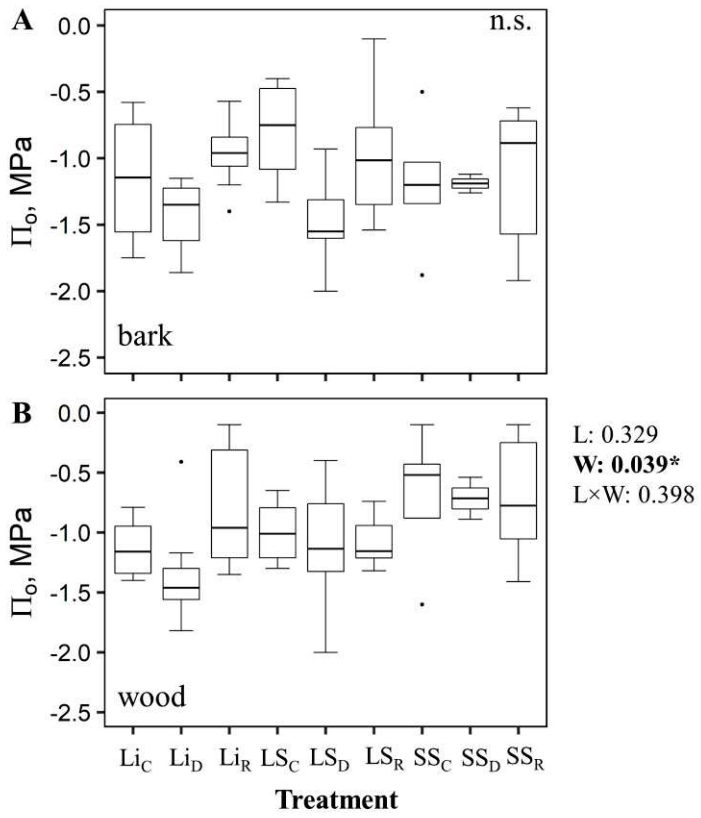

Fig. 6 Median values, 25th and 75th percentiles of A) bark and B) wood osmotic potential at full turgor (π_0), measured in light (Li), long-shaded (LS) and short-shaded (SS) control (Li_C, LS_C, SS_C), drought (Li_D, LS_D, SS_D) and recovery (Li_R, LS_R, SS_R) *Fraxinus ornus* saplings. n.s. = not statistically significant. Explanatory variables (light treatment, L, and water treatment, W) and associated p-values are reported. * = $p < 0.05$; ** = $p < 0.01$; *** = $p < 0.001$.

Stem non-structural carbohydrates content

In general, Li plants showed different trends of NSC dynamics/content compared to LS and SS plants, especially under drought and in particular at wood level (Fig. 7, 8). Both soluble NSC and starch were lower in the wood of LS and SS plants compared to Li ones (Fig. 7D). Moreover, stem shading significantly affected the ability of LS and SS sample to mobilize the pool of NSC (starch + soluble sugars) in both bark and wood under drought stress, when compared to Li samples (Fig. 8). In fact, Specifically, drought induced a decrease of total NSC content both in the bark and wood, but only in Li plants, mainly due to the marked starch depletion (Fig. 7B, E), while LS and SS plants maintained lower NSC levels under well-watered conditions, that remained unchanged under drought or recovery. LS_D and SS_D samples also showed a significantly higher concentration of mannitol in bark compared to Li_D samples (Fig. 7C). The same pattern of NSC dynamics was observed in the analyses

of samples measured at the Synchrotron, although no statistically significant difference (Fig. S3) was found for each NSC quantified.

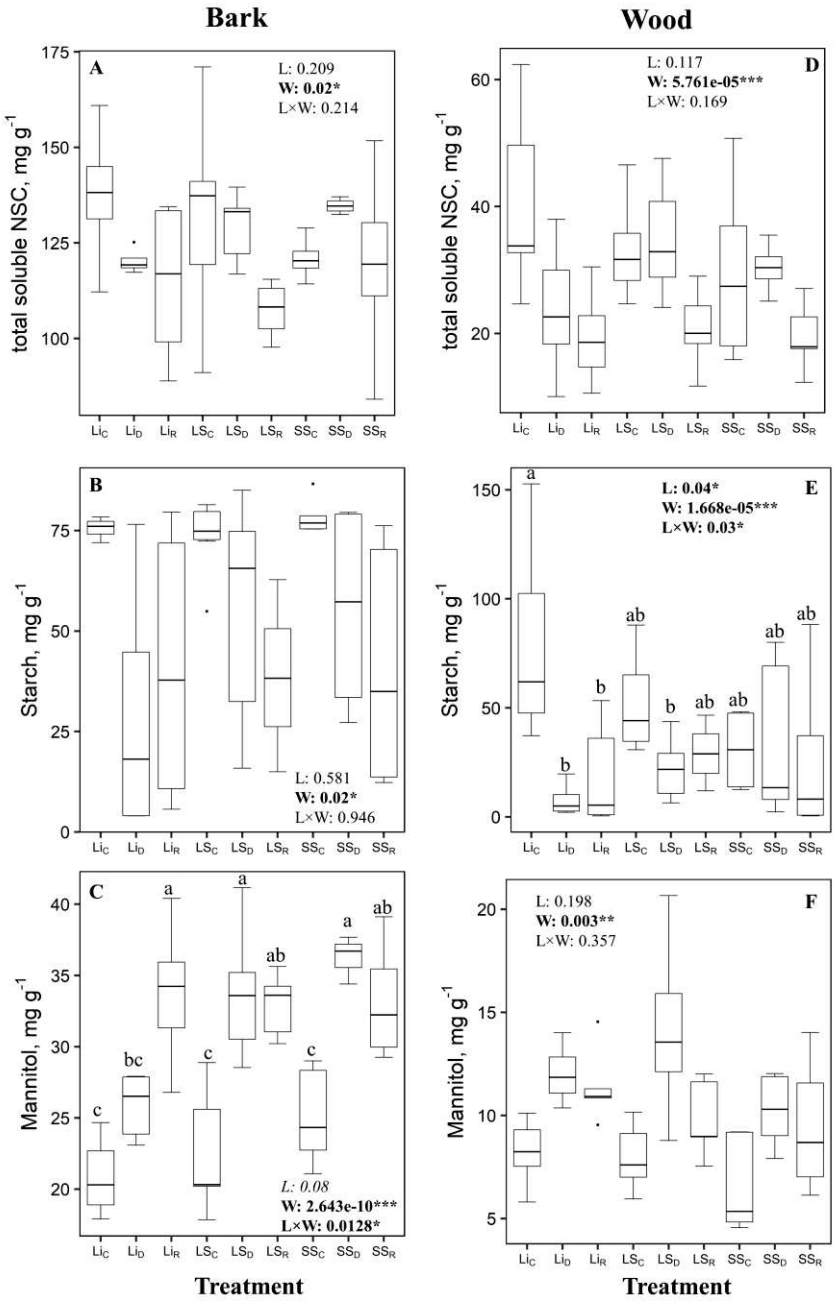

Fig. 7 Median values, 25th and 75th percentiles of stem A,D) total soluble non-structural carbohydrates (NSC), B,E) starch and C,F) mannitol measured in bark (A,B,C) and wood (D,E,F) of light (Li), long-shaded (LS) and short-shaded (SS) control (Li_C, LS_C, SS_C), drought (Li_D, LS_D, SS_D) and recovery (Li_R, LS_R, SS_R) *Fraxinus ornus* saplings. Different letters indicate statistically significant differences among treatments ($p < 0.05$). Explanatory variables (light treatment, L, and water treatment, W) and associated p-values are reported. * = $p < 0.05$; ** = $p < 0.01$; *** = $p < 0.001$.

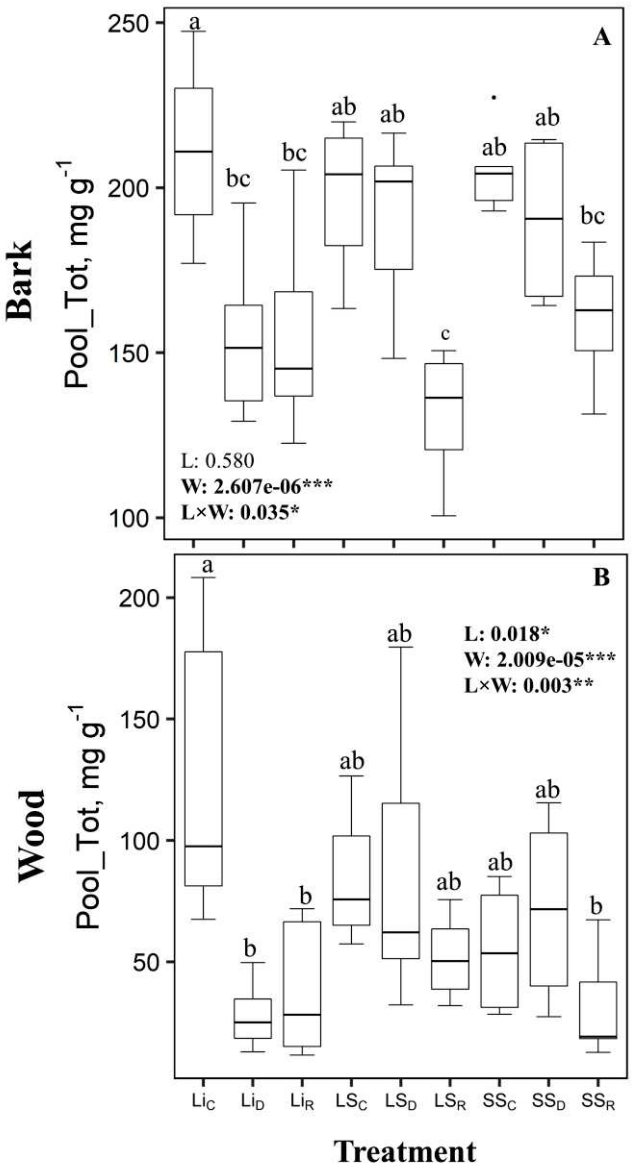

Fig. 8 Median values, 25th and 75th percentiles of stem total non-structural carbohydrates (Pool Tot) measured in A) bark and B) wood of light (Li), long-shaded (LS) and short-shaded (SS) control (Li_C, LS_C, SS_C), drought (Li_D, LS_D, SS_D) and recovery (Li_R, LS_R, SS_R) *Fraxinus ornus* saplings. Different letters indicate statistically significant differences among treatments ($p < 0.05$). Explanatory variables (light treatment, L, and water treatment, W) and associated p-values are reported. * = $p < 0.05$; ** = $p < 0.01$; *** = $p < 0.001$.

Discussion

Our data provide new insights on the possible roles played by stem photosynthesis in plant responses to drought stress. We found that plants exposed to a long-term stem shading increased their vulnerability to xylem embolism during drought compared to control plants, but no effect of stem shading was recorded during the recovery phase. Changes in xylem hydraulic vulnerability were coupled with modifications of the NSC pool and impaired osmoregulation processes, suggesting a possible role of parenchymatic cell turgor in xylem hydraulic functioning.

Stem shading had no impact on gas exchanges rates in well-irrigated plants, and under drought the magnitude of xylem water potential drop and g_L reduction was similar in all light treatments. Upon re-irrigation, plant water status returned promptly to control values but g_L remained low, at least 24 h after water re-supply. This might suggest some residual hydraulic limitation to gas exchange, or the presence of a chemical signal super-imposed on the hydraulic one, limiting g_L recovery. We can safely rule out the first hypothesis, as hydraulic measurements revealed that stem hydraulic functioning promptly returned to pre-drought levels upon re-watering (see below). Hence, it is possible that chemical signals (e.g. ABA) accumulated in leaves under drought, and were not promptly removed or de-activated upon re-irrigation. Similar observations have been previously reported for different woody species (Loewenstein and Pallardy 2002; Martorell et al. 2014; Tombesi et al. 2015; Hasan et al. 2021), and suggest the presence of a mechanism delaying stomatal aperture in some species, even after apparent recovery of hydraulic functioning and plant water status. This mechanism might be important to prevent water potential drop before embolism repair processes have been completed, considering that hydraulic recovery is energetically favored only when xylem water potential rises to near-zero values (Nardini et al. 2018).

Despite similar trajectories in terms of gas exchange and water status, saplings subjected to different light treatments showed different patterns of embolism accumulation and loss of hydraulic conductivity when exposed to drought conditions. In particular, PLC was about 30% in all groups when under full irrigation, and slightly increased to about 50% in Li_D plants. On the contrary, PLC markedly increased in LS_D plants (up to 80%) and SS_D ones (about 60%). These findings suggest that stem shading increased the vulnerability to xylem embolism, making plants more prone to the risk of hydraulic failure under drought. Our data are consistent with previous findings (Schmitz et al. 2012; Bloemen et al. 2016; Chen et al. 2021) and confirm that stem photosynthesis is an important modulator of plant hydraulic performance.

Changes in xylem anatomy induced by different light conditions can influence plant hydraulics (Plavcova et al. 2011). Although we did not measure anatomical traits in our study plants,

measurements of plant size at the start and the end of the experiment did not show any active growth during this period. Hence, it is unlikely that differences between groups/treatments derived from the production of new xylem conduits with different features. This is also confirmed by the fact that maximum stem hydraulic conductivity was similar in all experimental groups and treatments (Fig. 3C). However, we cannot rule out the possibility that shading induced modifications in the ultrastructure of pit membranes, as reported in some species (Plavcova et al. 2011) but not in others (Tomasella et al. 2021), with potentially important impacts on conduits' vulnerability to air-seeding (Thonglim et al. 2020). However, changes in pit membranes structure should also reflect on xylem hydraulic efficiency, which was not the case in our study plants.

The observed increase in vulnerability to xylem embolism induced by stem shading (Fig. 3) is intriguing, but in line with previous observations (De Baerdemaeker et al. 2017; Tomasella et al. 2021). Previous studies have suggested that a reduction in NSC availability induced by inhibition of stem photosynthesis would be at the basis of this phenomenon, and our data indeed confirm that NSC pool was reduced in the wood of shaded plants compared to controls. Furthermore, control plants showed a significant depletion of carbohydrates under drought, which was relatively minor in the NSC-limited shaded stems (Fig. 7). Interestingly, the levels of mannitol were tendentially higher in shaded plants compared to light ones during drought. Since shaded plants suffered from higher PLC values and mannitol is an osmoprotectant, its accumulation might be a tolerance strategy to drought stress to re-balance the soil water uptake and leaf water loss (Guicherd et al 1997; Fini et al. 2012; 2014a,b; Khaleghi et al. 2019). In future studies, it would undoubtedly be interesting to study in more detail the concentration of sucrose, fructose, glucose, maltose and mannitol to better understand which is the NSC that plays a major role in response to drought stress in *F. ornus*. The mechanistic link between NSC availability and xylem hydraulics remains elusive, although different hypotheses have been proposed. NSC might be required to modulate the surface tension of xylem sap, which can indeed affect xylem vulnerability (Losso et al. 2017; Tomasella et al. 2021). Also, NSC might represent energy sources for the synthesis of lipids and proteins that have been suggested to act as surfactants and stabilizers of gas nanobubbles in the xylem sap (Schenk et al. 2017). A third hypothesis was advanced by Tomasella et al. (2021), suggesting that NSC might be crucial for maintaining cell turgor and continuity between wood parenchyma cells and both phloem cells and xylem conduits under drought (De Roo et al. 2020). Indeed, vessel-associated cells (VACs) are known to exchange water and solutes with the xylem conduits (Morris et al. 2018). Under drought, it is likely that the water potential of VAC equilibrates with the negative pressure inside the conduits, possibly leading to cell turgor loss and shrinkage (Oparka 1994). In *F. ornus* the turgor loss point of leaf cells shifts on a seasonal basis from -2.5 MPa in spring to -3.2 MPa by the end of summer drought (Nardini

et al. 2003). This last value would be close the Ψ_{xyl} value of -3.5 MPa targeted in our drought experiment. Hence, it is possible that wood parenchyma of LS_D (and SS_D) plants experienced the risk of turgor loss and cell shrinkage due to lack of NSC and limited osmoregulation capacity, possibly increasing the risk of air seeding at the interface between VAC and xylem conduits. In fact, we observed a decrease in stem osmotic potential only in Li_D plants (Fig. 6), but not in LS_D or SS_D. Interestingly, changes in osmotic potential were not accompanied by significant changes in electrical conductivity, suggesting that osmoregulation was achieved at least partly via accumulation of sugars or other non-charged compounds, that were less available (and not mobilized under drought) in both LS and SS plants.

Previous studies have suggested that inhibition of stem photosynthesis can lead to an impairment of post-drought hydraulic recovery processes (Schmitz et al. 2012; Bloemen et al. 2016; Liu et al. 2019). In fact, embolism repair is an energy-dependent process likely based on an osmotic mechanism that involves release of sugars into refilling conduits (Savi et al. 2016; Tomasella et al. 2017; Secchi et al. 2021). Hence, a reduction in NSC pools as induced by inhibition of stem photosynthesis is expected to delay or prevent the recovery of hydraulic functions after re-irrigation (Trifilò et al. 2017). However, in our set of plants complete hydraulic recovery was observed in all light treatments. Changes in PLC under drought, as estimated on the basis of destructive hydraulic techniques, can arise because of artefacts caused by excision of stem samples while the xylem conduits are under substantial tension (Wheeler et al. 2013). On the other hand, relaxation procedures aimed at preventing such artefacts can induce artificial refilling of xylem conduits, more likely when xylem tension values are moderate (Trifilò et al. 2014). We can rule out the possibility of such artefacts in our dataset, because the same pattern of embolism build-up under drought and recovery after re-irrigation was observed in intact plants, based on micro-CT analysis. This suggests that hydraulic recovery was possible also in LS and SS plants, either because the residual amount of NSC was still sufficient to sustain the process, or because xylem tension transiently increased to near-atmospheric values under low-transpiration conditions, favoring spontaneous dissolution of the gas phase in xylem conduits (Konrad et al. 2018).

In conclusion, our results confirm that NSC produced by stem photosynthesis are important modulators of plant hydraulic performance under drought stress, favoring the long-term maintenance of xylem hydraulic function. We suggest that these effects are mediated by the direct or indirect role of NSC in osmoregulatory processes, but the mechanistic link between turgor loss of wood parenchyma and embolism build-up still awaits to be elucidated. In any case, our data suggest that enhanced photosynthetic capacity at stem level might be an important trait for selection of woody crops and forest trees with an improved tolerance to extreme drought events.

Author contributions

SN, AN, MT, and FP designed the experiment; SN performed the experiment and measurements, with help from SG, MT, FP, EB, VC and AN; SN and MT performed hydraulic measurements; EB performed leaf conductance to water vapor measurements; SN, SG and VC performed NSC extraction, analysis and data interpretation; SN, MT, FP, GT and AN performed measurements at Synchrotron; SN and FP analyzed the data; SN and AN wrote the manuscript, with contributions and revisions from all authors.

Acknowledgements

We are very grateful to the 'Direzione centrale risorse agroalimentari, forestali e ittiche – area foreste e territorio' of the 'Regione Autonoma Friuli Venezia Giulia', and to the public nursery Vivai Pascul (Tarcento, Italy) for providing the plant material for the glasshouse experiment. The access to the SYRMEP beamline was granted by Elettra Sincrotrone Trieste (proposal no. 20195384).

References

Adams HD, Guardiola–Claramonte M, Barron–Gafford GA, Villegas JC, Breshears DD, Zou CB, Troch PA, Huxman TE. 2009. Reply to Leuzinger et al.: drought-induced tree mortality temperature sensitivity requires pressing forward with best available science. *Proceedings of the National Academy of Sciences* **106:** E107.

Adams HD, Zeppel MJ, Anderegg WR, Hartmann H, Landhäusser SM, Tissue DT, et al. 2017. A multi–species synthesis of physiological mechanisms in drought–induced tree mortality. *Nature ecology & evolution* **1:** 1285–1291.

Allen CD, Macalady AK, Chenchouni H, Bachelet D, McDowell N, et al. 2010. A global overview of drought and heat– induced tree mortality reveals emerging climate change risks for forests. *Forest Ecology and Management* **259:** 660–684.

Aschan G, Wittmann C, Pfanz H. 2001. Age-dependent bark photosynthesis of aspen twigs. *Trees* **15:** 431–437.

Aschan G, Pfanz H. 2003. Non-foliar photosynthesis-a strategy of additional carbon acquisition. *Flora-Morphology, Distribution, Functional Ecology of Plants* **198:** 81–97.

Ávila E, Herrera A, Tezara W. 2014. Contribution of stem CO_2 fixation to whole-plant carbon balance in nonsucculent species. *Photosynthetica* **52:** 3–15.

Ávila–Lovera E, Zerpa AJ, Santiago LS. 2017. Stem photosynthesis and hydraulics are coordinated in desert plant species. *New Phytologist* **216:** 1119–1129.

Bergmeyer HU, Bernt E. 1974. Sucrose. In: HU Bergmeyer, eds. *Methods of Enzymatic Analysis*. Academic Press, New York, USA: 1176–1179.

Bloemen J, Overlaet–Michiels L, Steppe K. 2013. Understanding plant responses to drought: how important is woody tissue photosynthesis? *Acta Horticulturae* **991:** 149–157.

Bloemen J, Vergeynst LL, Overlaet-Michiels L, Steppe K. 2016. How important is woody tissue photosynthesis in poplar during drought stress? *Trees* **30:** 63–72.

Brun F, Pacile S, Accardo A, Kourousias G, Dreossi D, Mancini L, Tromba G, Pugliese R. 2015. Enhanced and flexible software tools for X-ray computed tomography at the italian synchrotron radiation facility Elettra. *Fundamenta Informaticae* **141:** 233–243.

Cernusak LA, Hutley LB. 2011. Stable. isotopes reveal the contribution of corticular photosynthesis to growth in branches of *Eucalyptus miniata*. *Plant physiology* **155:** 515–523.

Cernusak LA, Cheesman AW. 2015. The benefits of recycling: how photosynthetic bark can increase drought tolerance. *New Phytologist* ***208*****:** 995–997.

Chen X, Zhao P, Zhao X, Wang Q, Ouyang L, Larjavaara M, et al. 2021. Involvement of stem corticular photosynthesis in hydraulic maintenance of Eucalyptus trees and its effect on leaf gas exchange. *Environmental and Experimental Botany* **186:** 104451.

De Baerdemaeker NJ, Salomón RL, De Roo L, Steppe K. 2017. Sugars from woody tissue photosynthesis reduce xylem vulnerability to cavitation. *New Phytologist* **216:** 720–727.

De Roo L, Salomón RL, Oleksyn J, Steppe, K. 2020. Woody tissue photosynthesis delays drought stress in *Populus tremula* trees and maintains starch reserves in branch xylem tissues. *New Phytologist* **228:** 70–81.

Eyles A, Pinkard EA, O'Grady AP, Worledge D, Warren CR. 2009. Role of corticular photosynthesis following defoliation in Eucalyptus globulus. *Plant, Cell &Environment* **32:** 1004–1014.

Fini A, Guidi L, Ferrini F, Brunetti C, Di Ferdinando et al. 2012. Drought stress has contrasting effects on antioxidant enzymes activity and phenylpropanoid biosynthesis in *Fraxinus ornus* leaves: an excess light stress affair?. *Journal of plant physiology*, **169:** 929–939.

Fini A, Guidi L, Giordano C, Baratto MC, Ferrini F, Brunetti C, et al. 2014a. Salinity stress constrains photosynthesis in *Fraxinus ornus* more when growing in partial shading than in full sunlight: consequences for the antioxidant defence system. *Annals of botany* **114:** 525–538.

Fini A, Ferrini F, Di Ferdinando M, Brunetti C, Giordano C, Gerini F, Tattini M. 2014b. Acclimation to partial shading or full sunlight determines the performance of container-grown *Fraxinus ornus* to subsequent drought stress. *Urban Forestry & Urban Greening* **13:** 63–70.

Gibson AC. 1983. Anatomy of photosynthetic old stems of nonsucculent dicotyledons from North American deserts. *Botanical Gazette* **144:** 347–362.

Guicherd P, Peltier JP, Gout E, Bligny R, Marigo G. 1997. Osmotic adjustment in *Fraxinus excelsior* L.: malate and mannitol accumulation in leaves under drought conditions. *Trees* **11:** 155–161.

Hasan MM, Gong L, Nie ZF, Li FP, Ahammed GJ, Fang XW. 2021. ABA-induced stomatal movements in vascular plants during dehydration and rehydration. *Environmental and Experimental Botany* **186:** 104436.

Hember RA, Kurz WA, Coops NC. 2017. Relationships between individual-tree mortality and water-balance variables indicate positive trends in water stress-induced tree mortality across North America. *Global Change Biology* **23:** 1691–1710.

Hölttä T, Mencuccini M, Nikinmaa E. 2009. Linking phloem function to structure: analysis with a coupled xylem-phloem transport model. *Journal of Theoretical Biology* **259:** 325–337.

Hubeau M, Steppe K. 2015. Plant-PET scans: in vivo mapping of xylem and phloem functioning. *Trends in Plant Science* **20:** 676–685.

Kawai K, Minagi K, Nakamura T, Saiki ST, Yazaki K, Ishida A. 2022. Parenchyma underlies the interspecific variation of xylem hydraulics and carbon storage across 15 woody species on a subtropical island in Japan. *Tree Physiology* **42:** 337–350.

Khaleghi A, Naderi R, Brunetti C, Maserti BE, Salami SA, Babalar M. 2019. Morphological, physiochemical and antioxidant responses of *Maclura pomifera* to drought stress. *Scientific reports* **9:** 1–12.

Konrad W, Katul G, Roth-Nebelsick A, Jensen KH. 2018. Xylem functioning, dysfunction and repair: a physical perspective and implications for phloem transport. *Tree physiology* **39:** 243–261.

Landhäusser SM, Chow PS, Dickman LT, Furze ME, Kuhlman I, Schmid S, et al. 2018. Standardized protocols and procedures can precisely and accurately quantify non-structural carbohydrates. *Tree Physiology* **38:** 1764–1778.

Lloret F, Sapes G, Rosas T, Galiano L, Saura-Mas S, Sala A, Martínez-Vilalta J. 2018. Non-structural carbohydrate dynamics associated with drought-induced die-off in woody species of a shrubland community. *Annals of Botany* **121:** 1383–1396.

Liu J, Gu L, Yu Y, Huang P, Wu Z, Zhang Q, Qian Y, Sun Z. 2019. Corticular photosynthesis drives bark water uptake to refill embolized vessels in dehydrated branches of *Salix matsudana*. *Plant, Cell & Environment* **42:** 2584–2596.

Loewenstein NJ, Pallardy SG. 2002. Influence of a drying cycle on post-drought xylem sap abscisic acid and stomatal responses in young temperate deciduous angiosperms. *New Phytologist* **156:** 351–361.

Losso A, Beikircher B, Dämon B, Kikuta S, Schmid P, Mayr S. 2017. Xylem sap surface tension may be crucial for hydraulic safety. *Plant Physiology* **175:** 1135–1143.

Lunn PG, Northrop CA, Northrop AJ. 1989. Automated enzymatic assays for the determination of intestinal permeability probes in urine. 2. Mannitol. *Clinica Chimica Acta* **183:** 163–170.

Martorell Lliteras S, Diaz-Espejo A, Medrano H, Ball M, Choat B. 2014. Rapid hydraulic recovery in *Eucalyptus pauciflora* after drought: linkages between stem hydraulics and leaf gas exchange. *Plant, Cell & Environment* **37:** 617–626.

McDowell NG. 2011. Mechanisms linking drought, hydraulics, carbon metabolism, and vegetation mortality. *Plant Physiology* **155:** 1051–1059.

McDowell NG, Beerling DJ, Breshears DD, Fisher RA, Raffa KF, Stitt M. 2011. The interdependence of mechanisms underlying climate-driven vegetation mortality. *Trends in Ecology & Evolution* **26:** 523–532.

McDowell NG, Coops NC, Beck PS, Chambers JQ, Gangodagamage C, Hicke JA, et al. 2015. Global satellite monitoring of climate-induced vegetation disturbances. *Trends in plant science* **20:** 114–123.

McDowell NG, Sapes G, Pivovaroff A, Adams HD, Allen CD, Anderegg WR, et al. 2022. Mechanisms of woody-plant mortality under rising drought, CO_2 and vapour pressure deficit. *Nature Reviews Earth & Environment* **3:** 294–308.

McDowell NG, Sapes G, Pivovaroff A, Adams HD, Allen CD, Anderegg WR, et al. 2022. Mechanisms of woody-plant mortality under rising drought, CO_2 and vapour pressure deficit. *Nature Reviews Earth & Environment* **3:** 294–308.

Morris H, Plavcová L, Gorai M, Klepsch MM, Kotowska M, Schenk HJ, Jansen S. 2018. Vessel-associated cells in angiosperm xylem: highly specialized living cells at the symplast-apoplast boundary. *American Journal of Botany* **105:** 1–10.

Nardini A, Salleo S, Trifilò P, Lo Gullo MA. 2003. Water relations and hydraulic characteristics of three woody species co-occurring in the same habitat. *Annals of Forest Science* **60:** 297–305.

Nardini A, Gascò A, Trifilò P, Lo Gullo MA, Salleo S. 2007. Ion-mediated enhancement of xylem hydraulic conductivity is not always suppressed by the presence of Ca^{2+} in the sap. *Journal of Experimental Botany* **58:** 2609–2615.

Nardini A, Gullo MAL, Salleo S. 2011. Refilling embolized xylem conduits: is it a matter of phloem unloading? *Plant Science* **180:** 604–611.

Nardini A, Savi T, Trifilò P, Lo Gullo MA. 2018. Drought stress and the recovery from xylem embolism in woody plants. In Cánovas FM, Luettge U, Matyssek R, eds. *Progress in Botany*. Berlin, DE, Springer, 197–231.

Neumann M, Mues V, Moreno A, Hasenauer H, Seidl R. 2017. Climate variability drives recent tree mortality in Europe. *Global Change Biology* **23**: 4788–4797.

Nilsen ET. 1995. Stem photosynthesis: extent, patterns and role in plant carbon economy. In: Gartner B, eds. *Plant stems: physiology and functional morphology*. San Diego, USA: Academic Press, 223–240.

Oparka KJ. 1994. Plasmolysis: new insights into an old process. *New Phytologist* **126:** 571–591.

Paganin D, Mayo SC, Gureyev TE, Miller PR, Wilkins SW. 2002. Simultaneous phase and amplitude extraction from a single defocused image of a homogeneous object. *Journal of microscopy* **206:** 33–40.

Pfanz H, Aschan G. 2001. The existence of bark and stem photosynthesis in woody plants and its significance for the overall carbon gain. An eco-physiological and ecological approach. In: Essr K, Luttge U, Kadereit JW, Beyshlag W, eds. *Progress in Botany*, Berlin, DE: Springer-Verlag, 477–510.

Pfanz H, Aschan G, Langenfeld-Heyser R, Wittmann C, Loose M. 2002. Ecology and ecophysiology of tree stems: corticular and wood photosynthesis. *Naturwissenschaften* **89:** 147–162.

Plavcova L, Hacke UG, Sperry JS. 2011. Linking irradiance-induced changes in pit membrane ultrastructure with xylem vulnerability to cavitation. *Plant, Cell & Environment* **34:** 501–513.

R Core Team. 2022. R: A language and environment for statistical computing. R Foundation for Statistical Computing, Vienna, Austria. URL https://www.R-project.org/.

Saveyn A, Steppe K, Ubierna N, Dawson TE. 2010. Woody tissue photosynthesis and its contribution to trunk growth and bud development in young plants. *Plant, Cell & Environment* **33:** 1949–1958.

Savi T, Andri S, Nardini A. 2013. Impact of different green roof layering on plant water status and drought survival. *Ecological Engineering* **57:** 188–196.

Savi T, Casolo V, Luglio J, Bertuzzi S, Trifilò P, Lo Gullo MA, Nardini A. 2016. Species–specific reversal ofstem xylem embolism after a prolonged drought correlates to endpoint concentration ofsoluble sugars. *Plant Physiology and Biochemistry* **106:** 198–207.

Schenk HJ, Espino S, Romo DM, et al. 2017. Xylem surfactants introduce a new element to the cohesion-tension theory. *Plant Physiology* **173:** 1177–1196.

Schmitz N, Egerton JJG, Lovelock CE, Ball MC. 2012. Light-dependent maintenance of hydraulic function in mangrove branches: do xylary chloroplasts play a role in embolism repair? *New Phytologist* **195:** 40–46.

Secchi F, Pagliarani C, Cavalletto S, Petruzzellis F, Tonel G, Savi T, et al. 2021. Chemical inhibition of xylem cellular activity impedes the removal of drought-induced embolisms in poplar stems-new insights from micro-CT analysis. *New Phytologist* **229:** 820–830.

Sevanto S, Mcdowell NG, Dickman LT, Pangle R, Pockman WT. 2014. How do trees die? A test of the hydraulic failure and carbon starvation hypotheses. *Plant, Cell & Environment* **37:** 153–161.

Steppe K, Sterck F, Deslauriers A. 2015. Diel growth dynamics in tree stems: linking anatomy and ecophysiology. *Trends in Plant Science* **20:** 335–343.

Sun Q, Yoda K, Suzuki M, Suzuki H. 2003. Vascular tissue in the stem and roots of woody plants can conduct light. *Journal of Experimental Botany* **54:** 1627–1635.

Sun Q, Yoda K, Suzuki H. 2005. Internal axial light conduction in the stems and roots of herbaceous plants. *Journal of Experimental Botany* **56:** 191–203.

Teskey RO, Saveyn A, Steppe K, McGuire MA. 2008. Origin, fate and significance of CO_2 in tree stems. *New Phytologist* **177:** 17–32.

Thonglim A, Delzon S, Larter M, Karami O, Rahimi A, Offringa R, et al. 2021. Intervessel pit membrane thickness best explains variation in embolism resistance amongst stems of *Arabidopsis thaliana* accessions. *Annals of Botany* **128:** 171–182.

Tixier A, Orozco J, Roxas AA, Earles JM, Zwieniecki MA. 2018. Diurnal variation in nonstructural carbohydrate storage in trees: remobilization and vertical mixing. *Plant Physiology* **178:** 1602–1613.

Tomasella M, Häberle KH, Nardini A, Hesse B, Machlet A, Matyssek R. 2017. Post-drought hydraulic recovery is accompanied by non-structural carbohydrate depletion in the stem wood of Norway spruce saplings. *Scientific Reports* **7:** 14308.

Tomasella M, Casolo V, Aichner N, Petruzzellis F, Savi T, Trifilò P, Nardini A. 2019a. Non-structural carbohydrate and hydraulic dynamics during drought and recovery in *Fraxinus ornus* and *Ostrya carpinifolia* saplings. *Plant Physiology and Biochemistry* **145:** 1–9.

Tomasella M, Petrussa E, Petruzzellis F, Nardini A, Casolo V. 2019b. The possible role of non-structural carbohydrates in the regulation of tree hydraulics. *International journal of molecular sciences* **21:** 144.

Tomasella M, Casolo V, Natale S, Petruzzellis F, Kofler W, Beikircher B, Stefan Mayr, Nardini A. 2021. Shade-induced reduction of stem nonstructural carbohydrates increases xylem vulnerability to embolism and impedes hydraulic recovery in *Populus nigra*. *New Phytologist* **231:** 108–121.

Tombesi S, Nardini A., Frioni T., Soccolini M, Zadra C, Farinelli D, Poni S, Palliotti A. 2015. Stomatal closure is induced by hydraulic signals and maintained by ABA in drought-stressed grapevine. *Scientific reports* **5:** 1–12.

Torres-Ruiz JM, Jansen S, Choat B, McElrone AJ, Cochard H, Brodribb, et al. 2015. Direct X-ray microtomography observation confirms the induction of embolism upon xylem cutting under tension. *Plant Physiology* **167:** 40–43.

Trifilò P, Raimondo F, Lo Gullo MA, Barbera PM, Salleo S, Nardini A. 2014. Relax and refill: xylem rehydration prior to hydraulic measurements favours embolism repair in stems and generates artificially low PLC values. *Plant, Cell & Environment* **37:** 2491–2499.

Trifilò P, Casolo V, Raimondo F, Petrussa E, Boscutti F, Lo Gullo MA, Nardini A. 2017. Effects of prolonged drought on stem non-structural carbohydrates content and post-drought hydraulic recovery in *Laurus nobilis* L.: the possible link between carbon starvation and hydraulic failure. *Plant Physiology and Biochemistry* **120:** 232–241.

Trifilò P, Natale S, Gargiulo S, Abate E, Casolo V, Nardini A. 2021. Stem photosynthesis affects hydraulic resilience in the deciduous *Populus alba* but not in the evergreen *Laurus nobilis*. *Water* **13:** 2911.

Vandegehuchte MW, Bloemen J, Vergeynst LL, Steppe K. 2015. Woody tissue photosynthesis in trees: salve on the wounds of drought? *New Phytologist* **208:** 998–1002.

Wang S, Xie Y, Niu S, Lin L, Liu C, Zhou YS, Wang ZL. 2014. Maximum surface charge density for triboelectric nanogenerators achieved by ionized-air injection: methodology and theoretical understanding. *Advanced Materials* **26:** 6720–6728.

Wheeler JK, Huggett BA, Tofte AN, Rockwell FE, Holbrook NM. 2013. Cutting xylem under tension or supersaturated with gas can generate PLC and the appearance of rapid recovery from embolism. *Plant, Cell & Environment* **36:** 1938–1949.

Wittmann C, Pfanz H. 2008. General trait relationships in stems: a study on the performance and interrelationships of several functional and structural parameters involved in corticular photosynthesis. *Physiologia Plantarum* **134:** 636–648.

Yemm EW, Willis A. 1954. The estimation of carbohydrates in plant extracts by anthrone. *Biochemical journal* **57:** 508.

Supplementary material

Treatment	h, cm			ø, mm	
	start of experiment	*end of experiment*		*start of experiment*	*end of experiment*
Li_C	82.90±18.85	82.73±18.88		9.00±1.27	9.88±1.66
Li_D	86.50±12.44	86.75±11.72		8.27±1.32	8.95±1.41
Li_R	81.70±19.45	87.20±26.62		8.15±1.01	9.35±1.16
LS_C	74.00±10.07	79.71±23.43		7.83±1.64	8.59±1.76
LS_D	91.25±15.20	91.48±15.38		8.11±0.86	8.45±1.11
LS_R	87.00±15.20	85.98±15.38		9.12±0.82	10.38±1.16
SS_C	80.40±20.68	79.50±20.63		7.89±1.02	8.91±1.71
SS_D	79.80±18.24	81.20±18.37		8.48±1.33	9.22±2.01
SS_R	80.58±12.18	80.60±12.19		8.50±1.34	9.21±1.07

Tab. S1 Plant's height (h) and the diameter of the stem base (ø) measured in light (L), long-shaded (LS) and short-shaded (SS) control (Li_C, LS_C, SS_C), drought (Li_D, LS_D, SS_D) and recovery (Li_R, LS_R, SS_R) saplings of *Fraxinus ornus*. Mean values are reported ± S.D (n=5-10) for measurements made at the start of the experiment and at the end of the experiment.

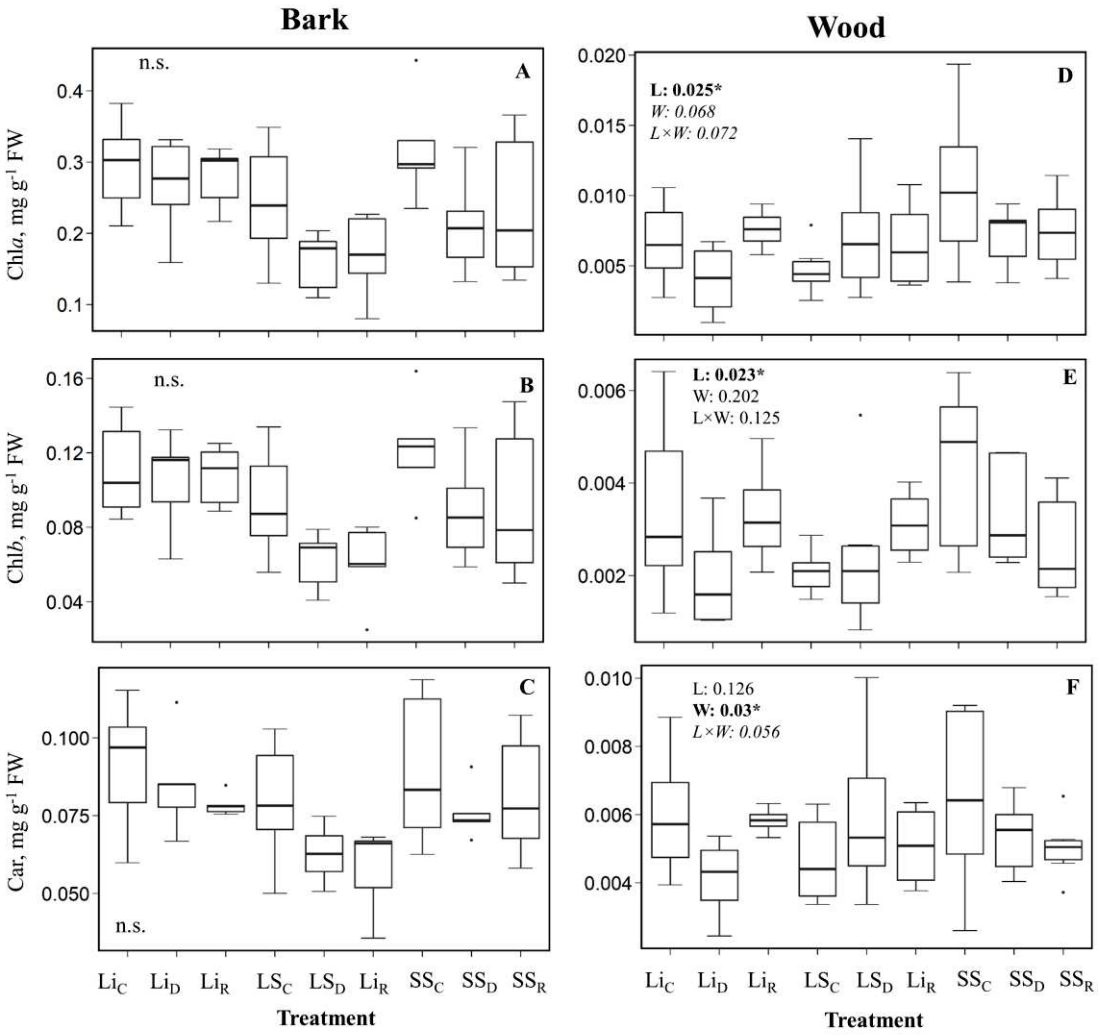

Fig. S1 Median values, 25th and 75th percentiles of A,D) Chl*a*, B,E) Chl*b*, C,F) Car for bark (A,B,C) and wood (D,E,F) of one-year-old stems of *Fraxinus ornus* measured in light (Li), long-shaded (LS) and short-shaded (SS) control (Li_C, LS_C, SS_C), drought (Li_D, LS_D, SS_D) and recovery (Li_R, LS_R, SS_R). n.s. = not statistically significant. Explanatory variables (light treatment, L, and water treatment, W) and associated p-values are reported. * = $p < 0.05$; ** = $p < 0.01$; *** = $p < 0.001$.

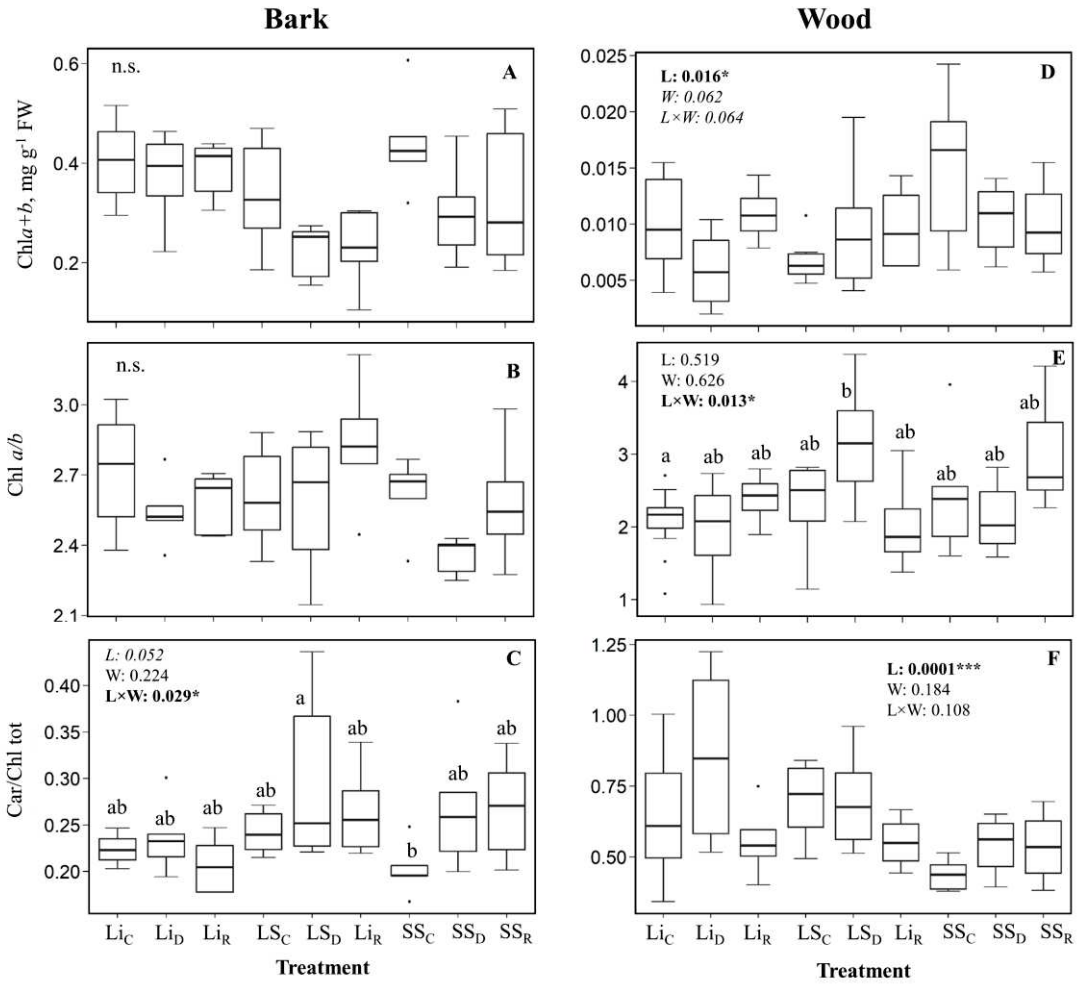

Fig. S2 Median values, 25th and 75th percentiles of A,D) Chl *a*+*b*, B,E) Chl *a*/*b*, C,F) Car/Chl tot for bark (A,B,C) and wood (D,E,F) of one-year-old stems of *Fraxinus ornus* measured in light (Li), long-shaded (LS) and short-shaded (SS) control (Li_C, LS_C, SS_C), drought (Li_D, LS_D, SS_D) and recovery (Li_R, LS_R, SS_R). Different letters indicate statistically significant differences among treatments ($p < 0.05$). n.s. = not statistically significant. Explanatory variables (light treatment, L, and water treatment, W) and associated p-values are reported. * = $p < 0.05$; ** = $p < 0.01$; *** = $p < 0.001$.

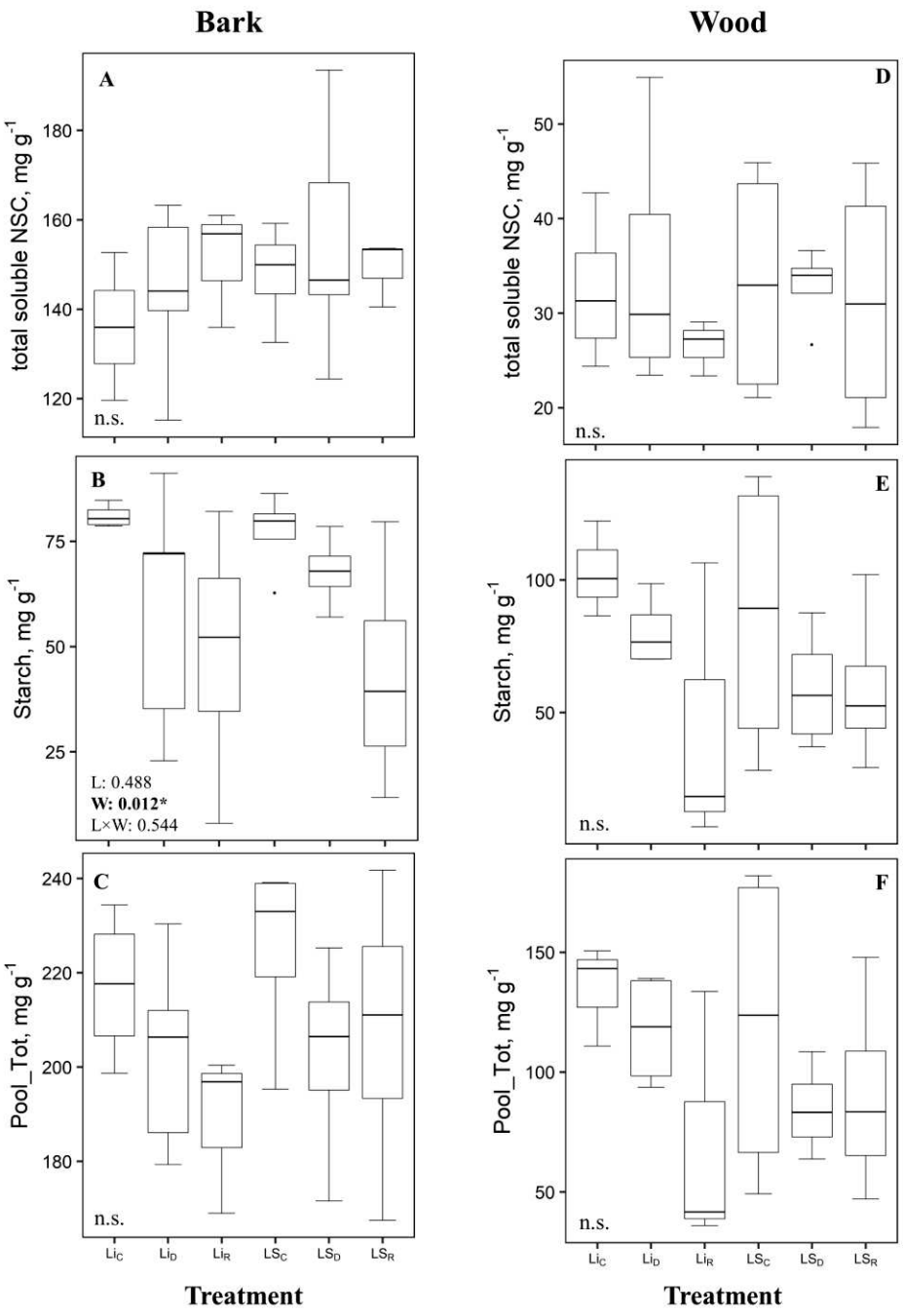

Fig. S3 Median values, 25th and 75th percentiles of A,D) total soluble non-structural carbohydrates (NSC), B,E) starch and C,F) stem total non-structural carbohydrates (Pool Tot) measured in bark (A,B,C) and wood (D,E,F) of light (Li) and long-shaded (LS) control (Li_C, LS_C), drought (Li_D, LS_D) and recovery (Li_R, LS_R) *Fraxinus ornus* saplings, used for the in vivo visualization by X-ray microtomography (micro-CT). Different letters indicate statistically significant differences among treatments ($P < 0.05$). n.s. = not statistically significant. Explanatory variables (light treatment, L, and water treatment, W) and associated p-values are reported. * = $p < 0.05$; ** = $p < 0.01$; *** = $p < 0.001$.

Variable	contrast	estimate	SE	df	t.ratio	p.value
Leaf conductance to water vapor (g_L)						
	C - D	2.200	0.176	35.900	12.476	**<.0001**
	C - R	1.190	0.167	41.200	7.165	**<.0001**
	D - R	-1.000	0.192	27.100	-5.228	**<.0001**
Midday stem xylem water potential (Ψ_{xyl})						
	C - D	2.880	0.090	20.900	31.370	**<.0001**
	C - R	-0.060	0.080	31.200	-0.810	0.422
	D - R	-2.940	0.090	24.300	-30.840	**<.0001**
Osmotic potential (wood)						
	C - D	0.100	0.174	48.000	0.623	0.800
	C - R	-0.070	0.153	48.000	-0.522	0.860
	D - R	-0.180	0.154	48.000	-1.210	0.440
Electrical conductivity (wood)						
	C - D	-30.700	44.100	33.600	-0.690	0.760
	C - R	-82.100	38.900	42.000	-2.100	0.100
	D - R	-51.400	39.600	49.000	-1.290	0.400
Percentage of total area of embolized vessels (AEV) over total area of mature xylem (AMX): AEV/AMX	C - D	-0.670	0.150	9.000	-4.490	**0.003**
	C - R	-0.220	0.160	9.000	-1.360	0.400
	D - R	0.440	0.150	9.000	2.840	**0.040**
Midday stem xylem water potential (Ψ_{xyl}) (micro-CT samples)	C - D	3.120	0.080	19.000	36.710	**<.0001**
	C - R	0.210	0.080	19.000	2.410	0.065
	D - R	-2.910	0.080	19.000	-34.240	**<.0001**
Total chlorophyll (a+*b*) (wood)						
	Li - LS	0.000	0.001	41.000	0.180	0.980
	Li - SS	-0.002	0.001	31.000	-1.700	0.190
	LS - SS	-0.003	0.001	32.000	-1.900	0.140
Carotenoid/Total chlorophyll (wood)						
	Li - LS	0.040	0.070	15.100	0.534	0.600
	Li - SS	0.180	0.060	14.700	2.730	**0.030**
	LS - SS	0.140	0.050	40.600	2.840	**0.020**
Carotenoid (wood)						
	C-D	0.001	0.001	37.900	0.924	0.629
	C-R	0.000	0.001	37.900	0.604	0.819
	D-R	0.000	0.001	42.000	-0.278	0.958
Chlorophyll *b* (wood)						
	Li - LS	0.000	0.000	42.000	0.698	0.539
	Li - SS	-0.001	0.000	42.000	-1.119	0.539
	LS - SS	-0.001	0.000	42.000	-1.828	0.224
Chlorophyll *a* (wood)						
	Li - LS	0.000	0.001	16.400	-0.082	0.996
	Li - SS	-0.002	0.001	14.300	-1.935	0.165
	LS - SS	-0.002	0.001	21.500	-1.853	0.177
Total non-structural carbohydrates (bark)						
	C - D	2.080	5.840	40.000	0.355	0.933
	C - R	16.330	5.720	40.000	2.858	**0.018**
	D - R	14.260	6.120	40.000	2.331	0.063
Starch (bark)						
	C - D	29.570	11.350	6.610	2.606	0.083
	C - R	35.690	9.450	16.570	3.776	**0.004**
	D - R	6.120	14.540	8.520	0.421	0.908
Total non-structural carbohydrates (wood)						
	C - D	4.940	3.350	43.000	1.475	0.313
	C - R	14.710	3.360	43.000	4.378	**0.000**
	D - R	9.770	3.570	43.000	2.734	**0.024**
Mannitol (wood)						
	C - D	-4.470	0.730	43.900	-6.110	**<.0001**
	C - R	-2.580	0.700	45.600	-3.689	**0.001**
	D - R	1.890	0.838	36.300	2.260	**0.030**
Starch (bark) (micro-CT samples)	C - D	15.900	5.950	16.950	2.665	**0.041**
	C - R	33.300	14.810	5.720	2.245	0.145
	D - R	17.400	15.470	6.220	1.125	0.534

Appendix 1 Summary of ANOVA model. The response variable is shown in the column "Variable", and control (C), drought (D), recovery (R) relative to drought stress and light-exposed stem (Li), long-shaded stems (LS) and short-shaded stems (SS) were the explanatory variables. P values are reported.

Study 5

Stem Photosynthesis Affects Hydraulic Resilience in the Deciduous *Populus alba* but Not in the Evergreen *Laurus nobilis*

Patrizia Trifilò[1], Sara Natale[2], Sara Gargiulo[3], Elisa Abate[1], Valentino Casolo[3], Andrea Nardini[2]

[1]Dipartimento di Scienze Chimiche, Biologiche, Farmaceutiche ed Ambientali, Università di Messina, Salita Stagno D, Alcontres, 31, 98166 Messina, Italy
[2]Dipartimento di Scienze della Vita, Università di Trieste, Via L. Giorgieri, 10, 34127 Trieste, Italy
[3]Dipartimento di Scienze AgroAlimentari, Ambientali e Animali, Università di Udine, Via delle Scienze, 91, 33100 Udine, Italy

Published as: **Trifilò P, Natale S, Gargiulo S, Abate E, Casolo V, Nardini A. 2021.** Stem photosynthesis affects hydraulic resilience in the deciduous *Populus alba* but not in the evergreen *Laurus nobilis*. *Water* **13:** 2911.

Abstract

Stem photosynthesis has been suggested to play relevant roles to cope with different biotic and abiotic stress factors, including drought. In the present study, we performed measurements of stem hydraulic conductance and non-structural carbohydrate content in the evergreen *Laurus nobilis* L. and the deciduous *Populus alba* L., subjected to inhibition of stem photosynthesis and successive exposure to a drought-recovery cycle in order to check if stem photosynthesis may be involved in allowing hydraulic recovery after drought stress relief. Stem shading affected the growth of *L. nobilis* but not of *P. alba* saplings. By contrast, inhibition of stem photosynthesis was coupled to inhibition of hydraulic recovery following embolism build-up under drought in *P. alba* but not in *L. nobilis*. The two study species showed a different content and behavior of non-structural carbohydrates (NSCs). The differences in NSCs' trend and embolism reversal ability led to a significant relationship between starch content and the corresponding hydraulic conductance values in *L. nobilis* but not in *P. alba*. Our findings suggest that stem photosynthesis plays a key role in the maintenance of hydraulic functioning during drought especially in the deciduous species. This, in turn, may increase their vulnerability under current global climate change scenarios.

Keywords: deciduous; drought; evergreen; hydraulic recovery; laurel; poplar; non-structural carbohydrates; starch; sugars; xylem embolism

Introduction

Most terrestrial plants perform photosynthesis at the leaf level, but some of them can only use stems to this purpose, as leaves have been eliminated or transformed into thorns or other organs serving different functions in peculiar habitats. However, even several leaf-bearing plants, including both herbaceous and woody species, do assimilate CO_2 at stem level, as suggested by the presence of chloroplasts in the bark and even in wood parenchyma and pith (Wiebe 1975; van Cleve et al. 1993; Berveiller et al. 2007; Rentzou et al. 2008). Photosynthetic activity of stems has been reported in many species and families, encompassing their biogeographic and phylogenetic features (Nilsen 1995; Teskey et al. 2008; Ávila-Lovera et al. 2014).

In trees and other woody plants, carbon assimilation is typically higher in current-year stems compared to older ones (Aschan and Pfanz 2003). The actual contribution of stem photosynthesis to plant carbon balance, compared to carbon uptake at leaf level, remains debated (Ávila-Lovera et al. 2014; Ehleringer et al. 1993; Nilsen and Sharifi 1997; Ávila-Lovera and Tezara 2018; Ávila-Lovera et al. 2019; Santiago et al. 2004). Different studies have suggested that carbon assimilation by tree stems can provide different functional advantages for plants. The increased carbon gain would offer additional carbohydrate availability for the production of new leaves, flowers and fruits under both optimal and stressful environmental conditions (Berveiller et al. 2007; Osmond et al. 1987; Nilsen et al. 1989; Nilsen et al. 1990; Tinoco-Ojanguren 2008; Damesin 2003; De Roo et al. 2020. In accordance, different studies have shown that stem photosynthesis contributes to stem growth and bud development, especially in young woody plants and in deciduous species (Saveyn et al. 2010; Bloemen et al. 2013; Cernusak and Hutley 2011; Simbo et al. 2013; Liu et al. 2018). Photosynthetic activity of stems also plays a relevant role to cope with defoliation caused by biotic or abiotic agents (Bossard and Rejmanek 1992; Pfanz and Aschan 2001; Eyles et al. 2009). Finally, it contributes to face thermal stress (Aschan and Pfanz 2003;Cernusak and Marshall 2002; Pfanz and Aschan 2002; Wittmann and Pfanz 2014; Wittmann and Pfanz 2018) and drought, as reported in different desert and semi-desert non-succulent species, as well as in Mediterranean plants (i.e., (Rentzou and Psaras 2008; Nilsen 1995; Aschan and Pfanz 2003; Nilsen 1997; Ávila-Lovera and Tezara 2018; Ávila-Lovera et al. 2019; Comstock and Ehleringer 1988; Dima et al. 2006).

Research on stem photosynthesis has recently received renewed interest because of its potential role in resistance and resilience of plants to severe global change-type droughts (Vandegehuchte et al. 2015). Hydraulic failure caused by massive xylem embolism is a major and recurrent cause of drought-induced tree mortality (Hartmann et al. 2013; Adams et al. 2017; Hammond et al. 2019), with an additional role suggested for carbon starvation. Interestingly, carbohydrate content decline,

even when non-lethal, has been reported to impact plant hydraulic efficiency (McDowell 2011; Hartmann et al. 206; Nardini et al. 2018; Tomasella et al. 2020; Sapes and Sala 2021). Non-structural carbohydrates (NSCs) are apparently involved in the maintenance of plant hydraulic function via different processes, which are only partially understood. NSCs are involved in xylogenesis, thus providing plants with the possibility to grow new xylem to increase or maintain their hydraulic capacity, despite possible occurrence of xylem embolism or mechanical damage impairing older conduits (Deslauriers et al. 2014; Falchi et al. 2020). Moreover, NSCs are also involved in osmoregulation processes that, at the level of wood parenchyma, might protect cells from damage caused by drought- or freeze-induced protoplast dehydration (Sala et al. 2012; Plavcova and Jansen 2015; Traversari et al. 2020).

Besides the relatively well-known role of NSCs in xylem growth and symplast osmoregulation, NSCs stored in wood parenchyma have also been reported to be involved in lowering the osmotic potential of xylem sap during and after stressful events. Xylem sap osmoregulation by soluble NSCs might lead to lowering its freezing point, thus limiting formation of ice in xylem conduits during freeze stress (Neuner 2014; Tixier et al. 2019). Accumulation of soluble NSCs in the xylem sap during and/or after freeze or drought stress might also provide the necessary driving force to refill embolized conduits with water once stress is relieved and the xylem pressure rises to near-atmospheric values (Nardini et al. 2018; Tomasella et al. 2020; Améglio et al. 2004; Mayer et al. 2014; Mayr and Améglio 2016; Secchi and Zwieniecki 2016; Pagliarani et al. 2019). An additional intriguing role of NSCs might be the direct or indirect contribution to the production of surfactants that, by modifying xylem sap surface tension or stabilizing gas nanobubbles, would modify the xylem vulnerability to embolism formation on diurnal or seasonal time scales (Pagliarani et al. 2019; Oroian et al. 2015; Losso et al. 2017; Schenk et al. 2017).

Based on the above, stem-level photosynthesis might play a primary role not only in the production of NSCs contributing to the whole plant carbon gain but also in the modulation and regulation of xylem hydraulic function. Indeed, some recent studies have reported experimental evidence for a role of stem photosynthesis in reducing xylem vulnerability to embolism and improving the capacity for xylem embolism reversal (Bloemen et al. 2016; De Baerdemaeker et al. 2017; Tomasella et al. 2021; Schmitz et al. 2012; Liu et al. 2019).

In the present study, we report measurements of stem hydraulic conductance in response to drought stress and re-irrigation in plants subjected to inhibition of stem photosynthesis via localized shading. We aimed at testing the hypotheses that the carbon gain obtained by stem photosynthesis is involved in allowing hydraulic recovery after drought stress relief. We focused on two woody species, namely the evergreen *Laurus nobilis* L. and the deciduous *Populus alba* L, because, for both of them, there

is available experimental evidence suggesting their capacity to reverse xylem embolism following drought stress, with an involvement of NSC stores (Pagliarani et al. 2019; Trifilò et al. 2015).

Materials and Methods

Plant Material and Growth Condition

Measurements were performed during spring and summer 2019 on *P. alba* and *L. nobilis* saplings (50 samples per species). In April, one-year-old cuttings of *P. alba* and *L. nobilis* growing in 4-liter pots were transferred to a greenhouse at University of Messina, Italy. Samples were randomly divided in two experimental groups: control (C) and shaded (S) samples. In S samples, the main stem and any lateral branch were wrapped with aluminum foil, similarly to the experimental procedure described by Saveyn et al. (2010). This treatment was expected to significantly reduce the presence of differentiated chloroplasts and, in any case, to inhibit stem photosynthesis, without blocking gas exchange between stem tissues and atmosphere (Saveyn et al. 2010; Bloemen et al. 2016).

In the greenhouse, plants received only natural light, with maximum photosynthetic photon flux density (PPFD) daily values averaging 1050 ± 180 μmol s^{-1} m^{-2}. Air temperature ranged from 22 ± 2 ˚C to 31 ± 3 ˚C (night/day) and the mean value of air humidity was 80 ± 3%. All plants were regularly irrigated to field capacity (FC), every second day from April until early June, when the drought treatment was imposed (Fig. 1). The drought treatment started after stem and leaf production and growth had ceased. Water stress was imposed by irrigating plants to 30% FC once per week, for 4 weeks (drought period). This irrigation regime induced a strong reduction of gas exchange and xylem water potential (Ψ_x), thus inducing substantial loss of stem hydraulic conductivity (see below). After the drought period, C and S samples were further divided in two groups. A first set of plants was used to immediately measure different physiological parameters (see below) at the end of drought. A second group of samples was re-irrigated to field capacity and measured 7 days later. Moreover, five additional plants per species were maintained fully irrigated during the whole experimental period and grew under the same environmental conditions experienced by C and S samples. These plants were used to collect samples for estimating NSC content (see below) in plants not experiencing drought.

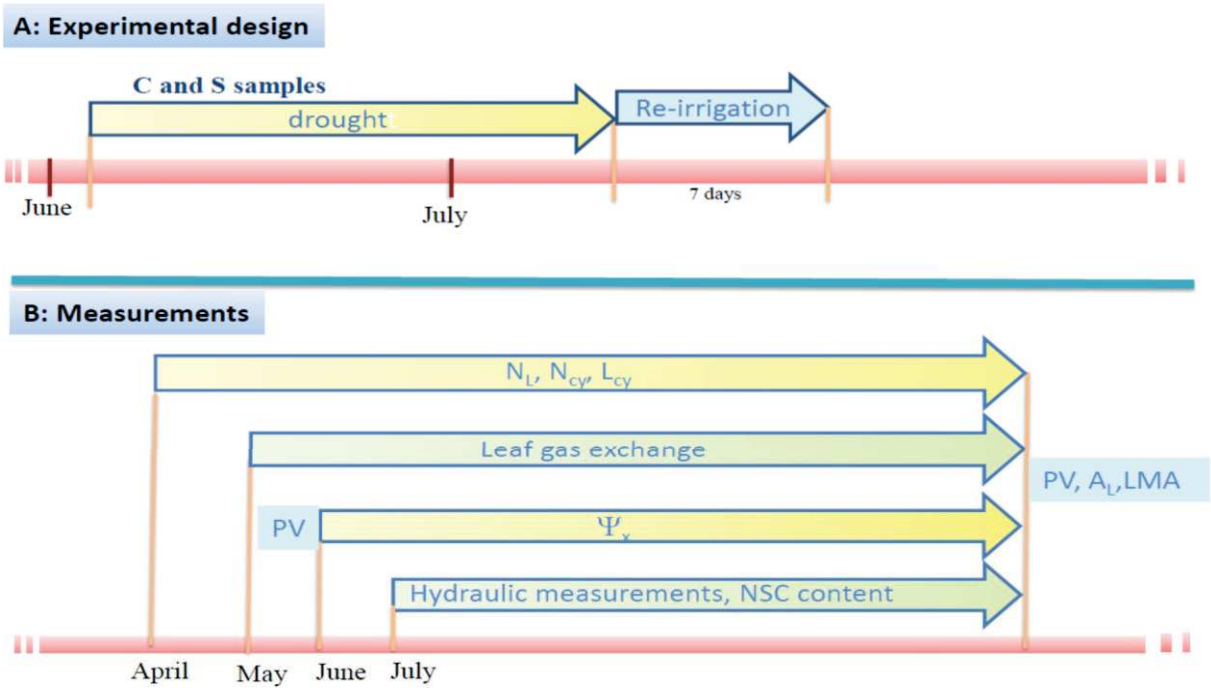

Fig. 1 (**A**) Experimental design and (**B**) measurements performed on control and stem-shaded samples (C and S, respectively) of *L. nobilis* and *P. alba* plants; (**A**) At the beginning of June, C and S samples were subjected to a water stress treatment. One month later, a set of samples was measured for different physiological parameters. Another set of plants was re-irrigated at field capacity and measured after 7 days to evaluate the capacity for recovery; (**B**) Leaf gas exchange rates were measured from May to the end of the experiment; xylem water potential (Ψ_x) values were recorded from June to the end of experiments; hydraulic measurements and NSC content were performed after the drought treatment and 7 days after re-irrigation. Moreover, PV-curves were measured before and at the end of the drought-recovery treatments. Leaf area and leaf mass per area were measured at the end of the experiments (for details, see the text). PV: pressure volume curves; N_L: number of leaves of the current-year branches; N_{cy}: number of current-year branches; L_{cy}: length of the current-year branches; A_L: leaf area; LMA: leaf mass area.

Morphological Measurements

To estimate the possible effect of stem shading on plant growth, the number (N_{cy}) and the length (L_{cy}, as recorded by a ruler) of current-year stems as well as the total number of leaves on current-year branches (N_L) were measured weekly during the whole experimental period (i.e., from April to July) in 3 C and 3 S samples per species.

Leaf area (A_L) and leaf mass per unit area (LMA) were estimated on 40 leaves randomly collected at the end of hydraulic measurements (see below). A_L was recorded by a scanner (HP Scanjet G4050,

Palo Alto, CA, USA) and image analysis based on the software ImageJ (http://imagej.nih.gov/ij/, accessed on 8 October 2021). Leaves were oven-dried for 3 days at 70 °C to obtain their dry weight (DW) and the leaf mass per unit area (LMA) was calculated as DW/A_L.

Leaf Water Potential Isotherms

At the beginning of June (i.e., before starting the drought treatment) and in July (i.e., after one month of water stress), leaf water potential isotherms (PV-curves) were performed on 5 C and 5 S leaves per species and per treatment, sampled from different plants. PVcurves were elaborated to obtain the leaf water potential at the turgor loss point (Ψ_{tlp}), the osmotic potential at full turgor (π_0), and the bulk modulus of elasticity (ε_{max}). In particular, Ψ_{tlp} was estimated as the flex point of the relationship between $1/\Psi_L$ and water loss, π_0 was calculated by the y-intercept of the linear region of this relationship, and ε_{max} was calculated by the ratio between the change of turgor pressure and the relative change of the leaf water content (Tyree and Hammel 1972).

Gas Exchange and Water Potential Measurements

In order to check gas exchange rates and water status in C versus S samples under drought and recovery, leaf conductance to water vapor (g_L) and photosynthetic rate (A_n) were measured from the beginning of May (i.e., when fully expanded leaves of poplar samples were observed) to the end of the experiment (Fig. 1). g_L and A_n were measured once per week until the beginning of the drought treatment and, afterwards, twice per week. Measurements were performed at midday on at least 4 leaves per group and per treatment, selected from different plants, using a porTab. LCi Analyzer System (ADC Bioscientific Ltd., Herts, UK). To avoid excessive defoliation, minimum diurnal xylem water potential (Ψ_x) was measured at midday only the week before starting the drought treatment, and then on the same days of gas exchange measurements. This experimental procedure allowed us to check that the applied water stress led plants to experience Ψ_x values of about –1.5 MPa (i.e., Ψ_x inducing significant loss of hydraulic conductivity for both species (Huckin et al. 2005; Nardini et al. 2017). Ψ_x was also measured at midday and in the morning (at about 6:00 a.m.) on the same samples used for hydraulic measurements. Measurements of Ψ_x were performed on 3 leaves from different plants per species and per treatment, using a porTab. pressure chamber (3005 Plant Water Status Console, Soilmoisture Equipment Corp., Goleta, CA, USA). Leaves were wrapped in cling film and aluminum foil 2–3 h before sampling.

Hydraulic Conductivity Measurements

Xylem-specific hydraulic conductivity (K_x) was measured in C and S samples after the drought period and upon recovery. Measurements were performed at midday (i.e., 12.00) and on the following morning (i.e., 6:00 a.m.) on about 10 cm-long current-year samples using a hydraulic apparatus (Sperry et al 1988; Lo Gullo and Salleo 1991). Perfusion solution was a commercial mineral water in which were added 15 mM KCl (Nardini et al. 2007). Samples were perfused at a pressure (P) of 8 kPa. When flow rate (F) became sTab., samples were flushed at P = 0.2 MPa for 15 min to remove embolism and F was re-measured at 8 kPa. K_x was computed as $(F/P) \times (L/A_x)$, where L is sample length and A_x is the xylem cross-sectional area. The initial branch hydraulic conductivity value (K) and the K value measured after embolism removal (K_{max}) were used to estimate the PLC as $PLC = 1 - (K/K_{max}) \times 100$.

To avoid possible cutting artifacts (Wheeler et al. 2013), 1 h before their collection, branches were girdled for their entire length at about 3 cm intervals, by removing about 3 mm wide bark rings. The exposed wood was immediately covered with a thin layer of silicone grease to avoid desiccation. After girdling, at least six samples per treatment per species were cut under water and maintained with their cut end immersed into the water for 1 h in order to relax xylem tension (Trifilò et al. 2014). Then, the current-year segment was collected and measured. All hydraulic measurements were performed at a temperature of 20 ˚C.

NSC Content

At least 5 samples from those used for hydraulic measurements were collected to estimate NSC content (sugars and starch). Moreover, at the end of drought treatment, five additional samples were collected from samples maintained fully irrigated during the whole experimental period and growing under the same environmental conditions experienced by C and S samples. After hydraulic measurements, stem samples were immediately microwaved at 700 W for 3 min to stop enzymatic activities, oven-dried at 70 ˚C for 24 h, and finally grounded to fine powder (particle size < 0.15 mm). NSC extraction followed the standardized method proposed by Quentin et al. [73] and Landhausser et al. (2018), with minor modifications to account for small amount of material. An aliquot of 15 ± 1 mg of dry sample was suspended in 0.5 mL of ethanol 80% (*v*/*v*), incubated at 80 ˚C for 30 min and centrifuged (with Mikro 120, Hettuch zentrifugen, Tuttlingen, Germany) at 14.000 RPM for three minutes. This step was repeated, suspending the pellet with 0.3 mL of ethanol 80%. Once mixed in the same Eppendorf tube, the extracts were dried till complete evaporation. The resulting crystalized carbohydrates were re-suspended with 0.5 mL of 50 mM Tris-HCl pH 7.5 and centrifuged at 14.000 RPM for three minutes. Sugars contained in supernatants were measured with Anthrone assay (Yemm

1954), using spectrophotometer at wavelength of 620 nm. The absorbance values were converted to mg glucose g^{-1} DW using a calibration curve prepared with known amounts of glucose. Pellets were resuspended in 1 mL of 0.2 M Sodium Acetate Trihydrate pH 4.6 and incubated at 100 °C for 1 h to allow starch gelatinization. The enzymatic hydrolysis—using 100 U of α-amylase and 25 U of amyloglucosidase per sample—was performed at 55 °C. To stop enzymatic activity, samples were boiled for 5 min. Glucose obtained from starch digestion was evaluated as NADPH (absorbance at 340 nm) by action of 0.3 U per sample of hexokinase and 0.5 U per sample of glucose-6-phosphate-deihydrogenase in 0.1 mL of buffer solution (50 mM Tris-HCl, 2 M $MgCl_2$, 50 mM $NADP^+$ and 0.4 M ATP) at 32 °C for 20 min. Starch content (mg g^{-1} DW) was calculated comparing NADPH obtained with known amounts of commercial amylose from potato (Sigma-Aldrich, Milan, Italy) that followed the same hydrolysis protocol of samples. Spectrophotometer analysis was performed in a VICTOR3 Multilabel Counter Plate Reader (Perkin Elmer, Boston, MA, USA), for both sugars and starch, using 300 µL per sample.

Statistical Analysis

All statistical analyses were performed with SigmaStat v. 12.0 (SPSS, Inc., Chicago, IL, USA). To test for differences between C and S samples in terms of N_{cy}, L_{cy}, A_L and LMA for each species, a Student's *t*-test ($\alpha = 0.05$) was performed after checking for normality assumption. Effects of stem shading and drought on N_L, gas exchange, water status, PVcurve data, PLC and NSC were assessed by two-way ANOVA. For statistically significant tests ($p < 0.05$), a Tukey's post hoc test using Holm-Sidak *p*-values correction was carried out to perform pairwise comparisons.

Results

Stem Shading Effects on Plant Growth

Plant growth ceased by the end of May, and no further production of branches and leaves was observed until the end of the experiment (July) in both *L. nobilis* and *P. alba*. Tab. 1 reports data of N_{cy}, L_{cy}, A_L and LMA as recorded at the end of the experimental period. Stem shading did not affect the growth of *P. alba*. In fact, the number and length of current-year branches were similar in C and S samples (Tab. 1). Similarly, no differences were recorded in terms of mean A_L (~ 17 cm^2) and LMA (~42 mg cm^{-2}) in this species. By contrast, S samples of *L. nobilis* showed significantly lower values of A_L compared to C plants (10.6 ± 3 versus 12.2 ± 3.2 cm^2, respectively), but similar values of N_{cy}, L_{cy} and LMA. The drought treatment affected the number of leaves per plant in *P. alba* but not in *L. nobilis*, and N_L decreased more in C than in S poplar (Tab. 2). This decrease was due to leaf shedding

in response to water stress. No leaf fall was observed over the same time interval in well-watered poplar samples used for NSC estimation (see above).

Parameter	*L. nobilis*		*P. alba*	
	C	S	C	S
N_{cy}	2.7 ± 0.3	2.7 ± 0.3	7.7 ± 1.1	9.3 ± 1.9
	(*p*-value = 1.0)		(*p*-value = 0.292)	
L_{cy} (cm)	13.3 ± 0.9	13.4 ± 2.3	17.6 ± 3.1	13.7 ± 1.7
	(*p*-value = 1.0)		(*p*-value = 0.201)	
A_L (cm^2)	12.2 ± 0.5	10.6 ± 0.6	17.4 ± 0.9	17.1 ± 1.1
	(*p*-value = **0.022**)		(*p*-value = 0.414)	
LMA ($g\ m^{-2}$)	104.0 ± 2.6	111.5 ± 2.9	41.1 ± 1.5	41.6 ± 1.3
	(*p*-value = 0.06)		(*p*-value = 0.797)	

Tab. 1 Mean ± SEM of the total number (N_{cy}) and length (L_{cy}) of current-year branches, mean leaf surface area (A_L) and leaf mass per area (LMA) as recorded in control (C) and shaded (S) samples of *L. nobilis* and *P. alba*. Differences between C and S samples were checked by a Student's *t*-test. *p*-Values are reported between brackets; n = 3 plants for N_{cy} and L_{cy}; n = 40 leaf samples for A_L and LMA.

Species	Time	N_L		*p-Value*
		C	S	
L. nobilis	June	32.3 ± 3.5	33.7 ± 5.5	T: 0.819
				L: 1
	July	32.3 ± 3.5	33.7 ± 5.5	T × L: 1
P. alba	June	177.3 ± 15.5a	168.7 ± 9.6a	**T: <0.001**
				L: 0.1
	July	38.7 ± 10.11b	95.7 ± 3.6c	**T × L: <0.05**

Tab. 2 Mean ± SEM (n = 3 plants) of total number of leaves (N_L) as recorded in June (before starting drought treatment) and in July (at the end of the experimental period, for details, see the text). Different letters indicate statistically significant differences based on two-way ANOVA. F values are reported as resulted by statistical analysis of N_L measurements by time, T (i.e., June, before drought, and July, at the end of experimental treatment) and light treatment, L (i.e., control and shaded samples).

Plant Water Relations

Stem shading did not affect plant water relations of the two study species. In accordance, no differences in Ψ_{tlp}, π_0 and ε_{max} values were recorded in C versus S samples (Tab.s 3 and 4). *L. nobilis* plants lowered their Ψ_{tlp} value by decreasing π_0 in response to drought. By contrast, no changes in these parameters were recorded in *P. alba*.

Midday values of g_L, A_n and Ψ_x during the experimental period were statistically similar in C versus S samples (Fig. 2). In response to drought, reductions of stomatal aperture and photosynthetic rates were recorded. Stomatal closure did not fully prevent the drop of xylem water potential to about −1.3 MPa, that, in turn, induced a significant loss of stem hydraulic conductivity (see below). In response to re-irrigation, g_L and A_n partially recovered but remained below pre-drought values. However, it can be noted that we recorded values only until 7 days after re-irrigation. Therefore, it cannot be excluded that a full recovery of gas exchange may have occurred after a longer time interval.

Parameter	Time	*L. nobilis*		*P. alba*	
		C	S	C	S
$-\Psi_{tlp}$ (MPa)	June	1.99 ± 0.05a	1.97 ± 0.06a	2.27 ± 0.03	2.21 ± 0.10
	July	2.64 ± 0.11b	2.62 ± 0.10b	2.19 ± 0.01	2.19 ± 0.09
$-\pi_o$ (MPa)	June	1.71 ± 0.04a	1.72 ± 0.04a	1.73 ± 0.03	1.72 ± 0.05
	July	2.07 ± 0.0.3b	2.08 ± 0.09b	1.53 ± 0.11	1.72 ± 0.09
ε_{max} (MPa)	June	27.4 ± 3.6	31.2 ± 4.4	18.2 ± 4.5	25.7 ± 3.5
	July	35.7 ± 2.5	37.9 ± 3.1	30.1 ± 3.9	27.6 ± 4.1

Tab. 3 Mean ± SEM (n = 5) of leaf water potential at turgor loss point ($-\Psi_{tlp}$), osmotic potential at full turgor ($-\pi_o$) and bulk modulus of elasticity (ε_{max}) as recorded in June (before starting drought treatment), and in July (at the end of the experimental period) in control (C) and shaded (S) samples of *L. nobilis* and *P. alba* plants. Different letters indicate statistically significant differences based on two-way ANOVA.

Parameter	*L. nobilis*			*P. alba*		
	T	L	T × L	T	L	T × L
Ψ_{tlp} (MPa)	**43.58** ***	0.025	0.0006	0.18	0.08	0.04
π_o (MPa)	**33.91** ***	0.05	0.01	1.23	0.91	1.11
ε_{max} (MPa)	**3.76**	0.58	0.05	2.36	1.30	1.24

Tab. 4 Results of the two-way ANOVA analysis of parameters determined from PV-curves' analysis by time of measurement, T (i.e., Before drought and at the end of experiment) and light treatment, L (i.e., control and shaded samples). Numbers represent F values; *** = $p < 0.001$.

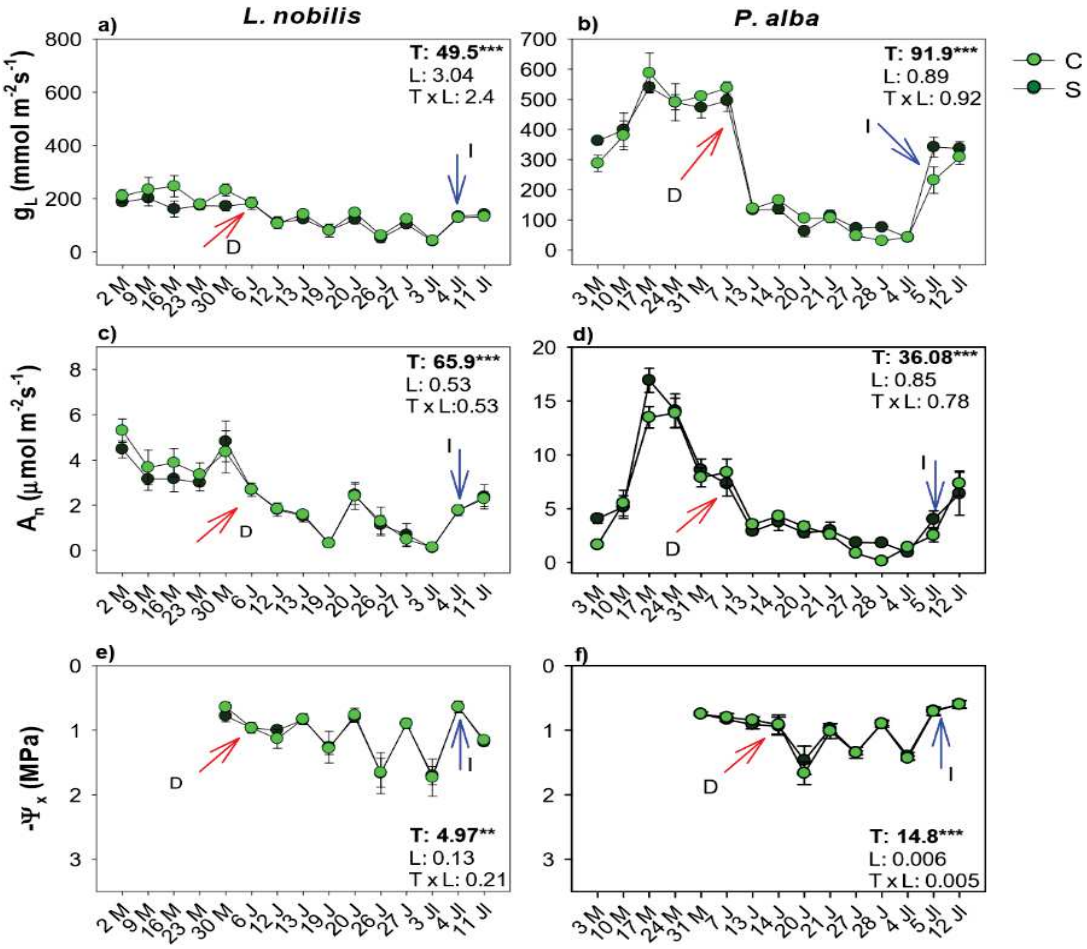

Fig. 2 Mean values ± SEM of (**a**,**b**) stomatal conductance to water vapor, g_L; (**c**,**d**) photosynthetic rate (A_n) and (**e**,**f**) xylem water potential (Ψ_X) as recorded in May (M), June (J) and July (Jl) in control (C, light green circle) and shaded samples (S, dark green circle) of *L. nobilis* and *P. alba* plants. Arrows indicate the day starting drought treatment (D) and re-irrigation (I). F values, as obtained by the two-way ANOVA analysis, are reported. Time of measurement, T, and light treatment, L (i.e., control and shaded samples) are the explanatory variables ** = $p < 0.01$; *** = $p < 0.001$.

Hydraulic Recovery and NSCs Content

Stem shading did not affect the ability to recover xylem hydraulic function upon re-irrigation in the evergreen species, but influenced this process in the deciduous one (Fig. 3). In fact, in poplar, a significant interaction between time and treatment (i.e., C versus S) was recorded. By contrast, changes in PLC were affected only by time in laurel samples. In accordance, C and S samples of *L. nobilis* had PLC of about 40% at midday and about 20% on the next morning (i.e., 6:00 a.m.) while under drought stress, and of about 10% in response to re-irrigation. By contrast, despite a similar value of PLC recorded at midday in C and S samples in *P. alba*, only controls showed hydraulic recovery after re-irrigation.

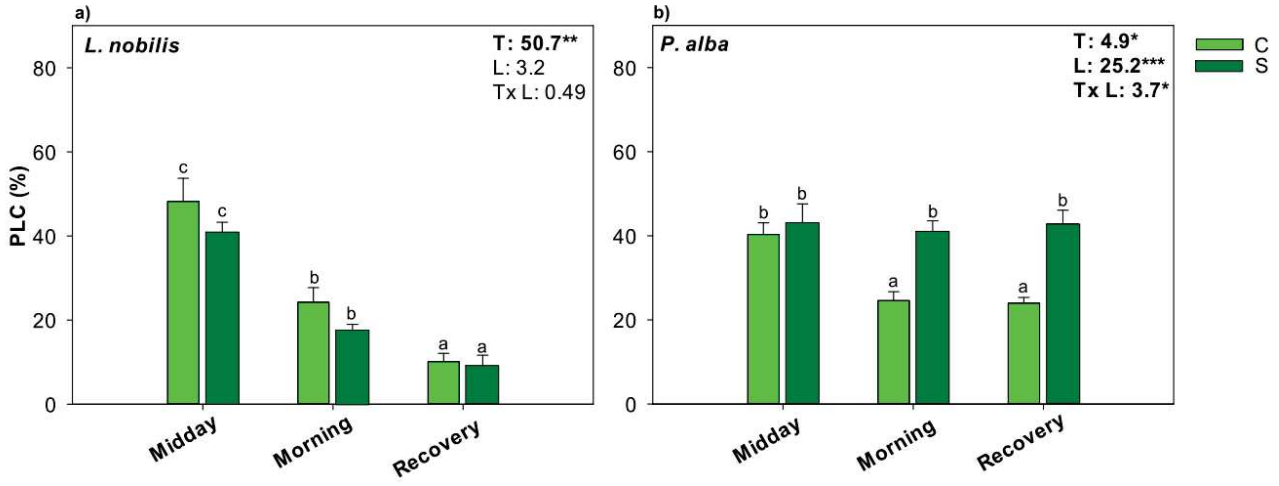

Fig. 3 Mean values ± SEM of percentage loss of hydraulic conductivity (PLC) as recorded in control (C) and shaded stem (S) samples of *L. nobilis* (**a**) and *P. alba* (**b**) as measured at midday, on the following morning (Morning) as well as in samples re-irrigated at field capacity and measured 7 days after re-irrigation (Recovery). Light green and dark green columns refer to C and S samples, respectively. F values, as obtained by the two-way ANOVA analysis, are reported. Time of measurement, T, and light treatment, L (i.e., control and shaded samples) are the explanatory variables. * = $p < 0.05$; ** = $p < 0.01$; *** = $p < 0.001$.

Laurel and poplar samples not experiencing drought (i.e., samples collected, at the end of drought treatment, by plants maintained fully irrigated during all experimental period) showed a soluble sugar content of about 14 mg g^{-1} DW^{-1}, and no differences in midday versus morning values were recorded (Tab.s 5 and 6). Starch content was about 20 mg g^{-1} DW^{-1} in *L. nobilis,* but only up to 10 mg g^{-1} DW^{-1} in *P. alba* (Tab.s 5 and 6).

Species	Soluble Sugars (mg g^{-1} DW^{-1})		Starch (mg g^{-1} DW^{-1})	
	Midday	Morning	Midday	Morning
L. nobilis	14.8 ± 7.3	13.2 ± 9.7	19.2 ± 1.8b	17.9 ± 2.5b
P. alba	13.1 ± 1.3	13.2 ± 1.2	6.9 ± 2.3a	10.5 ± 2.8ab

Tab. 5 Mean values ± SEM of soluble NSCs and starch content as recorded in well-watered samples of *L. nobilis* and *P. alba* at midday and on the following morning on the same days of hydraulic measurements in water-stressed samples. Different letters indicate statistically significant differences based on two-way ANOVA.

Parameters	Sp	T	Sp × T
soluble NSCs	0.53	0.41	0.62
starch	**16.71** ***	0.215	1.01

Tab. 6 Results of the two-way ANOVA analysis of parameters by species, Sp (i.e., laurel versus poplar) and time, T (i.e., Midday versus Morning). Numbers represent F values; *** = $p < 0.001$.

C and S samples of both species showed similar trends of soluble NSCs' content (Fig. 4a,b). Higher values of soluble NSCs were recorded at midday compared to morning and no significant differences were recorded in response to re-irrigation compared to values measured in the early morning (i.e., 6:00 am). However, in laurel, a significant interaction between time and treatment (i.e., C versus S) was recorded, due to a higher decrease of soluble NSCs in control in respect to shaded samples. A statistically significant increase of starch content was recorded in C and S stems of laurel in response to re-irrigation respect values recorded at midday. A similar trend was recorded in S samples of *P. alba*. By contrast, in C poplar stems, a significant decrease in starch content was recorded in response to re-irrigation in respect to value recorded at midday.

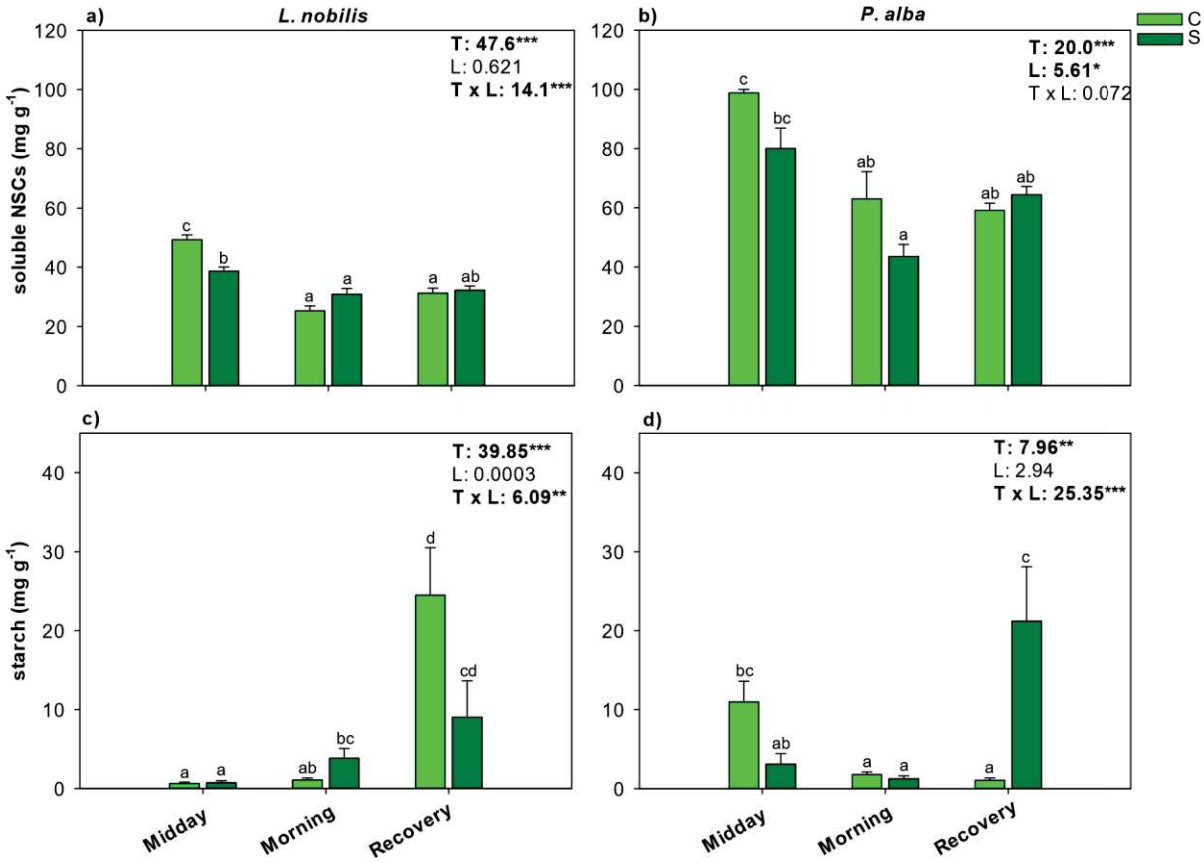

Fig. 4 Mean values ± SEM of (**a**,**b**) soluble NSCs and (**c**,**d**) starch content as recorded in control (C) and shaded stem (S) samples of *L. nobilis* and *P. alba* at midday, on the following morning (Morning) and at morning after re-irrigation at field capacity (Recovery). Light and dark green columns refer to C and S samples, respectively. F values, as obtained by the two-way ANOVA analysis, are reported. Time of measurement, T, and light treatment, L (i.e., control and shaded samples) are the explanatory variables. * = $p < 0.05$; ** = $p < 0.01$; *** = $p < 0.001$.

The differences in NSC and PLC trends led to a significant relationship between starch content and the corresponding PLC values in *L. nobilis* but not in *P. alba* (Fig. 5c, d). Moreover, a linear correlation near to be significant ($p = 0.06$) was also recorded between soluble NSCs and PLC values in laurel samples but not in poplar plants.

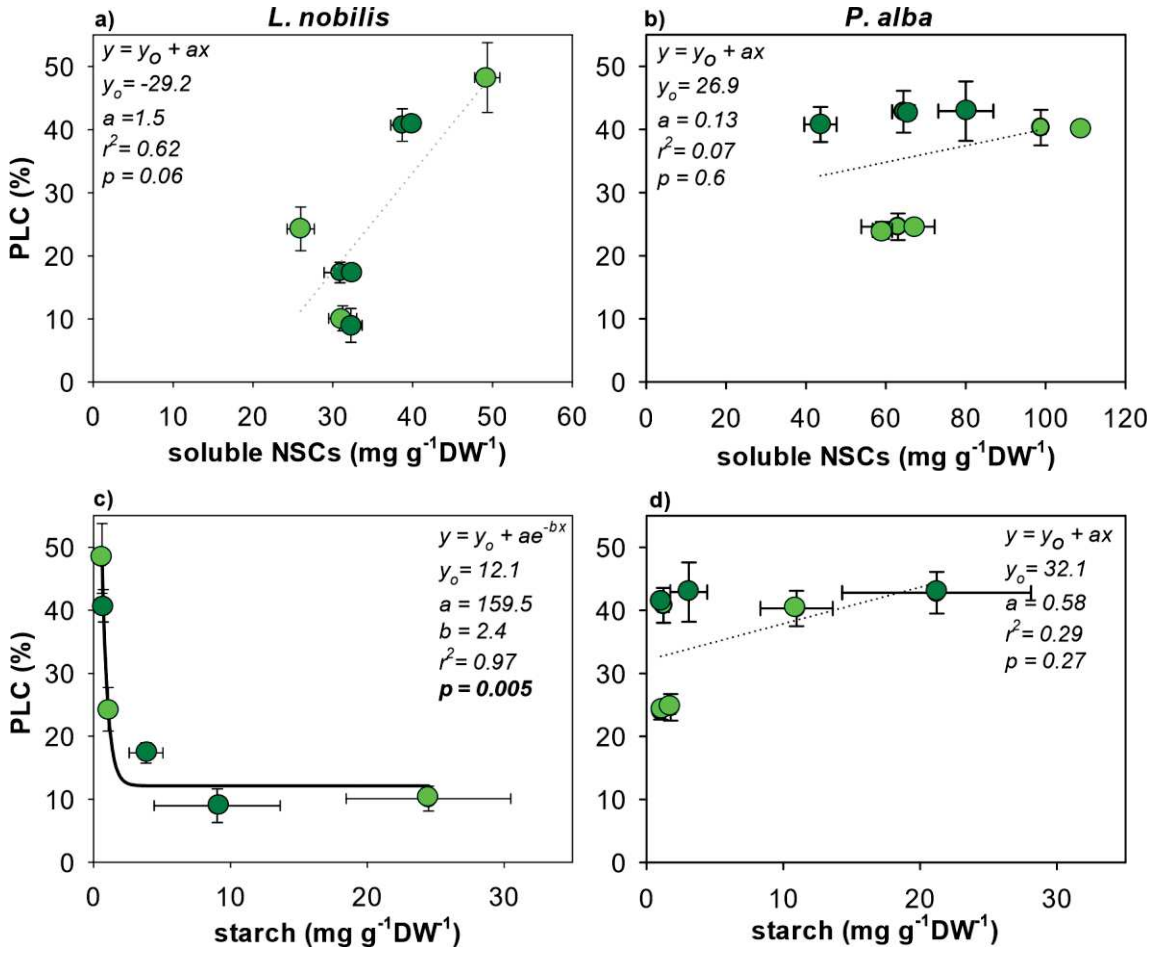

Fig. 5 Relationships between percentage loss of hydraulic conductivity (PLC) and (**a**, **c**) soluble NSCs and (**b**, **d**) starch content as recorded in control (light green) and woody tissue-shaded (dark green) stem of *L. nobilis* and *P. alba* stem samples. Regression equation (dotted and solid lines for correlation with $p > 0.05$ and $p < 0.05$, respectively), coefficient values, correlation coefficients (r^2) and *p*-values are also reported.

Discussion

Drought-induced hydraulic failure (i.e., whole blockage of the long-distance water transport system) poses a major threat to plant survival (Choat et al. 2018; Hartmann et al. 2018), but even carbon starvation can represent a significant challenge to plants facing water limitations (Sapes and Sala 2021; Kanneberg 2020). The maintenance of basal metabolism under drought, when leaf gas exchange is strongly reduced by stomatal closure, relies on the consumption of stored NSCs (McDowell et al. 2011). However, NSCs might play even more important indirect roles under drought, e.g., being involved in the maintenance of hydraulic conductance (Tomasella et al. 2020). Hence, the eventual extra carbon gain assured by stem photosynthesis under drought may be involved in the modulation of plant hydraulic functions (Ávila-Lovera et al. 2014; Vandegehuchte et al. 2015; Schmitz et al. 2012; Liu et al. 2019). Our results support the hypothesis that stem-level carbon gain plays a species-dependent role in the post-drought hydraulic recovery (Bloemen et al. 2013; Vandegehuchte et al. 2015; Cernusak and Cheeseman 2015). However, only in the deciduous poplar stem shading did affect the hydraulic recovery ability, while this was not the case for the evergreen laurel.

Inhibition of stem photosynthesis did not produce effects on the growth of poplar saplings. By contrast, smaller leaves were produced by S samples of *L. nobilis* compared to controls. Moreover, 5 weeks after the end of foliar expansion, lower starch content was recorded in well-watered samples of poplar compared to laurel (i.e., about 10 versus 20 mg g^{-1} DW^{-1}) but soluble sugars' content were similar (i.e., about 14 mg g^{-1} DW^{-1}).

Overall, these results strongly suggest that in *P. alba*, the decrease in stored NSCs, required to maintain similar annual growth in control and stem-shaded samples, affected the residual availability of NSCs to be used for the maintenance of hydraulic function under water stress. Sprouting is mainly supported by stored NSCs produced over the previous growing seasons, especially in deciduous species (Karlsson 1985; Hansen 1994; Piispanen and Saranpaa 2001; Schadel et al. 2009; Klein et al. 2016). Woody tissue carbon storage plays a key role in annual growth, as reported in a large number of species (Martínez-Vilalta et al. 2016; Furze et al. 2018). However, the impact of the remobilization of stored NSCs on the magnitude of growth is still unclear (Carbone et al. 2013; Trumbore et al. 2015; Piper and Paula 2020). Recently, Klein et al. (2016) reported that more than 95% of branch starch content was consumed for production of new leaves in saplings of three deciduous species (including species showing stem photosynthesis), and the recovery of carbon reserves occurred only 2–6 weeks after complete leaf expansion. On this basis, it is reasonable to suppose that, in deciduous species, even when performing stem photosynthesis, annual growth is mainly sustained by already available

wood NSCs' stores. This, in turn, is expected to lead to relevant depletion of NSC reserves that may be recovered over weeks by mature leaf and, at least in some species, by stem photosynthesis. In accordance, in well- watered samples, where no stem photosynthesis inhibition occurred, lower NSCs' content was recorded in the deciduous compared to evergreen species. Therefore, the inability to recover hydraulic function following embolism build-up under drought as recorded in S poplar samples was likely the consequence of inhibition of stem photosynthesis coupled to lower NSC reserves for the maintenance of hydraulic function during water stress, compared to laurel plants subjected to the same treatment. In accordance, xylem recovery occurred in control *P. alba* samples that, with equal NSC reserves of S samples, can rely on stem photosynthesis as well as in C and stem-shaded plants of *L. nobilis*.

In response to experimental drought, we observed a significant reduction in leaf gas exchange in the study species, leading to a severe reduction of leaf-level carbon assimilation. Under such conditions, plant metabolism of C plants was probably maintained by stored carbon compounds as well as by stem photosynthesis products. By contrast, in S samples, only stored carbon could be used. Soluble NSCs derived from photosynthesis or by starch hydrolysis are also necessary for osmoregulation processes and/or ROS scavenging (Sala et al. 2012; Plavcova and Jansen 2015; Traversari et al. 2020; Khaleghi et al. 2019). Sugars lead to generation of local positive pressures to drive water inflow into embolized conduits when water potential rises upon re-irrigation, leading to hydraulic recovery, i.e., (Tomasella et al. 2021; Salleo et al. 2004; Secchi and Zwieniecki 2014; Trifilò et al. 2017). In accordance, *L. nobilis* plants under drought showed a significant increase in soluble NSC content, and a parallel decrease in starch concentration in both C and S samples, compared to well-watered plants. Moreover, in this species, changes in NSC content were clearly related to changes in PLC. A different trend was recorded in *P. alba*. In fact, despite (i) the significant increase in soluble NSCs' content as recorded in C and S poplar samples in respect to well-watered plants and (ii) soluble sugars' content showing similar trend of changes in C and S poplar and laurel plants in response to drought-recovery cycle, no correlation between NSCs and PLC values was recorded in *P. alba*. These results clearly suggest that, in poplar stems, modulation of soluble NSCs and starch content was not involved in restoring hydraulic function, at least in S samples, where no refilling occurred even after re-irrigation.

Our data invite to depict the following scenario, that might orient future studies on the role of stem photosynthesis in modulation of plant hydraulic functioning. In evergreens, the maintenance of leaf photosynthesis over the whole year may assure sufficient carbon uptake, so that carbon stores would be normally available and usable under stress conditions. Hence, for these species, stem photosynthesis could represent an extra carbon gain to be used only when leaf photosynthesis is

severely inhibited. By contrast, in deciduous species, the extra carbon gain derived by stem photosynthesis might play a key role in whole plant metabolism, especially under drought. In these species, stem photosynthesis would not provide an "extra" carbon gain but would contribute to whole plant carbon assimilation.

Conclusions

In conclusion, our experiment has tried to disentangle the impact of leaf and stem photosynthesis on post-drought hydraulic recovery, showing that carbon assimilation at stem level differentially affects the maintenance of hydraulic functions in an evergreen versus a deciduous species. Our results, if confirmed in a wider number of deciduous versus evergreen species, will provide key information to predict the vulnerability of tree species under current global climate changes. Nevertheless, further studies investigating the impact of long- and short-term stem shading on species-specific drought resilience are needed.

Author Contributions

Conceptualization, P.T., A.N. and V.C.; investigation, E.A., S.G., S.N., P.T. and V.C.; resources, P.T. and V.C.; data curation, P.T.; writing—original draft preparation, P.T; writing— review and editing, P.T., A.N. and V.C. All authors have read and agreed to the published version of the manuscript.

Acknowledgments

We are very grateful to Dipartimento Regionale Azienda Foreste Demaniali, Messina, Sicily, Italy, for kindly providing plant material.

References

Adams HD, Zeppel MJ, Anderegg WR, Hartmann H, Landhäusser SM, Tissue DT, Huxman TE, Hudson PJ, Franz TE, Allen CD, et al. 2017. A multispecies synthesis of physiological mechanisms in drought-induced tree mortality. *Nature Ecology & Evolution* **1:** 1285–1291.

Améglio T, Decourteix M, Alves G, Valentin V, Sakr S, Julien J, Guillot A, Lacointe A. 2004. Temperature effects on xylem sap osmolarity in walnut trees: Evidence for a vitalistic model of winter embolism repair. *Tree Physiology* **24:** 785–793.

Aschan G, Pfanz H. 2003. Non foliar photosynthesis-A strategy of additional carbon acquisition. *Flora–Morphology, Distribution, Functional Ecology of Plants* **198:** 81–97.

Ávila-Lovera E, Herrera A, Tezara W. 2014. Contribution of stem CO_2 fixation to whole-plant carbon balance in nonsucculent species. *Photosyntica* **52:** 3–15.

Ávila-Lovera E, Tezara W. 2018. Water use efficiency is higher in green stems than in leaves of a tropical tree species. *Trees* **32:** 1547–1558.

Ávila-Lovera E, Urich R, Coronel I, Tezara W. 2019. Seasonal gas exchange and resource-use efficiency in evergreen versus deciduous species from a tropical dry forest. *Tree Physiology* **39:** 1561–1571.

Berveiller D, Kierzkowski D, Damesin C. 2007. Interspecific variability of stem photosynthesis among tree species. *Tree Physiology* **27:** 53–61.

Bloemen J, Overlaet-Michiels L, Steppe K. 2013. Understanding plant responses to drought: How important is woody tissue photosynthesis? *Acta Horticulturae* **991:** 149–155.

Bloemen J, Vergeynst L, Overlaet-Michielis L, Stepps K. 2016. How important is woody tissue photosynthesis in poplar during drought stress? *Trees* **30:** 63–72.

Bossard CC, Rejmanek M. 1992. Why have green stems? *Functional Ecology* **6:** 197–205.

Carbone MS, Czimczik CI, Keenan TF, Murakami PF, Pederson N, Schaberg PG, Xu X, Richardson AD. 2013. Age, allocation and availability of nonstructural carbon in mature red maple trees. *New Phytologist* **200:** 1–11.

Cernusak LA, Marshall JD. 2000. Photosynthetic refixation in branches of western white pine. *Functional Ecology* **14:** 300–311.

Cernusak LA, Hutley LB. 2011. Stable isotopes reveal the contribution of corticular photosynthesis to growth in branches of *Eucalyptus miniata*. *Plant Physiology* **155:** 515–523.

Cernusak LA, Cheeseman AW. 2015. The benefits of recycling: How photosynthetic bark can increase drought tolerance. *New Phytologist* **208:** 995–997.

Choat B, Brodribb TJ, Brodersen CR, Duursma RA, Lopez R, Medlyn BE. 2018. Triggers of tree mortality under drought. *Nature* **558:** 531–539.

Comstock JP, Ehleringer JR. 1988. Contrasting photosynthetic behaviour in leaves and twigs of *Hymenoclea salsola*, a green-twigged warm desert shrub. *American Journal of Botany* **75:** 1360–1370.

Damesin C. 2003. Respiration and photosynthesis characteristics of current-year stems of *Fagus sylvatica*: From the seasonal pattern to an annual balance. *New Phytologist* **158:** 465–475.

De Baerdemaeker NJF, Salomon RL, De Roo L, Steppe K. 2017. Sugars from woody tissue photosynthesis reduce xylem vulnerability to cavitation. *New Phytologist* **216:** 720–727.

De Roo L, Salomon RL, Steppe K. 2020. Woody tissue photosynthesis reduces stem CO_2 efflux by half and remains unaffected by drought stress in young *Populus tremula* trees. *Plant, Cell & Environment* **43:** 981–991.

Deslauriers A, Beaulieu M, Balducci L, Giovannelli A, Gagnon MJ, Rossi S. 2014. Impact of warming and drought on carbon balance related to wood formation in black spruce. *Annals of Botany* **33:** 335–345.

Dima E, Manetas Y, Psaras GH. 2006. Chlorophyll distribution pattern in inner stem tissues: Evidence from epifluorescence microscopy and reflectance measurements in 20 woody species. *Trees* **20:** 515–521.

Ehleringer JR, Phillips SL, Comstock JP. 1992. Seasonal variation in the carbon isotopic composition of desert plants. *Functional Ecology* **6:** 396–404.

Eyles A, Pinkard EA, Mohammed C. 2009. Shifts in biomass and resource allocation patterns following defoliation in *Eucalyptus globulus* growing with varying water and nutrient supplies. *Tree Physiology* **29:** 753–764.

Falchi R, Petrussa E, Braidot E, Sivilotti P, Boscutti F, Vuerich M, Calligaro C, Filippi A, Herrera JC, Sabbatini P, et al. 2020. Analysis of non-structural carbohydrates and xylem anatomy

of leaf petioles offers new insights in the drought response of two grapevine cultivars. *International Journal of Molecular Sciences* **21:** 1457.

Furze ME, Trumbore S, Hartmann H. 2018. Detours on the phloem sugar highway: Stem carbon storage and remobilization. *Current Opinion in Plant Biology* **43:** 89–95.

Hammond WM, Yu K, Wilson LA, Will RE, Anderegg WRL, Adams HD. 2019. Dead or dying? Quantifying the point of no return from hydraulic failure in drought- induced tree mortality. *New Phytologist* **223:** 1834–1843.

Hansen J, Beck E. 1994. Seasonal changes in the utilization and turnover of assimilation products in 8-year-old Scots pine (*Pinus sylvestris* L.). *Trees* **8:** 172–182.

Hartmann H, Ziegler W, Kolle O, Trumbore S. 2013. Thirst beats hunger declining hydration during drought prevents carbon starvation in Norway spruce saplings. *New Phytologist* **200:** 340–349.

Hartmann H, Trumbore S. 2016. Understanding the roles of non-structural carbohydrates in forest trees from what we can measure to what we want to know. *New Phytologist* **211:** 386–403.

Hartmann H, Moura CF, Anderegg WRL, Ruehr NK, Salmon Y, Allen CD, Arndt SK, Breshears DD, Davi H, Galbraith D, et al. 2018. Research frontiers for improving our understanding of drought-induced tree and forest mortality. *New Phytologist* **218:** 15–28.

Huckin K, Cochard H, Dreyer E, Le Thiec D, Bogeat-Triboulot MB. 2005. Cavitation vulnerability in roots and shoots: Does *Populus euphratica* Oliv., a poplar from arid areas of Central Asia, differ from other poplar species? *Journal of Experimental Botany* **418:** 2003–2010.

Kanneberg AS, Philips RP. 2020. Non-structural carbohydrate pools not linked to hydraulic strategies or carbon supply in tree saplings during severe drought and subsequent recovery. *Tree Physiology* **40:** 259–271.

Karlsson PS. 1985. Effects of water and mineral nutrient supply on a deciduous and an evergreen dwarf shrub: *Vaccinium uliginosum* L. and *V. vitisidaea* L. *Ecography* **8:** 1–8.

Khaleghi A, Naderi R, Brunetti C, Maserti BE, Salami SA, Babalar M. 2019. Morphological, physiochemical and antioxidant responses of *Maclura pomifera* to drought stress. *Scientific Reports* **9:** 19250.

Klein T, Vitasse Y, Hoch G. 2016. coordination between growth, phenology and carbon storage in three coexisting deciduous tree species in a temperate forest. *Tree Physiology* **7:** 847–855.

Landhausser SM, Chow PS, Dickman LT, Furze ME, Kuhlman I, Schmid S, Wiesenbauer J, Wild B, Gleixner G, Hartmann H, et al. 2018. Standardized protocols and procedures can precisely and accurately quantify non-structural carbohydrates. *Tree Physiology* **38:** 1764–1778.

Liu J, Gu L, Yu, J, Ju G, Sun Z. 2018. Stem photosynthesis of twig and its contribution to new organ development in cutting seedlings of *Salix Matsudana* Koidx. *Forests* **9:** 207.

Liu J, Gun L, Yu Y, Huang P, Wu Z, Zhang Q, Qian Y, Wan X, Sun Z. 2019. Corticular photosynthesis drives bark water uptake to refill embolized vessels in dehydrated branches of *Salix matsudana. Plant, Cell & Environment* **42:** 2584–2596.

Lo Gullo MA, Salleo S. 1991. Three different methods for measuring xylem cavitation and embolism: A comparison. *Annals of Botany* **67:** 417–424.

Losso A, Beikircher B, Damon B, Kikuta S, Schimd P, Mayr S. 2017. Xylem sap surface tension may be crucial for hydraulic safety. *Plant Physiology **175:*** 1135–1143.

Martínez-Vilalta J, Sala A, Asensio D, Galiano L, Hoch G, Palacio S, Piper FI, Lloret F. 2016. Dynamics on non-structural carbohydrates in terrestrial plants: A global synthesis. *Ecological Monographs* **86:** 495–516.

Mayr S, Kartusch B, Kikuta S. 2014. Evidence for air-seeding: Watching the formation of embolism in conifer xylem. *Journal of Plant Hydraulics* **1:** e0004.

Mayr S, Ameglio T. 2016. Freezing stress in tree xylem. In: Luttge, U., Canovas, F., Matyssek, R., eds. *Progress in Botany.* Springer: Berlin, DE: 381–414.

McDowell NG, Beerling DJ, Breshears DD, Fisher RA, Raffa KF, Stitt M. 2011. The interdependence of mechanisms underlying climate-driven vegetation mortality. *Trends in Ecology & Evolution* **26:** 523–532.

Nardini A, Gascó A, Trifilò P, Lo Gullo MA, Salleo S. 2007. Ion-mediated enhancement of xylem hydraulic conductivity is not always suppressed by the presence of Ca^{2+} in the sap. *Journal of Experimental Botany* **58:** 2609–2615.

Nardini A, Savi T, Losso AA, Petit G, Pacilè S, Tromba G, Mayr S, Trifilò P, Lo Gullo MA, Salleo S. 2017. X-ray microtomography observations of xylem embolism in stems of *Laurus nobilis* L. are consistent with hydraulic measurements of percent loss of conductance. *New Phytologist* **213:** 1068–1075.

Nardini A, Savi T, Trifilò P, Lo Gullo MA. 2018. Drought stress and the recovery from xylem embolism in woody plants. In Cánovas FM, Luettge U, Matyssek R, eds. *Progress in Botany*. Berlin, DE, Springer, 197–231.

Neuner G. 2014. Frost resistance in alpine woody plants. *Frontiers in Plant Science* **5:** 654.

Nilsen ET, Meinzer FC, Rundel PW. 1989. Stem photosynthesis in *Psorothamnus spinosus* (smoke tree) in the Sonorandesert of California. *Oecologia* ***79*:** 193–197.

Nilsen ET, Bao Y. 1990. The influence of water stress on stem and leaf photosynthesis in *Glycine max* and *Spartium junceum* (leguminosae). *American Journal of Botany* **77:** 1007–1015.

Nilsen ET. 1995. Stem photosynthesis: extent, patterns and role in plant carbon economy. In: Gartner B, eds. *Plant stems: physiology and functional morphology*. San Diego, USA: Academic Press, 223–240.

Nilsen ET, Sharifi MR. 1997. Carbon isotopic composition of legumes with photosynthetic stems from mediterranean and desert habitats. *American Journal of Botany* **84:** 1707–1713.

Oroian M, Ropciuc S, Amariei S, Gutt G. 2015. Correlations between density viscosity, surface tension and ultrasonic velocity of different mono- and di-saccharides. *Journal of Molecular Liquids* **207:** 145–151.

Osmond CB, Smith SD, Gui-Ying B, Sharkey TD. 1987. Stem photosynthesis in a desert ephemeral, *Eriogonum inflatum*. Characterization of leaf and stem CO_2 fixation and H_2O vapor exchange under controlled conditions. *Oecologia* **72:** 542–549.

Pagliarani C, Casolo V, Beiragi MA, Cavalletto S, Siciliano I, Schubert A, Gullino ML, Zwieniechi MA, Secchi F. 2019. Priming xylem for stress recovery depends on coordinated activity of sugar metabolic pathways and changes in xylem sap pH. *Plant, Cell & Environment* **42:** 1775–1787.

Pfanz H, Aschan G. 2001. The existence of bark and stem photosynthesis in woody plants and its significance for the overall carbon gain. An eco-physiological and ecological approach. In: Essr K, Luttge U, Kadereit JW, Beyshlag W, eds. Progress in Botany, Berlin, DE: Springer-Verlag, 477–510.

Pfanz H, Aschan G, Langenfeld-Heyser R, Wittmann C, Loose M. 2002. Ecology and ecophysiology of tree stems: Corticular and wood photosynthesis. *Naturwissenschaften* **89:** 147–162.

Piispanen R, Saranpaa P. 2001. Variation of non-structural carbohydrates in silver birch (*Betula pendula* Roth) wood. *Trees* **15:** 445–451.

Piper F, Paula S. 2020. The role of nonstructural carbohydrates storage in forest resilience under climate change. *Current Forestry Reports* **6:** 1–13.

Plavcova L, Jansen S. 2015. The role of xylem parenchyma in the storage and utilization of non-structural carbohydrates. In *Functional and Ecological Xylem Anatomy*; Hacke, U., Ed, Springer: Berin, Germany; pp. 209–234.

Quentin AG, Pinkard EA, Ryan MG, Tissue DT, Baggett LS, Adams HD, Maillard P, Marchand J, Landhäusser SM, Lacointe A, et al. 2015. Non-structural carbohydrates in woody plants compared among laboratories. *Tree Physiology* **35:** 1146–1165.

Rentzou GK, Psaras A. 2008. Green plastids, maximal PSII photochemical efficiency and starch content of inner stem tissues of three Mediterranean woody species during the year. *Flora* **203:** 350–357.

Sala A, Woodruff DR, Meinzer FC. 2012. Carbon dynamics in trees: Feast or famine? *Tree Physiology* **32:** 764–775.

Salleo S, Lo Gullo MA, Trifilò P, Nardini A. 2004. New evidence for a role of vessel-associated cells and phloem in the rapid xylem refilling of cavitated stems of *Laurus nobilis* L. *Plant, Cell & Environment* **27:** 1065–1076.

Santiag LS, Goldstein G, Meinzer FC, Fisher JB, Machado K, Woodruff D, Jones T. 2004. Leaf photosynthetic traits scale with hydraulic conductivity and wood density in Panamanian forest canopy trees. *Oecologia* **140:** 543–550.

Sapes G, Sala A. 2021. Relative water content consistently predicts drought mortality risk in seedling populations with different morphology, physiology, and times to death. *Plant, Cell & Environment* **44:** 3322–3335.

Saveyn KA, Steppe N, Ubierna TE. 2010. Woody tissue photosynthesis and its contribution to trunk growth and bud development in young plants. *Plant, Cell & Environment* **33:** 1949–1958.

Schadel C, Blochl A, Richter A, Hoch G. 2009. Short-term dynamics of non-structural carbohydrates and hemicelluloses in young branches of temperate forest trees during bud break. *Tree Physiology* **29:** 901–911.

Schenk HJ, Espino S, Romo DM, Nima N, Do AY, Michaud JM, Papahadjopoulos-Sternberg B, Yang J, Zuo YY, Steppe K, et al. 2017. Xylem surfactants introduce a new element to the Cohesion-Tension theory. *Plant Physiology* **173:** 1177–1196.

Schmitz N, Egerton JJG, Lovelock CE, Ball MC. 2012. Light-dependent maintenance of hydraulic function in mangrove branches: Do xylary chloroplasts play a role in embolism repair? *New Phytologist* **195:** 40–46.

Secchi F, Zwieniecki MA. 2014. Down-regulation of plasma intrinsic protein1 aquaporin in poplar trees. Is detrimental to recovery from embolism? *Plant Physiology* **164:** 1789–1799.

Secchi F, Zwieniecki MA. 2016. Accumulation of sugars in the xylem apoplast observed under water stress conditions is controlled by xylem pH. *Plant, Cell & Environment* **39:** 2350–2360.

Simbo DJ, Van den Bilcke N, Samson R. 2013. Contribution of corticular photosynthesis to bud development in african baobab (*Adansonia digitata* L.) and castor bean (*Ricinus communis* L.) seedlings. *Environmental and Experimental Botany* **95:** 1–5.

Sperry JS, Donnelly JR, Tyree MT. 1988. A method for measuring hydraulic conductivity and embolism in xylem. *Plant, Cell & Environment* **11:** 35–40.

Teskey, R.O, Saveyn, A, Steppe, K, McGuire, M.A. 2008. Origin, fate and significance of CO_2 in tree stems. *New Phytologist* **177:** 17–32.

Tinoco-Ojanguren C. 2008. Diurnal and seasonal patterns of gas exchange and carbon gain contribution of leaves and stems of *Justicia californica* in the Sonoran Desert. *Journal of Arid Environments 72***:** 127–140.

Tixier A, Gambetta GA, Godfrey J, Zwieniecki MA. 2019. Non-structural carbohydrates in dormant woody perennials: The tale of winter survival and spring arrival. *Frontiers in Forests and Global Change* **2:** 18.

Tomasella M, Petrussa E, Petruzzellis F, Nardini A, Casolo V. 2020. The possible role of non-structural carbohydrates in the regulation of tree hydraulics. *International Journal of Molecular Sciences* **21:** 144.

Tomasella M, Casolo V, Natale S, Petruzzellis F, Kofler W, Beikircher B, Mayr S, Nardini A. 2021. Shade-induced reduction of stem nonstructural carbohydrates increases xylem vulnerability to embolism and impedes hydraulic recovery in *Populus nigra*. *New Phytologist* **231:** 108–121.

Traversari L, Neri M, Traversi L. 2020. Daily osmotic adjustments in stem may be good predictors of water stress intensity in poplar. *Plant Physiology and Biochemistry* **146:** 13–22.

Trifilò P, Raimondo F, Lo Gullo MA, Barbera PM, Salleo S, Nardini A. 2014. Relax and refill: Xylem rehydration prior to hydraulic measurements favours embolism repair in stems and generates artificially low PLC values. *Plant, Cell & Environment* **37:** 2491–2499.

Trifilò P, Nardini A, Lo Gullo MA, Barbera PM, Raimondo F. 2015. Diurnal changes in embolism rate in nine dry forest trees: Relationship with specie-specific xylem vulnerability, hydraulic strategy and wood traits. *Tree Physiology* **35:** 694–705.

Trifilò P, Casolo V, Raimondo F, Petrussa E, Boscutti F, Lo Gullo MA, Nardini A. 2017. Effects of prolonged drought on stem non-structural carbohydrates content and post-drought hydraulic recovery in *Laurus nobilis* L.: The possible link between carbon starvation and hydraulic failure. *Plant Physiology and Biochemistry* **120:** 232–241.

Trumbore S, Czimczik CI, Sierra CA, Muhr J, Xu X. 2015. Non-structural carbon dynamics and allocation relate to growth rate and leaf habit in California oaks. *Tree Physiology* **35:** 1206–1222.

Tyree MT, Hammel HT. 1972. The measurement of the turgor pressure and the water relations of plants by the pressure-bomb technique. *Journal of Experimental Botany* **23:** 267–282.

Van Cleve B, Apel K. 1993. Induction by nitrogen and low temperature of storage-protein synthesis in poplar trees exposed to long days. *Planta* **189:** 157–160.

Vandegehuchte MW, Bloemen J, Vergeynst LL, Steppe K. 2015. Woody tissue photosynthesis in trees: Salve on the wounds of drought? *New Phytologist* **208:** 998–1002.

Wheeler JK, Huggett BA, Tofte AN, Rockwell FE, Holbrook NM. 2013. Cutting xylem under tension or supersaturated with gas can generate PLC and the appearance of rapid recovery from embolism. *Plant, Cell & Environment* **36:** 1938–1949.

Wiebe HH. 1975. Photosynthesis in wood. *Physiologia Plantarum* **33:** 245–246.

Wittmann C, Pfanz H. 2007. Temperature dependency of bark photosynthesis in beech (*Fagus sylvatica* L.) and birch (*Betula pendula* Roth.) trees. *Journal of Experimental Botany* **58:** 4293–4306.

Wittmann C, Pfanz H. 2014. Bark and woody tissue photosynthesis: A means to avoid hypoxia or anoxia in developing stem tissue. *Functional Plant Biology* **41:** 940–953.

Wittmann, C, Pfanz, H. 2018. More than just CO_2-recycling: Corticular photosynthesis as a mechanism to reduce the risk of an energy crisis induced by low oxygen. *New Phythologist* **219:** 551–564.

Yemm EW, Willis AJ. 1954. The estimation of carbohydrates in plant exctract by anthrone. *Biochemical Journal* **57:** 508–514.

Study 6

No Evidence for Light-Induced Embolism Repair in Cut Stems of Drought-Resistant Mediterranean Species under Soaking

Martina Tomasella[2], Sara Natale[1], Francesco Petruzzellis[1,2], Sara Di Bert[1], Lorenzo D'Amico[3,4], Giuliana Tromba[3] and Andrea Nardini[1]

[1]Dipartimento di Scienze della Vita, Università di Trieste, Via L. Giorgieri 10, 34127 Trieste, Italy;
[2]Dipartimento di Scienze Agroalimentari, Ambientali e Animali, Università di Udine, Via delle Scienze 91, 33100 Udine, Italy
[3]Elettra-Sincrotrone Trieste, Area Science Park, 34149, Basovizza, Italy;
[4]Dipartimento di Fisica, Università di Trieste, Via A. Valerio 2, 34127 Trieste, Italy

Published as: **Tomasella M, Natale S, Petruzzellis F, Di Bert S, D'Amico L, Tromba G, Nardini A. 2022.** No evidence for light-induced embolism repair in cut stems of drought-resistant mediterranean species under soaking. *Plants* **11:** 307.

Abstract

(1) Recent studies suggested that stem photosynthesis could favor bark water uptake and embolism recovery when stem segments are soaked in water under light conditions, but evidence for this phenomenon in drought-resistant Mediterranean species with photosynthetic stems is missing. (2) Embolism recovery upon immersion in water for 2 h–4 h under light was assessed (i) via a classical hydraulic method in leafless *Fraxinus ornus* and *Olea europaea* branch segments stressed to xylem water potentials (Ψ_{xyl}) inducing ca. 50% loss of hydraulic conductivity (PLC) and (ii) via X-ray micro-CT imaging of the stem segments of drought-stressed potted *F. ornus* saplings. Hydraulic recovery was also assessed in vivo in intact drought-stressed *F. ornus* saplings upon soil re-irrigation. (3) Intact *F. ornus* plants recovered hydraulic function through root water uptake. Conversely, the soaked stem segments of both species did not refill embolized conduits, although Ψ_{xyl} recovered to pre-stress levels (between −0.5 MPa and −0.2 MPa). (4) We hypothesize that xylem embolism recovery through bark water uptake, even in light conditions, may not be a common phenomenon in woody plants and/or that wounds caused by cutting short stem segments might inhibit the refilling process upon soaking.

Keywords: stem photosynthesis; hydraulic recovery; soaking; X-ray micro-CT; bark water uptake; embolism

Introduction

Most terrestrial plants rely on root-level water absorption to maintain their hydration status. However, water can also be absorbed from the surface of aboveground plant organs under particular biophysical conditions, i.e., when liquid water is wetting plant surfaces or the water potential of the surrounding atmospheric boundary layer is higher than that of cells (Berry et al. 2019). This occurs when water vapor pressure in the air is at (or close to) saturation and, most importantly, when liquid water forms or falls on a plant surface due to fog, rain or snow melting, allowing local rehydration and partial xylem tension relief, especially when plants are experiencing a soil water deficit (Breshears et al. 2008).

Water uptake through leaves has been widely observed in many plant lineages (Dawson et al. 2020; Carmichael et al. 2020). Leaf trichomes, depending on their density, composition and structure, are the major media for water absorption in a Mediterranean (*Quercus ilex*) and a temperate (*Fagus sylvatica*) species (Fernández et al. 2014; Schreel et al. 2020). In addition, in two species without leaf trichomes or hydathodes, open stomata have been observed to play a major role in water uptake over cuticles when exposed to fog (Guzmán-Delgado et al. 2021). Leaf water absorption can also be involved in the recovery of leaf (Fuenzalida et al. 2019) and stem (Mayr et al. 2019; Laur and Hacke 2014) hydraulic functions after drought- or frost-induced xylem embolism.

The stems of woody plants, even when covered with suberized tissue, are also able to absorb water when the bark becomes wet, allowing partial xylem tension relief (Katz et al. 1989). There is some evidence that leafless dehydrated branches soaked in water for at least some hours partially recover their xylem hydraulic function in a conifer (*Sequoia sempervirens,* (Mason Earles et al. 2016)) and in an angiosperm (*Salix matsudana*, (Liu et al. 2019)). Xylem hydraulic recovery would require radial water movement from the phloem to the xylem through parenchyma rays, as proven in a dying experiment on wetted stems (Katz et al. 1989). Liu et al. (2019) soaked short *S. matsudana* stem segments in water and observed faster embolism repair (within 2 h) when under light conditions compared to dark conditions, where partial refilling nevertheless occurred. The enhanced refilling effect under light was ascribed to the sugars produced by stem photosynthesis, which provide the driving (osmotic) force for the process. In fact, embolism repair can occur as the result of a water potential gradient between the xylem apoplast, where sugars are accumulated, and parenchyma cells surrounding the conduits (Salleo et al. 2004; Zwieniecki and Holbrook 2009; Secchi et al. 2017). Independently of the mechanisms involved in the process, such soaking experiments on short leafless stem segments on other woody species performing stem photosynthesis are underrepresented, and

they might constitute an interesting experimental model to investigate the biology of post-drought hydraulic recovery.

In the past decade, some methodological issues have arisen regarding stem hydraulic vulnerability assessment and the study of embolism recovery via classic hydraulic methods due to the possible overestimation of embolism rates, which may be generated when cutting xylem under tension (Wheeler et al. 2013). At the same time, prolonged xylem relaxation prior to hydraulic measurements, which is suggested to avoid artefactual embolism appearance, can favor refilling, leading to the underestimation of embolism levels (Trifilò et al. 2014). In well-established sample preparation procedures for hydraulic measurements, stems are often kept under water prior to hydraulic measurements, even for long time intervals, based on the principle that the very low pressure head upon immersion would avoid embolism dissolution (Sperry et al. 1988). However, the above-mentioned soaking experiments in short leafless branch segments (Mason Earles et al. 2016; Liu et al. 2019) indicated that the active accumulation of solutes at the wood parenchyma–conduit interface drives water into the apoplast and might refill the conduits under soaking. If this happens, soaking stems for a prolonged period would induce overestimation of xylem hydraulic conductivity.

These controversies can be overcome using X-ray micro-computed tomography (micro-CT), an important tool to visualize embolized xylem conduits at a proper resolution and to quantify in vivo xylem vulnerability, as well as possible hydraulic recovery in intact plants (Broadersen et al. 2010; Secchi et al. 2020). Therefore, this method has been exploited to validate destructive hydraulic methods (e.g., (Savi et al. 2017; Venturas et al. 2019)) and related sample preparation procedures (Torres-Ruiz et al. 2015).

In this study, we hypothesized that bark water uptake in the presence of light would induce the recovery of hydraulic function in two embolism-resistant Mediterranean angiosperm species performing stem photosynthesis, namely, *Fraxinus ornus* and *Olea europaea*. We tested this hypothesis both with a classical hydraulic method in dehydrated leafless cut branches of adult plants of both species, and in vivo through X-ray micro-CT imaging of segments of drought-stressed potted young saplings of *F. ornus*. There is evidence suggesting that *O. europaea* is capable of partial hydraulic recovery following drought-induced xylem embolism (Trifilò et al. 2014), making this species a good candidate to investigate the eventual process of conduit refilling under soaking conditions. Similarly, intact *F. ornus* plants have already been reported to recover hydraulic function when the soil is re-watered after substantial drought-induced loss of xylem hydraulic conductivity (Tomasella et al. 2019), but in vivo evidence is missing. For this reason, we additionally tested the hydraulic recovery capability of this species through root water uptake via micro-CT imaging of intact potted plants.

Materials and Methods

Plant Material

The experiment was carried out on two Mediterranean tree species, namely, manna ash (F*raxinus ornus* L.) and olive (*Olea europaea* L.), between mid-June and the end of July 2021. In order to test the hydraulic recovery capability upon soaking under light conditions, embolism was measured both with a classical hydraulic conductivity apparatus and in vivo via micro-CT, but on different plant material. Hydraulic measurements were performed on sun-exposed branches taken from several *F. ornus* trees and one *O. europaea* tree growing in the Botanical Garden of the University of Trieste (Italy, 45°39′40.9″ N, 13°47′40.1″ E). For micro-CT experiments, 2-year-old and 1-year-old *F. ornus* saplings provided by a local public nursery (Vivai Pascul, Regional Forestry Service, Tarcento, Italy) were transplanted in 3.4 L and 1 L pots in March 2020 and 2021, respectively. Pots were filled with a lightweight substrate for green roof installations (for the 2-year-old plants) or with red soil (for the 2-year-old plants) sampled from a vineyard in the Italian Karst (Duino-Aurisina, Italy). Plants were grown in a greenhouse of the University of Trieste, supplied with tap water twice a day to soil field capacity through a clock irrigation system.

To check the capability of the study species to perform bark and wood photosynthesis, some stem segments were analyzed with an imaging PAM chlorophyll fluorometer (Photon Systems Instruments, Brno, Czech Republic) to obtain the maximum quantum yield of PSII (Fv/Fm). Stem segments of approx. 2 cm length were dark adapted for 1 h, longitudinally sectioned and positioned on a plate with a layer of paper towels, keeping them hydrated through partial immersion in a film of water. Outer bark, outer xylem and xylem longitudinal section (sapwood + pith) were measured (see Fig. 1a).

Hydraulic Measurements

F. ornus and *O. europaea* branches were collected in the late afternoon and rehydrated overnight while covered with a black plastic bag after cutting the basal 5 cm underwater. In the early morning, full hydration was checked to ensure that xylem water potential (Ψ_{xyl}) was above −0.3 MPa. A group of hydrated branches was used for hydraulic measurements to check possible residual embolism (hydrated group, H, $n = 5$). The remaining branches were dehydrated on the bench, covering several leaves with cling film and aluminum foil to stop transpiration and favor equilibration between leaf and stem xylem in order to measure Ψ_{xyl} with a pressure chamber (mod. 1505D, PMS Instrument co., Albany, OR, USA). For olive, before bench dehydration, about 15 cm of the 2-year-old stem portions selected for hydraulic measurements and soaking treatment were deprived of leaf blades by cutting

them at the insertion point at the petiole and sealing the cut section with impermeable glue (Super Attack, Loctite). Branches were dehydrated until reaching the target Ψ_{xyl}, fixed to -(3.5–3.9) MPa for *F. ornus* and to -(4.2–4.7) MPa for *O. Europaea,* based on preliminary assessments. At that point, a group of branches was immediately processed for hydraulic conductivity measurements (dehydration group, D, n = 5–6), while a third group was subjected to the soaking treatment as follows. Stem segments, obtained as described below, were sealed at the cut ends with wax tape (Parafilm® M), kept under water and then immersed in a white rectangular bowl containing distilled water, lying horizontally 1 cm below the water level. Stems were rotated by 180° every hour to allow whole stem light exposure. A LED panel (red/blue 96/24) was mounted above the bowl to produce a photosynthetic photon flux density (PPFD) at the water level of about 400 μmol m^{-2} s^{-1}. According to Liu et al. (2019), most of the embolized vessels of *S. matsudana* refilled already 2 h after branch segment immersion in light conditions. Therefore, duration of soaking was fixed to 2 h for both species (S_{2h} group, n = 6). For *F. ornus,* a second set of branches was immersed for 4 h to check if longer rehydration times were needed for hydraulic recovery (S_{4h} group, n =7). After soaking, branch segments were prepared for hydraulic measurements as described below, while a 3 cm adjacent stem segment was taken for Ψ_{xyl} measurements, performed with a dew point hygrometer (WP4-C, Meter Group, Inc., Pullman, WA, USA). To this aim, the segment was quickly wiped with paper towel, cut longitudinally in half, placed in a sample holder and measured upon Ψ_{xyl} stabilization (reached in 30 min–40 min).

Measurements were performed on 3 cm–4 cm long segments of H, D, S_{2h} and S_{4h} stems. For all samples, the base of the branch was trimmed under clean tap water at a distance higher than the maximum vessel length. Maximum vessel length, determined with the "air method" described by Wang et al. (2014), averaged 29 cm and 45 cm in *F. ornus* and *O. europaea* branches, respectively. Then, a selected ~15 cm long segment was cut and kept under water. S_{2h} and S_{4h} segments were sealed at both ends with Parafilm and soaked as described above. For hydraulic conductivity measurements, a shorter segment was obtained; the bark was removed from both cut ends, and several thin sharp slides were made with a razorblade at both ends to obtain a 3 cm–4 cm long segment; and the basal end was inserted in a hydraulic apparatus (see (Tomasella et al. 2019)).

Xylem hydraulic conductance was measured gravimetrically under a water head of 3.5 kPa, perfusing stems with filtered (0.45 μm) and degassed mineral water added with 10 mM KCl (Nardini, et al. 2007). Hydraulic conductance was measured before (initial hydraulic conductance, k_i) and after (maximum hydraulic conductance, k_{max}), flushing the sample at high pressure (0.15 MPa) for 3 min to remove xylem embolism. Xylem hydraulic conductivity (K) was calculated as

$$K = k \times L/A \quad (1)$$

where L is the length of the segment, and A is the sapwood area, calculated as the average sapwood areas measured at the cut ends of the sample.

Percentage loss of hydraulic conductivity (PLC) was then calculated as

$$PLC = 100 \times [1 - (k_i \, k_{max}^{-1})] \quad (2)$$

Micro-CT Scans and Image Processing

Micro-CT scans were performed at the SYRMEP beamline of the Elettra Synchrotron light source (Trieste, Italy).

To check the capability of *F. ornus* to recover xylem embolism after soil rewetting, four 3-year-old saplings were dehydrated in pots to reach the target Ψ_{xyl} (−3.5 MPa) on 17–21 July 2020. The 2-year-old stem portion of two plants was scanned right after reaching the target Ψ_{xyl} (D_{pot} plants), while the other two were scanned 24 h after re-irrigation to soil field capacity (recovery, R_{pot} plants). Two additional well-watered plants were measured as controls (C_{pot}). In all plants, Ψ_{xyl} was measured prior to scanning.

The soaking experiment was performed on potted *F. ornus* saplings on 1 August 2021. All plants were dehydrated by withholding irrigation for about 5 days. Three of them were scanned to detect the embolism level at the target Ψ_{xyl} (D plants). These plants were also used to tests the sample preparation effect on embolism formation, scanning the stem at the same point in three different steps: (i) the intact plant, (ii) the plant cut underwater right above the root collar after immersing the pot (sealed in a plastic bag) in water and (iii) the final stem segment obtained by cutting the stem 14 cm–21 cm above the previous cut, keeping the sample underwater. The length of the segment depended on the length of the 2-year-old stem segment portion, while the scan was always 8 cm–9 cm above the basal cut. After every cut, the cut surface was tightly sealed underwater with Parafilm. An additional scan was performed after cutting the stem segment a few mm above the scanned region in order to observe the fully embolized xylem.

The remaining three plants were prepared in the same way as the D plants, but they were only scanned after soaking the stem segment (obtained at step iii) in water for 2 h (S_{2h} samples) as described above for branches measured with the hydraulic apparatus. This was carried out to avoid the possibility of multiple scans inhibiting cellular activity and possible related processes involved in water uptake and hydraulic recovery (Petruzzellis et al. 2018).

Before micro-CT scanning, all samples were quickly wrapped in cling film and Parafilm to avoid water loss and fixed to the sample holder. The CT studies were performed in propagation-based phase

contrast modality using an Orca Flash 4.0 SCMOS, coupled with a 17 μm GGG scintillator, as a detector. The sample was placed 15 cm from the detector, and the pixel size was set at 2.1 μm. The experiment was performed in white beam mode, and 1.0 mm of silica was applied, resulting in a mean X-ray energy of about 22 keV. For each scan, 1800 projections were acquired during the sample rotation over 180°.

The slice reconstructions were performed using SYRMEP Tomo Project (STP) software [39]. A phase retrieval pre-processing algorithm (Paganin et al. 2002) was applied prior to the conventional filtered back-projection algorithm to increase the image contrast.

Reconstructed images were processed using ImageJ (https://imagej.nih.gov/ij/, accessed on 30 November 2021). Due to the larger diameter of the stems compared to the field of view (ca. 4 mm × 4 mm), analyses were conducted on about one-quarter of the stem section, excluding the immature xylem next to the vascular cambium (see Fig. 3, 4, S1 and S2). The embolized sapwood area (A_{embol}) was calculated by dividing the embolized pixel area by the analyzed sapwood area, expressed as percentage. The embolized vessel area (EVA) was calculated by dividing A_{embol} by the A_{embol} after the final cut above the scanned region (representing the percentage of sapwood area occupied by conduits), expressed as percentage.

Statistics

Statistical analyses were carried out with R (R Core Team 2019). Boxplot panels were obtained with the "ggplot2" package in R. Bar charts were prepared with SigmaPlot (v. 12.0, Systat Software Inc., Berkshire, UK). For PLC and Ψ_{xyl}, the one-way ANOVA test (response variable ~f(treatment)) through the *aov* function was applied, followed by Tukey's HSD post hoc test (only for significant ANOVA, $p < 0.05$) through the *TukeyHSD* function in the "stats" package after checking for normality of residuals and homogeneity of variances. When homogeneity of variance assumption was violated, generalized least squares (GLS) models were calculated with the *gls* function, including a "varIdent" variance structure, in the "nlme" R package [41], followed by Tukey's HSD post hoc analysis (for significant tests), with *p*-values adjusted using the Bonferroni–Holm method. The effect of progressive cuttings on A_{embol} and EVA in the micro-CT test experiment was tested using linear mixed models (LMMs) through the *lme* function. Specifically, one LMM was fitted by separately setting A_{embol} or EVA as the response variable and by setting the cutting stage as the explanatory one, with the plant replicate as the random effect. Pairwise comparisons were performed through *lsmeans* function in R package "emmeans" (Lenth 2020).

Results

The stem segments used for the soaking experiments, i.e., 2-year-old *F. ornus* and 1-year-old *O. europaea* branch portions, as well as the 1-year-old stem portions of *F. ornus* saplings, showed a relatively high capability of performing photosynthesis (Fig. 1). In particular, the maximum quantum yield of PSII (Fv/Fm) in the outer bark was about 0.8 in all three different samples. Similar values were also measured in the outer wood and in the longitudinal section of the wood (sapwood + pith) of the 1-year-old branch and stem segments of both species. Lower (but still relatively high) Fv/Fm values were measured in the outer wood (0.65) and in the longitudinal section of the wood (0.49) of *F. ornus* 2-year-old branch portions.

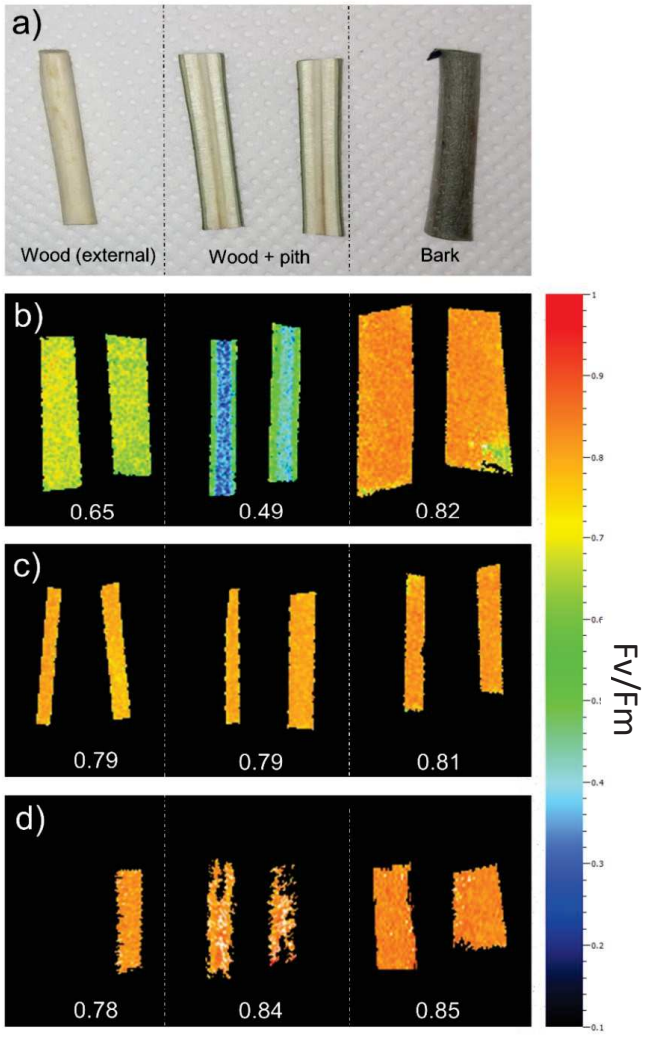

Fig. 1 Maximum quantum yield of PSII (Fv/Fm) measured in branch/stems used for the experiment. Wood (exposing the side next to the vascular cambium), wood + pith (exposing the cut side) and bark were analyzed separately (**a**). Measurements were performed on 2-year old *F. ornus* branch segments (**b**), in 1-year old *O. europaea* branch segments (**c**) and in 1-year old stems of *F. ornus* saplings (**d**). Values in b–c are the average value of the sample.

Hydraulic Measurements

Some native embolism was detected in the hydrated branches of *F. ornus* and *O. europaea* (H samples), with PLC averaging 17% and 5%, respectively (Fig. 2). After dehydration on the bench, PLC at the target Ψ_{xyl} (−3.7 MPa and −4.4 MPa in *F. ornus* and *O. europaea*, respectively) significantly increased to 56 ± 4% in *F. ornus* and to 54 ± 10% in *O. europaea*. After the soaking treatment in distilled water for 2 h (S_{2h} samples), Ψ_{xyl} increased to pre-stress levels, averaging −0.46 MPa in *F. ornus* and −0.33 MPa in *O. europaea*, but stem PLC did not recover in either species. Moreover, prolonged immersion in water (four hours, S_{4h} stems) did not induce xylem hydraulic recovery in *F. ornus,* albeit xylem tension further and significantly decreased with respect to the S_{2h} samples (Ψ_{xyl} = −0.19 ± 0.06 MPa, $p < 0.05$).

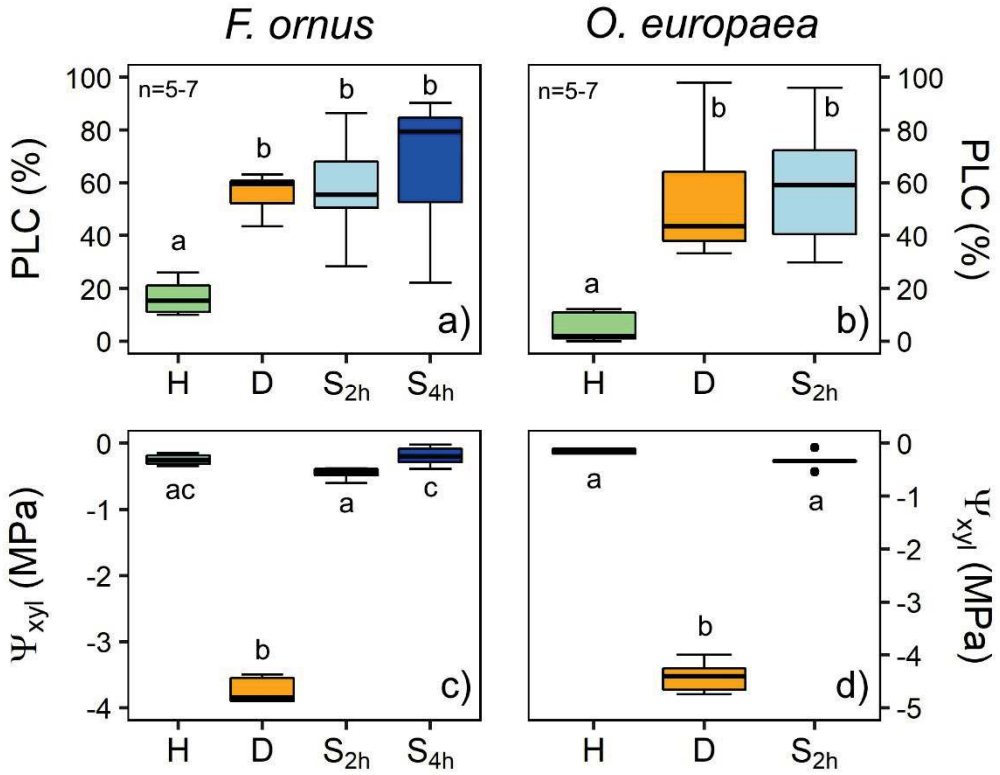

Fig. 2 Percentage loss of xylem hydraulic conductivity (PLC, **a**,**b**) and xylem water potential (Ψ_{xyl}, **c**,**d**) measured in *F. ornus* (**a**,**c**) and *O. europaea* (**b**,**d**) in hydrated (H, n = 5), drought-stressed (D, n = 5–6) and soaked (for 2 and 4 h, S_{2h} and S_{4h}, respectively, n = 6–7) stems. Note the different scales for Ψ_{xyl} between the two species. The 4 h soaking treatment was performed only for *F. ornus*. Different letters denote statistically significant differences among groups ($p < 0.05$).

Micro-CT Analyses

The micro-CT experiment on the potted plants of *F. ornus* proved the capability of xylem hydraulic recovery in intact plants through root water uptake 24 h after soil rehydration to field capacity. In fact, the embolized vessel area (EVA) was around 40–50% in drought-stressed (D_{pot}) plants, which reached Ψ_{xyl} of −3.50 MPa, and it was restored to pre-stress control (C_{pot}) values in the two re-irrigated (R_{pot}) plants (6% and 21% in the two scanned plants, Fig. 3), which relieved Ψ_{xyl} to −0.25 MPa and −0.70 MPa.

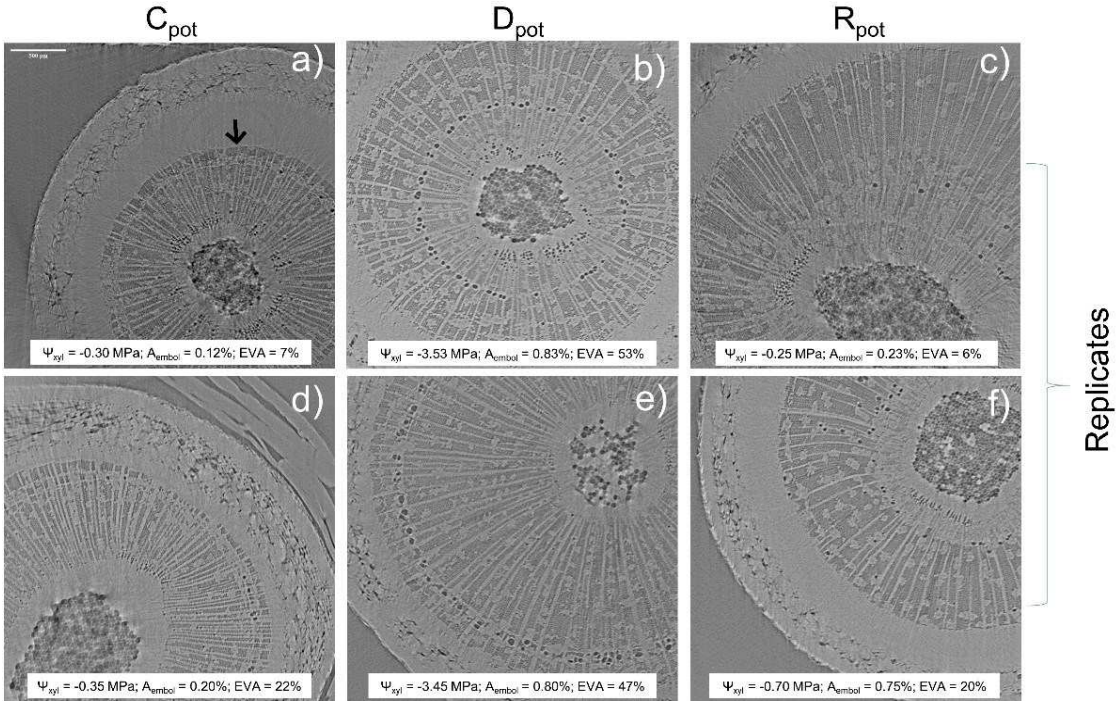

Fig. 3 Transverse reconstructed images of the 1-year-old stem portion obtained with X-ray micro-CT in well-hydrated (C_{pot}, **a**,**d**), drought-stressed (D_{pot}, **b**,**e**) and re-irrigated (R_{pot}, **c**,**f**) intact *F. ornus* plants. Ψ_{xyl} = xylem water potential, A_{embol} = percentage of embolized sapwood area, EVA = percentage of embolized vessel area; all calculated excluding the immature sapwood close to the cambium (see arrow delimiting mature/immature sapwood in **a**).

The consecutive micro-CT scans performed on the 2-year-old *F. ornus* drought-stressed (D) plants after each progressive sample preparation step are shown in Fig. S1. The first cut at the base of the stem did not significantly increase the embolized sapwood area (A_{embol}) or EVA. However, the second cut made to obtain the final D segment significantly increased EVA from 44 ± 7% (measured in the shoots cut at the base) to 63 ± 11%, with an overall increase of 27% compared to the intact plant (Fig. S2).

The stem segments did not refill their embolized conduits after the 2 h soaking treatment under light, as the values of A_{embol} and EVA (1.07 ± 0.06% and 58 ± 1%, respectively) were similar to those calculated for D stem segments ($p > 0.05$; Fig. 4 and S3).

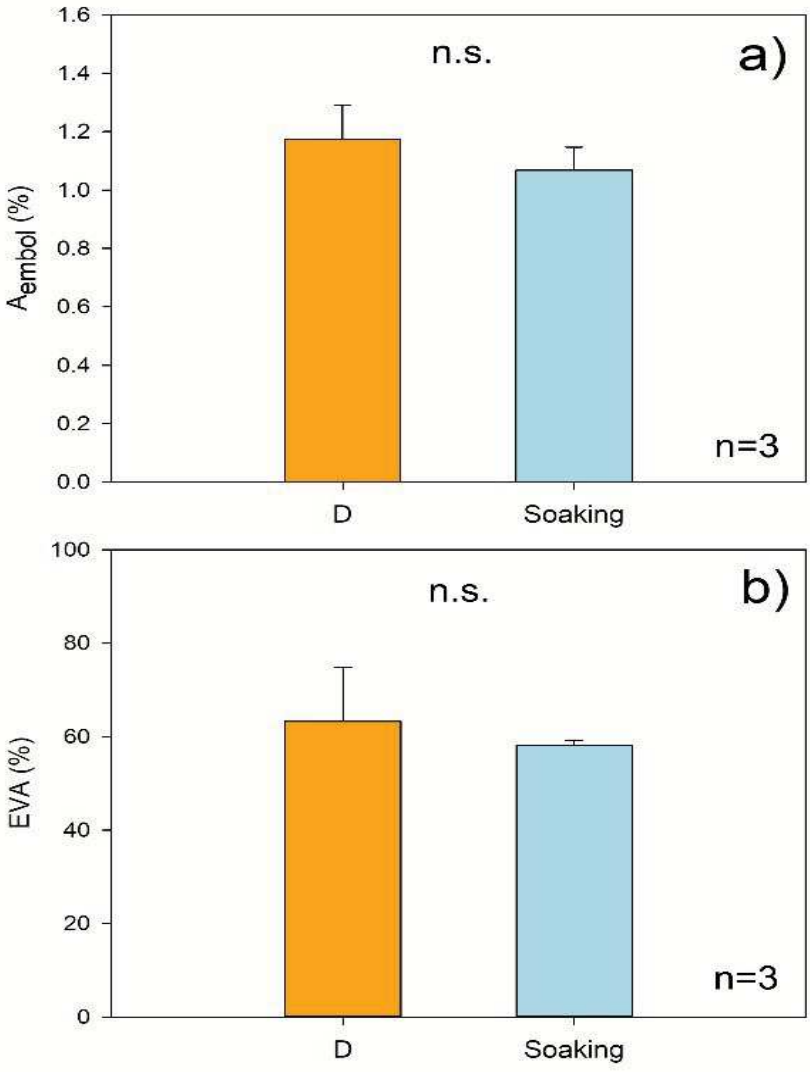

Fig. 4 Percentage of embolized sapwood area (A_{embol}, **a**) and percentage of embolized vessel area (EVA, **b**) measured in micro-CT transverse reconstructed images of *F. ornus* stem segments. D = segments of drought-stressed plants ($n = 3$). Soaking = segments of additional D plants scanned upon soaking in water for 2 h ($n = 3$). Values are means ± SE. n.s. = difference not significant among groups.

Discussion

No Evidence for Hydraulic Recovery in Stem Segments upon Soaking

The in vivo micro-CT analyses showed that *F. ornus* plants can recover xylem hydraulic function through root water uptake after experiencing substantial embolism levels under drought, confirming the previous classical hydraulic measurements of cut stems (Tomasella et al. 2019). In addition, embolism recovery occurred even though plants were still experiencing overall negative xylem pressure, supporting previous observations. However, the leafless stem segments of *F. ornus* and *O. europaea* that reached about 50% PLC (i.e., the same target PLC used in the pot re-irrigation experiment) did not recover xylem hydraulics after immersion in water under light conditions (Fig. 2). This outcome was additionally validated by the micro-CT scans of the *F. ornus* cut stems, obtained from the drought-stressed potted saplings (Fig. 4 and S2).

The hydraulic measurements of *F. ornus* branches (Fig. 2) were in agreement with the micro-CT measurements of intact plants (Fig. 3), confirming the lack of cutting artifacts. Likewise, the PLC values obtained in our study for *O. europaea* at the target Ψ_{xyl} were consistent with the vulnerability curves obtained for the same species both via hydraulic measurements and X-ray micro-CT scans (Torres-Ruiz et al. 2014, 2017), making us confident that sample preparation artefacts were avoided. However, with the methodological test performed at the micro-CT beamline on the dehydrated saplings of *F. ornus*, we aimed to examine if the sample preparation procedure used to obtain the final stem segments for soaking would induce additional non-native embolism. The progressive cuts made on the stem of the potted saplings increased the embolized vessel area (Fig. S1 and S2). In this test, we first made a cut underwater at the base of the shoot, and then a second cut was made at a distal position (ca. 20 cm from the previous one) to obtain a stem segment in the basal part of the stem. Given that the maximum vessel length of the saplings (40 cm on average) was higher than the obtained stem segment, it is likely that air entry upon cutting under substantial xylem tension induced embolism in the stem portion where the micro-CT scans were made (at 8 cm–9 cm from the first cut). Given that we aimed to perform the soaking experiment on the lower 1-year-old stem portion and that the plants were relatively small, we were forced to obtain the stem segment in that proximal stem region. With this simple test, we underline that experiments with in vivo imaging techniques should be further exploited to better identify the possible artefacts of sample preparation. However, the results of our cutting test do not influence the outcome of the soaking experiment because the samples scanned prior (D) or after (Soaking) immersion in water (Fig. 4) were prepared with the same procedure.

The results of the soaking experiments contradict those obtained for *S. matsudana* stem segments soaked in water under light conditions, where bark water uptake contributed to refill about 75% of the previously embolized vessels after 2 h of immersion (Liu et al. 2019). Here, we also showed that *F. ornus* and *O. europaea* stems can perform photosynthesis both at wood and bark levels (Fig. 1), which should provide additional sugars to enhance the process of water uptake by generating an osmotic gradient.

There is evidence that local xylem tension relief is important to refill xylem conduits (Zwieniecki and Holbrook 2000; Secchi and Zwieniecki 2016). In *S. sempervirens*, partial hydraulic recovery was observed upon soaking when branch water potential slightly increased with respect to dehydrated conditions, but it was still quite negative (ca. −4 MPa, (Mason Earles et al. 2016). Similarly, recovery under substantial tension occurred in *Picea glauca* leafy twigs exposed to fog (Laur et al. 2014), suggesting possible localized hydraulic isolation in the xylem. Xylem tension in our two study species was even relaxed to Ψ_{xyl} above −0.5 MPa (Fig. 2). These values are comparable to those measured in the intact potted plants of *F. ornus*, which recovered xylem hydraulics when re-irrigated in pots (Fig. 3). Therefore, we note that the residual xylem tension of the cut stems was comparable to that of intact plants, and it was expected to promote the refilling of conduits through bark water uptake.

Earles et al. 2016 suggested that tall trees, such as redwoods, which, due to their height, must develop low Ψ_{xyl} even under well-hydrated conditions, may profit from bark water uptake during prolonged fog periods to partially restore xylem functionality. It is suggested that trees adapted to climates with prolonged periods of rain and/or fog (Burgess and Dawson 2004) and trees at the timberline with crowns covered with snow that melts in spring (Mayr et al. 2014; Losso et al. 2021) may have evolved bark characteristics that favor water uptake and subsequent hydraulic recovery. Indeed, radial water uptake may depend on outer (rhytidome) and/or inner (phloem) bark characteristics. For example, bark porosity and density influence hygroscopicity (Ilek et al. 2021), while the hydrophobicity of cork cells in the outer bark limits water absorption (Schönherr and Ziegler 1980; Groh et al. 2002). It is possible that species adapted to Mediterranean climates, commonly not exposed to prolonged fogs/rainy periods, may not have evolved such bark characteristics that would favor radial water uptake. However, we might rule out this hypothesis because, although we did not directly measure bark water uptake, the marked Ψ_{xyl} relief upon soaking indicated substantial stem rehydration (Fig. 2b). Alternatively, sample preparation/experimental conditions could have been responsible for the lack of hydraulic recovery. Previous experiments have highlighted the role of phloem in xylem hydraulic recovery (Nardini et al. 2011). In particular, stem girdling in *O. europaea* prevented embolism refilling upon branch rehydration, while hydraulic recovery was observed in samples with intact phloem (Trifilò et al. 204). Hence, it is possible that the wounds caused by the preparation of

stem segments for soaking had similar inhibitory effects on the refilling process. Tests on different species could help improve our understanding as to whether refilling through bark water uptake might be species specific, as well as the possible limits of the soaking method when applied to cut stem segments.

Conclusions

In this work, we tested the hypothesis that the immersion of photosynthesizing stem segments in distilled water for some hours in the presence of light would induce hydraulic recovery through bark water uptake in the embolized branches of two drought-resistant Mediterranean tree species (*F. ornus* and *O. europaea)*. Hydraulic recovery was previously reported for the soaked stem segments of *S. matsudana*, and it was related to the generation of an osmotic gradient (Liu et al. 2019). However, for the two species analyzed in this study, which are known to be capable of hydraulic repair under moderate tension (additionally demonstrated here by an in vivo micro-CT analysis of the potted saplings of *F. ornus*), refilling by bark water uptake did not occur. Our data suggest that refilling does not commonly occur in cut stems soaked under water, thus suggesting that this common procedure in hydraulic measurements is not likely to produce artefactual results. Clearly, further soaking studies under light conditions should be performed on photosynthesizing stems of other species to better understand both the potential and the limits of this process, as well as the possible consequences in terms of the accuracy of hydraulic measurements of xylem embolism.

Author Contributions

Conceptualization and experimental design, A.N., M.T. and S.N.; methodology, M.T., S.N. and A.N.; formal analysis, M.T. and S.N.; investigation, M.T., S.N., F.P., S.D.B., L.D. and G.T.; data curation, M.T.; visualization, M.T.; writing—original draft preparation, M.T. and A.N.; writing—review and editing, A.N.; supervision, A.N. All authors have read and agreed to the published version of the manuscript.

Acknowledgments

We thank the "Direzione centrale risorse agroalimentari, forestali e ittiche–area foreste e territorio" of the "Regione autonoma Friuli Venezia Giulia" and the public nursery Vivai Pascul (Tarcento, Italy) for providing us with the potted plant material. The beamtime access to the SYRMEP beamline was granted by Elettra Sincrotrone Trieste (proposal no. 20195384 and no. 20210284).

References

Berry ZC, Emery NC, Gotsch SG, Goldsmith GR. 2019. Foliar water uptake: processes, pathways, and integration into plant water budgets. *Plant, Cell & Environment* **2019 42:** 410–423.

Breshears DD, McDowell NG, Goddard KL, Dayem KE, Martens SN, Meyer CW, Brown KM. 2008. Foliar absorption of intercepted rainfall improves woody plant water status most during drought. *Ecology* **89:** 41–47.

Brodersen CR, McElrone AJ, Choat B, Matthews MA, Shackel KA. 2010. The dynamics of embolism repair in xylem: in vivo visualizations using high-resolution computed tomography. *Plant Physiology* **154:** 1088–1095.

Brun F, Pacilè S, Accardo A, Kourousias G, Dreossi D, Mancini L, Tromba G, Pugliese R. 2015. Enhanced and flexible software tools for x-ray computed tomography at the italian Synchrotron Radiation Facility Elettra. *Fundamenta Informaticae* **141:** 233–243.

Burgess SSO, Dawson TE. 2004. The contribution of fog to the water relations of sequoia sempervirens (d. don): foliar uptake and prevention of dehydration. *Plant, Cell & Environment* **27:** 1023–1034.

Dawson TE, Goldsmith GR. 2018. The value of wet leaves. *New Phytologist.* **219:** 1156–1169.

Carmichael MJ, White JC, Cory ST, Berry ZC, Smith WK. 2020. Foliar water uptake of fog confers ecophysiological benefits to four common tree species of south eastern freshwater forested wetlands. *Ecohydrology* **13:** e2240.

Fernández V, Sancho-Knapik D, Guzmán P, Peguero-Pina JJ, Gil L, Karabourniotis G, Khayet M, Fasseas C, Heredia-Guerrero JA, Heredia A, et al. 2014. Wettability, polarity, and water absorption of holm oak leaves: effect of leaf side and age. *Plant Physiology* **166:** 168–180.

Fuenzalida TI, Bryant CJ, Ovington LI, Yoon H, Oliveira RS, Sack L, Ball MC. 2019. Shoot surface water uptake enables leaf hydraulic recovery in *Avicennia marina*. *New Phytologist* **224:** 1504–1511.

Groh B, Hübner C, Lendzian K. 2002. Water and oxygen permeance of phellems isolated from trees: the role of waxes and lenticels. *Planta* **215:** 794–801.

Guzmán-Delgado P, Laca E, Zwieniecki MA. 2021. Unravelling foliar water uptake pathways: the contribution of stomata and the cuticle. *Plant, Cell & Environment* **44:** 1728–1740.

Ilek A, Siegert CM, Wade A. 2021. Hygroscopic contributions to bark water storage and controls exerted by internal bark structure over water vapor absorption. *Trees* **35:** 831–843.

Katz C, Oren R, Schulze ED, Milburn JA. 1989. Uptake of water and solutes through twigs of *Picea abies* (L.) Karst. *Trees* **3:** 33–37.

Laur J, Hacke UG. 2014. Exploring *Picea glauca* aquaporins in the context of needle water uptake and xylem refilling. *New Phytologist* **203:** 388–400.

Lenth, R.V. 2020. Emmeans: estimated marginal means, aka least-squares means. r package version 1.5.0. available online: https://CRAN.R-project.org/package=emmeans (accessed on 30 November 2021).

Liu J, Gu L, Yu Y, Huang P, Wu Z, Zhang Q, Qian Y, Wan X, Sun Z. 2019. Corticular photosynthesis drives bark water uptake to refill embolized vessels in dehydrated branches of *Salix matsudana*. *Plant, Cell & Environment* **42:** 2584–2596.

Losso A, Bär A, Unterholzner L, Bahn M, Mayr S. 2021. Branch water uptake and redistribution in two conifers at the alpine treeline. *Scientific Reports* 11: 22560.

Mason Earles J, Sperling O, Silva LC, McElrone AJ, Brodersen CR, North MP, Zwieniecki MA. 2016. Bark water uptake promotes localized hydraulic recovery in coastal redwood crown. *Plant, Cell & Environment* **39:** 320–328.

Mayr S, Schmid P, Laur J, Rosner S, Charra-Vaskou K, Dämon B, Hacke UG. 2014. uptake of water via branches helps timberline conifers refill embolized xylem in late winter. *Plant Physiology* **164:** 1731–1740.

Nardini A, Lo Gullo MA, Salleo S. 2011. refilling embolized xylem conduits: is it a matter of phloem unloading? *Plant Science* **180:** 604–611.

Nardini A, Gasco A, Trifilo P, Lo Gullo MA, Salleo S. 2007. Ion-mediated enhancement of xylem hydraulic conductivity is not always suppressed by the presence of ca^{2+} in the sap. *Journal of Experimental Botany* **58:** 2609–2615.

Paganin D, Mayo SC, Gureyev TE, Miller PR, Wilkins SW. 2002. Simultaneous phase and amplitude extraction from a single defocused image of a homogeneous object. *Journal of microscopy* **206:** 33–40.

Petruzzellis F, Pagliarani C, Savi T, Losso A, Cavalletto S, Tromba G, Dullin C, Bär A, Ganthaler A, Miotto A, et al. 2018. The pitfalls of in vivo imaging techniques: evidence for cellular damage caused by synchrotron x-ray computed micro-tomography. *New Phytologist* **220:** 104–110.

Pinheiro J, Bates D, DebRoy S, Sarkar D. R Core Team. 2019. Nlme: linear and nonlinear mixed effects models. available online: https://cran.r-project.org/package=nlme (accessed on 30 November 2021).

Salleo S, Lo Gullo MA, Trifilo P, Nardini A. 2004. New evidence for a role of vessel-associated cells and phloem in the rapid xylem refilling of cavitated stems of *Laurus nobilis* L. *Plant, Cell & Environment* **27:** 1065–1076.

Savi T, Miotto A, Petruzzellis F, Losso A, Pacilè S, Tromba G, Mayr S, Nardini A. 2017. Drought-induced embolism in stems of sunflower: a comparison of in vivo micro-ct observations and destructive hydraulic measurements. *Plant Physiology and Biochemistry* **120:** 24–29.

Schönherr J, Ziegler H. 1980. Water permeability of betula periderm. *Planta* **147:** 345–354.

Schreel JDM, Leroux O, Goossens W, Brodersen C, Rubinstein A, Steppe K. 2020. Identifying the pathways for foliar water uptake in beech (*Fagus sylvatica* L.): a major role for trichomes. *Plant Journal* **103:** 769–780.

Secchi F, Pagliarani C, Zwieniecki MA. 2017. The functional role of xylem parenchyma cells and aquaporins during recovery from severe water stress: response of xylem parenchyma cells to embolism. *Plant, Cell & Environment* **40:** 858–871.

Secchi F, Zwieniecki MA. 2016. Accumulation of sugars in the xylem apoplast observed under water stress conditions is controlled by xylem pH. *Plant, Cell & Environment* **39:** 2350–2360.

Secchi F, Pagliarani C, Cavalletto S, Petruzzellis F, Tonel G, Savi T, Tromba G, Obertino MM, Lovisolo C, Nardini A, et al. 2020. Chemical inhibition of xylem cellular activity impedes the removal of drought-induced embolisms in poplar stems-new insights from micro-CT analysis. *New Phytologist* **229:** 820–830.

Sperry JS, Donnelly JR, Tyree MT. 1988. A method for measuring hydraulic conductivity and embolism in xylem. *Plant, Cell & Environment* 11: 35–40.

Tomasella M, Casolo V, Aichner N, Petruzzellis F, Savi T, Trifilò P, Nardini A. 2019. Non-structural carbohydrate and hydraulic dynamics during drought and recovery in *Fraxinus ornus* and *Ostrya carpinifolia* saplings. *Plant Physiology and Biochemistry* **145:** 1–9.

Torres-Ruiz JM, Cochard H, Mayr S, Beikircher B, Diaz-Espejo A, Rodriguez-Dominguez CM, Badel E, Fernández JE. 2014. Vulnerability to cavitation in *olea europaea* current-year shoots: further evidence of an open-vessel artifact associated with centrifuge and air-injection techniques. *Physiologia Plantarum* **152:** 465–474.

Torres-Ruiz JM, Jansen S, Choat B, McElrone AJ, Cochard H, Brodribb TJ, Badel E, Burlett R, Bouche,PS, Brodersen CR, et al. 2015. Direct x-ray microtomography observation confirms the induction of embolism upon xylem cutting under tension. *Plant Physiology* **167:** 40–43.

Torres-Ruiz JM, Cochard H, Choat B, Jansen S, López R, Tomášková I, Padilla-Díaz CM, Badel E, Burlett R, King A, et al. 2017. Xylem resistance to embolism: presenting a simple diagnostic test for the open vessel artefact. *New Phytologist* **215:** 489–499.

Trifilò P, Raimondo F, Lo Gullo MA, Barbera PM, Salleo S, Nardini A. 2014. Relax and refill: xylem rehydration prior to hydraulic measurements favours embolism repair in stems and generates artificially low plc values. *Plant, Cell & Environment* **37:** 2491–2499.

Venturas MD, Pratt RB, Jacobsen AL, Castro V, Fickle JC, Hacke UG. 2019. Direct comparison of four methods to construct xylem vulnerability curves: differences among techniques are linked to vessel network characteristics. *Plant, Cell & Environment* **42:** 2422–2436.

Wang R, Zhang L, Zhang S, Cai J, Tyree MT. 2014. Water relations of *robinia pseudoacacia* l.: do vessels cavitate and refill diurnally or are r-shaped curves invalid in *robinia*? *Plant, Cell & Environment* **37:** 2667–2678.

Wheeler JK, Huggett BA, Tofte AN, Rockwell FE, Holbrook NM. 2013. Cutting xylem under tension or supersaturated with gas can generate plc and the appearance of rapid recovery from embolism. *Plant, Cell & Environment* **36:** 1938–1949.

Zwieniecki MA, Holbrook NM. 2000. Bordered pit structure and vessel wall surface properties. implications for embolism repair. *Plant Physiology* **123:** 1015–1020.

Zwieniecki MA, Holbrook NM. 2009. Confronting maxwell's demon: biophysics of xylem embolism repair. *Trends in Plant Science* **14:** 530–534.

Supplementary material

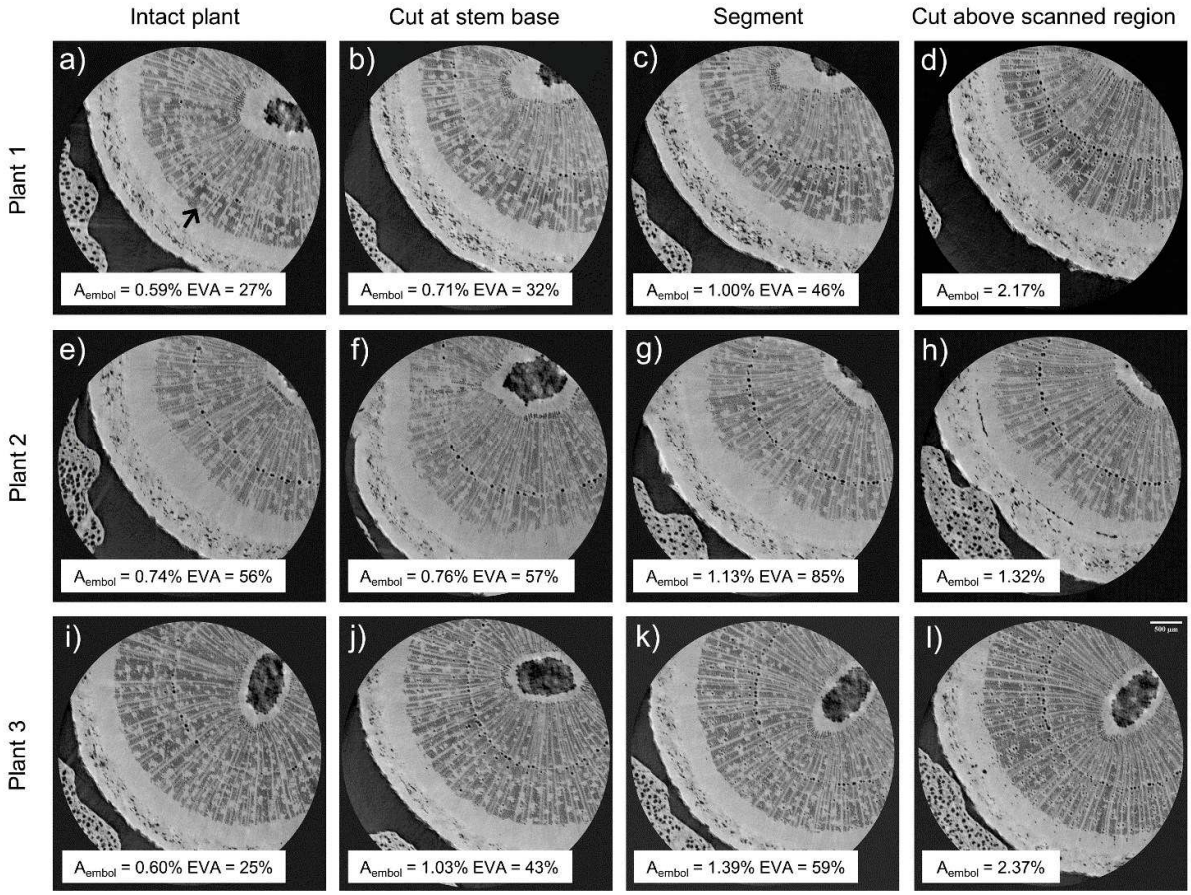

Fig. S1 X-ray Micro-CT transverse images of drought stressed 2-year-old *F. ornus* saplings (n=3). Scans were performed in drought-stressed intact plants (a,e,i), after subsequent cut underwater at the base of the stem (b,f,j), after a second cut underwater to obtain a stem segment (c,g,k) and after cutting above the scanned region to embolize all mature conduits (d,h,l). A_{embol} = percentage of embolized sapwood area; EVA = percentage of embolized vessel area, all calculated excluding the immature sapwood close to the cambium (see arrow delimiting mature-immature sapwood in a).

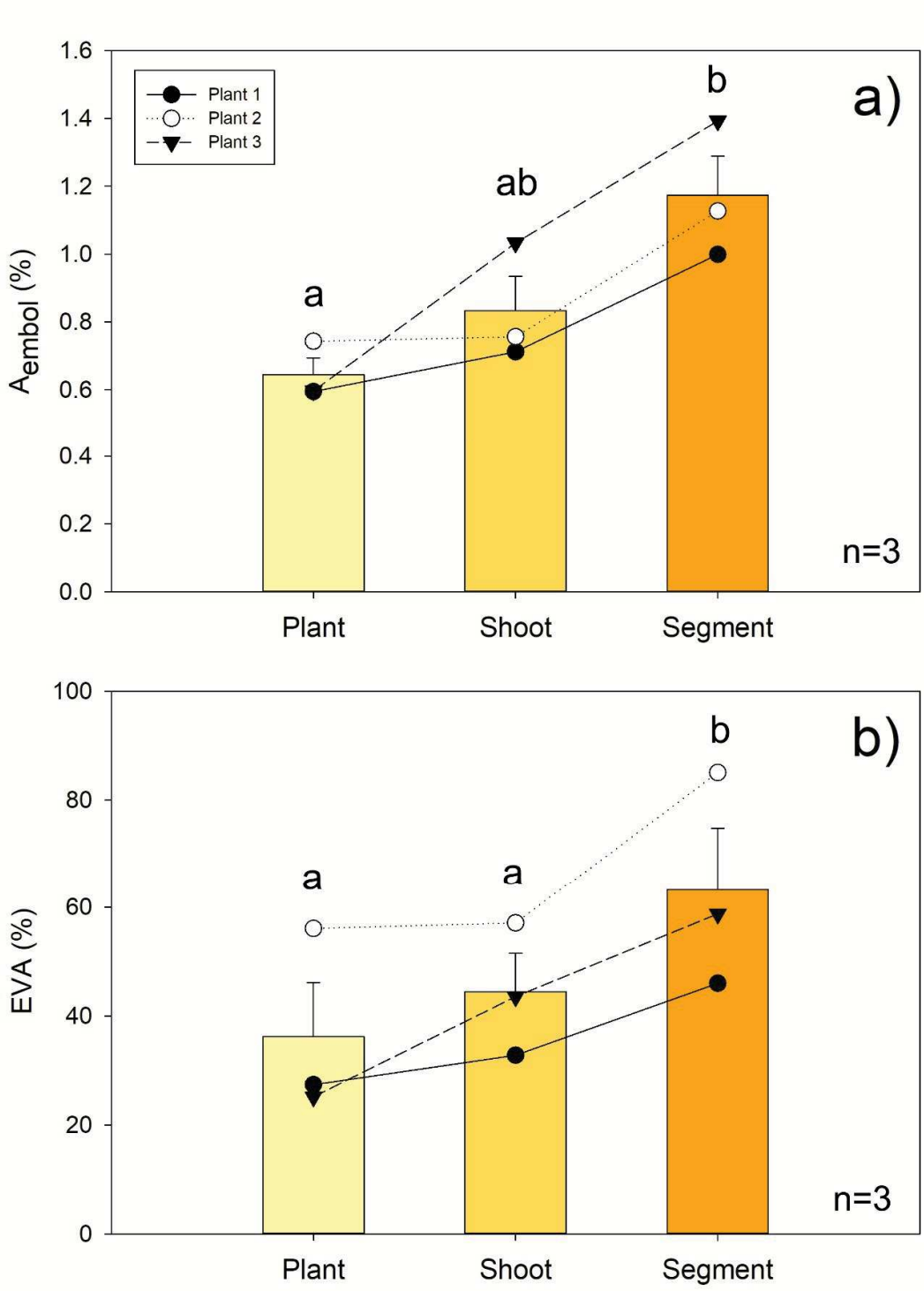

Fig. S2 Cutting effect on embolism formation in *F. ornus* potted saplings visualized with Micro-CT. **a**) Percentage of embolized sapwood area (A_{embol}) and **b)** percentage of embolized vessel area (EVA) measured in Micro-CT transverse images of drought-stressed saplings. Plants (1-3, indicated by symbols, n=3) were consecutively scanned when intact (Plant), after subsequent cut underwater at the base of the stem (Shoot) and after a second cut underwater to obtain a stem segment (Segment). Values are means ± SE. Different letters denote statistically significant differences among Plant, Shoot and Segment ($P < 0.05$).

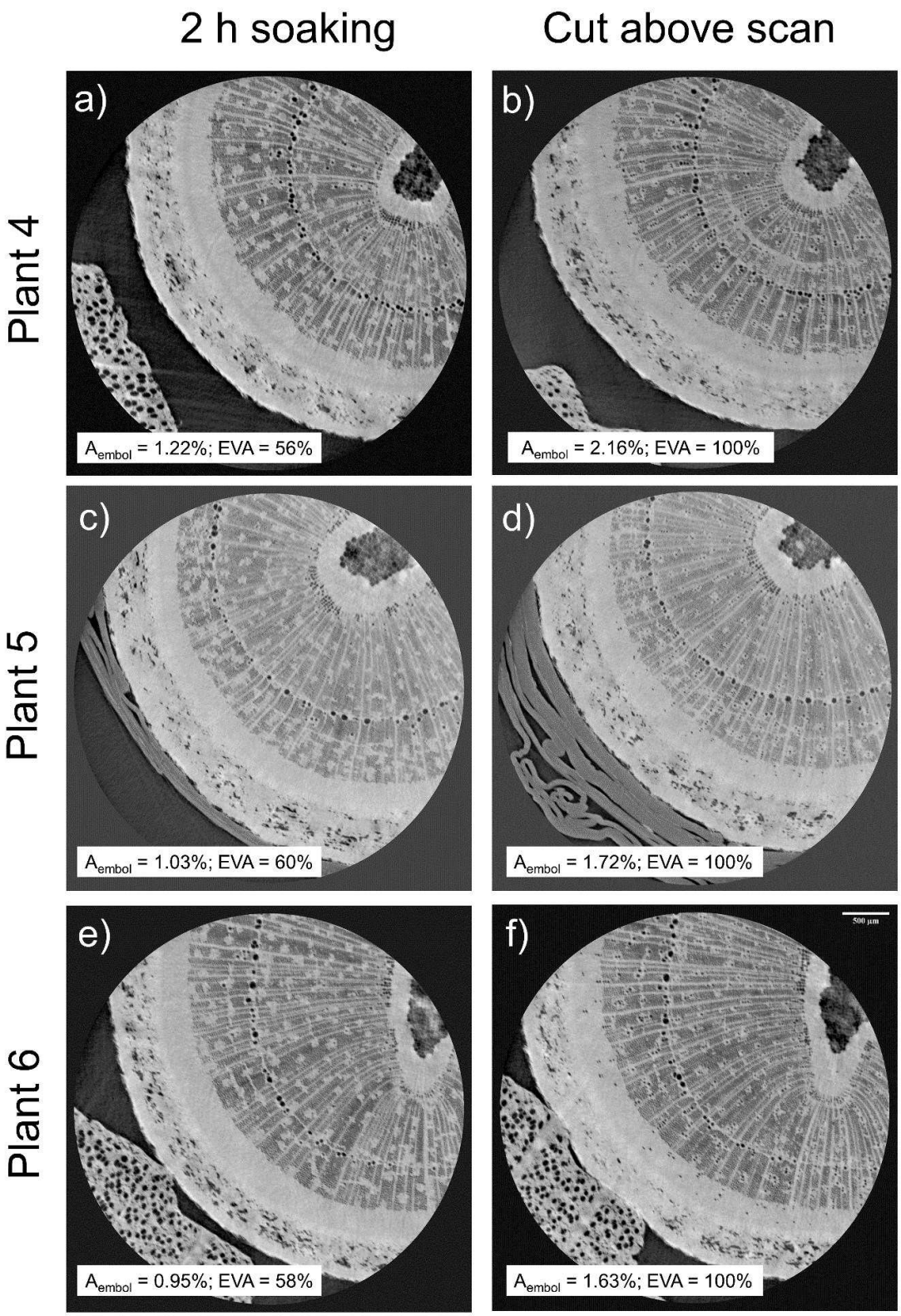

Fig. S3 X-ray Micro-CT transverse images of 2-year-old *F. ornus* stem segments after the soaking treatment (S_{2h}, n=3). Scans were performed in drought-stressed segments soaked under light for 2 hours (a,c,e) and after cutting above the scanned region to embolize all mature conduits (b,d,f). A_{embol} = percentage of embolized sapwood area; EVA = percentage of embolized vessel area.

General conclusions

General research outcomes and scientific contributions

The main objective of my PhD research project was to improve our knowledge of the structural and functional characteristics of stem chloroplasts. Furthermore, the broad goal was to explore the role of stem photosynthesis in tree resistance/resilience to drought stress due to the current threats of climate change to which all the plants are exposed. In this concluding chapter, the main findings of the study are discussed. Finally, remaining unanswered questions and suggestions for promising future lines of research on the role of stem photosynthesis in tree drought resistance are identified and discussed.

Advances on stem photosynthesis

A classical hypothesis in plant science is that any tissue that is visually green contains chloroplasts. A corollary is that greenish stems they must have chloroplasts too, and therefore they should be able to perform photosynthesis (e.g. Pfanz and Aschan 2001). However, an in-depth evaluation of the actual properties and functioning of stem chloroplasts is still missing in the literature.

In this light, the first chapter of this Thesis aimed to deeply investigate the structural and functional characteristics of stem chloroplasts, compared to those of the leaf. I also applied methods so far used only for leaves and/or roots, to estimate the efficiency of electronic transport (Study 1) and the production of oxygen (Study 2) in the stem of a drought-tolerant woody species, *Fraxinus ornus* (*F. ornus*).

Specifically, in Study 1 I reported the first detailed characterization of stem chloroplasts of *F. ornus*. In addition to classical experimental techniques (e.g. spectral reflectance, fluorescence microscopy, chlorophyll fluorescence imaging), I also applied spectroscopy measurements in stem samples. I provided evidence for a decreasing chlorophyll concentration gradient from the outer bark to the pith, in compliance with the light gradient found along the stem radial direction (blue light was mainly absorbed by the bark whereas the far-red light reached the xylem and the pith). I further investigated the functional features of stem chloroplasts, by finally proving that bark chloroplasts resembled those of the leaves, whereas wood chloroplasts are coherently optimized to photosynthesize in their particular micro-environmental conditions.

In Study 2, I provided a new framework for oxygen measurements based on dedicated MicroSensors. Due to their precision, these devices allow to measure oxygen production *in situ* at very low

concentrations. Our results proved that bark chloroplasts can perform net photosynthesis, whereas wood chloroplasts can only counterbalance respiration.

The diversity of stem photosynthesis in drought tolerant and drought sensitive species

While the ultrastructural, biochemical, fluorescence and functional properties of stem wood and bark chloroplasts have been identified (Chapter 1), it remains largely unknown whether the presence of chloroplasts in the stem of woody species is different between drought tolerant and drought sensitive species. Our approach, presented in Chapter 2, constitutes quite a novelty in stem photosynthesis research. For instance, chloroplasts' presence in the wood seems to be associated with the amount of volume occupied by parenchyma, since Gymnosperms, that generally have low amounts of parenchyma in their wood (in the range of 5-10% of the total volume), in sharp contrast with Angiosperms (25-50%), presented lower values of Fv/Fm. Probably, differences in wood characteristics might also alter the light transmission efficiency with consequences on chloroplasts abundance/distribution. Indeed, Fv/Fm values decreased with increasing stem age, and this perfectly matches with higher deposition of cork layers and wood in older stems. Furthermore, results obtained in Chapter 2, allowed to pinpoint the potential adaptive role of stem photosynthesis in drought tolerant species, thriving under arid conditions likely leading to prolonged stomatal closure and halt of leaf-level carbon gain, since Fv/Fm both at the bark and wood level was higher for drought tolerant Angiosperms compared to drought sensitive ones. These findings support the already presented hypothesis [summarized by Vandegehuchte et al. (2015)] that stem photosynthesis is less reduced than leaf photosynthesis during drought. Furthermore, since it takes advantage also on the endogenously respired CO_2, stem photosynthesis is more efficient in carbon fixation than leaves during drought, increasing also the plant water use efficiency (Cernusak and Marshall 2000; Wittman and Pfanz 2008). The specific key role of stem photosynthesis during drought, when leaf photosynthesis is partially impaired, might be the production of photosynthates at sink level necessary to sustain plant metabolism. In this light, stem photosynthesis might sustain turgor and phloem functioning, hence maintaining the hydraulic functioning of the plant and increasing the drought resistance of the species (Sevanto et al. 2014; Bloemen et al. 2013b).

Key findings and implications of stem photosynthesis in tree resilience to drought stress

From Chapter 1 I found active chloroplasts in bark and wood of *F. ornus* and in Chapter 2 I found that drought-tolerant species tend to have higher values of Fv/Fm in stems that might be fundamental to sustain carbon metabolism during drought. Indeed, during drought stress, one of the earliest responses of plants is to close stomata at leaf level, limiting water loss but also the uptake of

atmospheric CO_2 with consequent decrease of leaf photosynthesis activity (Chaves et al. 2002; Flexas and Medrano 2002). Stem photosynthesis instead is also supplied with endogenously respired CO_2, with a consequent higher water use efficiency compared to leaves (Ávila-Lovera and Tezara 2018). The stem light exclusion treatment, that prevented stem photosynthesis to occur in the three experiments reported in Chapter 3, resulted in reduced growth for the evergreen *Laurus nobilis* (*L. nobilis*, Chapter 3 – study 5) but not for the deciduous *Populus alba* (*P. alba*, Chapter 3 – study 5) and *Fraxinus ornus* (Chapter 3 – study 4). This demonstrated that stem photosynthesis has a species-specific impact on the overall plant status, although it did not alter leaf gas exchange rates in any of the species investigated.

The shading of the stem had different consequences on the three species investigated during water stress and recovery, compared to control-light plants:

- had no effect in *L. nobilis*,
- inhibited the hydraulic recovery following embolism build-up under drought in *P. alba*,
- increased the percent loss of conductance (PLC) during drought but did not alter the hydraulic recovery in *F. ornus*.

These three different results let me to conclude that stem photosynthesis plays a species-specific key role in the maintenance of hydraulic functioning during drought, especially for the deciduous species. Indeed, it seems that in the drought-sensitive deciduous species (*P. alba*) stem photosynthesis provides an extra carbon gain useful for the whole plant metabolism, especially under drought. By contrasts, in the two drought-tolerant species (*F. ornus* and *L. nobilis*), stem photosynthesis could represent an extra carbon gain to be used mainly when leaf photosynthesis is impaired.

The main achieved conclusions rely on the fact that stem photosynthesis affects the hydraulic resilience of some woody species, mainly contributing to the NSC reserves and mobilization.

Directions for future research

In this Thesis, I mainly focused on one model species (*Fraxinus ornus*) and I have conducted experiments on saplings grown and treated under greenhouse conditions. The chance to measure other stem photosynthesis traits (e.g. electron transport rate) on a large set of species would allow widening the scale of the analyses provided in this Thesis, to further prove whether stem photosynthesis is related to tree drought resistance/resilience as described here.

Since the role of stem chloroplasts in embolism repair remains unclear, further studies both on saplings and branches of adult trees are needed. To further prove a relationship between stem photosynthesis and hydraulic responses, it could be useful to design experiments that monitor

hydraulic traits (e.g. with a stem psychrometer, a stand-alone instrument for stem water potential measurement, which indicates plant water stress), simultaneously with photosynthetic traits (e.g. with PAM instruments to measure photosynthesis).

Moreover, recent advances in isotopic techniques might contribute to clarify patterns and processes in tree carbon cycling at a yet unprecedented resolution (e.g. Bloemen et al. 2013, 2014). Of particular interest might be including measurements of starch carbon isotope composition (^{13}C, ^{12}C), that could provide useful information about the source of CO_2 used by bark and wood chloroplasts in the photosynthetic process. Specifically, these measurements could finally elucidate if stem chloroplasts, with particular attention to those located in the wood, rely on recycling internal CO_2 from recently assimilated photosynthates or stored carbon reserves. Hence, the use of this approach would further deepen the knowledge of the ability and significance of internal CO_2 recycling by stem chloroplasts, that is particularly important if we consider that internal CO_2 recycling is less susceptible to the drying power of the atmosphere due to climate change and water loss via the stem is reduced compared to those of the leaves, leading to an increased plant water use efficiency under the ongoing drought extremes events.

In conclusion, I suggest that the inclusion of stem photosynthesis in the study of the ability of trees to face drought stress might give a more comprehensive understanding on how different woody species can acclimate to variation of environmental conditions.

References

Ávila-Lovera E, Tezara W. 2018. Water-use efficiency is higher in green stems than in leaves of a tropical tree species. *Trees* **32:** 1547–1558.

Bloemen J, McGuire MA, Aubrey DP, Teskey RO, Steppe K. 2013. Internal recycling of respired CO_2 maybe important for plant functioning under changing climate regimes. *Plant Signaling & Behavior* **8:** e27530.

Bloemen J, Overlaet-Michiels L, Steppe K. 2013b. Understanding plant responses to drought: how important is woody tissue photosynthesis? *Acta Horticulturae* **991:** 149–157.

Bloemen J, Agneessens L, Van Meulebroek L, Aubrey DP, McGuire MA, Teskey RO, Steppe, K. 2014. Stem girdling affects the quantity of CO_2 transported in xylem as well as CO_2 efflux from soil. *New Phytologist* **201:** 897–907.

Cernusak LA, Marshall JD. 2000. Photosynthetic refixation in branches of western white pine. *Functional Ecology* **14:** 300–311.

Chaves MM, Pereira JS, Maroco J, Rodrigues ML, Ricardo CPP, Osorio ML, Carvalho I, et al. 2002. How plants cope with water stress in the field. Photosynthesis and growth. *Annals of Botany* **89:** 907–916.

Flexas J, Medrano H. 2002. Drought-inhibition of photosynthesis in C_3 plants: stomatal and non-stomatal limitations revisited. *Annals of Botany* **89:** 183–189.

Pfanz H, Aschan G. 2001. The existence of bark and stem photosynthesis in woody plants and its significance for the overall carbon gain. An eco-physiological and ecological approach. In: Essr K, Luttge U, Kadereit JW, Beyshlag W, eds. *Progress in Botany*, Berlin, DE: Springer-Verlag, 477–510.

Sevanto S, Mcdowell NG, Dickman LT, Pangle R, Pockman WT. 2014. How do trees die? A test of the hydraulic failure and carbon starvation hypotheses. *Plant, Cell & Environment* **37:** 153–161.

Vandegehuchte MW, Bloemen J, Vergeynst LL, Steppe K. 2015. Woody tissue photosynthesis in trees: salve on the wounds of drought? *New Phytologist* **208:** 998–1002.

Wittmann C, Pfanz H. 2008. Antitranspirant functions of stem periderms and their influence on corticular photosynthesis under drought stress. *Trees* **22:** 187–196.

Publication list

Published papers related to this Thesis

Tomasella M, Natale S, Petruzzellis F, Di Bert S, D'Amico L, Tromba G, Nardini A. 2022. No evidence for light-Induced embolism repair in cut stems of drought-resistant mediterranean species under soaking. *Plants* **11:** 307.

Trifilò P, Natale S, Gargiulo S, Abate E, Casolo V, Nardini A. 2021. Stem photosynthesis affects hydraulic resilience in the deciduous *Populus alba* but not in the evergreen *Laurus nobilis*. *Water* **13:** 2911.

Side papers published in the course of the PhD

Petruzzellis F, Natale S, Reščič J, Bariviera L, Calderan A, Lisjak K, Sivilotti P, Šuklje K, Vanzo A, Nardini A. 2022. High spatial heterogeneity of water stress level in Refošk grapevines cultivated in Classical Karst. *Agricultural water management* **260:** 107288.

Nardini A, Petruzzellis F, Marusig D, Tomasella M, Natale S, Altobelli A, Calligaris C, Floridda G, Cucchi F, Forte E, Zini L. 2021. Water "on the rocks": a summer drink for thirsty trees?. *New Phytologist* **229:** 199–212.

Tomasella M, Casolo V, Natale S, Petruzzellis F, Kofler W, Beikircher B, Mayr S, Nardini A. 2021. Shade induced reduction of stem nonstructural carbohydrates increases xylem vulnerability to embolism and impedes hydraulic recovery in Populus nigra. *New Phytologist*: **231:** 108–121.

Petruzzellis F, Tordoni E, Bonaventura A, Tomasella M, Natale S, Panepinto F, Bacaro G, Nardini A. 2021. Turgor loss point and vulnerability to xylem embolism predict species-specific risk of drought-induced decline of urban trees. *Plant Biology*. https://doi.org/10.1111/plb.13355

Petruzzellis F, Tomasella M, Miotto A, Natale S, Trifilò P, Nardini A. 2020. A leaf selfie: using a smartphone to quantify leaf vulnerability to hydraulic dysfunction. *Plants* **9:** 234.